Department of Chemical and Environmental

Engineering

Improving the carbon efficiency in the bio-production of citramalic acid in *Escherichia coli*

Juliana Laurence Dominique LEBEAU

Thesis submitted to the University of Nottingham for the degree of

Doctor of Philosophy

September 2017

…quand le vent siffle dans les aiguilles des filaos…

J.M.G. Le Clézio, *Le chercheur d'or*, 1985.

Abstract

Methacrylic acid (MAA) is a bulk chemical used in the synthesis of acrylic polymers as well as for the manufacture of many different products such as resins, and paints. However, the industrial manufacturing processes for MAA production involve toxic raw materials that are reliant on availability and economic variability of petroleum derived compounds. Global consumption and market of acrylics keep growing, rendering constant production processes as well as price stability highly desirable.

To date, there is no direct bio-process available for the biosynthesis of MAA itself. Fortunately, a bio-production route of citramalic acid, which was previously demonstrated to be converted readily to MAA in a simple chemical patented hot pressurised water process, was demonstrated in *Escherichia coli* with promising titres of product (130 g/L). The enzyme citramalate synthase was used, and catalysed the condensation of two central cellular metabolites, pyruvate and acetyl-CoA, to (*R*)-citramalate in a one-step reaction. However, the biocatalytic reaction is limited by the availability of the starting materials. Acetyl-CoA is mainly produced *via* the decarboxylation of pyruvate, resulting in losing carbon by the formation of CO_2, and is known as one of the major limitation for the development of cost-effective microbial bio-production of commodity bio-chemicals.

In this thesis, *E. coli* strains were engineered to be able to co-consume carbohydrate and/or non-carbohydrate sources, in order to address the metabolic limitation due to pyruvate decarboxylation. In *E. coli*,

both acetate and ethanol are directly linked to acetyl-CoA *via* different reversible enzyme pathways and were thus identified as potential external sources of acetyl-CoA. The introduction of either an acetate or an ethanol assimilation pathway with the appropriate co-feeding of glucose/acetate or glucose/ethanol resulted in increasing the specific productivities of (*R*)-citramalate in *E. coli* up to 50% in comparison to bio-production systems based on glucose only. Thus, acetate and ethanol co-feeding strategies provided promising outcomes for the bio-production of MAA.

Acknowledgments

There. On the day of my 28th birthday. A life's bit of 4 years has just finished. Paced with ups and downs, new intellectual and emotional challenges, but most of all enormous support from the solid and patient family kernel, and that despite the distance, and also from the new friends I made here. The completion of this thesis would not have been possible without all of this.

I would like to thank my PhD supervisors, Gill Stephens and Steve Hall, for their constant help, guidance and patience along my studies. Thanks you so much for everything! I am also grateful of the support and inputs of my industrial supervisors, Graham Eastham and David Johnson.

Beyond the lab and the work, the endless days, nights and weekends following bacterial cell's growth had been so much better thanks to the warm-hearted and delightful presence of my lab mates! Alanna, the kindness embodied; Camille, always up for chatting about anything while listening to Radio FIP, Angela and her Canadian inputs, Andy and Luca (the big brothers we love) for their always good advices and reassuring presences. A very unique biotope! And without forgetting the lately arrived members, Floriane, always up for a hot chocolate (or anything food-related) and a diner with friends! And Charlotte for the hugs when needed during writing up!

Nottingham has been a huge piece. And this is its conclusion, that I dedicate it to my beloved parents, my friends and all my labmates, who all have brought their inputs in this work!

Thank you!

Acknowledgements – French version

Voilà un pan de vie de 4 ans qui s'achève, et ce le jour de mes 28 ans. Rythmé par des hauts et des bas, de nouveaux challenges intellectuels et émotionnels mais aussi et surtout beaucoup de support de la part du socle solide et patient, bien qu'éloigné, familial, et des nouveaux amis rencontrés ici. L'aboutissement de cette thèse n'aurait pas été possible sans tout cela.

Je tiens tout particulièrement à remercier mes directeurs de thèse, Gill Stephens et Steve Hall, qui m'ont guidée et encouragée constamment tout au long de ces années ! Merci de leur bienveillance ! Un grand merci également à mes directeurs industriels, Graham Eastham et David Johnson, pour leur suivi constant pendant ce projet.

Au-delà de l'aspect laborantin et professionnel, les longues journées, soirées et week-ends à faire mes suivis bactériens ont été tellement plus agréables grâce à la présence chaleureuse et diablement amicale de mes comparses de paillasse ! Alanna, toujours là pour remonter le moral, Camille pour discuter de tout et de rien en écoutant Radio FIP, Angela et ses influences canadiennes, Andy et Luca (les grands frères qu'on adore) pour leurs conseils et leurs rassurantes présences ! Tout un biotope unique ! Et la dernière arrivée, Floriane, toujours partante pour un chocolat chaud (ou toute forme de nourriture) et une soirée entre amis ! Sans oublier Charlotte et ses « hugs » pour consoler quelques moments difficiles !

Nottingham a été un sacré morceau. Ceci en est la conclusion, et elle est dédiée à mes chers parents, mes amis et mes collègues qui auront plus qu'apporté leurs pierres à l'édifice !!

Merci !

Table of contents

1. Introduction 1

2. Literature review 6

2.1 Manufacture and use of methyl methacrylate: 6

2.2 Biological production of MMA and MAA..... 11

2.3 Carbon efficiency for the production of bio-chemicals in *E. coli* 17

3. Aims and objectives 26

4. Design of a carbon efficient citramalate producing strain..... 28

4.1 Acetate as alternative carbon source..... 28

4.1.1 Description of the acetate assimilation route 28

4.1.2 Development of an acetate co-feeding strategy 31

4.1.3 Metabolic considerations for acetate feeding..... 33

4.2 Identification of an ATP-forming alternative carbon assimilation route 35

4.3 Ethanol as an alternative source of acetyl-CoA 36

4.3.1 Background..... 36

4.3.2 Identification and selection of enzyme candidates for an ethanol assimilation pathway 42

4.3.2.1 Database and literature search for alcohol dehydrogenases..... 42

4.3.2.2 Database and literature search for acetaldehyde dehydrogenases..... 51

4.3.2.3 Metabolic considerations for ethanol consuming route 55

4.4 Conclusions..... 56

5. Materials & methods 58

5.1 Reagents 58

5.2 Thermodynamic considerations 58

5.3 *E. coli* growth, maintenance and media 59

5.3.1 *E. coli* strains 59

5.3.2 Growth media 59

5.3.3 Cultivation conditions 61

5.4 DNA techniques and strain construction 63

5.4.1 Genes, plasmids and primers 63

5.4.2 Polymerase chain reaction 64

5.4.3 Restriction enzyme cloning 66

5.4.4 DNA purification 68

5.5 Protein overexpression: 70

5.6 Enzyme assays 71

5.6.1 Crude extract preparation 71

5.6.2 Alcohol dehydrogenase assay 72

5.6.2.1 Alcohol dehydrogenase from *Aspergillus nidulans* . 72

5.6.2.2 Alcohol dehydrogenase from *Corynebacterium glutamicum* 73

5.6.3 Acetaldehyde dehydrogenase assay 74

5.6.4 Citramalate synthase purification and assay 76

5.6.4.1 Citramalate synthase partial purification 76

5.6.4.2 Citramalate synthase assay 76

5.7 Production of citramalate in whole-cell systems 77

5.7.1 Production of citramalate from glucose and acetate in flask 77

5.7.2 Production of citramalate from glucose and ethanol in flask 77

5.8 Analytical techniques 78

5.8.1 Biomass 78

5.8.2 Glucose concentration 79

5.8.3 Agarose gel electrophoresis..... 79

5.8.4 Sodium dodecyl polyacrylamide gel electrophoresis.... 80

5.8.5 DNA concentration 81

5.8.6 Measuring protein concentration 81

5.8.7 HPLC..... 82

6. Thermodynamic considerations on the acetate and ethanol pathways 83

6.1 Introduction..... 83

6.2 Acetate and glucose co-consumption route for (*R*)-citramalate production 84

6.3 Ethanol and glucose co-consumption route for (*R*)-citramalate production 86

6.4 Conclusions..... 88

7. Construction of the production strain..... 89

7.1 Host strain and expression plasmid selection..... 89

7.2 Cloning of the acetate consuming route using the pBAD24 expression system 90

7.2.1 Construction of the AckA-Pta route into pBAD24 90

7.2.2 Optimisation of the expression of the *ackA-pta* genes from pBAD24 93

7.2.3 *In vivo* activity of the AckA-Pta assimilation route and citramalate production in flask experiments 96

7.3 Cloning of the ethanol consuming route using the pBAD24 expression system 100

7.3.1 Construction of the ADH I-ALDH A and ADH A-ALDH routes into pBAD24 100

7.3.2 Expression of the proteins ADH I-ALDH A and ADH A-ALDH 103

7.3.3 *In vitro* enzyme assays.....109

7.3.3.1 Alcohol dehydrogenases enzyme assays.....109

7.3.3.2 Acetaldehyde dehydrogenase enzyme assays 118

7.3.3.3 *In vitro* citramalate synthase assay 121

8. *In vivo* production of (*R*)-citramalate from two carbon sources 125

8.1 Production of (*R*)-citramalate from the co-consumption of glucose and acetate in *E. coli* BW25113 Δ*ldhA*.....125

8.1.1 Determination of optimal concentration of acetate for cell growth and (*R*)-citramalate conversion efficiency.....125

8.1.2 Conclusions from small-scale flask experiments.....131

8.1.3 Production of (*R*)-citramalate from glucose and acetate in fed-batch fermentation.....132

8.1.3.1 Introduction 132

8.1.3.2 Benchmark fed-batch fermentation of *E. coli* BW25113 Δ*ldhA* for the production of (*R*)-citramalate from glucose only 138

8.1.3.3 Fed-batch fermentation of *E. coli* BW25113 Δ*ldhA* for the production of (*R*)-citramalate from glucose and acetate142

8.1.3.4 Identification of a new strategy to improve carbon efficiency using a co-feed of glucose and acetate 147

8.1.3.5 Fed-batch fermentation *E. coli* BW25113 Δ*aceF* for the production of (*R*)-citramalate from glucose and acetate150

8.1.3.6 Conclusions 154

8.2 Production of (*R*)-citramalate from the co-consumption of glucose and ethanol in *E. coli* BW25113 Δ*aceF* 155

8.2.1 Demonstration of the co-consumption of glucose and ethanol and determination of the optimal concentration of ethanol for cell growth and *bio-production*.....155

8.2.2 Fed-batch fermentation of *E. coli* BW25113 Δ*aceF* for the production of (*R*)-citramalate from glucose and ethanol.....160

8.2.3 Conclusions.....168

9. Conclusions, discussion and future direction 172

10. References:.....182

11. Appendices 220

11.1 Wood-Ljungdahl pathway: 220

11.2 Nucleotide sequence of the *E. coli* native *ackA:* 221

11.3 Nucleotide sequence of the *E. coli* native *pta*.....222

11.4 Matrix analysis for ADHs selection –Satisfactory percentage table 223

11.5 Nucleotide sequence of the *alcA* gene encoding alcohol dehydrogenase from *A. nidulans:* 224

11.6 Nucleotide sequence of the *adhA* gene encoding alcohol dehydrogenase from *C. glutamicum:* 225

11.7 Paired comparison table for weighing each factor considered in the selection process against each others 226

11.8 Relative importance of the factors used for the selection of ALDHs 227

11.9 Matrix analysis for ALDHs selection - Satisfactory percentage table 228

11.10 Growth profiles of *E. coli* BW25113 Δ*ldhA* pBAD24-*ackA-pta-cimA3.7* and *E. coli* BW25113 Δ*ldhA* pBAD24 in flask experiment 229

11.11 Example of SDS-PAGE of insoluble ADH I-ALDH A-CimA3.7 230

11.12 DC assay calibration curve 231

11.13 2-Mercaptoethanol calibration curve 232

11.14 HPLC calibration curves 233

11.15 Growth profiles of *E. coli* BW25113 Δ*ldhA* pBAD24-*ackA-pta-cimA3.7* 234

11.16 Sample calculation of yield of carbon source conversion to citramalate 235

11.17 Fed-batch fermentation set-up 236

11.18 Comparison of efficiency parameters in fed-batch fermentation with different glucose and acetate co-feeds 237

11.19 Growth profiles of *E. coli* BW25113 Δ*aceF* pBAD24-*alcA-aldA-cimA3.7* 238

12. Addendum: DTP- PIP placement 239

List of figures

Figure 1: Diagram for (*R*)-citramalate biosynthesis from glucose 4

Figure 2: Summary of the metabolic pathways 5

Figure 3: Chemical route of the acetone cyanohydrin process (ACH) 7

Figure 4: Chemical route of the C_4 direct oxidation process developed by Mitsubishi Gas Chemical 8

Figure 5: Alpha process route 9

Figure 6: Potential pathways leading to biocatalytic routes producing methacrylic acid (MAA) from cellular metabolism intermediates 12

Figure 7: The main steps involved in the conversion of several organic acids to MAA in the hot pressurised water system using an aqueous base (NaOH) catalyst 14

Figure 8: Bio-production route of (*R*)-citramalate from pyruvate and acetyl-CoA catalysed by CimA3.7 16

Figure 9: Structure of the cyclic non-oxidative glycolysis (NOG). .. 20

Figure 10: Pathway design for the biosynthesis of isobutyl acetate (IBA) from glucose and acetate. 23

Figure 11: Structure of the acetate node 28

Figure 12: Main stress effects of acetic acid on *E. coli*. 32

Figure 13: Simplified view of the central metabolism of *E. coli* highlighting the potential competition for CoA-SH between the TCA cycle and an overexpressed acetate assimilation route. 34

Figure 14: General organisation of ethanol assimilation pathways in most ethanol-consuming microbes 38

Figure 15: Impact of ethanol on *E. coli* cells 40

Figure 16: pBAD24-*ackA-pta* (A) and pBAD24-*ackA-pta-cimA3.7* (B) expression vectors maps 92

Figure 17: SDS-PAGE of soluble and insoluble AckA-Pta expressed alone (A and C) and co-expresssed with CimA3.7 (B and D) at various growth conditions 95

Figure 18: Citramalate production from glucose and acetate in *E. coli* BW25113 Δ*ldhA* pBAD24-*ackA-pta-cimA3.7* and *E. coli* BW25113 Δ*ldhA* with an empty pBAD24 97

Figure 19: pBAD24-*alcA-aldA* (A) and pBAD24-*adhA-ALDH* (B) expression vectors maps 101

Figure 20: pBAD24-*alcA-aldA-cimA3.7* (A) and pBAD24-*adhA-ALDH-cimA3.7* (B) expression vectors maps 102

Figure 21: SDS-PAGE of soluble and insoluble ADH I – ALDH A expressed alone (A and C) and co-expressed with CimA3.7 (B and D) at various growth conditions 106

Figure 22: SDS-PAGE of soluble and insoluble ADH A - ALDH expressed alone (A) and co-expressed with CimA3.7 (B) at 30°C. 108

Figure 23: Alcohol dehydrogenase (ADH I) oxidation assay.....110

Figure 24: Alcohol dehydrogenase, ADH I, reduction assay.....112

Figure 25: Determination of the presence in the crude extract of native enzymes consuming NADH instead.....114

Figure 26: Oxidation assay on alcohol dehydrogenase ADH A.....117

Figure 27: Acetaldehyde dehydrogenase, ALDH A, activity assay.120

Figure 28: Reaction scheme for Ellman's reagent, DTNB, as colorimetric indicator for the formation of citramalic acid.....122

Figure 29: CimA3.7 activity assays 123
Figure 30: Glucose and acetate consumption and citramalate production in *E. coli* BW25113 ∆*ldhA* pBAD24-*ackA-pta-cimA3.7*.130
Figure 31: Benchmark aerobic fermentation of *E. coli* BW25113 ∆*ldhA* pBAD24-*cimA3.7* for the production of (*R*)-citramalate from glucose 141
Figure 32: Aerobic fermentation of *E. coli* BW25113 Δ*ldhA* pBAD24-*ackA-pta-cimA3.7* for the production of (*R*)-citramalate from glucose and acetate 145
Figure 33: Structure of the pyruvate dehydrogenase complex.....148
Figure 34: Aerobic fermentation of *E. coli* BW25113 Δ*aceF* pBAD24-*ackA-pta-cimA3.7* for the production of (*R*)-citramalate from glucose and acetate 153
Figure 35: Glucose and ethanol consumption, citramalate and organic acids production in *E. coli* BW25113 Δ*aceF* pBAD24-*alcA-aldA-cimA3.7* when supplementing culture medium containing 1% glucose with 0% ethanol (A), 1% ethanol (B), 3% ethanol (C) and 5% ethanol (D). 159
Figure 36: Aerobic fermentation of *E. coli* BW25113 Δ*aceF* pBAD24-*alcA-aldA-cimA3.7* for the production of (*R*)-citramalate from glucose and ethanol 163
Figure 37: Citramalate and organic acids production (g/L) in fed-batch fermentation of *E. coli* BW25113 Δ*aceF* pBAD24-*alcA-aldA-cimA3.7* 166
Figure 38: Schematic of future metabolic engineering to perform on *E. coli* BW25113 Δ*aceF*.....175

Figure 39: Overview of the Wood-Ljungdahl pathway for the production of acetyl CoA and pyruvate from the fixation of CO and CO_2 220
Figure 40: Growth profiles of *E. coli* BW25113 Δ*ldhA* pBAD24 and *E. coli* BW25113 Δ*ldhA* pBAD24-*ackA-pta-cimA3.7* in glucose and acetate co-feed in flask experiment 229
Figure 41: Example of SDS-PAGE showing insoluble ADH I –ALDH A –CimA3.7 when expressed on Lund medium supplemented with glycerol as sole carbon source at 37°C and 30°C. 230
Figure 42: Bovine Serum Albumin concentration calibration curve 231
Figure 43: 2-Mercaptaethanol concentration calibration curve 232
Figure 44: HPLC calibration curves 233
Figure 45: Growth profile of *E. coli* BW25113 Δ*ldhA* pBAD24-*ackA-pta-cimA3.7* in presence of various concentrations of acetate.....234
Figure 46: Description of the fed-batch fermentation devices and set-up 236
Figure 47: Growth profile of *E. coli* BW25113 Δ*aceF* pBAD24-*alcA-aldA-cimA3.7* in presence of various concentrations of ethanol 238

List of tables

Table 1: List of potential candidates for the selection alcohol dehydrogenase 45

Table 2: Paired comparison table for weighing each factors considered in the decision against each others 48

Table 3: Relative importance of the factors used for the selection of ADHs 49

Table 4: Details of the result for the selection of appropriate alcohol dehydrogenases enzymes 50

Table 5: List of potential candidates for the selection of an acetaldehyde dehydrogenase 53

Table 6: Details of the result for the selection of appropriate aldehyde dehydrogenases enzymes 54

Table 7: List of primers 64

Table 8: Typical thermocycler conditions used for either high fidelity or colony polymerase chain reactions 66

Table 9: Standard Gibbs Free energy calculated for each part of the glucose and acetate co-consumption pathway for citramalate production 86

Table 10: Standard Gibbs free energy calculated for each part of the glucose and ethanol co-consumption pathway for citramalate production 87

Table 11: Table of expression strains constructed 93

Table 12: Table of expression strains constructed 103

Table 13: Determination of the solubility of recombinant proteins of ADH I, ALDH A, ADH A, ALDH and citramalate synthase CimA3.7 in

SDS-PAGE of *E. coli* BW25113 Δ*ldhA* grown under various conditions 105

Table 14: Growth rates of *E. coli* BW25113 Δ*ldhA* pBAD24 *ackA-pta-cimA3.7* challenged with increased acetate concentrations.....126

Table 15: Citramalate titres (g/L) and carbon efficencies (g/g) under various concentrations of acetate supplemented to Lund medium 128

Table 16: Efficiency parametres of the production phases (phase 3) in the benchmark *E. coli BW25113 ΔldhA* pBAD24-*ackA-pta-cimA3.7* fed-batch fermentations 144

Table 17: Efficiency parameters of the production phases (phase 3) in the benchmark *E. coli* BW25113 Δ*ldhA* pBAD24-*cimA3.7* and *E. coli* BW25113 Δ*aceF* pBAD24-*ackA-pta-cimA3.7* fed-batch fermentations 152

Table 18: Growth rates, citramalate titres and yields of *E. coli* BW25113 Δ*aceF* pBAD24 *alcA-aldA-cimA3.7* challenged with increased ethanol concentrations.....156

Table 19: Efficiency parameters of the production phases (phase 3) in the benchmark *E. coli* BW25113 Δ*ldhA* pBAD24-*cimA3.7* and *E. coli* BW25113 Δ*aceF* pBAD24-*alcA-aldA-cimA3.7* fed-batch fermentations 161

Table 20: Comparison of efficiencies parameters obtained for all fermentations during the production phase 170

Table 21: Comparison of efficiencies parameters obtained for all fermentations during the total length of the fermentations 171

Table 22: Glucose and acetate consumed for the production of citramalate, and yields of carbon source conversion to citramalate when 0% and 2.5% of acetate was supplemented to the medium235
Table 23: Comparison of efficiency parameters obtained in the benchmark fed-batch fermentation and in various glucose/acetate co-feeding regimes 237

List of equations

Equation 1: Equation for the calculation of the percentage of satisfaction for each enzyme candidate 49

Equation 2: Calculation of the overall standard Gibbs free energy of the complete pathway..... 58

Equation 3: Equations for the oxidative and reductive activity of alcohol dehydrogenase (EC 1.1.1.1) 72

Equation 4: Catalytic reaction of acetaldehyde dehydrogenase (ALDH) 74

List of abbreviations

1,4-BDO	1,4-Butanediol
2-ME	2-Mercaptoethanol
ACH	Acetone cyanohydrin
acs	Acetyl-CoA synthase
aceF	Dihydrolipoamide acetyltransferase
ackA	Acetate kinase
alcA	Alcohol dehydrogenase (*Aspergillus nidulans)*
aldA	Acetaldehyde dehydrogenase (*Aspergillus nidulans)*
adhA	Alcohol dehydrogenase (*Corynebacterium glutamicum)*
aldh	Acetaldehyde dehydrogenase (*Acinetobacter HSB2)*
ADP	Adenosine-5'-diphophate
AMP	Adenosine-5'-monophophate
ATP	Adenosine-5'-triphophate
bp	Base pair
BSA	Bovine serum albumin
cimA3.7	Citramalate synthase
CoA	Coenzyme A
DCW	Dry cell weight
dH_2O	Deionised water
DNA	Deoxyribonucleic acid
DO	Dissolved oxygen
DNTB	5,5'-Dithio-*bis*-(2-nitrobenzoic acid)
g	Gram
g/g	Gram per gram
g/L	Gram per litre
g/L/h	Gram per itre per hour
H	Hydrogen
h	Hour
h^{-1}	Per hour
HPLC	High performance liquid chromatography
kDa	Kilodalton

LB	Lysogeny brot
ldhA	Lactate dehydrogenase
MAA	Methacrylic acid
MMA	Methylmethacrylic acid
mL	Millilitre
mM	Millimolar
MTBE	Methyl *tert* butyl ether
NAD^+	Nicotiamide adenine dinucleotide (oxidized form)
NADH	Nicotiamide adenine dinucleotide (reduced form)
OD	Optical density
PAGE	Polyacrylamide gel electrophoresis
PCR	Polymerase chain reaction
PDH	Pyruvate dehydrogenase complex
PEP	Phosphoenolpyruvate
PMMA	Poly(methylmethacrylate)
poxB	Pyruvate oxidase
pta	Phosphotransacetylase
pts	Phosphotransferase system
ptsG	Glucose specific phosphotransferase system
SDS	Sodium dodecyl sulphate
spp	*Species pluralis*
TCA	Tricarboxylic acid
UV	Ultraviolet
WLP	Wood-Ljungdahl pathway
WT	Wild type

1. Introduction

Methacrylic acid (MAA) is a bulk chemical used in the synthesis of poly(methylmethacrylate) (PMMA), an acrylic polymer manufactured by Lucite International. PMMA is used to produce materials such as Perspex® or Plexiglas®. Global consumption of acrylics is estimated to be 2.1 million tonnes [1] and the global market is projected to reach $7.4 billion by 2019. Considering such economic potential, it is highly desirable for Lucite International to maintain a leadership position. Most commodity chemicals and conventional fuels are manufactured using crude oil-based processes, and have been essential to worldwide social, economic and technological development. Indeed, the processes used to manufacture these products have been the backbone of industrial chemicals manufacture for many decades, suggesting it is unrealistic to stop producing them [2]. Current industrial manufacturing processes for MAA production involve high pressures and temperatures, and raw materials derived from crude oil. Furthermore, depending on the process, toxic substances such as corrosive acids and rare-earth metal catalysts may be required. However, the rising global concern of sustainability, carbon dioxide emissions, oil price fluctuations and the polluting impact of industrial waste means that there is an absolute need to produce drop-in commodity chemicals from sustainable and economically competitive processes. The growing demand for bio-based products [3] has led to the development of environmentally sustainable processes for the manufacture of such commodity chemicals, including MAA. The main

challenge facing this approach is the design of a competitive biological route compared to conventional petrochemical processes [4]–[6].

MAA is highly toxic to the cells [7], rendering its direct biological synthesis rather difficult. Fortunately, (*R*)-citramalic acid, a naturally occurring organic acid, was previously identified in the thesis of J. Webb (2015, [7]) as a promising precursor of MAA. It is a non-toxic compound that can be converted readily to MAA in a simple chemical process. This process is known as the hot pressurised water process, and was developed by Carlsson and co- workers [8]. Thus, a new biotechnology-based route for citramalate production was developed using citramalate synthase (CimA3.7), an enzyme which catalyses the condensation of pyruvate and acetyl-CoA (Fig. 1; [7]). This pathway was successfully cloned and expressed in *Escherichia coli* and produced promising titres of citramalate (130 g/L). However, the efficiency of the biocatalytic reaction is limited by the loss of at least a third of the total carbon as carbon dioxide, due to the production of acetyl-CoA *via* the decarboxylation of pyruvate.

Such carbon loss is uneconomical in a bio-process designed for the production of a bulk chemical precursor, where profit margins are very narrow (about $1800-$2000/tonne of MAA; www.icis.com). Indeed, the decarboxylation of pyruvate is one of the major limitations for the development of cost-effective manufacture of bioproducts at large scale [9]. To address this, one approach was to engineer *E. coli* strains to co-consume carbohydrate and/or non-carbohydrate sources from low-cost feedstocks, such as lignocellulosic wastes [10]–[12]. This strategy aims to render the

waste of CO_2 affordable in the bio-process; however, it does not address the reduction of CO_2 emissions and the associated environmental impact. By contrast, building a complete *in vitro* synthetic enzymatic pathway system can appear as a promising solution regarding both conversion efficiency of feedstocks and engineering flexibility [13], [14]. Unfortunately, cell-free biosynthesis techniques remain challenging and costly to develop due to the requirement of all the elements to mimic cellular activity and maintain protein stability over time. Therefore, such methodology is not yet suitable for the manufacture of low-margins commodity chemicals, and the use of living cells such as *E. coli* as optimised biocatalyst for carbon efficiency remains the most appropriate system to investigate considering the purpose of this work. Only a few studies have aimed to improve the inherent carbon efficiency of biosynthetic routes [9], [15]. Bogorad and co-workers (2013) approached this problem by reprogramming glucose metabolism in *E. coli* to a cyclic non-oxidative glycolysis (NOG) pathway, which involved intensive metabolic engineering. However, the advantageous result of stoichiometric conversion of glucose or xylose to acetyl-CoA was offset by a strain, which grew poorly. By contrast, Tashiro and co-workers (2015) were able to reduce carbon emissions in the bio-production of isobutyl acetate (IBA) by co-feeding glucose and acetate, with no requirement of complex metabolic engineering. Therefore, the overall aim of this body of work was to build on this approach with the aim of optimising the carbon efficiency of the biosynthetic pathway for citramalate production, previously developed in the work performed by J. Webb

(2015, [7]), by using alternative carbon sources in co-feeding strategies (Fig. 1).

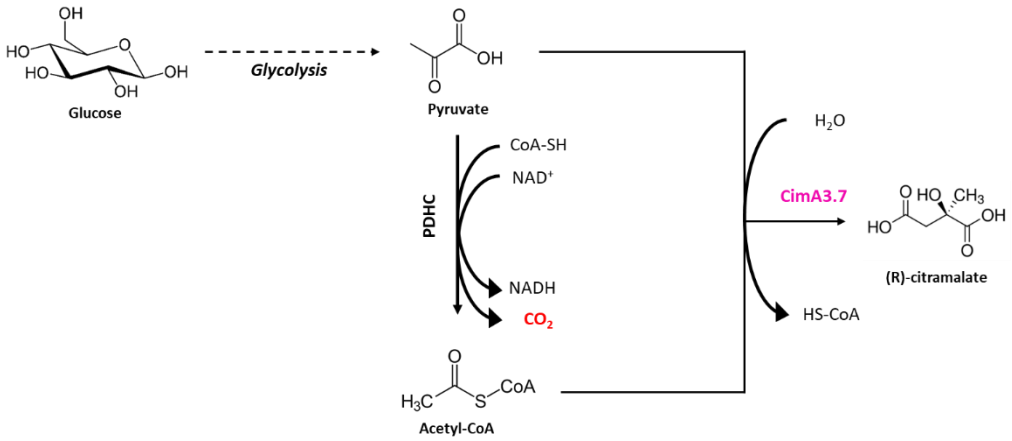


Figure 1: Diagram for (*R*)-citramalate biosynthesis from glucose

PDHC: Pyruvate dehydrogenase complex; CimA3.7: citramalate synthase; HS-CoA: Coenzyme A; NAD: Nicotinamide adenine dinucleotide, oxydised form; NADH: Nicotinamide adenine dinucleotide, reduced form. Black font indicates native enzymes and pathways, while pink font expresses exogenous enzymes.

Since carbon neutral ethanol and acetate can be produced using homoacetogenic gas fermentations [16], we engineered *E. coli* to use ethanol or acetate as co-substrates to produce acetyl-CoA, with pyruvate production from glucose (Fig. 2), to improve carbon efficiency.

Synthetic routes for the co-assimilation of ethanol or acetate with glucose were constructed in *E. coli*, and citramalate bio-production from the co-consumption of glucose/acetate or glucose/ethanol was demonstrated in both flask and fed-batch fermentations. To our knowledge, this was the first demonstration of co-utilisation of acetate or ethanol with glucose for the bio-production of citramalate.

Furthermore, this was also the first report of the utilisation of ethanol as carbon source for the biosynthesis of a platform chemical.

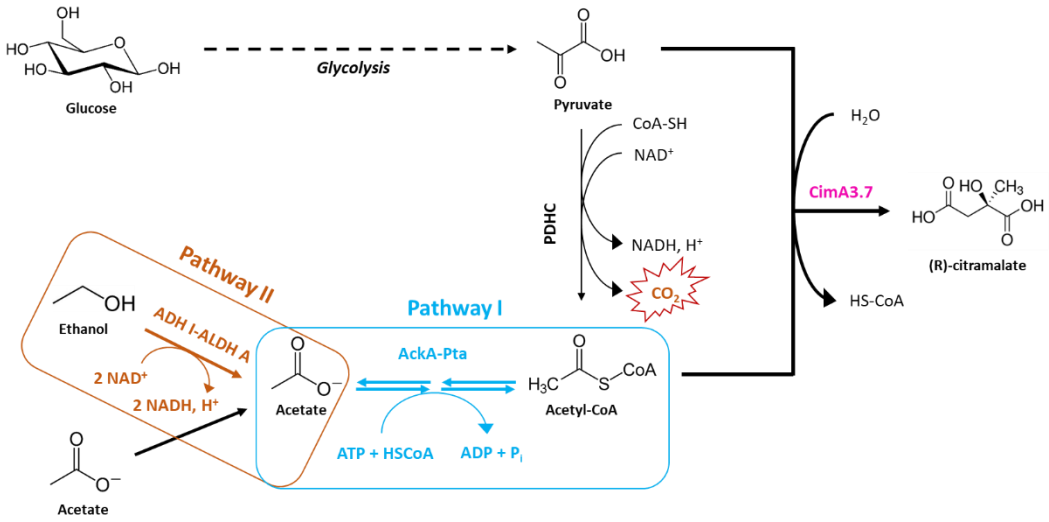


Figure 2: Summary of the metabolic pathways

A summary of the two metabolic pathways investigated in this project. Each colour corresponds to one particular type of pathway: Pathway I corresponds to the over-expression of the native acetate assimilation route of *E. coli* composed of the acetate kinase (AckA) and phophotransacetylase (Pta), while Pathway II describes the sequential exogenous alcohol dehydrogenase (ADH I) and acetaldehyde dehydrogenase (ALDH) associated to enable ethanol consumption by the strain. These two routes were tested individually.
CimA3.7: citramalate synthase; PDHC: Pyruvate dehydrogenase complex; HS-CoA: coenzyme A; NAD^+ : Nicotinamide adenine dinucleotide, oxydised form; NADH, H^+: Nicotinamide adenine dinucleotide, reduced form, P_i: inorganic phosphate.

These bio-processes provided proof of principle for the potential of the simultaneous use of multiple carbon sources for the bio-production of commodity chemicals with reduced carbon losses.

2. Literature review

2.1 Manufacture and use of methyl methacrylate:

Methyl methacrylic acid (MMA) is one of the major building blocks used in the production of thermoplastics, such as polymethyl methacrylate (PMMA), and other materials. One of the main uses of PMMA is as an alternative to glass as it is two times lighter but eight fold less brittle than conventional glass [17], and is sold under the brand name Lucite®, Perspex® and Plexiglas®. These materials can be coloured, moulded, cut and formed, and are used in a wide range of applications, including outdoor signage, optical fibre, windscreens and lenses. PMMA is also biocompatible and is used as bone cement and in dental prostheses. MMA is also widely used for the manufacture of surface coatings, paints, resins and adhesives [18]. Overall, the global market for PMMA is worth more than £3 billion.

Several methods for the production of MMA at large scale have been developed over the last thirty years. MMA can be obtained directly, or from the further esterification of methacrylic acid (MAA). Therefore, MAA is equally important as a key intermediate in the acrylic industry. Although its main application is for the production of MMA, crude MAA is also used in its own right for the manufacture of a wide range of resins, automobile coatings and cement modifiers, all of which have different physical and textural properties than the MMA-based polymers.

In industrial processes, three main families of manufacturing route can be described: C2, C3 and C4. These classifications are based upon the number of carbon atoms of the chemicals used as starting materials. The ACH route (C3 route, Fig. 3) was the first commercial route developed for the direct production of MMA, and remains, to this day. This route is the most widely used manufacturing process in North America and Europe [18] and accounts for around 80% of the global production of MMA.

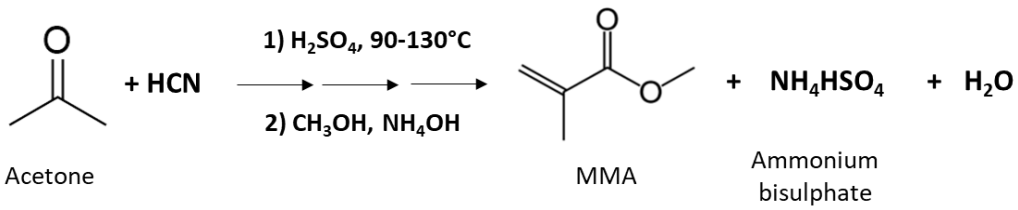


Figure 3: Chemical route of the acetone cyanohydrin process (ACH)

The process starts with a reaction mixture of acetone and hydrogen cyanide (HCN) which in presence of excess sulphuric acid (H_2SO_4), yields methacrylamide sulphate. Aqueous methanol is then applied for the esterification of methacrylamide sulphate, resulting in direct production of a mixture of MMA and ammonium bisulphate [19]. The main advantage of this route is the feedstock efficiency, which is about 85-90%. However, the availability and price stability of HCN, as well as the recovery cost of H_2SO_4 greatly affect the final price of the process, and have enhanced the need for the development of cleaner processes [20], [21].

The second largest MMA manufacturing technology is the C4 route with the C_4 direct oxidation process, developed by Mitsubishi Gas Chemical (Fig. 4). This route is mainly used in Asia. The process consists of two-step catalytic oxidation of isobutene or *tert*-butanol to methacrolein and then MAA. MAA is then esterified to MMA using methanol. The main limitations impairing the competitiveness of this route are the low overall efficiency (65-75%), the need of performant catalysts, especially in the second oxidative step, and the requirement of large amounts of water, resulting in intensive downstream treatments to recover MMA and recycle the water.

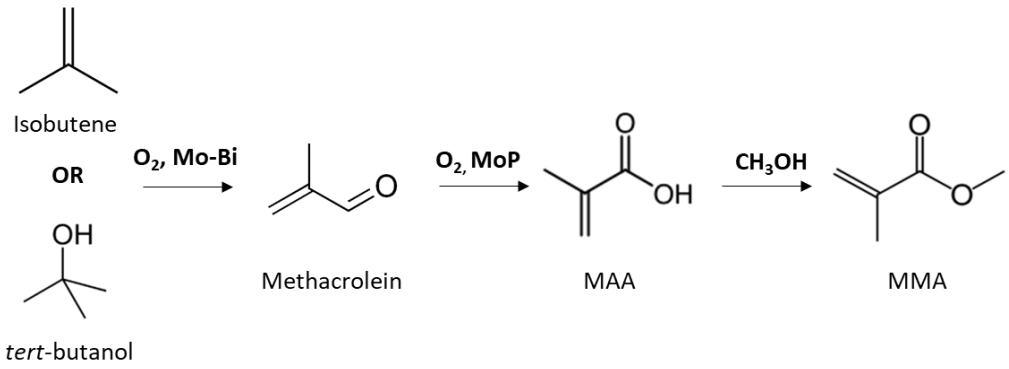


Figure 4: Chemical route of the C_4 direct oxidation process developed by Mitsubishi Gas Chemical

Lucite International has developed a C_2 route for the direct production of MMA, which helps to solve some critical points encountered in both the ACH and C_4 methods. The patented Alpha Technology (Fig. 5) uses readily available raw materials, which yield less hazardous components and reduced amounts of by-products [22]. The initial

mixture of ethylene, carbon monoxide and methanol produces methyl propionate with no or very little by-products. The methyl-propionate is then reacted with formaldehyde and converted into MMA and water.

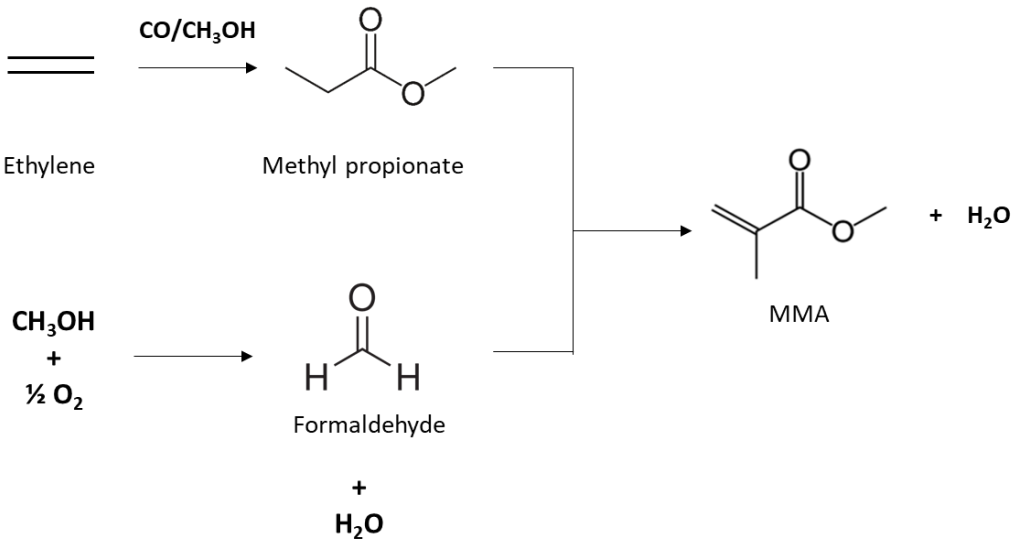


Figure 5: Alpha process route

The Alpha Technology yields direct production of MMA, and also allows better feedstock efficiency (about 93%) than the ACH and C4 processes, and an overall lower reliance on petroleum derivatives. However, the prices of the feedstock materials remain linked to the cost of crude oil and can affect significantly the cost-effectiveness of this route.

Therefore, alternative manufacturing routes for platform chemicals are required. The fossil oil sources currently exploited are subject to shortage, rising oil prices and constant volatility, therefore new sources of raw materials are needed. As a quick and easy answer to

the global energy challenge, many governments and oil industries are in favour of beginning the extraction of oil and shale gas from the few remaining untapped sources. However, such options are highly controversial due to the political instability brought by the questions of the ownership and exploitation of the new fossil sources, as well as the environmental impact and the expense of the extraction methods involved. Moreover, continued use of fossil energy sources tremendously hinders the global international commitment to cutting GreenHouse Gas (GHG) emissions and prioritising sustainable development. Therefore, there is a need to replace oil with other sources, which are most preferably carbon neutral or low carbon emitting, with no political or ethical threats [23]. However, it is challenging to find appropriate energy sources that would satisfy the current global growing demand at a competitive scale. Given all the economic, political and environmental burdens brought by the current use of fossil resources, the development of bio-based routes provide promising options from a sustainability perspective [24]. Sugars are renewable feedstocks produced from the fixation of CO_2 *via* photosynthesis, therefore bio-processes based on the fermentation of sugars is a first step towards a more neutral carbon and less energy intensive society [25]. There are various challenges underpinning whole-cell bio-processes, such as the complexity of developing a stable and continuous system, however there are also many benefits [26]. These include the economic benefits from the stable price of biomass feedstock, the milder reaction conditions in use in bio-processes, and the environmental friendliness of such route, are all in

favour of investigating bio-routes for MMA or MAA production. Moreover, such approaches pave the way to leading novel opportunities in a new market by Lucite International.

2.2 Biological production of MMA and MAA

Currently, there are no competitive biological routes for the direct biosynthesis of MAA or MMA. However, various strategies can be adopted to develop bio-based manufacturing processes [27], [28]. One of them is to engineer metabolic pathways for the biosynthesis of the chemical feedstocks required in the Lucite Alpha process. Thus, it would require the conversion of biomass into the starting materials. Both carbon monoxide and methanol can be provided from Syngas produced from biomass [29]. Similarly, ethylene can be obtained by dehydration of bioethanol, and formaldehyde can be produced from conversion of methanol synthesized from Syngas. Unfortunately, further economic modelling performed by Lucite (Graham Eastham, personal communication), has concluded that the numerous processing and purifications steps needed for the production of the different raw materials, render this bio-based route economically ineffective [30].

Therefore, a direct bio-based route for the production of MMA or precursors is desired, which would limit the number of bio-process steps for the manufacture of MMA. International patents filed by Genomatica describe enzymes able to catalyse the conversion of naturally occurring metabolites to MAA and its esters (Fig. 6;[31]–

[33]). Further thermodynamic analysis of the catalytic reactions involved and the availability of the associated substrates identified methacrylyl-CoA, mesaconic, itaconic and citraconic acids as the more favourable substrates for MAA conversion. This remains theoretical as none of these catalytic routes were demonstrated. However a recent patent from Lucite International demonstrated direct MAA production from the hydrolysis of methacrylyl-CoA [34] in whole-cell fermentation of *E. coli*.

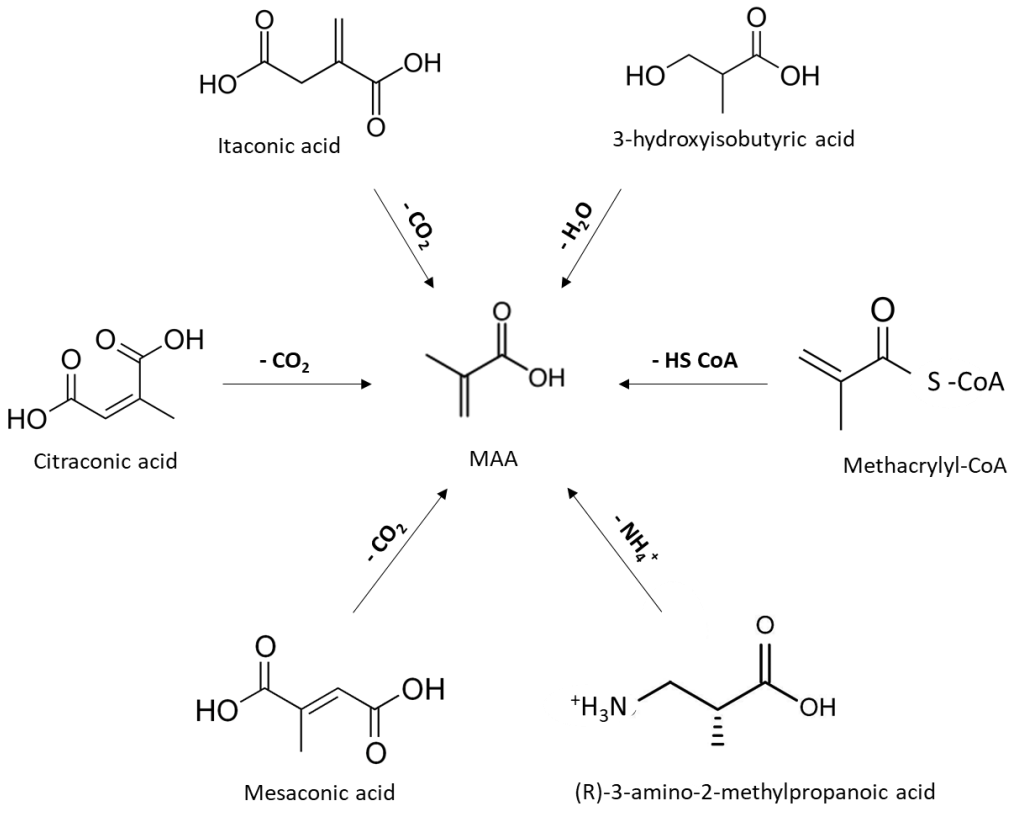


Figure 6: Potential pathways leading to biocatalytic routes producing methacrylic acid (MAA) from cellular metabolism intermediates.

Adapted from Burk et al. (2012).

However, the problem was the toxicity of MAA, which resulted in low product titres. MAA is highly toxic to cells [35]–[38], with a reported EC_{50} of 13.2±1.7mM in minimal medium in *E. coli* [7]. There are various strategies available to overcome toxicity issues [39]–[46], but, these involve additional and complex metabolic engineering of the host cell, and have not yet led to significant improved product titres.

Therefore, an alternative route has been developed in which a metabolic intermediate is first produced and subsequently converted to MAA using a chemo-catalytic process. A chemical process for the conversion of several organic acids to MAA (Fig. 7) was developed by Carlsson et *al.* (1994), and further optimised by Lucite International. Carlsson and co-workers [8] demonstrated the rapid and high yield conversion of citric acid, *cis*-aconitate, measaconic acid, citramalic acid to itaconic acid, which is then converted into MAA by applying increased temperature and pressure to the system. The process was optimised to be functional under lower temperatures and yielded up to an overall 90% conversion efficiency for the generation of MAA. Further purification of the MAA is conducted by lowering the pH to less than 5, so that the carboxy group of the acid becomes protonated (the pKa of MAA is 4.65), and the acid precipitates [47].

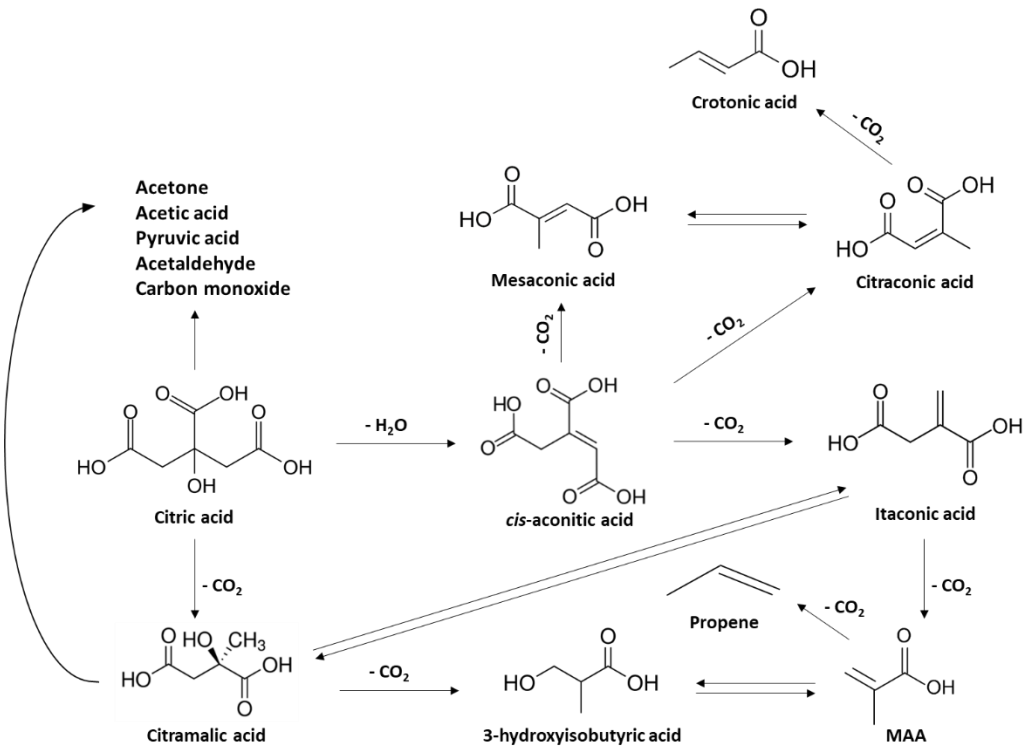


Figure 7: The main steps involved in the conversion of several organic acids to MAA in the hot pressurised water system using an aqueous base (NaOH) catalyst

Taken from Carlsson et *al.* 1994.

Citric and itaconic acids are already produced at industrial scale by the fungal fermentation of *Aspergillus sp* [48]–[51]. However these are costly manufacturing processes, due to the intensive aeration costs and limited possibility of yields improvement [52], [53]; consequently this renders these acids inappropriate for the production of a low profit-margin compound such as MAA.

Furthermore, enantiomers of (*S*)- and (*R*)-citramalate were described and both can be converted into MAA *via* the patented hot pressurised water process. Metabolic pathways for the bio-production of both

enantiomers of citramalate have been constructed in *E. coli* and validated *in vitro* [7]. However, the available metabolic pathways for (*S*)-citramalate bio-production have major drawbacks. (*S*)-citramalate is a product of the bio-degradation pathway of itaconic acid, and can be produced from toluenised cells of *Alcaligenes xylosoxydans* [54], [55]. Here, both the uses of itaconic acid as feedstock, and toluene as a facilitator for carbon source uptake were concluded as too expensive and counter-productive, as itaconic acid can directly be converted into MAA. (*S*)-citramalate is also a product of the glutamate degradation pathway (EcoCyc), and can be produced by the catalytic conversion of mesaconate, or *via* the citramalate lyase. Similarly to itaconic acid, mesaconic acid is not a suitable raw material for industrial production, as buying it would be too expensive [55], its metabolic conversion would require a glutamate overproducing strain, and most of all mesaconate can be directly converted into MAA using the hot pressurised water process [8]. Lastly, citramalate lyase was not proven to be effective enough for the production of (*S*)-citramalate, as it favoured its degradation to pyruvate and acetate [56].

By contrast, in a previous thesis [7], an (*R*)-citramalate producing *E. coli* strain was successfully constructed, which produced up to 130g/L of (*R*)-citramalate from glucose in fed-batch fermentations. The main net advantage of this strain construction was that it involved only a single enzymatic step with no cofactors requirement (Fig. 8), and no reported reversibility of the enzymatic reaction. The reaction is catalysed by the stereospecific (*R*)-citramalate synthase, CimA3.7,

which is a mutated enzyme that was developed through a direct evolution program by Atsumi & Liao [57]. It resulted in improvements to the catalytic activity and stability of the enzyme under mesophilic temperature, as well as removing feedback inhibition by isoleucine.

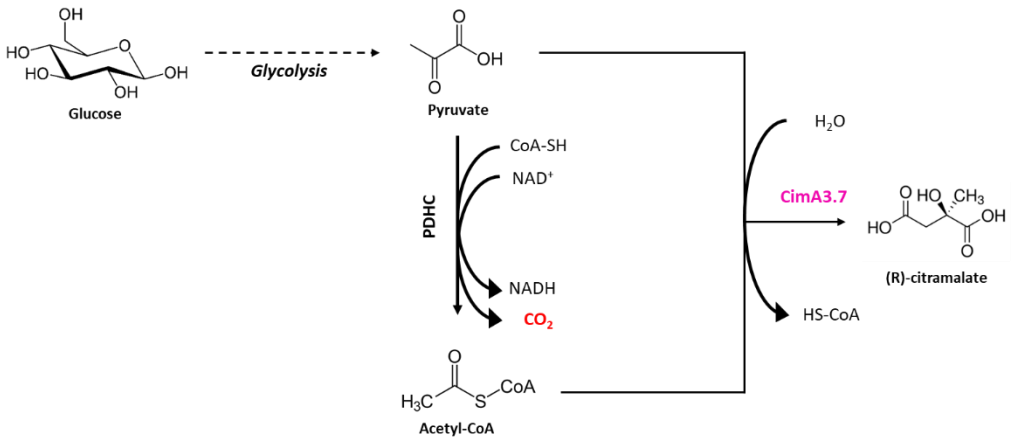


Figure 8: Bio-production route of (*R*)-citramalate from pyruvate and acetyl-CoA catalysed by CimA3.7

PDHC: Pyruvate dehydrogenase complex. CimA3.7: Citramalate synthase.

(*R*)-citramalate is produced from the condensation of pyruvate and acetyl-CoA (Fig. 8), which are common central metabolic intermediates produced from the glycolysis. However, acetyl-CoA is formed from the decarboxylation of pyruvate catalysed by the pyruvate dehydrogenase complex (PDHC). This results in CO_2 emission, and consequently in the loss of a third of the total carbon atoms initially supplied by glucose. Such carbon loss reduces the overall carbon efficiency of the bio-route, and affects the final cost-

effectiveness of the process. However, given the non-toxic profile of citramalate, its easy conversion into MAA with the hot pressurised water process and the already in-place fermentation system for its bio-production, it was then concluded in this project that there is great interest in further optimising the carbon atom efficiency of the citramalate producing strain of *E. coli*.

2.3 Carbon efficiency for the production of bio-chemicals in *E. coli*

The main challenge associated with the application of biotechnological routes for low profit margin, high-volume commodity chemicals at industrial scale, is the optimisation of the product yields and productivity [58], [59]. This is due to the large impact of raw material expenses, fermentation duration and maintenance on the final cost-effectiveness of the bio-process [30], [60]–[64]. Fermentation of sugars mixtures from hydrolysed ligno-cellulosic biomass was thoroughly investigated for the production of a wide range of bio-chemicals, such as bioethanol [65], [66], platform chemicals [67], polymers [68], and other pharmaceutical and food industry target compounds [69], [70], with the end goal of developing high yield and cost-effective bio-processes [10]. Furthermore, non-carbohydrates carbon sources, such as glycerol and acetate, have also been investigated as co-feedstocks with glucose for the bio-production of *D*-glucaric acid [60] and aromatic compounds [71], [72] in *E. coli,* respectively. Unfortunately, using all of the carbon atoms present in a medium does not indicate carbon efficiency of a bio-route, as the

decomposition and degradation of plant biomass through fermentation still generates carbon emissions. Thus, at industrial scale, the carbon emissions occurring in biotechnological processes remain an economical weight, this is exacerbated by the demanding environmental legislations, taxes on carbon emissions and waste management fees applied by governments [73].

In this instance, limiting CO_2 emissions during bio-processes becomes the key challenge to address. The most mature zero carbon emission fermentation systems which have reached the market use gas fermenting acetogenic microorganisms (*Clostridium autoethanogenum*) which are capable of fixing CO_2 and CO to produce bio-chemicals through the Wood-Lungdahl pathway (WLP) [16], [74]. LanzaTech is one of the leading companies in gas fermentation, with commercialised processes for the bio-production of bioethanol and 2,3-butanediol. Considering the apparent advantage of carbon neutrality of gas fermentation, the use of gas-fermenting strain such as *C. autoethanogenum* as single host appears as a promising option. In this extend, the WLP would be used in place of glycolysis, allowing the fixation of CO and CO_2 by the carbon monoxide dehydrogenase (CODH) to supply acetylCoA (Appendix 11.1). Then, the reversible pyruvate:ferredoxin oxidoreductase (PFOR) enables the generation of pyruvate from the carboxylation of acetylCoA [75]. Both substrates for the biosynthesis of citramalate would then be readily available and generated from carbon fixation. However, development and optimisation of gas fermentation bio-processes are highly limited yet due to the lack of genetic techniques and tools available for

acetogenic microorganisms. Therefore, building heterologous pathways is challenging. Moreover, gas fermentations are technically delicate. Oxygen has a strong inhibitory impact, therefore hermetic fermenters are required for gas-fermentation, which represents a heavy capital investment at first, and limits the overall cost-effectiveness of biochemical production. If the main advantage for industrial use of gas-fermenting bacteria is their anaerobic profiles, unfortunately, this is also the major disadvantage of this system. Anaerobic growth is known to be significantly slower on gaseous substrate, resulting in lower cell density and productivity. Additionally, the gasification of the feedstock can be incomplete and resulting in contaminant components that can impair growth and productivity of the targeted biochemical [76], [77]. Furthermore, the synthesis of energy molecules (ATP) is slow and low, which automatically greatly limits any bioprocess and even more when complex routes are involved. To date only a few examples have shown some success with small amounts being produced at laboratory-scale fermentation (acetone, isopropanol, 1-butanol and 3-hydroxybutyrate) [16]. And, only over-production of native chemicals could hit the market yet (ethanol, acetate and 2,3-butanediol). In the light of the limitations for using gas-fermenting bacteria, pursuing metabolic engineering of *E. coli* strains appeared as the best option in this project. It provided several advantages such as the ease of genetic manipulation, the well-known metabolism, the fast growing pace on glucose *via* glycolysis, and most of all it allowed good repeatability of the experiments conducted. Several efforts were performed for the

transfer of CO_2-fixing pathways into *E. coli*, but with limited success due to inefficient metabolic energy supply of the engineered pathway [78].

Other strategies for developing carbon neutral bio-processes in *E. coli* are thus needed. To address the carbon loss issue, Bogorad and co-workers (2013) created a cyclic non-oxidative glycolysis (NOG; Fig. 9) by rewriting the central metabolism of *E. coli* [9].

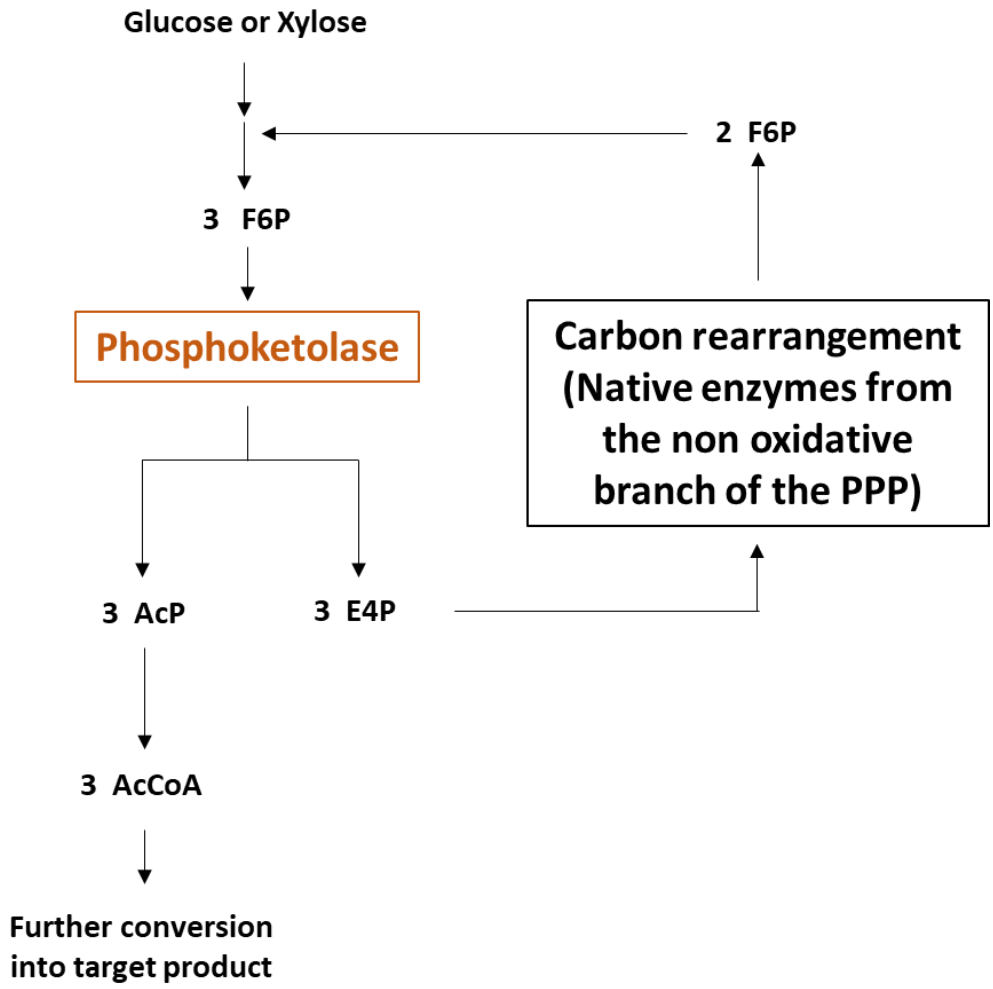


Figure 9: Structure of the cyclic non-oxidative glycolysis (NOG).

PPP: Pentose phosphate pathway. F6P: Fructose 6-Phosphate; AcP: Acetyl Phosphate; E4P: Erythro 4-Phosphate; AcCoA: Acetyl CoA. Orange colour describes the insertion of exogenous enzymes, phosphoketolase with F6P and xylulose-5-phosphate activities (F/Xpk).

Adapted from Bogorad et *al* 2013.

The aim was to enable complete carbon conversion of any C6-C5 sugars into the stoichiometric equivalent of acetyl-CoA without carbon emission. In the NOG, fructose 6-phosphate (F6P) becomes the starting molecule of the pathway. The driving force for the system relies on the insertion of the phosphoketolase, which catalysed the irreversible conversion of three F6P into three acetyl-phosphate and three erythrose 4-phosphate (E4P). The E4P can regenerate F6P for the NOG to go on, while the acetyl-phosphate provides key intermediate of acetyl-CoA, which can be further converted for potential target bio-chemical production. To prevent native fermentation pathways from competing with NOG for the use of F6P, deletions of *ldhA, adhE, frdBC* and *pflB* are required to remove the lower part of the glycolysis and side consumption routes. Additionally, to design the NOG for the efficient use of xylose and other pentose sugars, it was necessary to delete the PTS system and to use a phosphoketolase with both F6P and xylulose 5-phosphate activity (F/Xpk), as well as fructo 1,6-biphosphatase (Fbp). Although the restructuring of glycolysis allowed the successful stoichiometric conversion of carbon atoms from glucose or xylose into acetyl-CoA, it was performed at the price of the ease to grow and manipulate *E. coli* due to the intensive metabolic engineering performed. Moreover, the use of NOG for strain growth involves the external supply of reducing agents such as hydrogen or formic acid. Although, the cyclic NOG claimed complete carbon stoichiometry once settled, starting the pathway required the initial investment of two F6P. Furthermore, to our knowledge, the few applications reported of the NOG for bio-

chemical production yielded limited success [79], essentially due to the requirement of nutrient supplementation for cell growth. Thus, the use of such complex systems renders the NOG not yet applicable in an industrial process.

Instead of improving the carbon efficiency of glucose only, Tashiro and co-workers developed a co-feeding strategy of glucose and acetate for the bio-production of isobutyl acetate (IBA; Fig. 10; [15]). Using acetate as a feedstock has several advantages. Acetate is a cheap, available, non-food competitive substrate, with a low price volatility. Currently, it is already less costly than glucose: $340/metric ton and $400-600/metric ton on average, respectively [80]. Moreover, being a common product of anaerobic fermentation, it can be recovered from sludge from treated waste water [81]. Similarly, acetic acid bacteria (AAB) are well known in food processing, and have been in use for vinegar production for centuries, carrying the oxidation of ethanol into acetic acid [82], [83]. Furthermore, acetate is also an important by-product of the hydrolysis of ligno-cellulosic biomass, where typical enzymatic pre-treatments can generate hydrolysate mixtures containing acetate concentrations of about 13.2 to 16 g/L [84]. Acetate can be produced from CO_2 using acetogenic microbes such as *Clostridium* or *Acetobacter* sp [16], [77], which provide the net advantage of generating a greenhouse gas consuming biosynthetic route to acetate.

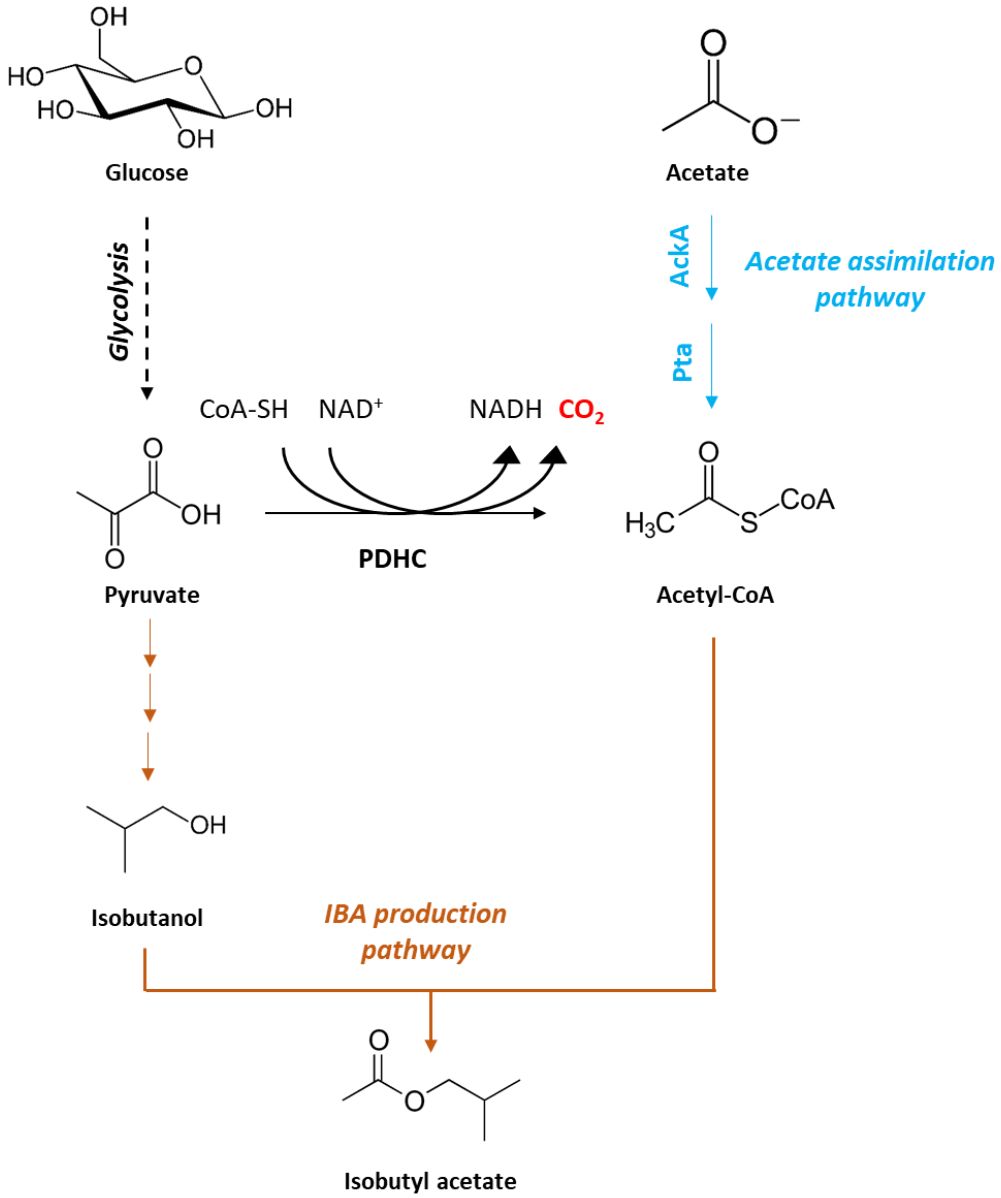


Figure 10: Pathway design for the biosynthesis of isobutyl acetate (IBA) from glucose and acetate.

PDHC: Pyruvate dehydrogenase complex; CoA-SH: coenzyme A; NAD^+: Nicotiamide dinucleotide (oxidised); NADH: Nicotiamide dinucleotide (reduced). The overexpression of the native acetate assimilation pathway was highlighted in blue and is composed of acetate kinase (AckA) and phosphotransacetylase (Pta). The heterologous pathway for the biosynthesis of IBA was highlighted in orange.

Adaptated from Tashiro et *al*. 2015.

In the study performed by Tashiro and co-workers, IBA is produced from the conversion of acetyl-CoA with isobutanol (Fig. 10). Unfortunately, both acetyl-CoA and isobutanol are formed from pyruvate, resulting in overall limited carbon efficiency. For this reason, an acetate assimilation pathway was introduced for the supply of acetyl-CoA, while pyruvate is produced from glucose, and can be completely used for the formation of isobutanol.

The metabolic engineering performed was simple and efficient, as it involved only the insertion of the IBA synthesis route from pyruvate and an assimilation pathway for acetate (Fig. 10). From the different native acetate assimilation pathways tested, which included the overexpression of either the acetate kinase-phosphotransacetylase (AckA-Pta) pathway, the acetyl-CoA synthetase (ACS) pathway, or the two acetaldehyde dehydrogenases (AldB-MhpF) pathway, Tashiro and co-workers concluded that only the overexpression of the native AckA-Pta pathway enabled growth on high acetate concentration (10 g/L). Therefore, AckA-Pta appeared to be the most appropriate route for the production of acetyl-CoA, which was further used for the bio-production of IBA. To enhance the carbon yield of the bio-route, the genes encoding pyruvate consuming enzymes were deleted, this included *adhE*, *ldhA*, *pflB* and *fnr*.

In parallel, another strain with the deletion of the pyruvate dehydrogenase complex (PDHC), which catalyses the decarboxylation of pyruvate was produced (Δ*aceEF*), and its effect on the final carbon efficiency for IBA production was investigated. At the end of the study, it was concluded that higher titres and carbon yields were obtained

from the co-feeding of glucose and acetate to a strain overexpressing AckA-Pta but with the wild type PDHC. The main issue with the Δ*aceEF* strain was the low consumption rate of both carbon sources. Furthermore, since the growth of the AckA-Pta engineered *E. coli* was not impaired, the strain remained perfectly appropriate for industrial applications. Thus, Tashiro and co-workers developed a co-feeding strategy with promising outcomes for improving the carbon efficiency of bio-routes.

3. Aims and objectives

The main aim of this PhD project was to improve the carbon efficiency of a previously developed microbiological process for the production of (*R*)-citramalate [7]. Citramalate is formed from the condensation of one pyruvate and one acetyl-CoA catalysed by CimA3.7. Improving the carbon yield in this reaction means maximising the availability of both pyruvate and acetyl-CoA, while maintaining low biomass production. However, the loss of CO_2 *via* the decarboxylation of pyruvate to acetyl-CoA is the major economic drawback of this bio-route. However, another strategy, in which pyruvate is provided from glucose and acetyl-CoA is supplied *via* an alternative carbon source was proposed and studied.

The first objective was to design and construct a microorganism capable of the simultaneous utilisation of two carbon sources for the carbon efficient production of citramalic acid. Tashiro and co-workers (2015) demonstrated that co-feeding of acetate gave successful results for the carbon efficient production of isobutyl acetate in *E. coli* (see Section 2.3). Therefore, it was decided to apply this strategy to a citramalate producing *E. coli* strain as a first task.

However, a major drawback of Tashiro study was the consumption of ATP for the activation of acetate, which may affect growth. Thus, the second task was to identify alternative carbon source candidates for the supply of acetyl-CoA. This involved a literature search to select suitable compounds that could be easily converted to acetyl-CoA while generating a net positive production of ATP. Decision on alternative

carbon candidates were made based on minimising the complexity of the pathway, and their cost-effectiveness as feedstocks.

The following task was the design of the alternative carbon source assimilation pathways in *E. coli*. This involved selecting appropriate genes and performing thermodynamic and stoichiometric calculations to provide primary conclusions on the feasibility of the bio-routes selected to be further explored. The next task was the construction of the pathways in *E. coli* and the demonstration of enzyme expression and activity *in vitro*.

The second main objective of the project was to demonstrate the co-utilisation of glucose and alternative carbon sources for the carbon efficient production of citramalic acid in whole cell fermentation systems. The first step was to demonstrate co-consumption of carbon sources and the production of citramalate in small scale whole cell biotransformations and flask assays. Following this, fed-batch fermentation protocols were developed to assess the carbon conversion ratio. Finally, further metabolic and co-feeding studies were performed to optimise carbon efficiency and product yield.

4. Design of a carbon efficient citramalate producing strain

4.1 Acetate as alternative carbon source

4.1.1 Description of the acetate assimilation route

Acetate is an important compound in *E. coli* metabolism and can be either used as a carbon and energy source for growth, or be excreted when cells are grown on excess glucose for ATP regeneration. The metabolic mechanisms involved in acetate assimilation and excretion routes are well-documented, and are referred as 'acetate node', 'acetate switch' or 'acetate futile cycle' (Fig. 11; [85]–[91]).

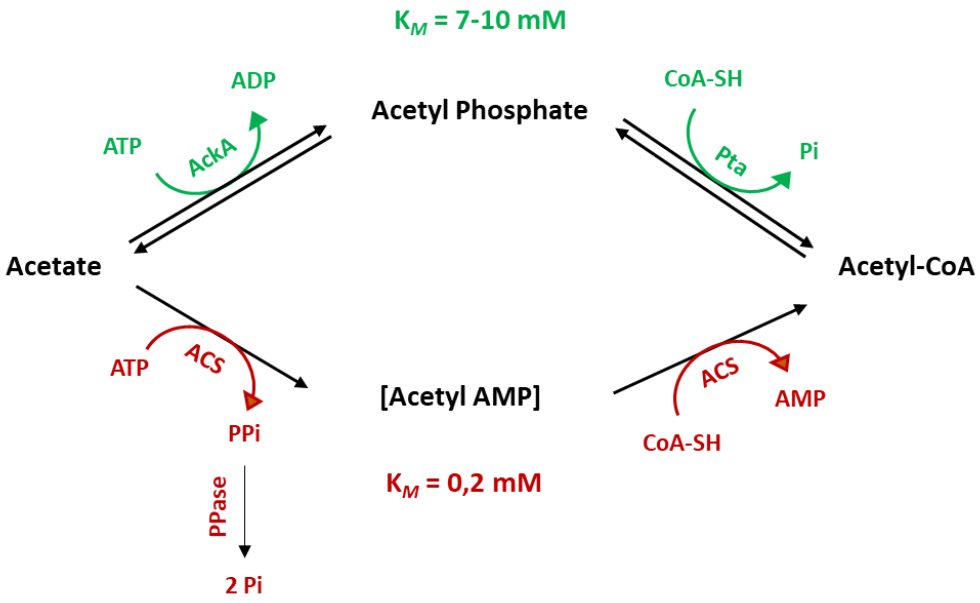


Figure 11: Structure of the acetate node

AckA-Pta:acetate kinase-phosphotransacetylase (green); AMP-ACS: AMP forming acetyl-CoA synthase (red); PPase: Pyrophosphatase; P_i: inorganic phosphate; CoASH: Acetyl Coenzyme A; ATP: Adenoside triphosphate; ADP: Adenoside diphosphate; AMP: Adenoside monophosphaste.

Interestingly, recent studies which focused on the use of acetate as a carbon source succeeded in enabling acetate assimilation by overexpressing the native genes of the acetate node from *E. coli*. This had the double benefit of ensuring proper expression and activity, as well as removing the transcriptional regulation pressure of the catabolic repression system. Acetate was shown to be suitable as a sole carbon source for the bio-production of various types of bio-compounds such as native fatty acids [92], succinate [80], [93], and a recombinant single chain derivative of the sweet plant protein monellin (MNEI; [94]). Acetate was also investigated as a promising carbon source for enhancing the accumulation of acetyl-CoA [95]. Acetyl-CoA is a central cellular building block, that can be used in biosynthetic pathways for the bio-production of valuable products [96] for food, drugs and fuels applications, such as fatty acids, higher chain acyl-CoA (butyryl-CoA), isoamyl acetate, amino acids, terpenoid and arteminisin [96]–[100].

As described previously (see section 2.3; Fig. 10), Tashiro and co-workers produced an acetate and glucose co-consuming strain for the bio-production of IBA, with an overall improved carbon efficiency. Acetate consumption was enabled by the overexpression of the native AckA-Pta route (Fig. 11) from *E. coli*. Although this route is reversible and is usually referred as the "acetate excreting route", when acetate concentrations exceed 2.5 mM (0.15g/L) the AckA-Pta becomes the main consuming pathway.

Since pyruvate and acetyl-CoA are the substrates required for the bio-production of citramalate, we decided to apply the same acetate co-

feeding strategy as Tashiro and co-workers. The *ackA-pta* operon was extracted from the genomic DNA of the wild-type *E. coli* MG1655 and cloned into our citramalate producing strain. The AckA protein is made of one subunit of 43 kDa, while Pta is a hexamer with a subunit weight of 77 to 80 kDa. Both are cytosolic proteins. The sequences of both *ackA* and *pta* genes are available on NCBI under the NCBI gene IDs 946775 and 946778, respectively (Appendix 11.2 and 11.3).

Traditionally, acetate is produced from plant-based fermentation through glycolysis consequently resulting in the generation of CO_2. Thus, using acetate as a feedstock could seem at first counter-productive with our aim to optimise the carbon efficiency of the biosynthesis of citramalate. Fortunately, acetate can be readily produced in a carbon neutral manner from gas fermentation using anaerobic acetogenic microbes such as *Clostridium* or *Acetabacter* spp [16], [77]. By fixing CO_2 and CO through the Wood-Ljundahl pathway (WLP), gas-utilising microorganisms are able to produce a wide range of cellular metabolites of commercial interest like acetate, lactate, ethanol, 2,3-butanodiol. The WLP, also named the reductive acetyl-CoA pathway, is the only non-photosynthetic route for linear CO_2 fixation, providing therefore an appropriate supply of acetate for the purpose of this work. As previously mentioned (Section 2.3), LanzaTech is the leading company for the production of carbon neutral acetate, and therefore could be considered as a potential future supplier, then avoiding Lucite Int the need of any capital investment for gas-fermentation facilities.

4.1.2 Development of an acetate co-feeding strategy

Although acetate is a well-reported possible carbon source for *E. coli*, it is also a toxic compound above a certain threshold (Fig. 12). Accumulation of acetate is a known inhibitor for biomass synthesis, recombinant protein production, and final product yield, and thus represents a limitation in the efficient utilisation of carbon sources [94].

In order to develop a fermentation system based on acetate feeding, we needed to understand the toxicity mechanism to identify ways to prevent it. Wild type *E. coli* can generally tolerate up to a maximum of 5 g/L of acetate (~up to 84 mM; [101]). Acetic acid is a weak acid (pKa of 4.75) and is more troublesome in its undissociated form (CH_3COOH), as it can permeate the membrane by passive diffusion [85]. In the cell, the acetic acid dissociates and liberates a proton, which uncouples the membrane pH gradient, required for ATP formation [102], and transport processes. After deprotonation, the anionic form of acetate (CH_3COO^-) is trapped within the cytoplasm and cannot diffuse through the membrane anymore [39], and this inhibits methionine biosynthesis, resulting in an accumulation of the toxic metabolite of homocysteine [103].

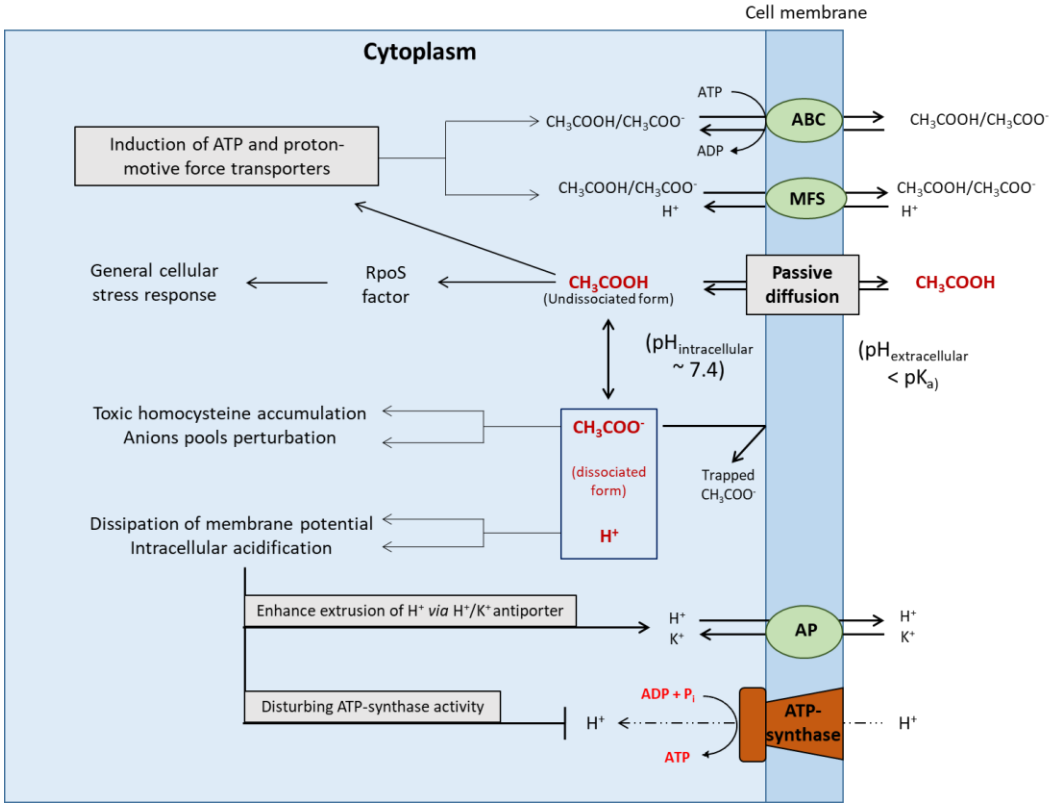


Figure 12: Main stress effects of acetic acid on *E. coli*.

Grey boxes represent major toxic effects and cellular stress responses.
ABC: ATP transporter; MFS: major facilitator family including proton motive force transporters. AP: H^+/K^+ antiporters.

Adapted from Trcek et al. (2015)

Toxicity of acetate is also modulated by the environmental growth conditions. In traditional fermentation systems, the external pH decreases due to the excretion of organic acids by the strain, resulting in moving the chemical equilibrium of acetate toward its undissociated, and therefore more troublesome form. However, by monitoring and maintaining the growth medium pH to create slightly more alkaline conditions (pH 7.5 instead of 6.5), Wang et *al*. (2014) demonstrated that the intracellular acetate concentration (and therefore its toxicity impact) can be reduced by 50% [104].

Therefore, it was concluded that the toxicity of acetate can be controlled by enhancing the assimilation ability of acetate in an engineered *E. coli* strain [105], in addition to carrying out a limited acetate feed to minimise the concentration of acetate in the fermentation medium, as well as maintaining a culture pH of 7 during the bio-process.

4.1.3 Metabolic considerations for acetate feeding

Although the use of acetate as a carbon source was proven to be a promising route for the supply of acetyl-CoA, there are questions about the carbon atom efficiency and putative energetic metabolic burdens to be considered. The generation of acetyl-CoA from acetate at efficient rates requires the availability of sufficient amounts of coenzyme A (CoA-SH) and ATP. Under aerobic growth of *E. coli*, there is direct competition for CoA-SH from both the phosphotransacetylase (Pta) and the α-ketoglutarate dehydrogenase complex (encoded by *sucAB* and *lpd*), which catalyses the production of succinate-CoA and feeds the TCA cycle (Fig. 13; [86]). Such competition is likely to impair growth due to the generation of a bottleneck in the TCA cycle, as well as a reduced acetate assimilation rate as the optimal catalytic activity of Pta would be hindered by the lack of available CoA-SH. A way to minimize the competition for CoA-SH is to activate the additional acetate assimilation pathway at a later stage in growth, when the TCA cycle is not as necessary as in early growth phase.

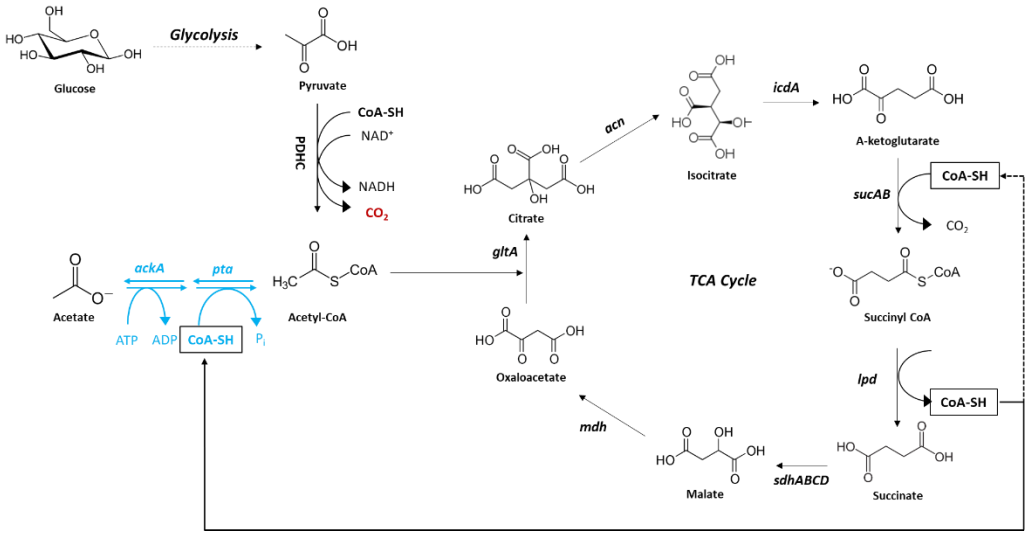


Figure 13: Simplified view of the central metabolism of *E. coli* highlighting the potential competition for CoA-SH between the TCA cycle and an overexpressed acetate assimilation route.

PDHC: Pyruvate dehydrogenase complex; CoA-SH: Coenzyme A; NAD: Nicotinamide adenine dinucleotide, oxydised form; NADH: Nicotinamide adenine dinucleotide, reduced form; *ackA*: acetate kinase; *pta*: phosphatransacetylase; *gltA*: citrate synthase; *acn*: aconitase; *icdA*: isocitrate dehydrogenase; *sucAB*: α-ketoglutarate dehydrogenase; *lpd:* succinyl-CoA synthase; *sdhABCD:* succinate dehydrogenase; *mdh*: malate dehydrogenase. Light blue colour indicates the overexpression of the native AckA-Pta node from *E. coli*.

Adapted from Shiloach and Rinas, 2009.

Moreover, the assimilation of acetate is an energy-demanding route, and involves the net consumption of one molecule of ATP for each acetate consumed (Fig. 11). From glycolysis, 2 ATP and 2 NADH are generated. The NADH produces 6 ATP equivalent *via* the membrane respiratory chain of *E. coli* under aerobic conditions. Thus, to limit the impact of ATP consumption by the acetate assimilation route and to maintain function of the citramalate biosynthetic route, the glucose-acetate co-feeding fermentation system needs to be carried out aerobically.

4.2 Identification of an ATP-forming alternative carbon assimilation route

To address the issue of the ATP-consumption involved in an acetate assimilation route, another carbon source for the supply of acetyl-CoA was also researched. From both promiscuity and energetic perspectives, the two other immediate carbon sources to be considered were fatty acids and ethanol.

Fatty acids of various lengths can be used as carbon sources by *E. coli* [106], [107]. They are degraded *via* the *β*-oxidation cycle, resulting in the formation of one acetyl-CoA for each two-carbon segment of a fatty acid and reduced cofactors of one $FADH_2$ and one NADH, which can generate 5 ATP together. However, the native *β*-oxidation cycle is tightly regulated in wild-type *E. coli*, suggesting that the pathway would need to be completely re-engineered into *E. coli* to alleviate inhibition from the *fadR* repressor. Thus, engineering the fatty acid degradation route would require the insertion of at least 5 enzymes for the degradation of long chain fatty acids, including *fadL* (fatty acid transport), *fadD* (acyl-CoA synthase), *fadE* (acyl-CoA dehydrogenase), *fadB* (Fatty acid oxidation complex subunit α), and *fadA* (3-ketoacyl-CoA thiolase), as well as at least two other enzymes for the degradation of medium and short chain fatty acids (*atoD* and *atoA*) [108]. Moreover, not only is the metabolic engineering required intensive, but growth of *E. coli* on fatty acids was also demonstrated to be significantly slower than on sugars. Therefore, co-using glucose and fatty acids as carbon substrates may result in an uncoupled assimilation rate of each carbon source, which would drastically

impair both growth and citramalate bio-production. Thus, fatty acids were not further considered as candidate alternative carbon source.

In contrast, ethanol appeared to be more promising. In *E. coli*, ethanol is produced *via* the reversible successive reduction of acetyl-CoA to acetaldehyde, and then to ethanol [107], [109]–[113]. This two-step reduction is catalysed by the same multifunctional alcohol dehydrogenase enzyme, AdhE, and consumes NADH. Unfortunately, *adh*E is repressed at the transcriptional level and the enzyme itself is highly oxygen sensitive due to metal catalytic oxidation of its two iron-containing active sites. Although, the native AdhE cannot be used for the consumption of ethanol in this instance, associating a recombinant alcohol dehydrogenase with an acetaldehyde dehydrogenase appeared as a promising solution. Indeed, reverse oxidation of ethanol to acetyl-CoA would generate two NADH per ethanol oxidised, resulting in the net production of 6 ATP through the respiratory chain of *E. coli*. Given the energetic advantage provided by the NADH-forming ethanol consuming route, ethanol was concluded as the additional candidate carbon source to investigate and compare to acetate for the construction of a carbon efficient strategy for the bio-production of citramalate.

4.3 Ethanol as an alternative source of acetyl-CoA

4.3.1 Background

Considering that the aim of this project is to use an additional carbon source to maximize the carbon efficiency of the citramalate route, the

use of carbon neutral ethanol is of interest. Although cheap bioethanol produced from first, second and third generation biomass fermentations is widely available [114]–[118], the carbon emission occurring during these bio-processes render traditional plant derived bioethanol an unsuitable carbon feedstock for the purpose of this project. Fortunately, recent advances in gas fermentation have enabled the production of bioethanol from CO_2-fermenting microorganisms that fix CO_2 and CO, resulting in carbon neutral production of ethanol at a commercial scale [16]. Moreover, Ineos Bio, Coskata, and LanzaTech [74] have successfully developed pre-commercial plants in the U. S. (Ineos Bio, Vero Beach, Florida; Madison, Pennsylvania) and in various locations in China, and continue to increase the production capacities of their facilities [76]. Carbon-neutral ethanol generated from CO_2 fixation becomes thus just as advantageous as the carbon neutral acetate, described previously (see Section 2.3).

Interestingly, from a biotechnological approach, ethanol has only been considered as an end-product as a biofuel so far from first through third biofuel generation, to syngas production processes [114]–[118]. In the early 1970s, a few patents were filed on the utilisation of ethanol as a substrate in the bio-production of amino acids such as *L*-lysine and glutamic acid in ethanol-consuming yeasts [119], [120]. Indeed, yeasts possess a wider enzymatic toolkit for ethanol metabolism, and most of the tolerance enhancement strategies applied to other microbes involved enzymes taken from the ethanol metabolisms of yeasts [121]. However, bioethanol was too

expensive at this time to further develop ethanol as a feeding substrate in a cost-effective bio-process. Despite the reversal of the bioethanol price trends and availability, to date, little work was further pursued to develop the potential of ethanol as carbon source in bio-processes in utilising *E. coli* or yeasts. Therefore, the use of ethanol as a feedstock for bacterial bio-processes is novel.

The mechanism involved in the degradation of ethanol (Fig. 14) is highly conserved between microbial taxonomic groups, and is built upon the successive oxidative reactions catalysed by an alcohol dehydrogenase (ADH), followed by an acetaldehyde dehydrogenase (ALDH).

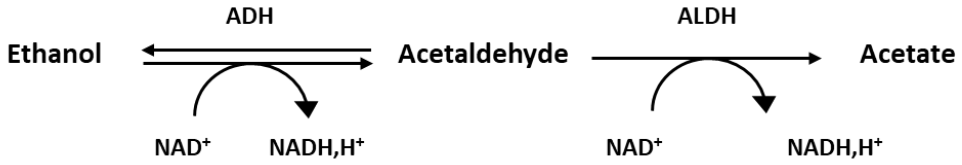


Figure 14: General organisation of ethanol assimilation pathways in most ethanol-consuming microbes

Adapted from Flipphi et *al* 2001

ADH catalyses the reversible oxidation of ethanol to its aldehyde equivalent, acetaldehyde. It is a polymeric oxidoreductase requiring NAD(P) as a cofactor [122]–[124]. Most studies tend to show lower K_M values for acetaldehyde compared to ethanol, but the k_{cat} usually favours the oxidation reaction. Once formed, acetaldehyde is further oxidized to acetate *via* the irreversible reaction catalysed by

acetaldehyde dehydrogenase. Similarly to ADHs, ALDHs are NAD(P)-dependent polymeric enzymes. The irreversibility of the reaction they catalyse, associated with their high affinity for acetaldehyde (low K_M values) generate the driving force which enable the complete oxidation of ethanol into acetate [125], and at the same time prevents the accumulation of toxic aldehyde metabolites. Thus, the well-coordinated activity of ADHs and ALDHs play a crucial role not only for the metabolism of alcohols, but also as a protection mechanisms towards the toxicity of alcohols and aldehydes.

Ethanol is a known biocide chemical to many microorganisms [126], and like most toxic compounds, increased extracellular and intracellular concentrations inhibit cell growth, metabolism and activity of bio-routes (Fig. 15). *E. coli* can carry out exponential growth, in the presence of up to 30 g/L of ethanol, however growth rate is depressed. No growth has been reported for ethanol concentrations above 50 g/L [127]. The toxicity of ethanol is essentially due to its negative impact on the cellular membrane. Ethanol can passively permeate the membrane resulting in weakening hydrophobic interactions between phospholipids and membrane proteins, which lead to cell leakage and lysis [121], [128]–[131].

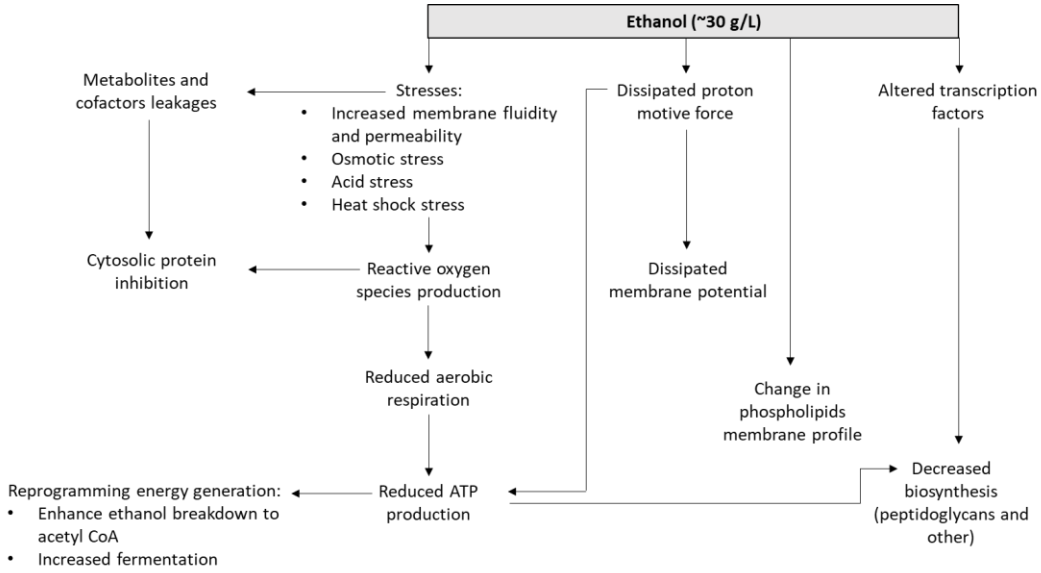


Figure 15: Impact of ethanol on *E. coli* cells

Adaptated from Cao et *al*. 2007.

Although ethanol is rather toxic to *E. coli*, a strain bearing a mutated version of the native alcohol dehydrogenase, AdhE, (encoded by the mutated gene *adhC*) was reported to breakdown ethanol, and to use it as a carbon and energy source [132]. It was claimed that only two changes in the amino acid sequence of the native AdhE (*i. e.* Ala 267 → Thr and Glu568→Lys) were enough to enable its aerobic expression and activity, as well as increasing its stability [133]. Moreover, the ADHs from *E. coli* are acetylating enzymes, and therefore directly generate acetyl-CoA.

Many other organisms have been reported to use short-chain alcohols like ethanol as carbon and energy source. Gram negative bacteria such as the acetic acid bacteria (AAB), *Acetobacter, Gluconobacter* and *Zymomonas* have long been referred to as the "brewers burdens"

as they can spoil beer and cider casks [134], [135]. *Corynebacterium glutamicum* has been shown to grow on short chain alcohols such as ethanol or methanol as sole carbon sources [136]. More uncommon microbes including wild-type yeasts such as *Candida* sp, [137] as well as *Lactobacilli*, [123], and other extremophiles such as *Thermoanaerobacter ethanolicus*, *Natronomonas pharaonis* and *Bacillus stearothermophilus* [138]–[140] have been reported for their higher tolerance towards higher alcohols as well as ethanol and their ability to use them as feedstock. Alcohols also occur as intermediates of metabolic pathways. For example, *n*-alkane-degrading bacteria, such as *Geobacillus thermodenitrificans* NG80-2 [141]–[143] or *Acinetobacter* sp [144], [145], are often reported for their ability to perform successive oxidative steps from *n*-alkane to the corresponding primary alcohol and to fatty acids, which can then enter *β*-oxidation and the TCA cycle. Filamentous fungi, particularly *Aspergillus nidulans*, have also been widely reported and studied for their ability to grow on ethanol [125], [146], [147]. Furthermore, in most of microbes mentioned above, ethanol utilisation is possible only in the presence of an active acetate assimilation route [148]. Indeed, mutants of acetic acid bacteria lacking functional acetate assimilation routes were not able anymore to metabolise ethanol [149], [150].

Therefore, it was concluded that associating an alcohol dehydrogenase with an acetaldehyde dehydrogenase was the most suitable strategy to use in this project in order to enable an engineered *E. coli* strain to use ethanol as a carbon source. Given the goal set in this PhD to enable an *E. coli* strain to consume ethanol as

a carbon and energy source, the identification and selection of suitable enzymes catalysing the oxidation of ethanol to acetate was required and is described in the following sections.

4.3.2 Identification and selection of enzyme candidates for an ethanol assimilation pathway

To our knowledge, no precedent was reported for building an ethanol consuming route in *E. coli*, therefore we carried out a paired database and literature search to identify appropriate ADHs and ALDHs that would work together in a host organism [151]–[154]. It was previously demonstrated that ethanol-consuming microorganisms (*n*-alkane degrading bacteria, acetic acid bacteria, yeasts and fungi) preferably performed the oxidation of ethanol to acetaldehyde, then to acetate, before using the acetate node to produce acetyl-CoA. Based on this it was decided to investigate ADHs for the oxidation of ethanol to acetaldehyde, and ALDHs for the oxidation of acetaldehyde to acetate.

4.3.2.1 Database and literature search for alcohol dehydrogenases

ADHs are catalysts of great interest for the production of drugs, pharmaceuticals, and food ingredients [155], and therefore have been well-documented. Amongst ADHs, NAD(P)-dependent ADHs (class 1) are the more widely applied and documented enzymes in bio-processes either as purified biocatalysts or in whole-cell system,

due to the requirement of common cofactors. By contrast, classes 2 and 3 involved rare co-factors, required to be coupled to membranous proteins or are membranous enzymes themselves, and are therefore too difficult and costly biocatalysts to use. Interestingly, over the last decade, most of the documented NAD(P)-dependent ADHs are used for the synthesis of asymmetric chiral alcohols [156], platform alcoholic compounds (1,3-butanediol; [157]), and bioethanol [65], [76], [114], [158], [159]. Consequently, database report abundant ADHs favourably reducing aldehydes to alcohols.

To identify potential ADH candidates, which could efficiently carry the oxidation of ethanol, the online databases BRENDA [160], UniProt [161] and KEGG [162] were searched. Based on the enzyme commission number (EC number; [163]), ADHs were searched amongst the enzymes classified as:

>Oxido-reductase (EC 1)

>> acting on the CH-OH group of the donor (EC 1.1)

>>> with $NAD(P)^+$ as cofactor (EC 1.1.1).

It was then decided to focus on NAD-dependent enzymes (EC 1.1.1.1) for two main reasons. First, using an NAD cofactor was necessary in order to satisfy the ATP-forming requirement that we set in this project when designing an ethanol assimilation route (See in section 4.2). Second, based on kinetic studies it was noticed very early that the use of NADP showed a tendency of lower oxidation activity compared to the use of NAD. The search launched for EC 1.1.1.1 enzymes generated 8850 results, including enzymes from all living

organisms. However, and as mentioned earlier, most of the ADHs reported were described for their ability to highly reduce aldehydes and produce secondary and branched alcoholic chemicals. Therefore, from the list of the substrates and reactions reported for the 8850 enzymes, we investigated only the 48 entries that were categorised for the reversible reduction of acetaldehyde to ethanol. We then decided to use enzymes only from microbial origin, based on the assumption that it would better facilitate the cloning steps as well as increasing the chance that the enzymes would be active in the host strain, *i. e. E. coli*. This narrowed the list down to 29 entries. Furthermore, another of our requirements was the availability of kinetic data on ethanol as a substrate. Thus, regarding the lack of kinetic data on ethanol amongst the 29, it was decided to produce a manual selection of 7 ADHs candidates from the remaining candidates. This was based on a literature survey specifically reporting ethanol oxidation activity on each. At the end of this selection process, we produced the following preliminary candidates list (Table 1).

Table 1: List of potential candidates for the selection alcohol dehydrogenase

Name	Organism	Organism type	References
ADH C	*E. coli* DC272	Mesophilic, aerobic bacteria	[110], [111], [132], [133], [164], [165]
ADH II	*Acetobacter pasteurianus* SKU1108		[82], [83], [124], [166]–[168]
ADH	*Acinetobacter* sp HBS-2		[144], [145], [169], [170]
ADH A	*Corynebacterium glutamicum*		[149], [150], [171]–[173]
ADH 2	*Geobacillus thermodenitrificans*	Thermophilic bacteria	[141], [143], [174], [175]
ADH	*Geobacillus stearothermophilus*		[140], [176], [177]
ADH I	*Aspergillus nidulans*	Filamentous fungus	[125], [146], [147], [178]–[181]

Additionally, another enzyme, alcohol oxidase (AOX; EC 1.1.3.13), was briefly considered. Indeed, AOXs catalyse the irreversible oxidation of alcohol to their corresponding aldehyde, which was first assumed to be an interesting reaction to further drive the assimilation of ethanol into the metabolism of the host strain. Yeasts and filamentous fungi were reported as being able to degrade and/or grow on *n*-alkane, lignin and alcohol substrates [124], [137], [182]–[184] using oxidases. A vast variety of AOXs have been reported and studied mainly from methylotrophic yeasts and some moulds. However, AOXs have never been reported in prokaryotes. AOXs catalyse alcohol oxidation using O_2 as an electron acceptor, resulting in the stoichiometric formation of H_2O_2, a well-known cell damaging

agent, particularly due to its oxidative effect on DNA [185]. In yeast and fungi, AOXs are located in peroxisomes, where laccases are also found. These latter enzymes can therefore further degrade H_2O_2, thus negating the toxic effect. Despite the absence of a cellular compartment, *E. coli* contains several oxidases that yield H_2O_2 [186]. Scavenging enzymes, in particular NADH peroxidase and catalase, are also largely available to quickly balance the toxic end-product of oxidases. However, due to the extremely rapid damaging reactivity of H_2O_2 on both DNA and metabolic enzymes, an increase of its intracellular concentration, due to a recombinant pathway overexpression would be challenging to the host strain. Therefore, using an AOX would involve the insertion of an additional gene, encoding a laccase. Moreover, the irreversibility of the alcohol oxidation was assumed to be a risk in terms of toxic accumulation of aldehyde in addition to the increased generation of H_2O_2, causing too many metabolic burdens at once. For these combined reasons, AOXs were not further investigated.

To further narrow down the list of ADHs, we performed a decision matrix-analysis based on a set of selection criteria. They are as follows:

- Low K_M values for ethanol
- Higher K_M values for acetaldehyde
- High reported catalytic activity of the enzyme for the substrate
- Mesophilic activity
- Availability of the nucleotide sequence
- Previously reported successful heterologous expression in *E. coli*

The matrix method used integrates multiple factors that need to be considered. First, all the options (*i. e*. ADH candidates) and factors needed to be determined and listed as rows and columns in a table. Secondly, each of the options was scored according to the degree of satisfaction reached against each of the factors considered. The following rating score was set such as 0 was poor and 5 suited all the expectations. The scores for the different factors from the same enzyme candidate did not have to be different. However, in the final decision-making process, each factor was not given the same relative importance therefore they needed to be weighted.

The Paired Comparison Analysis Tool (MindTool Website[MindTool]) was used to set the importance of each factor by analysing the relative importance of each factor against each other (Table 2). All the factors to be compared were listed and marked as row and column headings in a new table. Then, each factor in the rows was compared with each

factor in columns. Within each cell, the main factor was noted, and a score on how much more important it was compared to the other factor was allocated. Scores were usually ranked between 0, when considered as not crucial, to 3 when estimated as essential.

Table 2: Paired comparison table for weighing each factors considered in the decision against each other

Factors		A	B	C	D	E	F
		K_M (EtOH)	K_M (Ald)	K_{cat} (EtOH ox.)	Mesophilic activity	DNA seq. available	Heterol Expr. *E. coli*
A	K_M(EtOH)		A, 1	C, 2	D, 2	E, 3	A, 2
B	K_M(Ald)			C, 2	D, 1	E, 3	B, 2
C	K_{cat} (EtOH ox.)				D, 2	E, 3	C, 2
D	Mesophilic activity					E, 1	D, 2
E	DNA sequence available						F,1
F	Heterol. Expr. in *E. coli*						

Then, by adding the scores for each factor and dividing it by the total sum of all the scores noted, a percentage value was obtained, which yielded the relative weight of the factor (Table 3) in the analysis matrix.

Table 3: Relative importance of the factors used for the selection of ADHs

Factors	Score	Relative weight	Rank
K_M (ethanol)	3	10%	4
K_M (acetaldehyde)	2	7%	5
K_{cat} (ethanol oxidation)	6	21%	3
Mesophilic activity	7	24%	2
DNA sequence available	10	35%	1
Heterologous expression in *E. coli*	1	3%	6
Total	29	100%	-

Once each factor was weighted, and each option rated against all factors, the final score of each option could be determined by multiplying the rating score of each factor by its relative weight and summing up all the factor scores for each enzyme option. The final result was given as a percentage of overall satisfaction (Eq. 1).

$$\%satisfact_{candidate\ i} = \frac{\Sigma_{candidate\ i;}\ (score_{Factor\ j} \times relative\ weight_{Factor\ j})}{\Sigma\ (maximum\ score\ possible \times relative\ weight_{Factor\ j})}$$

Equation 1: Equation for the calculation of the percentage of satisfaction for each enzyme candidate

As a calculation example, the satisfactory percentage of the AdhC from *E. coli* was estimated as follow, with j representing the successive six factors to be considered for ranking the candidate enzyme from *E. coli* (Table 3), and the 'maximum score possible' being 5, resulting the numeral application:

$$\%\text{satisfact.} = \frac{[(3x0.1)+(0x0.07)+(2x0.21)+(5x0.24)+(4x0.35)+(5x0.03)]}{[(5x0.1)+(5x0.07)+(5x0.21)+(5x0.24)+(5x0.35)+(5x0.03)]}$$

$$= (3.27/5)\ x100$$

$$= 65\%$$

The satisfactory percentages obtained for all ADHs candidates were detailed in Appendix 11.4.

Table 4: Details of the result for the selection of appropriate alcohol dehydrogenases enzymes

ADHs		
Features	*A. nidulans*	*C. glutamicum*
Protein name (Encoding gene)	ADH I *(alcA)*	ADH A *(adhA)*
Nucl. Seq. ID	NT_107002.1/ AN8979.2 NCBI ID :2868277KREGG - alcA gene	NC_006958.1 AP009044.1 adhA gene
Protein structure **Subunit weight** **Amino acids seq.** **ADHs group**	Homo-octopolymer 37kDa 350 AA 1 Zn^{2+}/subunit (group I)	Homo-dimer 36kDa 345 AA 1 Zn^{2+}/subunit (group I)
***K_M* (ethanol)**	0.9 mM	6.8 mM
***K_M* (acetaldehyde)**	0.35 mM	0.92 mM
K_{cat}	32 U/mg	7.8 U/mg
	Under cellular condition, oxidation of ethanol is favourised. Reaction pulled by the furhter oxidation of acetaldehyde	
Score matrix	88%	79%
References	[125]	[171]

The final results of the analysis matrixes with further details are shown in Table 4. Alcohol dehydrogenase genes from *A. nidulans* and *C. glutamicum*, gave the highest scores through the decision-making matrixes. These two enzymes were then selected for building the first step for an ethanol pathway in *E. coli*. The nucleotide sequences of *alcA (A. nidulans)* and *adhA* (*C. glutamicum*) are given in Appendix 11.5 and 11.6, respectively.

4.3.2.2 Database and literature search for acetaldehyde dehydrogenases

ALDHs represent a wide superfamily of enzymes. They are important enzymes in the metabolism as they catalyse the irreversible oxidation of aldehydes, thus acting as a detoxification mechanism [187], [188]. Additionally, in microbes and animals ALDHs are also crucial for the generation of highly bio-active compounds vital to the organism, such as retinoic acid (essential for the vision) or γ-aminobutyric acid (GABA), the prime regulatory compound involved in regulation of neurotransmitters metabolism. Interestingly, ALDHs have been extensively studied for their implications in cellular mechanisms from pathogenicity of microbial strains to oxidative stress responses, or for their non-catalytic functions such as binding proteins for regulatory purposes [189], but little was reported for their use in bio-processes. Overexpression of ALDH was performed to improve the vinegar production in A*cetobacter aceti* [190], however only very recently have ALDHs been acknowledged as valuable biotechnological biocatalysts for the bio-production of high value compounds such as

retinoids [191], or platforms chemicals from lignin hydrolysates for the manufacture of polymers (syringate; [192]). Consequently, the literature available focused mainly on the oxidation of secondary and branched aldehydes.

To identify potential ALDH candidates, capable of carrying out the second oxidation step of acetaldehyde to acetate, the BRENDA [160] and UniProt [161] databases were searched using the same reasoning steps as described for the ADHs selection. We started to screen the enzymes by their EC numbers [163], as follows:

>An oxidoreductase enzyme (EC 1)

>>acting on the aldehyde group of donors (EC 1.2)

>>>with $NAD(P)^+$ as acceptor (EC 1.2.1) and preferably NAD^+ (EC 1.2.1.3).

In a similar strategy to that used for ADHs, we narrowed the ALDH (EC 1.2.1.3) results to 48 entries by focusing on acetaldehyde oxidation to acetate given in BRENDA. From the different organisms on the list, only microbes were kept, which yielded 16 hits. However, in order to build the complete ethanol-consuming pathway, ADH and ALDH needed to be coupled. When expressed in a host strain (*E. coli*), concomittant activity between the ADH and ALDH selected was assumed to be largely enhanced either by selecting an ADH and ALDH from the same microorganism, or by choosing enzymes which work with the same cofactor, NAD. Therefore, from the 16 candidate list, we screened for ALDHs from the same microorganisms as the ADHs previously identified. We were not able to identify ALDHs in all of the

organisms where ADHs are present, making the ALDH list slightly shorter with 6 candidates (Table 5).

Table 5: List of potential candidates for the selection of an acetaldehyde dehydrogenase

Name	Organism	Organism type	References
ADH C	*E. coli* DC272	Mesophilic, aerobic bacteria	[110], [111], [132], [133], [164], [165]
ALDH	*Acinetobacter* sp HBS-2		[193]
ALDH A	*Corynebacterium glutamicum*		[136], [148]–[150]
ALDH	*Geobacillus thermodenitrificans*	Thermophilic bacteria	[174]
ALDH	*Geobacillus stearothermophilus*		[194]
ALDH A	*Aspergillus nidulans*	Filamentous fungus	[125], [147]

The decision matrix method was similarly applied for selecting two final ADLHs enzymes to pair with ADHs. In the paired comparison table, the relative importance of the different factors and satisfactory percentage table are detailed in Appendices 11.7, 11.8 and 11.9. The criteria considered were the same as those previously detailed, except that this time we were looking for low K_M values for acetaldehyde. The two highest ranking enzymes were the ALDH from *A. nidulans* and the ALDH from *Acinetobacter* sp HBS-2; their characteristics are described in Table 6.

Table 6: Details of the result for the selection of appropriate aldehyde dehydrogenases enzymes

ALDHs		
Features	*A.nidulans*	*Acinetobacter sp. HBS-2*
Protein name (Encoding gene)	ALDH A *(aldA)*	ALDH *(ALDH)*
Nucl. Seq. ID	NCBI ID: 2876330 KREGG KREGG - aldhA gene	EF566941
Protein structure **Subunit weight** **Amino acids seq.**	Monomer 54kDa 497 AA	Monomer 57kDa 489 AA
***K_M* (acetaldehyde)**	Not given but said as best activity [147]	0.0152 mM
K_{cat}	100 U/mg	1.406 µM/min
	Irreversible reaction	
Score matrix	95%	90%
References	[125], [147]	[193]

Given that amongst our final candidates, we identified an ADH and an ALDH from *A. nidulans*, we decided to pair them together for building an ethanol assimilation route. We then produced a second ethanol route by coupling the ADH from *C. glutamicum* with the ALDH from *Acinetobacter* sp. HBS-2. Each of these associations were designed in such a way based on the previously drawn assumptions that ADH-ALDH enzymes from the same microbial origin, or with similar catalytic conditions (co-factor in this case) should work better together.

4.3.2.3 Metabolic considerations for ethanol consuming route

One challenge to consider when using ethanol as a carbon source is the increased production of NADH while ethanol is being oxidised into acetate. Accumulation of NADH can drastically impair both cell maintenance and biosynthetic routes, therefore ways to recycle NADH to its oxidised form need to be investigated. Cell respiratory membranous chain is widely recognised as a very effective way for cofactor regeneration *via* ATP formation, rendering aerobic fermentation an easy and practical solution, here. However, nor is cellular excess of ATP a desired feature. Here, two scenarii were considered. First, the excess of NADH produced from the oxidation of ethanol into acetate would be converted into ATP, and part of this ATP pool would fuel regular cellular mechanisms, while the rest would support the further utilisation of acetate to form acetyl CoA for the biosynthesis of citramalate. A second scenario would imply that the NADH would be too much of a risk and would require to be balanced through other means. From a carbon efficiency perspective, producing reduced compound (*e.g.* lactate) to recycle NADH is not a possible option. Manipulation of cell respiration by altering the air feed was a method investigated in other studies [195], but it demonstrated technical difficulties to ensure steady growth and productivity rates, and most of all it is economically unrealistic at industrial scale. A more sensible option would the insertion of NADH oxidase, enabling the consumption of excess NADH without any carbon loss by reduced compounds formation. Here, we favoured the occurrence of the first

scenario, based on the production of acetate, which can serve as an ATP-balancing route.

4.4 Conclusions

In this chapter, we described the selection process performed for the selection of suitable enzymes for the construction of an acetate and ethanol assimilation route, as well as the potential metabolic burdens associated with each route and ways to solve them.

Interestingly, glucose remains an unavoidable feedstock and/or co-feedstock in most of the studies performed on carbon efficiency. This is mainly due to the fact it is the favoured substrate of *E. coli*, allowing its fast growth, as well as being involved in numerous cellular regulatory mechanisms. For the purpose of the current work, efficient carbon sources of pyruvate and acetyl-CoA were desired. The sole use of either acetate or ethanol as carbon source was not kept as an interesting solution as slower growth rates, carbon loss *via* the activation of the glyoxylate shunt pathway to supply pyruvate, metabolic burdens regarding energy supply, co-factors regeneration, as well as reduction in yields and titres for the biosynthesis of citramalate were to be expected. Therefore, co-feeding systems involving glucose as the main supply of pyruvate was concluded as the most appropriate option regarding carbon efficiency and growth rate.

As stated earlier, we applied the same strategy as Tashiro and co-workers by overexpressing the native AckA-Pta from *E. coli* for the

construction of an acetate assimilation route. For the construction of an ethanol consuming pathway, two candidates routes were designed: one built with the ADH and ALDH enzymes which originated from the same filamentous fungus, *A. nidulans*; and the second one resulting from the association of an ADH and an ALDH from different microbial backgrounds, but using the same co-factor, NAD, as the electron acceptor. In order to confirm that citramalate can be produced from the co-consumption of two carbon sources, all the citramalate pathway and either the acetate or the ethanol pathways needed to be cloned into the host strain and expressed together. Therefore, three main *E. coli* strains were produced bearing the citramalate route co-expressed with either the AckA-Pta route to enable acetate co-feeding, or either ADH I-ALDH A from *A. nidulans* or both ADH A from *C. glutamicum* and the ADLH from *Acinetobaster* sp. HSB-2 to enable the ethanol co-use with glucose. The production of citramalate from the co-assimilation of either glucose/acetate or glucose/ethanol was then evaluated. The strains capable of producing citramalate from the co-assimilation of carbon sources were then scaled up to fed-batch fermentations to assess the carbon efficiency of the complete bio-route.

5. Materials & methods

5.1 Reagents

All reagents were purchased from Sigma-Aldrich UK and all enzymes were purchased from New England Biolabs Inc. unless otherwise stated in the text.

5.2 Thermodynamic considerations

Thermodynamic considerations were carried out to assess the feasibility of the biosynthetic pathways investigated for enabling the co-consumption of glucose with either acetate or ethanol for the bio-production of (*R*)-citramalate. Standard Gibbs free energy of reactions at 25°C and pH 7 for biological conditions, (notated as $\Delta_r G'^{\circ}$), were obtained from the MetaCyc Database [196]. The overall $\Delta_r G'^{\circ}$ value of the whole pathway studied was obtained by adding the different $\Delta_r G'^{\circ}$ values for each of the reaction steps together (Eq.2).

$$\Delta_r G'^{\circ}_{\text{complete pathway}} = \Sigma_1^{\,i} \, \Delta_r G'^{\circ}_{i}$$

Equation 2: Calculation of the overall standard Gibbs free energy of the complete pathway

Where $\Delta_r G'^{\circ}_{i}$ corresponded to the $\Delta_r G'^{\circ}$ value of each of the reaction steps involved in the complete pathway investigated.

A final negative $\Delta_r G'^{\circ}$ indicates a thermodynamically favourable pathway, while a positive $\Delta_r G'^{\circ}$ involves an energy-consuming reaction.

5.3 *E. coli* growth, maintenance and media

5.3.1 *E. coli* strains

E. coli JM107 was obtained from Novagen. *E. coli* MG1655 was from our laboratory stock. *E. coli* BW25113, *E. coli* BW25113 Δ*ldhA* and *E. coli* BW25115 Δ*aceF* were obtained from the Coli Genetic Stock Center (Yale, USA, [197]).

5.3.2 Growth media

Media components were sterilised by autoclaving (121 °C, 20 min, 15 psi), or where stated in the text by filtration (0.2 µm filter, Sarthorius), and mixed when cooled. Media solutions were prepared in deionised water (dH2O) and stored at room temperature unless otherwise stated. Where solid medium was required, agar (Sigma Aldrich; 15 g/L) was added to the medium prior to autoclaving. Where applicable, antibiotics were added to growth media. Antibiotics were prepared as a 1000 times concentrate of the working concentration. Kanamycin sulphate (Novagen; 100 mg/mL), and carbenicillin (Melford; 50 mg/mL) solutions were filter sterilised and stored at -20 °C. All overnight seed cultivations were performed at 37 °C, 200 rpm, in 20 ml cultures. All other cultivations were carried out at 30°C, 200 rpm and in baffled Erlenmeyer flasks, with nominal volumes five times the liquid culture volume unless otherwise stated.

Lund medium was used as experimental growth medium to generate biomass for protein expression and activity, and flask-scale

fermentations. Lund medium for all experiments contained: 5x salt concentrate (200 mL), glucose solution (20 mL; 500 g/L), $MgSO_4$ solution (2 mL; 1 M), trace elements (2 mL), carbenicillin (500 µL) and distilled H_2O (776 mL). Lund 5x salt solution contained: $(NH_4)_2SO_4$ (10 g/L), K_2PO_4 (73 g/L), NaH_2PO_4. $2H_2O$ (18 g/L) and (NH_4)2H-citrate (2.5 g/L). Lund trace elements solution contained: $Na_2EDTA.2H_2O$ (22.3 g/L), $FeCl_3$ (10.03 g/L), $CaCl_2.2H_2O$ (0.5 g/L), $ZnSO_4.7H_2O$ (0.18 g/L), $CoCl_2.6H_2O$ (0.18 g/L), $CuSO_4.5H_2O$ (0.16 g/L), $MnSO_4.H_2O$ (0.15 g/L).

Lund medium used for fermentations in 2L bioreactor contained: K_2HPO_4 (14.6 g/L), glucose solution (100 mL; 119 g/L), yeast extract solution (50 mL; 100 g/L), NaH_2PO_4.2H2O (3.6 g/L), $(NH_4)2SO_4$ (2 g/L), ammonium citrate (0.5 g/L), polypropylene glycol (0.1 mL), $MgSO_4.7H_2O$ solution (2 mL; 246.47 g/L), carbenicillin solution (1 ml) and fermentation trace elements (2 mL). Fermentation trace elements contained: $Na_2EDTA.2H_2O$ (22.3 g/L), $FeCl_3$ (10.03 g/L), $CaCl_2.2H_2O$ (0.5 g/L), $ZnSO_4$, $7H_2O$ (0.18 g/L), $CoCl_2.6H_2O$ (0.18 g/L), $CuSO_4.5H_2O$ (0.16 g/L), $MnSO_4.H_2O$ (0.15 g/L). Glucose, $MnSO_4$, H_2O, yeast extract (ThermoFisher Sc oxoid Ldt), trace elements and carbenicillin solutions were added to the fermenter vessel when cooled. All other components were autoclaved in the fermentation vessel.

5.3.3 Cultivation conditions

For general growth and maintenance, all strains were cultured on Lysogeny Broth (LB), which contain 25 g/L of LB granulated medium (Sigma Aldrich, L3522). Strains were routinely stored at -80°C as 20% glycerol stocks. Glycerol stocks were prepared by picking a single colony of the strain and culturing it overnight in LB containing the appropriate antibiotic (20 ml). After bacterial growth was obtained, 500 µl of a sterile 40% glycerol stock solution was added to 500 µl of the overnight culture.

Glycerol stocks (25 µL) of the strain to be fermented were used to inoculate Lund fermentation medium supplemented with carbenicilin (100 mL) and the cultures incubated overnight (37 °C, 250 rpm). The overnight culture was diluted in sterile Lund fermentation medium to give 50 ml of pre-culture at OD_{600nm} 0.1. The entire pre-culture was used to inoculate fermentation medium (1 L) to an initial OD of 0.005 in a New Brunswick™ BioFlo® /CelliGen® 115 (2 L; Eppendorf) maintained at 30 °C. The pH was controlled at 7.0 by the automatic addition of aqueous ammonium hydroxide (NH_4OH, 28 % v/v) or H_2SO_4 (2 M). Dissolved oxygen (DO) was controlled at a set point of 30 % saturation measured by a polarographic oxygen probe by automatic control of the stirrer speed between 400-1200 rpm. Filtered air was pumped into the fermenter at 1 volume vessel per minute (VVM) using a BAMBI VT250 air compressor. Once all of the carbon source was consumed in the batch medium, a glucose feed was used to maintain the pseudo-exponential growth rate at 0.25 h^{-1}. The glucose feed (1 L) contained: glucose (650 g), $MgSO_4.7H_2O$ solution

(50 mL; 246.47 g/L), fermentation trace elements (10 mL) and yeast extract (50 mL; 100 g/L). Glucose, yeast extract and $MgSO_4.7H_2O$ and trace elements solutions were prepared separately and mixed when cooled. The glucose feed was maintained until the culture OD_{600nm} reached approximately 45, at which point the culture was induced by adding *L*-arabinose (2 g/L). Subsequent paired glucose and acetate or glucose and ethanol feedings are described in the text.

Protein expression and activity experiments were performed by inoculating LB or Lund medium (20 mL) supplemented with carbenicillin with one single colony from a fresh LB plate supplemented with appropriate antibiotic of the strain to be tested, and the cultures incubated overnight at 37°C and 200 rpm. Overnight cultures were used to inoculate fresh LB or Lund medium (50 mL) supplemented with carbenicillin to an initial OD_{600nm} of 0.1 and the cultures incubated at 30°C. Protein expression was induced by the addition of *L*-arabinose (to a final concentrations of 0.2 %, from a 200 g/L stock solution sterilised by filtration) at an OD_{600nm} of 0.6. Induced cultures were incubated and harvested by centrifugation (5000 rpm, 10 min, 4 °C), 18 h post induction unless otherwise stated.

Specific growth rates of cultures were calculated in the exponential growth phase using the equation:

$$\ln OD_t / \ln OD_0 = \mu t$$

where OD_t is the arbitrary light scattering units at time t (h) and μ is the growth rate (h^{-1}).

5.4 DNA techniques and strain construction

5.4.1 Genes, plasmids and primers

The genes *alcA*, *aldA*, *adhA* and *ALDH* were custom-synthesized by Biomatik. The genes *ackA-pta* was PCR amplified from chromosomal DNA of *E. coli* MG1655. All primers were synthesized by Integrated DNA Technologies (IDT) and are detailed in Table 7. All primer pairs used for PCR amplification are given in the text. The plasmid vector pBAD24 was provided from a previous PhD project and is the expression system used for this project as well.

The restriction sites added via PCR are underlined and specified in the third column, while the ribosome binding site (RBS) is indicated in red and followed by the 8 bp spacing sequence. Both RBS and spacing sequences have been conserved for all constructions as it was demonstrated that they were functional in previous studies. The green colour indicates the part of the primer which annealed to the section DNA for gene amplification.

Table 7: List of primers

Name	Sequences	RE
5'ADH I pBAD	AAA**GCTAGC**AGGAGGAATTCACCATGTCCATC CCCACTAT	*Nhe*I
3'ADH I pBAD	CCGGGGGTACC**GAGCTC**TTATTCTGGCA	*Sac*I
5'ALDH A pBAD	AA**GAGCTC**AGGAGGAATTCACCATGTCTGATT TGTTCACCA	*Sac*I
3'ALDH A pBAD	CAGTGCC**AAGCTT**CTCGAGGCATGCTTAAGC GA	*Hind*III/ *Sph*I
5'ADH A pBAD	AAA**GCTAGC**AGGAGGAATTCACCATGACCAC TGCTGCACCCC	*Nhe*I
3'ADH A pBAD	TCAGGTGGGACCACCGCGCTACTGCC	*Sac*I
5'ALDH pBAD	AAA**GAGCTC**AGGAGGAATTCACCATGGCGAA GGAAATT	*Sac*I
3'ALDH pBAD	TGTTGGGAAGGGCGATCGGTGCGG	*Hind*III/ *Sph*I
5'acka-pta BAD	AAA**GCTAGC**AGGAGGAATTCACCATGTCGAG TAAGTTAGTACTGGTTCTGAACTGC	*Nhe*I
3'acka-pta pBAD	ACC**AAGCTT**GAT**GCATGC**TTACTGCTGCTGT GCAGACTGAATC	*Sph*I/ *Hind*III
5'cimA3.7 pBAD	AAA**GCATGC**AGGAGGAATTCACCATGATGGTT CGTATCTTCG	*Sph*I
3'cimA3.7 pBAD	TTT**AAGCTT**TTACAGTTTACCAGTAACCTCACG CACGATTGCCAG	*Hind*III

RE: Restriction enzyme

5.4.2 Polymerase chain reaction

High fidelity polymerase chain reaction (PCR) was carried out using KOD polymerase (Novagen) to amplify the gene targets of *alcA*, *adhA*, *aldA*, *ALDH*, *cimA3.7*, and *ackA-pta* without introducing mutations. PCR reaction mixes (50 µL) contained: 10 x buffer for KOD DNA polymerase (5 µL), $MgSO_4$ solution (25 mM; 2 µL), dNTPs (2 mM each; 5 µL), 5' primer (10 µM; 2 µL), 3' primer (10 µM; 2 µL),

template DNA (10 ng), KOD DNA polymerase (1 U) and PCR grade water. Typical thermocycler conditions (Table 8) were set accordingly to the recommendation of the manufacturer (EMD Millipore). 6x loading dye (New England Biolabs) was added (10 µL) to the reactions mixtures at the end of the PCR cycles, and analysed by gel electrophoresis (75 V, 45 min).

Colony PCR was performed to confirm the presence of inserted genes following a transformation. Between 5 and 10 single colonies were picked for each transformation and transferred to autoclaved dH_2O (50 µL). Colony PCR reaction mixes (50 µL) contained: 10X PCR buffer (5 µL), 10mM dNTPs (10 mM; 1 µL), 5' primer (10 µM; 1.5 µL), 3' primer (10 µM; 1.5 µL), colony suspension (2.5 µL) and JumpStart REDTaq polymerase (Sigma-Aldrich; 2.5 µL). Typical thermocycler conditions were set accordingly to the length of DNA to be amplified (Table 8). Following the reaction, samples were loaded directly into DNA agarose gels for analysis. When cloning had been successful, the remaining colony suspension in dH_2O was plated on LB supplemented with the appropriate antibiotic and incubated overnight at 37 °C. The resulting colonies were used to extract the plasmids for sequencing. Once confirmed by sequencing, glycerol stocks of the strain were prepared and stored at -80°C until further use. Sequence confirmed plasmids were used to produce recombinant *E. coli* strains to be further studied in this project.

Table 8: Typical thermocycler conditions used for either high fidelity or colony polymerase chain reactions

	KOD		JumpStart REDTaq	
Initial denaturation	98°C	30 sec	94°C	1 min
Denaturation	98°C	10 sec	94°C	30 sec
Annealing	55°C	20 sec	55°C	30 sec
Elongation	72°C	30 sec	72°C	1 min/kb expected
Final elongation	72°C	5 min	72°C	1 min/kb expected
Hold	4°C	∞	4°C	∞

30 cycles

The aforementioned parameters may varied accordingly to the length of the target gene being amplified.

5.4.3 Restriction enzyme cloning

Restriction enzyme cloning was used to insert *alcA*, *adhA*, *aldA*, *ALDH*, *cimA3.7*, and *ackA-pta* in various combinations into the pBAD24 plasmid. Plasmid DNA (1.5 µg) was prepared by digesting with the appropriate restriction enzyme for inserting the genes. Linear plasmid DNA was gel purified using a GenElute (Sigma-Aldrich) gel extraction kit. Gene inserts were digested with the same restriction enzymes and purified using a PCR purification kit. Gene inserts were ligated into the prepared plasmid DNA using a 3:1, 5:1 or 7:1 molar ratio of gene insert to plasmid. The ligation mixture (30 µL) was composed of linear plasmid DNA (50 ng), gene insert (varied depending on size), T4 ligase (5 U), 10 x T4 DNA ligase buffer (3 µL) and PCR grade water.

The reaction was incubated (room temperature, 1 h) and the enzymes inactivated by heating (70 °C, 10 min).

Cloning strain, *E. coli* JM107, was routinely transformed with engineered plasmids using TransformAid™ Bacterial Kit (LifeTechnology). Transformants were selected by growing cells on LB agar plates supplemented with carbenicillin (100 µL/mL) and incubated overnight (37°C).

Engineered plasmids were extracted using a Miniprep or Midiprep Kit (Sigma Aldrich) for analysis. The concentration of the extracted plasmids solution was determined using a Nanodrop ND. The quality of the DNA concentration readings was expressed by the protein contamination ratio (A_{260}/A_{280}), and the salt contamination ratio (A_{260}/A_{230}). Good quality of plasmids extraction was concluded when ratios were about 2.2 and 2.0, respectively.

Prior to sequencing, restriction digests were carried out to validate that the plasmid was correctly assembled. A restriction digest mixture contained: plasmid DNA (100 ng), restriction enzyme 1 (0.5 µL), restriction enzyme 2 (0.5 µL), polymerase buffer (5 µL) and autoclaved dH_2O. Restriction enzymes varied upon the section of the plasmid to be verified. Reaction mixtures were usually incubated 1 h at 37°C in water bath. When required, restriction enzymes were heat inactivated by incubating the reaction mixture at 65°C for 10 minutes on a heating block. Restriction digests reaction mixtures were then mixed with 6x blue loading dye and run onto agarose gel electroporation.

5.4.4 DNA purification

PCR products or restriction digested gene inserts were purified using a QIAquick PCR Product Purification Kit (Qiagen). Buffer PB (250 µL) was added to the PCR or restriction digest mix (50 µL). The DNA was loaded onto a QIAquick spin column in a collection tube and the DNA bound to the column by centrifugation (13,400 rpm, 1 min). The flow-through was discarded and the column washed with buffer PE (750 µL). The column was centrifuged (13,400 rpm, 1 min) and the flow-through discarded. To ensure any residual buffer was removed, the centrifugation step was repeated. Spin columns were transferred to a fresh microfuge tube and the DNA eluted by adding buffer EB or autoclaved dH_2O (30 to 50 µL, depending on the concentration needed). The column was allowed to stand for 5 min before centrifuging (13,400 rpm, 1 min). DNA was stored at -20 °C until required.

Miniprep kits (Qiaprep Spin Miniprep Kit; Qiagen) were used to purify high-copy number plasmids, and midiprep kits (Qiaprep Spin Midiprep Kit; Qiagen) were used to purify low copy number plasmids or where larger amounts of plasmid were required, such as for ligation reactions. LB medium (5 mL miniprep, 100 mL midiprep) supplemented with the appropriate antibiotic was inoculated with a single colony of the strain containing the target plasmid. The cultures were incubated overnight and harvested by centrifugation (5000 rpm, 10 min, 4 °C). Cell pellets were resuspended in buffer P1 (250 µL miniprep, 4 mL midiprep). Lysis buffer P2 (250 µL miniprep, 4 mL midiprep) was added to the suspension and mixed by inverting 4-6

times. The lysis reaction was incubated (5 min, room temp) and stopped by the addition of chilled buffer N3 (350 µL miniprep, 4 mL midiprep). The suspension was mixed by inverting 4-6 times and cell debris removed by centrifugation (13,400 rpm, 10 min miniprep, 13,400 rpm, 30 min midiprep). For minipreps, the supernatant was transferred to a QIAprep spin column in a collection tube. Spin columns were centrifuged (13,400 rpm, 1 min) and the flowthrough discarded. Trace nuclease activity was removed by washing the column with buffer PB (500 µL) and the column centrifuged (13,400 rpm, 1 min). The flow-through was discarded and the columns washed with buffer PE (750 µL). The column was centrifuged (13,400 rpm, 1 min) and the flowthrough discarded. To ensure any residual buffer was removed, the centrifuge step was repeated. Spin columns were transferred to a fresh microfuge tube and the DNA eluted by adding buffer EB (30 µL). The column was allowed to stand for 5 min before centrifuging (13,400 rpm, 1 min). For midipreps, the prepared supernatant was transferred to a fresh polypropylene tube (15 mL) and the centrifugation step repeated. The supernatant was loaded onto a QIAGEN-tip 100 column pre-equilibrated with buffer QBT (4 mL). Columns were allowed to drain by gravity flow and washed twice with buffer QC (10 mL). Columns were transferred to a fresh polypropylene tube (15 mL) and plasmid DNA eluted by adding buffer QF (5 mL). Plasmid DNA was precipitated by adding isopropanol (3.5 mL) and centrifuging (13,400 rpm, 30 min, 4 °C). The supernatant was discarded and the pellet washed with ethanol (70 % v/v, 2 mL). The suspension was centrifuged (13,400 rpm, 10 min, 4 °C) and the

supernatant discarded. Pellets were allowed to air dry and resuspended in buffer EB (500 µL). Plasmids were stored at -20 °C until required.

DNA was purified from agarose gels using Zymoclean Gel DNA Recovery Kits (Zymo Research). Target DNA was excised from agarose gels using a clean scalpel and transferred to a pre-weighed microfuge tube. The tube was reweighed and the weight of the gel slice calculated. Three volumes of buffer ABD was added to each volume of agarose gel. The suspension was incubated at 55 °C until the gel was completely dissolved. The dissolved agarose solution was transferred to a Zymo-Spin column, which was inserted in a collection tube. DNA was bound to the column by centrifugation (13,400 rpm, 1 min) and the flow-through discarded. The column was washed with DNA wash buffer (200 µL) and centrifuged (13,400 rpm, 1 min). The wash step was repeated. Zymo-Spin columns were transferred to a fresh microfuge tube. DNA elution buffer (30µL) or autoclaved distilled water (50µL) was added to the column to elute the DNA. The column was allowed to stand for 5 min before centrifuging (13,400 rpm, 1 min). The concentration of the eluted DNA was measured using a NanoDrop (Thermo Inc.). DNA was stored at -20 °C until further use.

5.5 Protein overexpression:

Glycerol stocks (20 µL) of the strains to be analysed were used to inoculate Lund medium supplemented with appropriate antibiotic and

the cultures incubated overnight (37°C, 200 rpm). Overnight cultures were used to inoculate fresh Lund medium (100 mL), unless otherwise stated, supplemented with the appropriate antibiotic to an OD_{600nm} of 0.1 and the cultures incubated at 30°C unless otherwise stated. Protein expression was induced by the addition of sterile *L*-arabinose (1 ml unless otherwise stated; 200 g/L autoclaved) at an OD_{600nm} of 0.6. Induced cultures were incubated and cell samples (1ml) were taken prior to induction and regularly after as further stated in the text. Samples were centrifuged and the pellets stored in -20°C freezer until performing sodium dodecyl sulphate polyacrylamide gel electrophoresis (SDS-PAGE).

5.6 Enzyme assays

5.6.1 Crude extract preparation

Cell free extracts of *E. coli* expressing the proteins of interest were prepared from 100mL cultures. Cells were harvested by centrifugation (600 rpm, 15 min, 4°C) after 18h of induction at 30°C. The pellets were resuspended in appropriate buffer (0.1M N-[tris(hydroxymethyl)methyl]-2-aminoethanesulfonic acid (TES) buffer containing 2 mM $MgCl_2$ and 1mM DTT, pH 7.4, 6 ml) containing benzoase nuclease (0.1 µL/mL) and EDTA-free protease inhibitor tablet (Sigma-Aldrich). The cells were lysed by two successive passages in the Constant Cell Disruption System (Constant Systems; 20,000 psi). Cells debris were removed by centrifugation (13,400 rpm, 4°C, 20 min). The supernatant was carefully transferred into a

new tube and stored on ice to be used the same day. Total protein concentration was determined by using DC protein assay kit (Bio-Rad).

5.6.2 Alcohol dehydrogenase assay

5.6.2.1 Alcohol dehydrogenase from *Aspergillus nidulans*

Oxidation and reduction activities of alcohol dehydrogenase from *Aspergillus nidulans*, ADH I, were assayed using a modified method described by Creaser et *al.* (1985) and Pateman et *al.* (1983). The oxidation of ethanol by alcohol dehydrogenase is coupled to the reduction of NAD^+ to NADH. The assay used to monitor alcohol dehydrogenase activity is based upon the rate of increase in absorbance at 340 nm at 30°C when cofactor NAD^+ is reduced to NADH (Eq. 3) using a UV-Vis spectrophotometer (Shimadzu). This reaction is reversible and so can be used to monitor reduction of acetaldehyde to ethanol, by measuring the decrease in absorbance at 340 nm, which corresponds to the oxidation of NADH to NAD^+. NADH has a molar extinction coefficient of 6,220 $M^{-1}.cm^{-1}$ at 340 nm, while NAD^+ does not absorb at this wavelength [198].

$$\text{Ethanol} + NAD^+ + H_2O \leftrightarrow \text{Acetaldehyde} + NADH$$

Equation 3: Equations for the oxidative and reductive activity of alcohol dehydrogenase (EC 1.1.1.1)

The oxidative activity of ethanol was performed in 1 mL quartz cuvettes. The reaction mixtures contained: TES buffer (100 mM, pH 8) containing $MgCl_2$ (2 mM) and dithiothreitol (DTT, 2 mM), NAD^+ (1 mM), ethanol (10 mM) and crude extract (50 µL). The reaction was initiated by the addition of NAD^+. A blank containing all components except NAD^+ was used. The formation of NADH was monitored by the increased in absorbance (5 min, 30°C).

The reductive activity of alcohol dehydrogenase was assayed by monitoring at 30°C the decrease of absorbance at 340nm due to the depletion of NADH. The reaction mixture contained: NADH (0.1 mM), acetaldehyde (10 mM), crude extract (50 µL) and up to 1 mL TES buffer (100 mM, pH 8) containing $MgCl_2$ (2 mM) and DTT (2 mM). The reaction was initiated by adding NADH. A blank containing all components except NADH was used.

5.6.2.2 Alcohol dehydrogenase from *Corynebacterium glutamicum*

The oxidative activity of alcohol dehydrogenase from *Corynebacterium glutamicum*, ADH A, was assayed accordingly to the protocol of Witthoff and co-workers [136]. Similarly, the oxidation of ethanol by ADH A is coupled to the reduction of NAD^+ to NADH, and therefore it was monitored by measuring the increase in absorbance at 340 nm (30°C). The reactional mixture (1 mL total volume) contained TES buffer (100 mM, pH 8) containing 100 µM $ZnCl_2$, 1 mM NAD^+, and 50 µL of cell extract. The reaction was initiated by the

addition of 1mM NAD^+ and monitored by following the increase in absorption at 340 nm (5 min, 30°C). For calibration, a blank containing all components except NAD^+ was used.

The reduction of acetaldehyde to ethanol was monitored by performing the same assay, but with the replacement of ethanol by acetaldehyde (10 mM) and NAD^+ by NADH (0.1 mM). The reaction was initiated by the addition of NADH (0.1 mM) and monitored by following the decrease in absorption at 340 nm (5 min, 30°C). A blank containing all components except NADH was used. The dependency of Zn^{2+} for the enzyme activity was also investigated by running the same tests in the presence/absence of Zn^{2+}.

5.6.3 Acetaldehyde dehydrogenase assay

Acetaldehyde dehydrogenase catalysed the irreversible conversion of acetaldehyde to acetate *via* the oxidation of NADH to NAD^+ (Eq. 4).

$$\text{Acetaldehyde} + NAD^+ + H_2O \rightarrow \text{Acetate} + NADH$$

Equation 4: Catalytic reaction of acetaldehyde dehydrogenase (ALDH)

Acetaldehyde dehydrogenases activity was then monitored by measuring the production of NADH at 340nm.

The assay used for the analysis of the acetaldehyde dehydrogenase from *Aspergillus nidulans* was adapted from the protocol used by Pateman and co-workers [146].The reaction mixture contained TES

buffer (100 mM, pH 8) supplemented with $MgCl_2$ (2 mM) and DTT (2 mM), NAD^+ (1 mM), acetaldehyde (10 mM) and crude extract (50 µL). The reaction was initiated by the addition of NAD^+. A blank containing all components except NAD^+ was used.

Catalytic activity assay of acetaldehyde dehydrogenase from *Acinetobacter* sp HBS-2 was adapted from the assay performed by Zhao and co-workers [193]. The reaction mixture contained in a 1ml quartz cuvette: TES buffer (100 mM, pH 8), 1mM NAD^+, 10mM acetaldehyde and crude extract (50 µL). NAD^+ was added to the mixture to initiate the reaction. A blank containing all components except NAD^+ was used.

In all assays, one unit of alcohol dehydrogenase oxidative or reductive activity is defined as the reduction of 1 µmol NAD^+ or the oxidation of 1 µmol NADH per minute, respectively. This also applies to the assays performed on acetaldehyde dehydrogenases.

Concentrations of NADH were calculated using the Beer-Lambert law:

$$A = \varepsilon . L . c$$

Where A is absorbance, ε is the molar extinction coefficient, c is concentration, and L is the path length of the solution in the spectrophotometer. In all the calculations, L = 1 (*i.e*. all measurements were made in a cuvette with a 1 cm path length). The molar extinction coefficient for NADH is 6220 M^{-1} cm^{-1}.

5.6.4 Citramalate synthase purification and assay

5.6.4.1 Citramalate synthase partial purification

CimA3.7 was partially purified from cell free extracts of *E. coli* BW25113 Δ*ldhA* pBAD24-*cimA3.7* and *E. coli* BW25113 Δ*ldhA* pBAD24-*alcA*-*aldA*-*cimA*3.7. Cell free extracts were prepared in TES buffer (0.1 M, pH 7.5, 6 ml) containing $MgCl_2$ (5 mM). CimA3.7 was partially purified by heating at 60°C for 10 minutes and separated from degraded proteins by centrifugation (13,400 rpm, 10 min). The supernatant was carefully transferred into a new tube and stored on ice to be used the same day.

5.6.4.2 Citramalate synthase assay

Citramalate synthase, CimA3.7, was assayed using a modified method previously described by Howell et *al*. (1999) [199]. The reaction mixture (1 mL) contained: partially heated purified CimA3.7 (200 µL), pyruvate (1 mM), acetyl-CoA (1 mM) and TES buffer (0.1 M, pH 7.5) containing $MgCl_2$ (5 mM). The mixture was incubated at 37°C and samples (100 µL) were taken at regular intervals (10 min), mixed with a sample analysis mix (900 µL), and the absorbance was measured at 412 nm. The sample analysis mix contained: 5,5'-dithio-*bis*-(2-nitrobenzoic acid) (DTNB; 0.56 mM), Tris-HCl (78 mM, pH 8) and dH_2O. A blank containing all of the aforementioned components but acetyl-CoA, was used. The concentration of free thiol groups generated was estimated using a calibration curve with 2-mercaptoethanol (Appendix 11.13).

5.7 Production of citramalate in whole-cell systems

5.7.1 Production of citramalate from glucose and acetate in flask

Evaluation of the strains overexpressing acetate assimilation pathways was carried in 500 ml flasks containing Lund medium with glucose (1%).

Overnight seed cultures of the acetate pathway expressing strains were prepared by inoculating Lund medium (20 mL, 37°C, 200 rpm) with 20 µL of the glycerol stocks of the strains to be analysed. Fresh Lund medium (100 mL) were inoculated at an initial OD_{600nm} of 0.1 using the overnight cultures. Protein expression was induced by the addition of *L*-arabinose (1 mL, 200 g/L) at an OD_{600nm} of 0.6. Directly after induction, acetate (2 mL, 250 g/L, autoclaved) was supplemented to the fermentation medium, and incubated (48 h, 30°C, 250 rpm). 24 h after induction, the glucose concentration was monitored using a glucose test strip (Merk-Millipore). The depletion of glucose being confirmed by the glucose test strip, both glucose (10 g/L) and acetate (5 g/L) were added again. Samples (1 mL) were taken frequently, spun down and supernatants filtered sterile for HPLC analysis.

5.7.2 Production of citramalate from glucose and ethanol in flask

Experiments were carried out in 500 mL flasks containing Lund medium with glucose (1%).

Overnight seed cultures were prepared by inoculating Lund medium (20 mL, 37°C, 200 rpm) with 20 µL of the glycerol stocks of the strains to be analysed. Fresh Lund medium (100 mL) were inoculated at an initial OD_{600nm} of 0.1 using the overnight cultures. Protein expression was induced by the addition of *L*-arabinose (1 mL, 200 g/L) at an OD_{600nm} of 0.6. Right after induction, the growth medium was supplemented with ethanol to a final concentration of 1%. Flasks were sealed and incubated at 30°C (48 h, 250 rpm). Samples (1 mL) were taken frequently, spun down and supernatants filtered sterile for HPLC analysis.

5.8 Analytical techniques

5.8.1 Biomass

Analysis of biomass was done by coupling optical density measurements and dry cell weight.

Optical density measurements were done using an Agilent 8453 Spectrophotometer set at 600nm. Samples of cell fermentation broth (1 mL) were transferred into polystyrene cuvettes (10 mm path length) for optical density reading. When the reading value was outside of a range from 0-0.8, samples were serial diluted 1 in 10 in dH_2O until they were within the linear measurement range.

Wet and dry cell weights measurements were done in pre-weighed Eppendorf tubes that had been dried in the oven for 48 h. Cell fermentation broth samples (1 mL) were centrifuged (13.400 rpm, 4 min, 4°C) and the supernatant carefully discarded. For wet cell

weights, the microfuge tubes were reweighed, and for dry cell weights, the cell pellets were incubated in the oven (48 h, 70 °C) to constant weight and reweighed. The difference between the empty microcentrifuge tube and the cell pellet was used to calculate the cell weight per litre of culture.

5.8.2 Glucose concentration

Glucose concentrations during fermentations were monitored using glucose monitoring strips (Glucose Test, Merck-Millipore). Test strips were immersed in the sample and were incubated for 30 seconds before reading the results (according to the manufacturer). Glucose at concentrations higher than 10 mg/L can be detected and were expressed by a change of colour of the test strip from white to different shades of blue, depending on the glucose concentration.

5.8.3 Agarose gel electrophoresis

Agarose gel electrophoresis was performed to analyse, and purify DNA fragments. Agarose gels (1% w/v) were prepared by dissolving agarose in tri acetate-EDTA buffer (TAE). TAE buffer was prepared by dissolving 50 x concentrate in dH_2O. The agarose was dissolved by microwaving the solution (800 W, 2 min), and allowed to cool down at room temperature. Ethidium bromide (1%, Fisher) was added to the solution, mixed by swirling, and the mixture poured into a pre-assembled electrophoresis rack. The gel was left to solidify and the comb removed to produce sample wells. DNA samples to be analysed

were mixed with 6 x concentrate of blue loading dye (Life Technology). The agarose gel was submerged in TAE buffer prior to the loading of DNA samples directly into the wells. The electrophoresis was carried out for 45 minutes at 75 V.

5.8.4 Sodium dodecyl polyacrylamide gel electrophoresis

SDS-PAGE was used to analyse protein expression. Success and strength of expression were determined by analysing cells samples taken prior to induction and at regular intervals after induction. The OD_{600nm} of the sample was measured and samples (1 mL) were harvested by centrifugation (13,400 rpm, 2 min). The supernatant was discarded and the cell pellets were frozen (-20 °C) until required. Cell pellets were resuspended in resuspension buffer containing 0.1M potassium phosphate buffer (pH 7.4), 10 x BugBuster™ (Merck-Millipore), and Benzonase® nuclease (0.1 µL/mL, Sigma-Aldrich). The volume of resuspension buffer to add is proportional to the OD_{600nm} of the sample in order to ensure the actual ratio of protein being expressed. It was calculated as followed and expressed in µL:

$$V_{\text{resusspendion buffer to add}} = OD_{600} \text{ of the sample x } 100$$

The resuspended pellets were incubated (20 min, room temperature, 250 rpm) before being centrifuged (6000 rpm, 10 min). Soluble fractions of the proteins were assayed by transferring 20 µL of the supernatant to clean 1.5 mL tubes. Insoluble fractions were prepared by resuspending the remaining pellet in same volume of resuspension buffer, and transferring 20 µL of the resuspension solution to clean

tubes. Soluble and insoluble fractions were mixed 1:1 with 2x Laemelli sample buffer (Bio-Rad) containing 2-mercaptoethanol (50 µl/ml) and boiled for 5 min (105°C). The samples (15 µl) were then loaded onto a polyacrylamide gel (Mini-PROTEAN® TGXTM precast gels, Bio-Rad; 150 V, 60 min). Gels were washed by soaking them in distilled water at room temperature with gentle agitation (50 rpm) for 5 minutes. The water was removed and the wash procedure was repeated a further three times. Gels were then stained by soaking in EZBlue™ Gel Staining Reagent (Sigma-Aldrich) at room temperature with gentle agitation for at least 1h to overnight (16h). Gels were rinsed with distilled water three times prior to analysis.

5.8.5 DNA concentration

DNA concentrations were measured by using a NanoDrop ND100. This was done by first washing the probe with nuclease free water (2 µl), then washing with elution buffer (EB, Sigma-Aldrich, GenElute Kit ®, 2 µl) and then loading the sample (2 µl) onto the probe. The quality of the DNA concentration readings were judged with both ratios A_{260}/A_{280}, expressing protein contamination, and A_{260}/A_{230} expressing salt contamination. Good quality ranges are 2.2 and 2.0 for each of ratio.

5.8.6 Measuring protein concentration

Protein concentration was measured using a DC protein assay kit (Bio-Rad). Cell free extracts were prepared on the day from lysed

cells, and were diluted 10 and 50 times. In a polypropylene tube (Falcon, 15 mL), sample to be analysed (100 µL), reagent A (500 µL) and reagent B (4 mL) were added and mixed immediately. Samples were incubated at room temperature (15 min), and the absorbance at 750 nm was measured. Measurement readings are stable for 1 h.

Solutions containing known concentrations of bovine serum albumin (BSA, 0-2 mg/L) were used to generate a standard curve. Protein concentrations of samples were determined using the BSA standard curve (Appendix 11.12).

5.8.7 HPLC

Samples to be analysed were centrifuged for 5 minutes (13,400 rpm), and the supernatant stored in -20°C freezer for further use. Before HPLC analysis, supernatants were thawed on ice, centrifuged for 5 minutes (13,400 rpm), and filtered into HPLC analysis vials (Agilent). Glucose, ethanol and organic acids were detected and concentrations measured using an Agilent 1200 series HPLC system equipped with a UV detector (210 nm) and refractive index detector. Glucose, ethanol and organic acids were separated using a Rezex column ROA organic acid H^+ (8%) from Phenomenex LC column. The column (300 x 7.8 mm) was equipped with a guard column and operated at 55^{o}C. A 0.5 ml/min mobile phase using 5 mM (0.01 N, pH 2) aqueous H_2SO_4 solution was applied. Standard curves were produced at every HPLC analysis for each compounds, and an example is given in Appendix 11.14.

6. Thermodynamic considerations on the acetate and ethanol pathways

6.1 Introduction

Several methodologies have been developed for the rational determination of the feasibility of a synthetic pathway, before targeting specific molecular engineering steps. This includes, but is not limited to, experimental techniques based on ^{13}C labelling, such as metabolic flux analysis (MFA) [200], or its mathematical counterpart known as flux balance analysis (FBA) [201], [202], which is based on stoichiometric models. However, both have limitations, as kinetic data, rate-limiting reactions as well as regulatory loops due to environmental and/or genetic variations causing changes in metabolites concentrations, are not well, if at all, taken into account. Fortunately, thermodynamic analysis offers a valuable complementary approach for the better understanding of the directions of metabolic reactions within a synthetic pathway, providing information about the overall spontaneity of the bio-route investigated thereby [203]–[205].

Thermodynamic feasibility can be determined from the difference in Gibbs formation energy of the reactants and products, noted $\Delta_f G'^{\circ}$. However, energy formation values of energetic intermediates, such as acetyl-CoA, are unavailable [206], [207] or difficult to estimate. In contrast, the standard Gibbs free energies of a reaction, $\Delta_r G'^{\circ}$, estimated the energy changes occurring between the reactant and product during a reaction, and taking all cofactors and energy

molecules (ATP) into account. $\Delta_r G^{o'}$ are additive values, thus the overall $\Delta_r G^{o'}$ of the complete reaction route can be determined by adding together the individual $\Delta_r G^{o'}$ of each of the several sub-reaction steps of the whole pathway. However, it provides information only about the spontaneity of a reaction under standards conditions, it does not supply any information as to whether or not the reaction will actually occur under physiological conditions, neither about the rate of the reaction or its mechanism.

In the following section, the thermodynamic feasibility analyses of the glucose/acetate and glucose/ethanol routes for the production of citramalate were determined by dividing the complete route into three main sub-reaction systems, and by calculating their respective $\Delta_r G^{o'}$. The global $\Delta_r G^{o'}$ for each alternative carbon source pathway was then further calculated by adding together the $\Delta_r G^{o'}$ of each of the three sub-reaction systems. The three sub-systems are as follows: the glycolysis sub-system, which expresses the formation of pyruvate from glucose, the ethanol or acetate route sub-system, expressing the formation of acetyl-CoA from either ethanol or acetate, and finally the citramalate synthesis sub-system, expressing the condensation of pyruvate and acetyl-CoA into citramalate.

6.2 Acetate and glucose co-consumption route for (*R*)-citramalate production

The MetaCyc Database [196] was searched for the standard Gibbs free energy of the reaction for the conversion of acetate to acetyl-

CoA. In the search tool for reaction, we requested acetate and ATP as reactants and acetyl-CoA as product. Two reactions were given as results: in the first reaction given ATP is hydrolysed to ADP, while in the second reaction given the ATP is fully hydrolysed to AMP.

In Chapter 4, we selected AckA-Pta for the construction of an acetate catalytic route in *E. coli*. AckA-Pta catalytic activity is coupled with the hydrolysis of ATP to ADP and pyrophosphate, Pi. Therefore, from the MetaCyc propositions, we selected the reaction paired with the formation of ADP only. The associated standard Gibbs free energy of reaction given was + 1.24 kJ/mol. Therefore, the conversion of acetate is energy consuming.

Fortunately, the glycolysis is a highly exergonic route with an overall estimated $\Delta G^{o'}$ value of -96 kJ/mol.

Furthermore, MetaCyc reported a $\Delta G^{o'}$ value of -43 kJ/mol for the citramalate synthase reaction.

To assess the complete $\Delta_r G^{o'}$ of a glucose and acetate co-utilisation route, the stoichiometry of the system needed to be taken into account. For each molecule of glucose going into the glycoslysis, two molecules of acetate need to be converted into two acetyl-CoA, which yields two molecules of citramalate. Therefore, in the overall $\Delta_r G^{o'}$ calculation, the $\Delta_r G^{o'}$ values of the acetyl-CoA and citramalate reactions needed to be counted twice. Thus, the overall $\Delta_r G^{o'}$ of the glucose and acetate co-consumption route for the production of citramalate yielded a $\Delta_r G^{o'}$ value of – 176.38 kJ/mol (Table 9).

Table 9: Standard Gibbs Free energy calculated for each part of the glucose and acetate co-consumption pathway for citramalate production

Name	Net Reaction	ΔrG'° MetaCyc (kJ/mol)
Glycolysis	Glucose + $2Pi^{2-}$ + $2ADP^{4-}$ + 2 NAD^+ => 2 Pyruvate + $2ATP^{4-}$ +2NADH, H^+ + $2H_2O$	- 96
Acetate ⇔ Acetyl-CoA	Acetate+ HS-CoA + ATP ⇔ Acetyl-CoA + ADP + P_i	+ 1.24
Citramalate conversion	Pyruvate + Acetyl-CoA +H_2O => Citramalate + HS-CoA	-41.43
Overall reaction	**Glucose + 2 Acetate + 2 NAD^+ => 2 Citramalate + 2NADH, H^+**	**- 96 + 2 x (+ 1.24) + 2 x (– 41.43) = -176.38**

The global $\Delta_rG^{o'}$ value estimated for the glucose and acetate co-consumption route for citramalate production described a thermodynamically feasible pathway. Therefore, this acetate route was confirmed as feasible and was incorporated into a citramalate producing *E. coli* strain.

6.3 Ethanol and glucose co-consumption route for (*R*)-citramalate production

Similar thermodynamic considerations were performed using ethanol as the starting point of the pathway for citramalate production.

In order to use the appropriate $\Delta_rG^{o'}$ value, the MetaCyc Database was searched for thermodynamic values of the oxidation of ethanol to acetaldehyde and the oxidation of acetaldehyde to acetate, both paired to the reduction of NAD^+ (Table 10). Standard Gibbs free energy value of + 12.9 kJ/mol was given for the oxidation of ethanol to acetaldehyde, which was concluded as endergonic, while the

oxidation of acetaldehyde to acetate yielded a $\Delta_r G^{o'}$ value of – 63.54 kJ/mol. Thus, the oxidation of ethanol to acetate corresponded to a thermodynamic feasible reaction, with a $\Delta_r G^{o'}$ of – 50.64 kJ/mol.

Table 10: Standard Gibbs free energy calculated for each part of the glucose and ethanol co-consumption pathway for citramalate production

Name	Net Reaction	ΔrG'° MetaCyc (kJ/mol)
Glycolysis	Glucose + $2Pi^{2-}$ + $2ADP^{4-}$ + 2 NAD^+ => 2 Pyruvate + $2ATP^{4-}$ +2NADH, H^+ + $2H_2O$	- 96
Ethanol ⇔Acetaldehyde	Ethanol + NAD^+ +H_2O => Acetaldehyde + NADH, H^+	+ 12.9
Acetaldehyde ⇨ Acetate	Acetaldehyde + NAD^+ +H_2O => Acetate + NADH, H^+	- 63.54
Acetate ⇔Acetyl-CoA	Acetate+ HSCoA + ATP ⇔ Acetyl-CoA + ADP + P_i	+ 1.24
Citramalate conversion	Pyruvate + Acetyl-CoA +H_2O => Citramalate + HS CoA	-41.43
Overall reaction	**Glucose + 2 Ethanol + 6NAD^+ + 4 H_2O => 2 Citramalate + 6NADH, H^+**	**- 96 + 2 x (+ 12.9) + 2 x (- 63.54) + 2 x (– 41.43) = -280.14**

To complete the overall $\Delta_r G^{o'}$ of the ethanol co-consumption route, we used the $\Delta_r G^{o'}$ calculated previously for the further oxidation of acetate to acetyl-CoA (see Section 6.2). Then, a global $\Delta_r G^{o'}$ value of – 280.14 kJ/mol for the ethanol co-consumming pathway was finally calculated (Table 10) after consideration of the stoichiometry of the overall pathway.

6.4 Conclusions

From a thermodynamic perspective, we concluded that both acetate or ethanol offered highly energetic feasible routes for the bio-production of citramalate. Furthermore, the $\Delta_r G'^{\circ}$ calculations confirmed that using acetate as the substrate was energetically less favourable compared to ethanol. Indeed, converting acetate to acetyl-CoA required the consumption of 1 ATP. In contrast, oxidising one molecule of ethanol yields 2 NADH, which can generate 6 ATP through the respiratory chain of *E. coli*. The further conversion of the acetate formed consumed 1 ATP, resulting in a net production of 5 ATP per ethanol consumed.

In conclusion, the potential of the two biosynthetic routes selected in this project for the glucose co-utilisation with acetate or ethanol was confirmed by overall highly favourable $\Delta_r G'^{\circ}$ values in each scenario. Therefore, the genes encoding either the acetate or ethanol assimilation routes were cloned and expressed in a citramalate-producing *E. coli* strain. Further tests will be performed in the next sections in order to confirm the preliminary results obtained from thermodynamic estimations.

7. Construction of the production strain

7.1 Host strain and expression plasmid selection

To examine the feasibility and efficiency of co-utilisation of alternative carbon sources with glucose for the bio-production of (*R*)-citramalate, the (*R*)-citramalate producing strain, that was previously successfully constructed in our laboratory [7], [208], was further engineered. Moreover, it was decided to use the same *E. coli* strain as host organism also to ensure comparison between the previous metabolic engineering done [7] and the ones performed in this body of work.

The gene encoding the citramalate synthase, *cimA3.7*, had been previously cloned in the pBAD24 expression vector, which yielded high expression and activity levels of the recombinant protein [7]. Therefore, both expression vector and induction systems were conserved, and used for the cloning of the additional genes to build either an acetate or ethanol assimilation pathway. Furthermore, cloning all the genes on the same plasmid avoided the use of multiple antibiotic and induction systems.

The pBAD24 expression vector is a low copy number plasmid and contains the promoter of the *araBAD* operon responsible for the arabinose metabolism. Plasmids of pBAD24 are meant to be cloned into strain of *E. coli* bearing inactivated arabinose metabolism (Δ*araD-araB)*. Thus, the expression of the target proteins is only triggered upon the addition of the inducer, arabinose, allowing to start the expression of the recombinant enzymes at the desired time in the process [154].

In the previous study, the host strain used was *E. coli* BW25113 Δ*pflB* Δ*ldhA*, but work in our laboratory showed that the strain had a tendency to foam (S. J. HALL, personal communication). However, when using *E. coli* BW25113 with only the deletion of *ldhA*, it removed the foaming problem. Thus, for the continuation of the present work, *E. coli* BW25113 and *E. coli* BW25113 Δ*ldhA* were used.

7.2 Cloning of the acetate consuming route using the pBAD24 expression system

7.2.1 Construction of the AckA-Pta route into pBAD24

The genes encoding the acetate route, *ackA-pta*, were cloned into the pBAD24 plasmid on their own as an operon, and also upstream of *cimA3.7* (Fig. 16A-B).

In previous work, the *cimA3.7* gene was cloned into pBAD24 using *Nhe*I and *Hind*III restriction sites, consequently removing the original ribosome binding site (RBS) of the expression vector, as well as all the restriction sites of the multiple cloning site (MCS). Thus, in order to insert the acetate route encoding genes upstream to *cimA3.7*, an additional restriction site was needed. Therefore, a PCR-modified insert containing *cimA3.7* with the upstream restriction site of *Nhe*I changed to *Sph*I was produced using the 5' *cimA3.7* pBAD primer (Table 7). The original optimised RBS sequence followed by an 8 bp spacing sequence, located upstream of the start codon of *cimA3.7,* was conserved. This small 8 bp spacing sequence ensured enough

space for optimal binding of the RNA polymerase onto the DNA, and consequently optimal gene transcription [7], [209], [210].

Tashiro and co-workers extracted the native operon encoding acetate kinase–phosphotransacetylase (*ackA-pta*) from the genomic DNA of wild-type strain of *E. coli* MG1655 by PCR amplification. The same technique was then used in this project. The only changes were the introduction of the restriction sites *Nhe*I and *Hind*III upstream and downstream to the *ackA-pta* operon using the forward and reverse primers, 5'-*ackA-pta* pBAD and 3'-*ackA-pta* pBAD, respectively (Table 7). The same RBS sequence (AGGAGG) as previously used in the initial expression vector of pBAD24-*cimA3.7* [7] was also inserted before the start codon of the *ackA* gene by the forward primer, 5'-*ackA-pta* pBAD. The reverse primer, 3'-*ackA-pta* pBAD, contained also the *Sph*I restriction site upstream to the *Hind*III to enable the insertion of the *cimA3.7* gene (Table 7). *Sph*I and *Hind*III were separated with a small spacing sequence to ensure proper cutting during enzyme digestion, as well as conservation of the restriction sites while performing ligations. Following this, the PCR insert containing the *ackA-pta* operon was double digested with *Nhe*I/*Hind*III and purified, before to be inserted into the pre-digested pBAD24 to form pBAD24-*ackA-pta* (Fig. 16A).

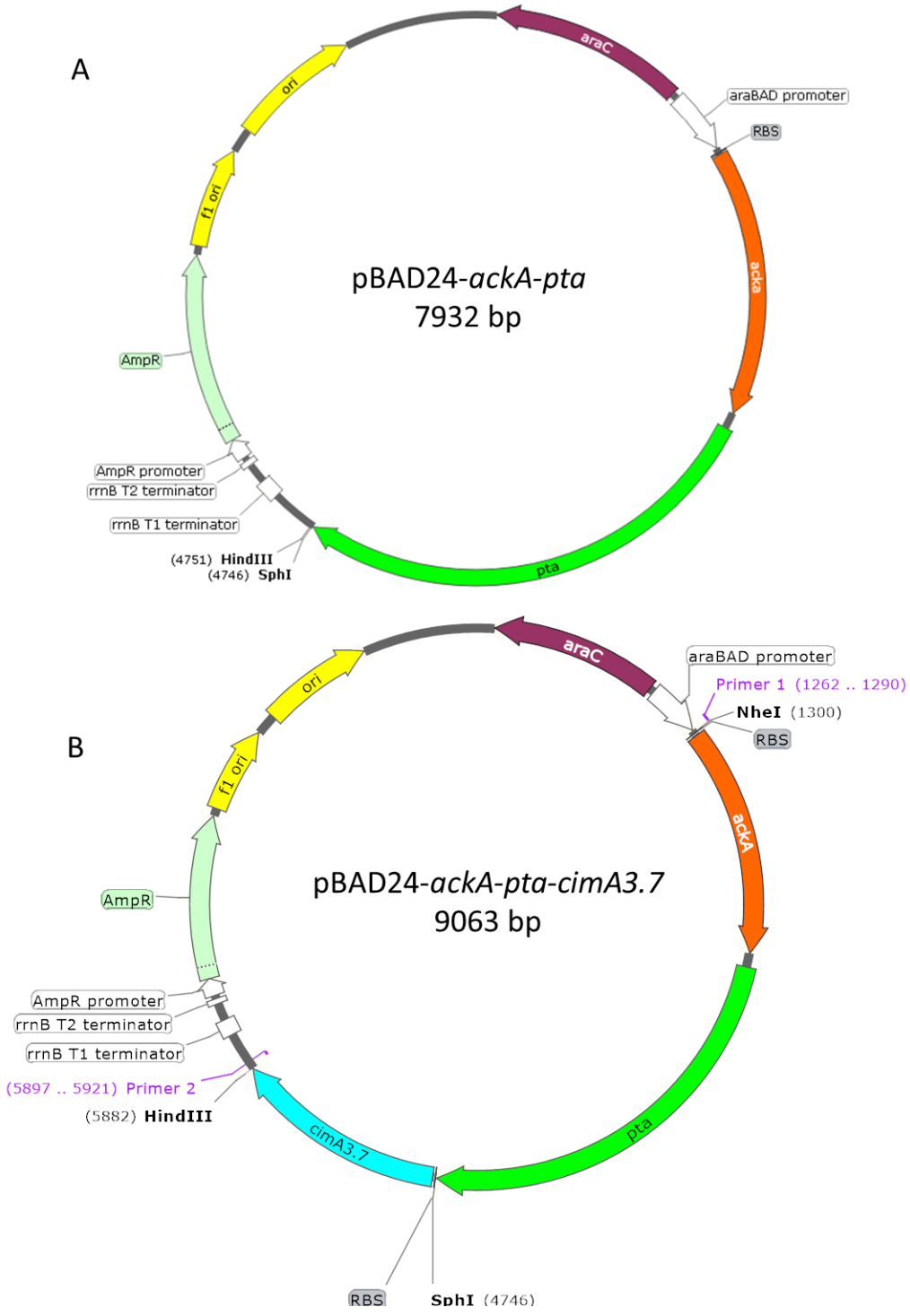


Figure 16: pBAD24-*ackA-pta* (A) and pBAD24-*ackA-pta-cimA3.7* (B) expression vectors maps

The PCR modified *cimA3.7* insert was then inserted into the previously made pBAD24-*ackA-pta* to form pBAD24-*ackA-pta-cimA3.7* (Fig.

16B). These two expression plasmids were then transformed into chemically competent *E. coli* BW25113 and *E. coli* BW25113 Δ*ldhA* (Table 11). A control strain of *E. coli* BW25113 transformed with the empty pBAD24 expression vector was also produced [28], [211].

Table 11: Table of expression strains constructed

Expression strain	Expression plasmid
E. coli BW25113	Empty pBAD24
E. coli BW25113 Δ*ldhA*	pBAD24-*ackA-pta*
	pBAD24-*ackA-pta-cimA3.7*

Cryostocks were prepared for each transformants, and the presence of the pBAD24 derived plasmids was confirmed by colony PCR. Gene inserts were sequenced to ensure that no mutations had been generated during the cloning.

7.2.2 Optimisation of the expression of the *ackA-pta* genes from pBAD24

The expression of the acetate kinase (AckA), phosphate acetyltransferase (Pta) and citramalate synthase (CimA3.7) from strains of *E. coli* BW25113 Δ*ldhA* pBAD24-*ackA-pta* and *E. coli* BW25113 Δ*ldhA* pBAD24-*ackA-pta-cimA3.7* was tested.

E. coli BW25113 Δ*ldhA* pBAD24-*ackA-pta, E. coli* BW25113 Δ*ldhA* pBAD24-*ackA-pta-cimA3.7* and the control strain of *E. coli* BW25113 with an empty pBAD24 were grown at 30°C or 37°C in Lund medium

supplemented with glucose as carbon source and induced at an OD_{600nm} of 0.6 with 0.2% of *L*-(+)-arabinose.

In *E. coli* BW25113 Δ*ldhA* pBAD24-*ackA-pta* grown at 37°C, AckA was expressed early (2 h post-induction) and as soluble protein, while Pta started to be expressed as soluble protein after 5 h of induction (Fig. 17A). When the citramalate synthase (CimA3.7) was co-expressed with AckA and Pta in *E. coli* BW25113 Δ*ldhA* pBAD24-*ackA-pta-cimA3.7*, an overall reduction of protein expression levels was observed with Pta expression level being apparently halved (Fig. 17B).

In contrast, *E. coli* BW25113 Δ*ldhA* pBAD24-*ackA-pta* grown at 30°C showed an accumulation of insoluble Pta after 5 h of induction, while the AckA protein seemed to be mainly located in the soluble fraction (Fig. 17C). Interestingly, in *E. coli* BW25113 Δ*ldhA* pBAD24-*ackA-pta-cimA3.7,* where citramalate synthase (CimA3.7) was co-expressed, Pta became more soluble while AckA and CimA3.7 were expressed in the soluble fraction (Fig. 17D). CimA3.7 and AckA have similar size (41 and 43 kDa respectively), thus they cannot be clearly distinguished on SDS-PAGE.

From these results, it was concluded that 30°C and 0.2% of *L*-(+)-arabinose would be the culture conditions to be used for further investigation of the impact of overexpressing the genes *ackA-pta* on acetate co-assimilation with glucose by recombinant strains of *E. coli* BW25113 Δ*ldhA* pBAD24-*ackA-pta* and *E. coli* BW25113 Δ*ldhA* pBAD24-*ackA-pta-cimA3.7*.

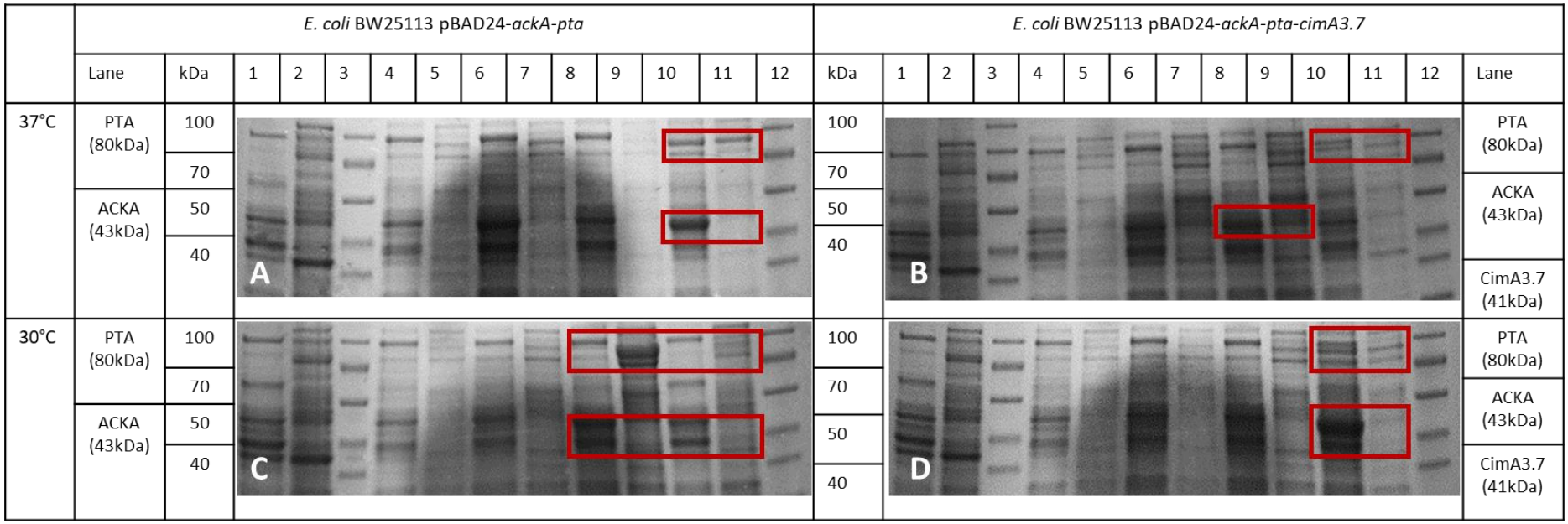


Figure 17: SDS-PAGE of soluble and insoluble AckA-Pta expressed alone (A and C) and co-expresssed with CimA3.7 (B and D) at various growth conditions

Overnight seed cultures of *E. coli* BW25113 Δ*ldhA* pBAD24-*ackA-pta* and *E. coli* BW25113 Δ*ldhA* pBAD24- *ackA-pta -cimA3.7* grown on Lund medium with glucose were used to inoculate fresh Lund medium containing glucose and incubated at 30°C or 37°C. When the OD_{600} of the 50 ml culture reached 0.4-0.6, 0.2% *L*-(+)-arabinose was added to induce protein production. Samples were taken at regular intervals to measure the OD_{600}. A control using empty pBAD24 vector was prepared in the same way. Cells were lysed using BugBuster protein extraction reagent and run on an SDS-PAGE. In all tests, a control containing an empty pBAD24 vector was prepared the same way. **Lane 1-2**: soluble and insoluble fractions of control at 24h. **Lane 3 and 12**: ladder. **Lane 4-5**: soluble and insoluble fraction of sample before induction. **Lane 6-7**: soluble and insoluble fraction of sample 2h after induction. **Lane 8-9**: soluble and insoluble fraction of sample 5h after induction. **Lane 10-11**: soluble and insoluble fraction of sample 24h after induction.

7.2.3 *In vivo* activity of the AckA-Pta assimilation route and citramalate production in flask experiments

The activity of the enzymes forming the acetate assimilation route, AckA-Pta, was directly tested in *in vivo* aerobic growth experiments of glucose and acetate in *E. coli* BW25113 Δ*ldhA* pBAD24-*ackA-pta-cimA3.7*. The aim of the experiment was, first, to confirm the ability of the engineered strain to co- use glucose and acetate, and second to demonstrate the production of citramalate.

Overnight cultures of *E. coli* BW25113 Δ*ldhA* pBAD24-*ackA-pta-cimA3.7* and the control strain of *E. coli* BW25113 pBAD24 were used to inoculate fresh Lund medium (100 ml) supplemented with glucose (1%) as sole carbon source for growth at 30°C in 500 mL flasks. Induction of expression of the plasmids was started at an OD_{600nm} of 0.6 by adding *L*-arabinose. Acetate was added directly after induction. The concentration of acetate to add was selected based on the known toxic level in wild-type *E. coli* [101]. Acetate was reported to reduce cell growth by half at concentration above 80 mM, for this initial experiment, a lower concentration of 40 mM was used.

The cultures were agitated at 250 rpm throughout the experiment. Samples were taken over 48 h, and the supernatants were analysed for concentrations of glucose, acetate, citramalate and other organic acid using by HPLC (Fig. 18).

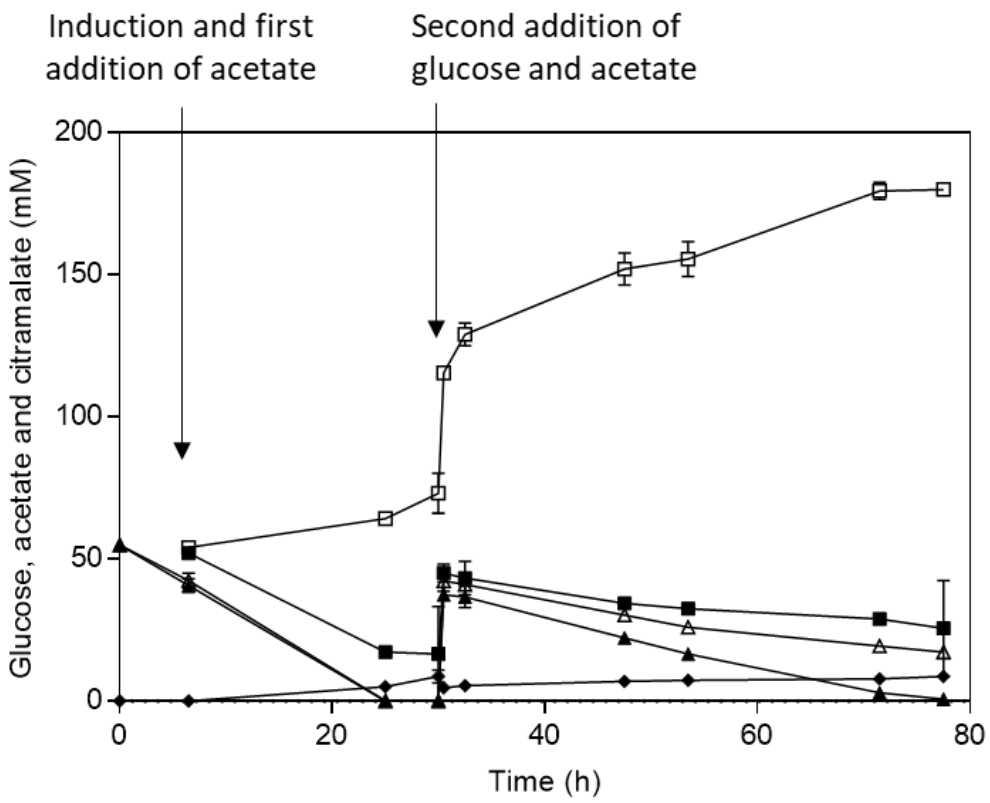


Figure 18: Citramalate production from glucose and acetate in *E. coli* BW25113 Δ*ldhA* pBAD24-*ackA-pta-cimA3.7* and *E. coli* BW25113 Δ*ldhA* with an empty pBAD24

Cultures of *E. coli* BW25113 pBAD24-*ackA-pta-cimA3.7* were grown in Lund medium containing glucose as sole carbon source. Proteins expression was induced by adding *L*-(+)-arabinose (0.2%) at an OD_{600} of 0.6-0.8. Right after induction, 40 mM acetate was supplemented to the culture medium. Samples were analysed for acetate consumption (■), glucose consumption (▲), and citramalate production (♦) using HPLC. A second addition of glucose (40 mM) and acetate (40 mM) was done at 30 h, and acetate and glucose consumptions as well as citramalate production were followed using HPLC analysis. A control experiment was performed similarly using the control strain *E. coli* containing an empty pBAD24 vector. Concentrations of acetate (□), glucose (△) were also monitored.

HPLC analysis showed that both control and *E. coli* BW25113 Δ*ldhA* pBAD24-*ackA-pta-cimA3.7* consumed all the glucose initially added to the medium within 25 h (Fig. 18). At the induction point, about 6 h

after inoculation, the glucose concentration remaining in the medium was about 40 mM, to which 40 mM of acetate was added. Over the 20 following hours, glucose and acetate were simultaneously consumed by *E. coli* BW25113 Δ*ldhA* pBAD24-*ackA-pta-cimA3.7*, while in the control strain only glucose was used and acetate accumulated. Interestingly, the rate of glucose consumption remained the same, 1.80 mM/h, before and after the induction point in both control and *E. coli* BW25113 Δ*ldhA* pBAD24-*ackA-pta-cimA3.7* strains. The successful integration of the acetate pathway within the host strain was also demonstrated in the growth profile of the AckA-Pta recombinant strain (Appendix 11.10). Indeed, both control and AckA-Pta overexpressing strains had the same growth profile throughout the pre-induction period. Post-induction, *E. coli* BW25113 Δ*ldhA* pBAD24-*ackA-pta-cimA3.7* showed a growth rate about 1.5-fold higher compared to the control strain, 0.15 h^{-1} and 0.1 h^{-1}, respectively (Appendix 11.10). As both cultures were supplemented with the same amount of glucose and acetate, it was concluded that acetate was successfully used as a carbon source, simultaneously with glucose by *E. coli* BW25113 Δ*ldhA* pBAD24-*ackA-pta-cimA3.7*, consequently enhancing the production of biomass. These assumptions were confirmed by the HPLC results showing the decrease of acetate concentration in the cultures of *E. coli* BW25113 Δ*ldhA* pBAD24-*ackA-pta-cimA3.7* (Fig. 18).

The second aim of this flask assay was to confirm the production of citramalate from the co-utilisation of both carbon sources. HPLC results showed that the CimA3.7 expressing strain yielded in average

a titre of 8.73 mM ±0.58 of (*R*)-citramalate at the end of the first 24 h (Fig. 18). Thus, it confirmed the production of citramalate while co-consuming glucose and acetate.

To assess if citramalate production continued in stationary phase, a fresh bolus of glucose (40 mM) and acetate (40 mM) were added 30 h after inoculation, once glucose was depleted. The control strain kept accumulating acetate, while consuming glucose at a slower rate compared to the first phase of the experimentation. Acetate accumulated to concentrations above 84 mM and up to 180 mM (10 g/L), which were reported as toxic concentrations for the cells. Therefore, it was concluded that the decrease in the glucose consumption rate was due to growth inhibitory effects generated from the elevated acetate concentrations in the control strain cultures. In contrast, *E. coli* BW25113 Δ*ldhA* pBAD24-*ackA-pta-cimA3.7* consumed the acetate and glucose together. In cultures of *E. coli* BW25113 Δ*ldhA* pBAD24-*ackA-pta-cimA3.7*, all the glucose was consumed by the end of the experiment (Fig. 18), while about half the acetate added was left in the control strain. It was assumed that the accumulation of acetate above the reported toxicity level impaired the cells growth and metabolism in the control strain.

It was demonstrated that *E. coli* BW25113 Δ*ldhA* pBAD24-*ackA-pta-cimA3.7* continued to co-consume glucose and acetate and produce citramalic acid in stationary phase.

Thus, AckA-Pta route was demonstrated as a suitable pathway for the bio-production of citramalate by co-consuming glucose and acetate.

7.3 Cloning of the ethanol consuming route using the pBAD24 expression system

7.3.1 Construction of the ADH I-ALDH A and ADH A-ALDH routes into pBAD24

The genes for the ethanol routes were also constructed as operons in pBAD24 in a similar manner as the AckA-Pta route (Fig. 19A-B). The same restriction sites sequences upstream (*Nhe*I) and downstream the ethanol operon (SphI and *Hind*III), as well as RBS and spacing sequences were used.

Genes of *alcA*, *aldA*, *adhA* and *ALDH* were custom synthesized and codon optimized for overexpression in *E. coli* by BioMatik corporation USA. Genes were ordered already associated in pairs: *alcA* and *aldA* as one of the operons for testing, and *adhA* and *ALDH* as a second operon. As described previously, the *Sph*I restriction site located after the stop codon of the acetaldehyde dehydrogenase gene of each operon, *aldA* and *ALDH* respectively, was added for the later addition of the PCR-modified *cimA3.7* insert (Fig. 20A-B).

The inserts with the different ethanol operons from each cloning vector were extracted from their plasmids of origin using double digestion with *Nhe*I/*HindIII*, and transferred into pre-digested pBAD24 to produce pBAD24-*alcA*-*aldA*, and pBAD24-*adhA*-*aldh* (Fig. 19A-B).

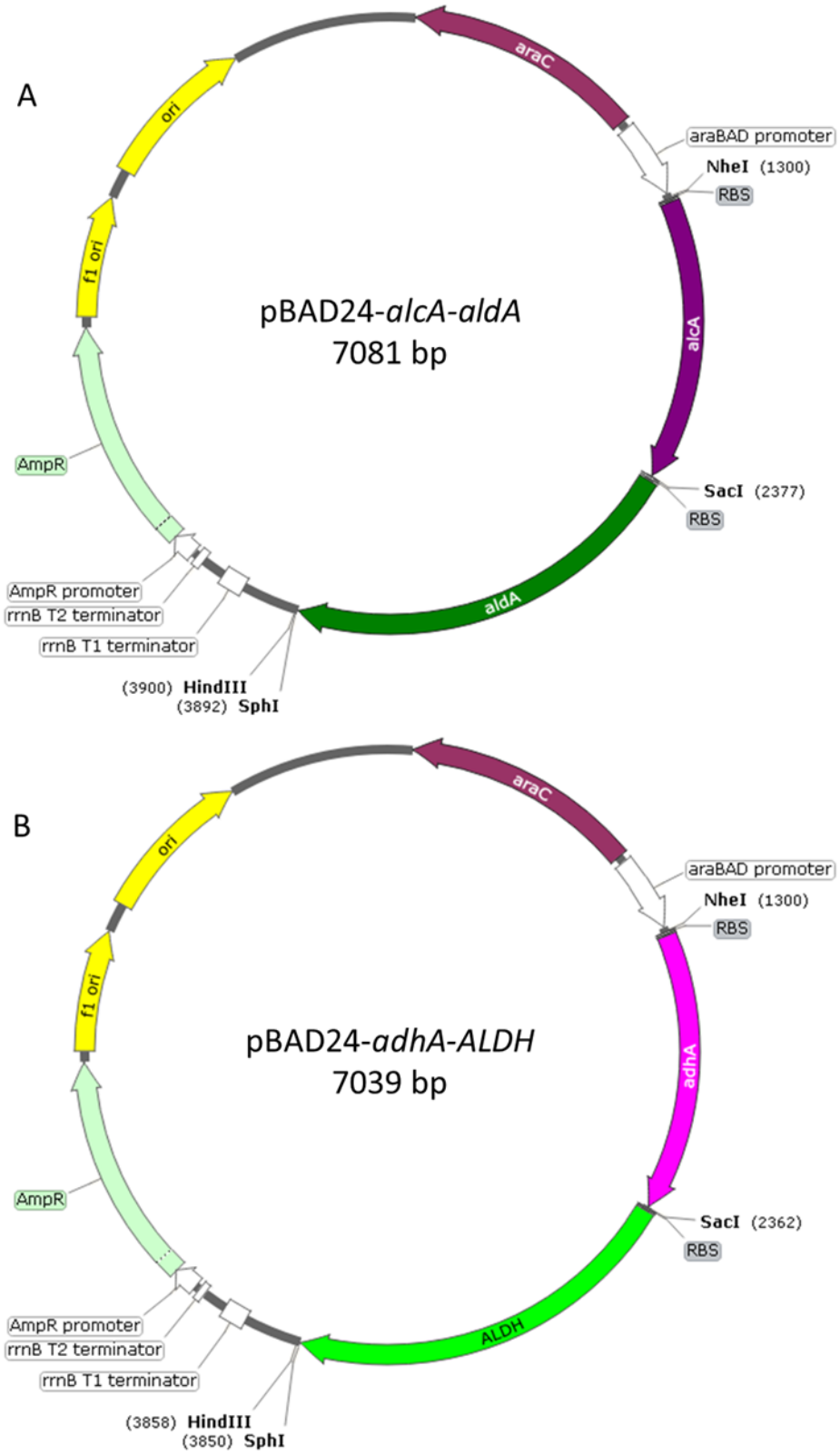


Figure 19: pBAD24-*alcA-aldA* (A) and pBAD24-*adhA-ALDH* (B) expression vectors maps

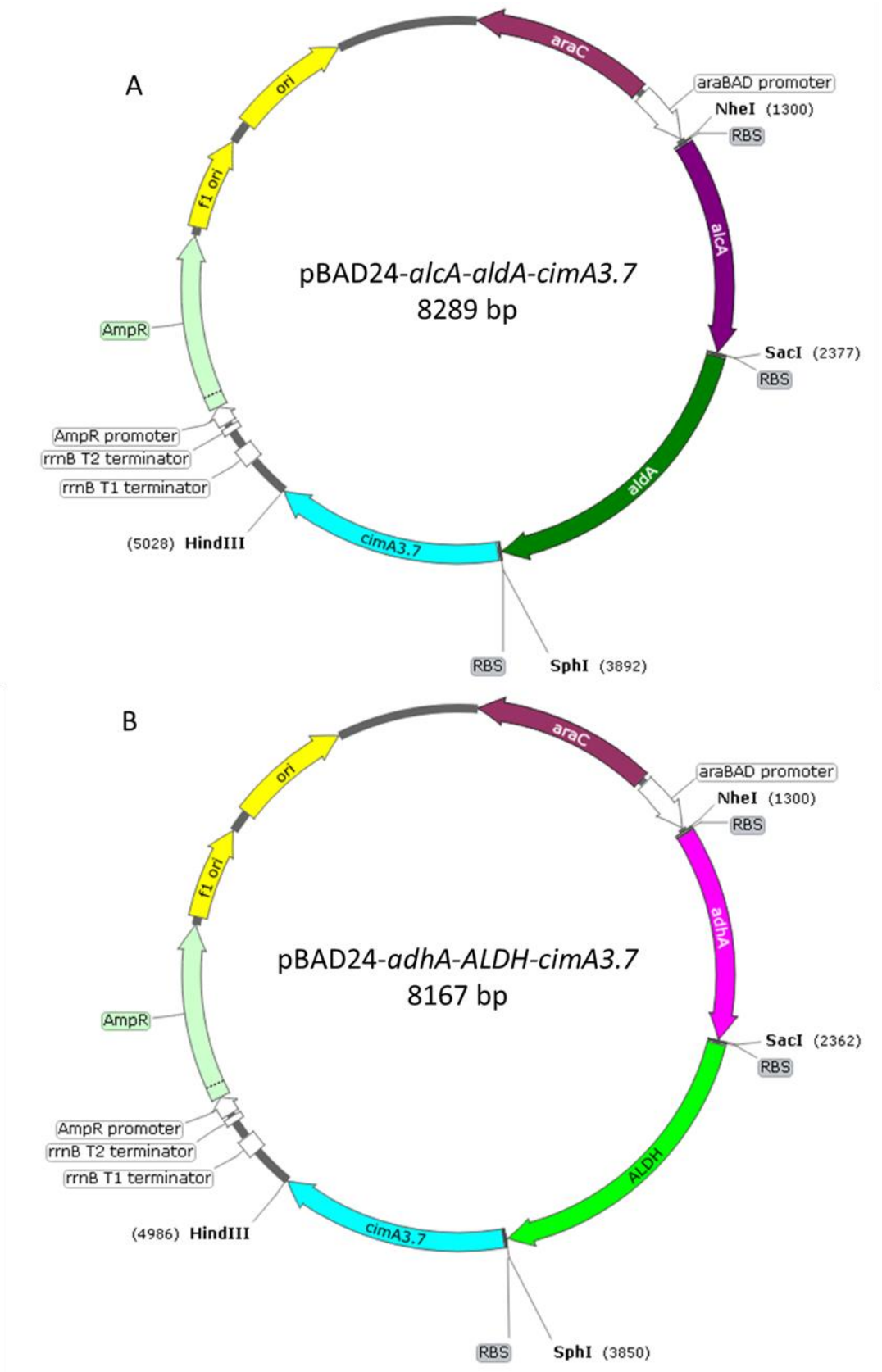


Figure 20: pBAD24-*alcA-aldA-cimA3.7* (A) and pBAD24-*adhA-ALDH-cimA3.7* (B) expression vectors maps

The PCR modified *cimA3.7* insert was then inserted into the previously made pBAD24-*alcA-aldA* and pBAD24-*adhA-ALDH* to form pBAD24-*alcA-aldA-cimA3.7* and pBAD24-*adhA-ALDH-cimA3.7*, respectively (Fig. 20A-B).

These expression plasmids were then transformed into chemically competent *E. coli* BW25113 and *E. coli* BW25113 Δ*ldhA* (Table 12).

Table 12: Table of expression strains constructed

Expression strain	Expression plasmid
E. coli BW25113	Empty pBAD24
E. coli BW25113 Δ*ldhA*	pBAD24-*alcA-aldA*
	pBAD24- *adhA-aldh*
	pBAD24- *alcA-aldA -cimA3.7*
	pBAD24- *adhA-aldh -cimA3.7*

7.3.2 Expression of the proteins ADH I-ALDH A and ADH A-ALDH

All strains bearing an ethanol consuming route on their own or coupled with CimA3.7, as well as the control strain, were grown using different temperatures (37°C, 30°C and 25°C) and inducer concentrations (0.2% and 0.02%) in order to determine the best conditions for expression of soluble proteins. Glycerol was first used as carbon source in the growth medium to prevent glucose catabolite repression from occurring and repressing expression from the pBAD24 promoter [212]. Recombinant protein expression was induced at OD_{600nm} of 0.6-0.7 by the addition of *L*-arabinose. The cells

were treated with BugBuster protein extraction reagent to extract the proteins, and the resulting soluble and insoluble fractions were run on SDS-PAGE to analyse both the protein expression level and solubility.

Performing growth and expression assays with glycerol as sole carbon source on minimal medium resulted in the production of insoluble proteins, despite changes made in temperature and inducer concentrations (Data sample given in Appendix 11.11). This growth condition was deemed inappropriate for expression of the proteins. Therefore, all the following expression assays were carried out using glucose instead of glycerol as carbon source.

Growth at 37°C of strains expressing either pBAD24-*alcA*-*aldA* or pBAD24-*alcA*-*aldA*-*cimA3.7* on minimal medium supplemented with glucose yielded mainly insoluble proteins whatever the concentration of *L*-arabinose added (Table 13). Growth at 30°C with the addition of 0.2% of *L*-arabinose improved the solubility of the proteins (Fig. 21). Although lowering the temperature to 30°C increased the solubility of the aldehyde dehydrogenase, ALDH A, half of the protein expressed remained insoluble. Unfortunately, lowering the temperature to 25°C did not improve further the solubility of any of the protein, but mainly resulted in drastically diminishing the overall level of expression as well as significantly decreasing the growth rate. For those reasons, conditions of 30°C and 0.2% of *L*-arabinose were selected for the growth of *E. coli* BW25113 pBAD24-*alcA*-*aldA* and *E. coli* BW25113 pBAD24-*alcA*-*aldA*-*cimA3.7.*

Table 13: Determination of the solubility of recombinant proteins of ADH I, ALDH A, ADH A, ALDH and citramalate synthase CimA3.7 in SDS-PAGE of *E. coli* BW25113 Δ*ldhA* grown under various conditions

Conditions		37°C				30°C				25°C			
		alcA-aldA	***alcA-aldA-cimA3.7***	***adhA-ALDH***	***adhA-ALDH-cimA3.7***	***alcA-aldA***	***alcA-aldA-cimA3.7***	***adhA-ALDH***	***adhA-ALDH-cimA3.7***	***alcA-aldA***	***alcA-aldA-cimA3.7***	***adhA-ALDH***	***adhA-ALDH-cimA3.7***
0.2% arabinose	ADH	I	I	I	N/A	S+I	S+I	-	S+I	Poor overall expression levels			
	ALDH	I	I	I		S+I	S+I	S	S+I				
	CimA3.7	-	I	-		-	S+I	-	S+I				
0.02% arabinose	ADH	I	I	I	S+I	I	S+I	-	-				
	ALDH	S+I	I	I	S+I	I	S+I	-	-				
	CimA3.7	-	I	-	S+I	-	S+I	-	-				

E. coli BW25113 strains containing either pBAD24-*alcA-aldA*, pBAD24-*alcA-aldA-cimA3.7,* pBAD24-*adhA-ALDH* or pBAD24-*adhA-ALDH* were inoculated into 20ml Lund medium containing glucose as carbon source, overnight. This seed culture was used to inoculate a further 50 ml of Lund medium with glucose. When the OD_{600} of the 50 ml culture reached 0.4-0.6, 0.2% or 0.02% of *L*-(+)-arabinose was added to induce protein production. Samples were taken at regular intervals to measure the OD_{600}. A control using empty pBAD24 vector was prepared in the same way. Cells were lysed using BugBuster protein extraction reagent and run on an SDS-PAGE. S: soluble protein; I: insoluble protein.

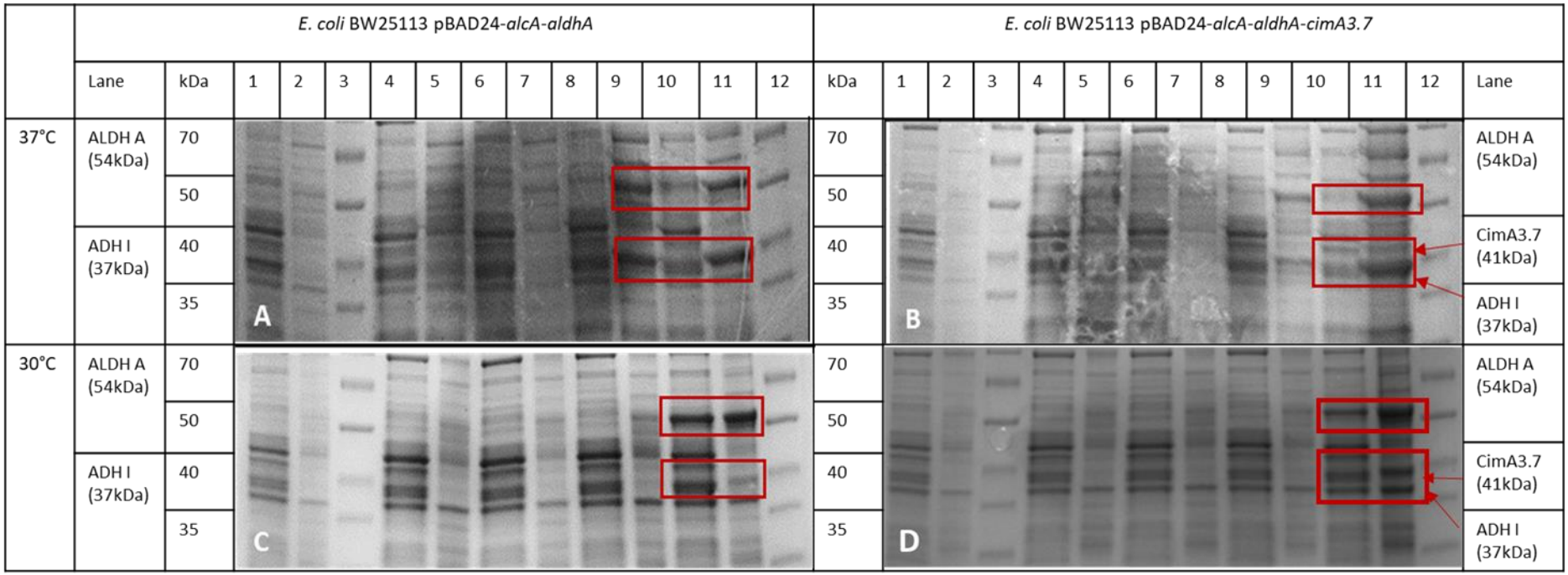


Figure 21: SDS-PAGE of soluble and insoluble ADH I – ALDH A expressed alone (A and C) and co-expressed with CimA3.7 (B and D) at various growth conditions

Overnight seed cultures of *E. coli* BW25113 Δ*ldhA* pBAD24-*alcA-aldA* and *E. coli* BW25113 Δ*ldhA* pBAD24-*alcA-aldA-cimA3.7* grown on Lund medium with glucose were used to inoculate fresh Lund medium containing glucose and incubated at 30°C or 37°C. When the OD_{600} of the 50 ml culture reached 0.4-0.6, 0.2% *L*-(+)-arabinose was added to induce protein production. Samples were taken at regular intervals to measure the OD_{600}. A control using empty pBAD24 vector was prepared in the same way. Cells were lysed using BugBuster protein extraction reagent and run on an SDS-PAGE. In all tests, a control containing an empty pBAD24 vector was prepared the same way. **Lane 1-2**: soluble and insoluble fractions of control at 0h. **Lane 3 and 12**: ladder. **Lane 4-5**: soluble and insoluble fraction of sample before induction. **Lane 6-7**: soluble and insoluble fraction of sample 4h after induction. **Lane 8-9**: soluble and insoluble fraction of sample 18h after induction. **Lane 10-11**: soluble and insoluble fraction of sample 24h after induction.

In *E. coli* BW25113 pBAD24-*adhA-ALDH* and *E. coli* BW25113 pBAD24-*adhA-ALDH-cimA3.7*, poor overall protein expression was obtained, with the proteins being insoluble, whatever the temperature or concentration of inducer tested (Table 13 & Fig. 22). Nevertheless, expression carried out at 30°C with 0.2% of *L*-arabinose yielded slightly more soluble proteins, but with a remaining poor overall expression level.

It was concluded that 30°C and 0.2% of *L*-(+)-arabinose provided the more appropriate growth conditions for *E. coli* BW25113 pBAD24-*alcA-aldA, E. coli* BW25113 pBAD24-*alcA-aldA-cimA3.7., E. coli* BW25113 pBAD24-*adhA-ALDH* and *E. coli* BW25113 pBAD24- *adhA-ALDH-cimA3.7* when grown on glucose, to produce reasonably soluble alcohol dehydrogenases, acetaldehyde dehydrogenases and citramalate synthase.

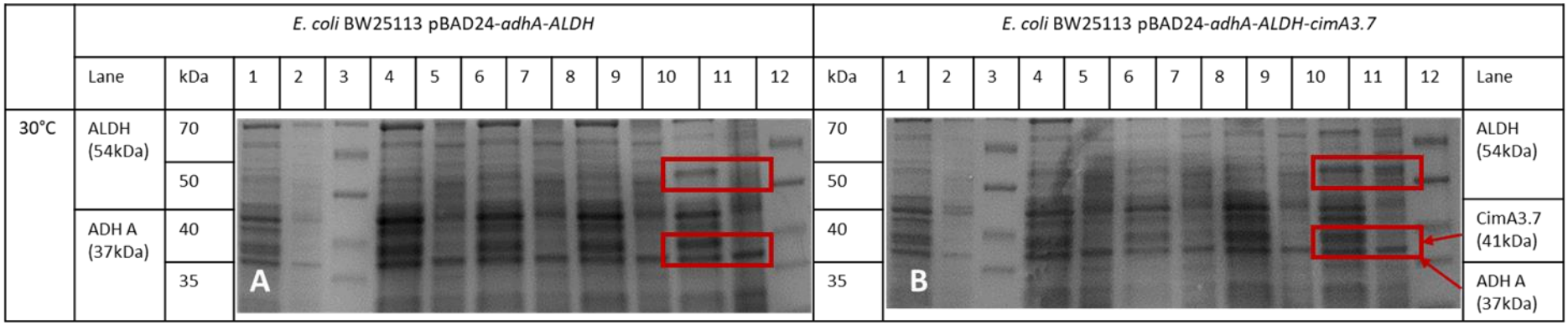


Figure 22: SDS-PAGE of soluble and insoluble ADH A - ALDH expressed alone (A) and co-expressed with CimA3.7 (B) at 30°C.

E. coli BW25113 Δ*ldhA* pBAD24-*adhA-ALDH* (A) and *E. coli* BW25113 Δ*ldhA* pBAD24- *adhA-ALDH -cimA3.7* (B) grown on Lund medium with glucose were used to inoculate fresh Lund medium containing glucose. When the OD_{600} of the 50 ml culture reached 0.4-0.6, 0.2% *L*-(+)-arabinose was added to induce protein production. Samples were taken at regular intervals to measure the OD_{600}. A control using empty pBAD24 vector was prepared in the same way. Cells were lysed using BugBuster protein extraction reagent and run on an SDS-PAGE. In all tests, a control containing an empty pBAD24 vector was prepared the same way. **Lane 1-2**: soluble and insoluble fractions of control at 0h. **Lane 3 and 12**: ladder. **Lane 4-5**: soluble and insoluble fraction of sample before induction. **Lane 6-7**: soluble and insoluble fraction of sample 4h after induction. **Lane 8-9**: soluble and insoluble fraction of sample 18h after induction. **Lane 10-11**: soluble and insoluble fraction of sample 24h after induction

7.3.3 *In vitro* enzyme assays

After cloning and expressing the genes of interest in *E. coli* BW25113, the next step was to characterise the recombinant enzymes using spectrophotometric assays.

7.3.3.1 Alcohol dehydrogenases enzyme assays

Cultures (100 ml) of *E. coli* BW25113 pBAD24-*alcA-aldA-cimA3.7*, *E. coli* BW25113 pBAD24-*adhA-ALDH-cimA3.7* and *E. coli* BW25113 pBAD24 were incubated for 5 h at 30°C after induction with *L*-arabinose. Cells were then harvested by centrifugation, and cell free extracts were prepared for each culture. As a negative control, independent activity assays were performed on crude extracts from the control strain containing the empty plasmid, pBAD24.

Extract of *E. coli* BW25113 pBAD24-*alcA-aldA-cimA3.7* contained alcohol dehydrogenase activity, confirming the activity of ADHI (Fig. 23).

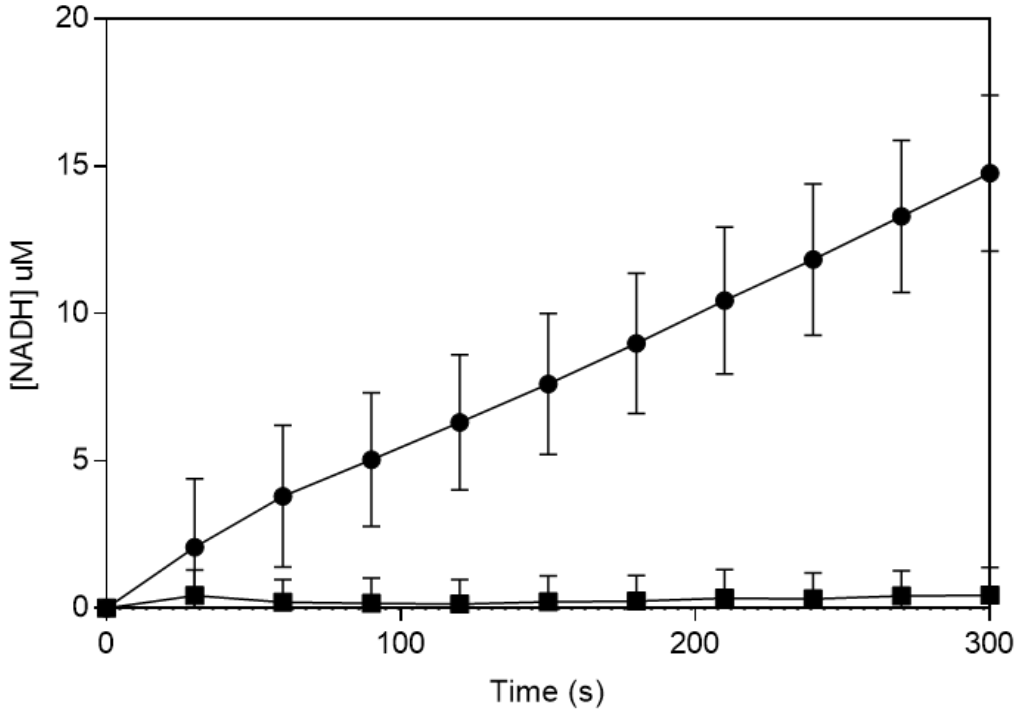


Figure 23: Alcohol dehydrogenase (ADH I) oxidation assay

Overnight cultures of *E. coli* BW25113 Δ*ldhA* pBAD24-*alcA-aldA-cimA3.7* and control strain of *E. coli* BW25113 Δ*ldhA* pBAD24 grown on Lund medium with glucose was used to inoculate fresh Lund medium containing glucose. When the OD_{600} of the 50 ml culture reached 0.4-0.6, 0.2% *L*-(+)-arabinose was added to induce protein production. The cells were harvested 4h post-induction and resuspended in TES buffer (0.1M, pH8). Crude extracts were prepared using cell disruption and cell debris were removed by centrifugation. Crude extracts were used on the day and stored on ice during the duration of the activity assays. The assay used to monitor the oxidation activity of ADH I was based upon the rate of increase in absorbance at 340 nm when cofactor NAD+ is reduced to NADH. The assay was conducted with ethanol (10 mM) and NAD^+ (1 mM) using extracts of *E. coli* BW25113 Δ*ldhA* pBAD24-*alcA-aldA-cimA3.7* expressing ADH I (●). A control using *E. coli* BW25113 containing an empty pBAD24 vector with ethanol (10 mM) and NAD (1 mM) was prepared, (■). Total protein concentration of the mixture was assayed using DC assay and estimated to 0.124mg of protein. Results represent the average of three repeated experiments.

As expected, no alcohol dehydrogenase was detected in the control reactions containing crude extract from an empty pBAD24 vector control strain (Fig. 23). Initial activity for ADH I was calculated to be

23.8 µmol of NADH formed/min/mg (23.8 U/mg), which is consistent with the literature [125], [147]. Although the reaction mixtures were blanked before starting the experiment, a slight delay in the absorbance reading was observed. This was due to technical reasons caused by the short time needed to add the enzyme to the reaction mix and start reading the absorbance.

The reduction of acetaldehyde by extract of *E. coli* BW25113 Δ*ldhA* pBAD24-*alcA*-*aldA*-*cimA3.7* was faster than the oxidation reaction, as all the NADH had been consumed within less than 2 minutes (Fig. 24). This was consistent with published data, as the reverse reaction is known to be preferential [147].

However, an acetaldehyde reduction activity was detected in the control strain. Furthermore, control assays in which no crude extract was used, showed that there was no spontaneous oxidation of NADH to NAD^+ (data not shown). The reduction observed in both crude extract samples from recombinant and control strains was due to the activity of a native enzyme present in the crude extract. Further tests were performed to identify activity of native enzymes either catalysing the reduction of acetaldehyde or using NADH.

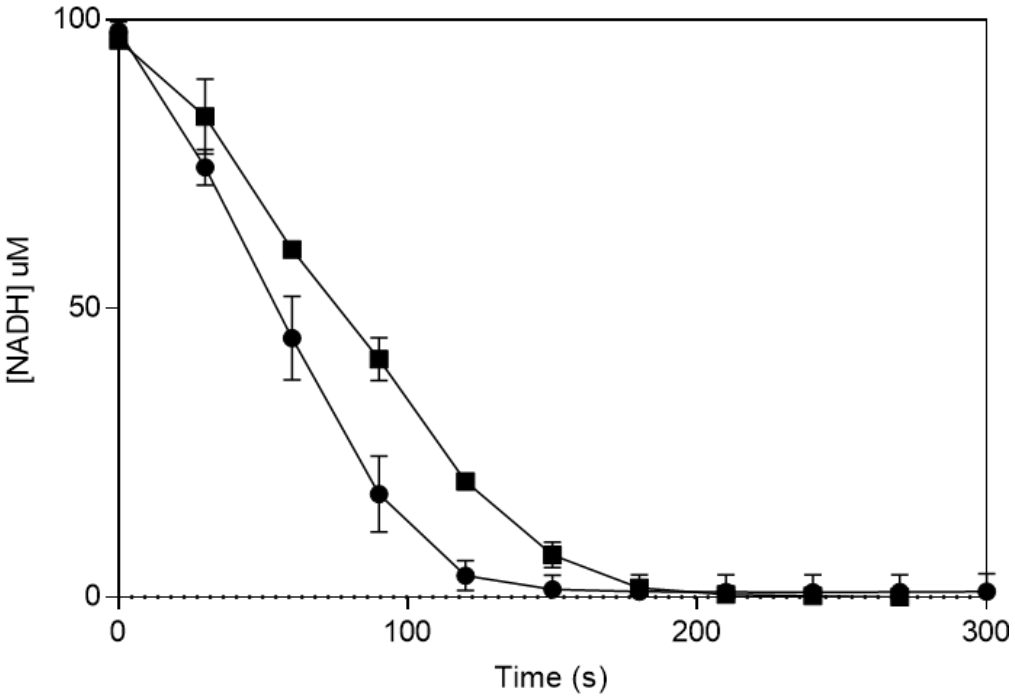


Figure 24: Alcohol dehydrogenase, ADH I, reduction assay

Overnight cultures of *E. coli* BW25113 Δ*ldhA* pBAD24-*alcA*-*aldA*-*cimA3.7* and control strain of *E. coli* BW25113 Δ*ldhA* pBAD24 grown on Lund medium with glucose was used to inoculate fresh Lund medium containing glucose. When the OD_{600} of the 100 ml culture reached 0.4-0.6, 0.2% *L*-(+)-arabinose was added to induce protein production. The cells were harvested 4h post-induction and resuspended in TES buffer (0.1M, pH8). Crude extracts were prepared using cell disruption and cell debris were removed by centrifugation. Crude extracts were used on the day and stored on ice during the duration of the activity assays. The assay used to monitor the reduction activity of ADH I was based upon the rate of decrease in absorbance at 340 nm when cofactor NADH is oxidized to NAD^+. The assay was conducted with acetaldehyde (10 mM) and NADH (0.1 mM) using extracts of *E. coli* BW25113 Δ*ldhA* pBAD24-*alcA*-*aldA*-*cimA3.7* expressing ADH I prepared in TES buffer (0.1M, pH8) (●). A control using *E. coli* BW25113 containing an empty pBAD24 vector with acetaldehyde (10 mM) and NADH (0.1 mM) was prepared, (■). Total protein concentration of the mixture was assayed using DC assay and estimated to 0.124mg of protein. Results represent the average of three repeated experiments. Standard deviations are shown on all curves, however some error bars are covered by the marker.

Assays were conducted where either only acetaldehyde or only NADH were added to the reaction mixture containing the crude extract of *E. coli* BW25113 Δ*ldhA* with an empty pBAD24 or *E. coli* BW25113 Δ*ldhA* pBAD24-*alcA*-*aldA*-*cimA3.7*. When only NADH without acetaldehyde was used, similar rates of consumption of NADH was observed in crude extracts of the control and *E. coli* BW25113 pBAD24-*alcA*-*aldA*-*cimA3.7* strain (Fig. 25).

This suggested that ADH I was not responsible for the NADH oxidation activity under the experimental conditions. Additionally, the sole addition of acetaldehyde in the crude extracts of either the control and *E. coli* BW25113 pBAD24-*alcA*-*aldA*-*cimA3.7* strains did not produce any change in absorbance (Fig. 25). Therefore, it was possible that a native NADH oxidase present in crude extract consumed the cofactor. Interestingly, no native enzymes from the crude extract reacted with NAD^+.

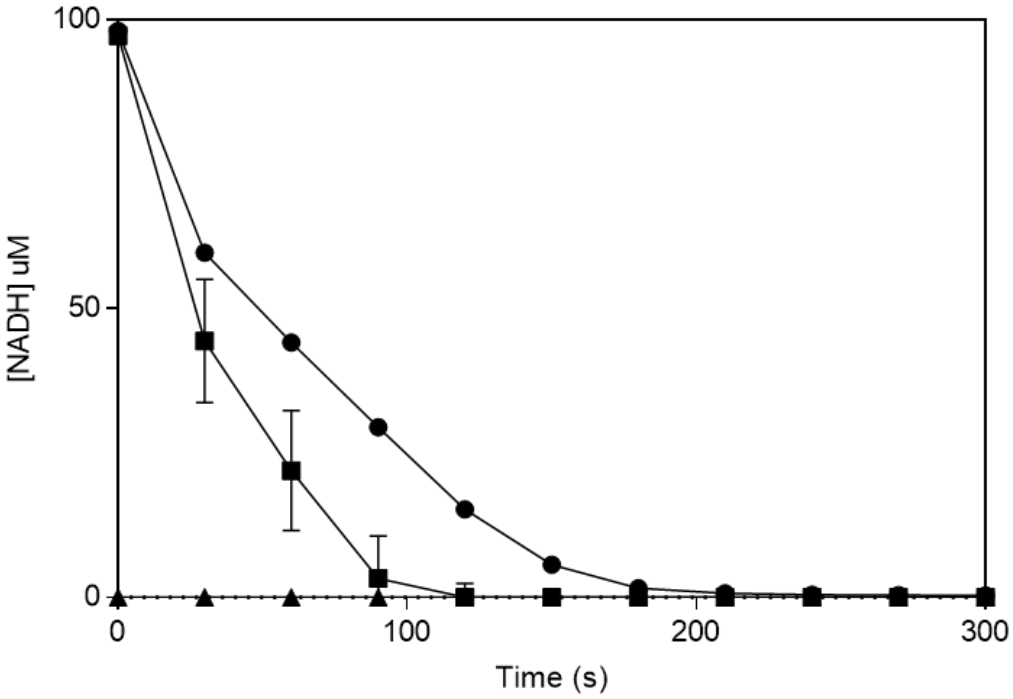


Figure 25: Determination of the presence in the crude extract of native enzymes consuming NADH instead

Overnight cultures of *E. coli* BW25113 Δ*ldhA* pBAD24-*alcA-aldA-cimA3.7* and control strain of *E. coli* BW25113 Δ*ldhA* pBAD24 grown on Lund medium with glucose was used to inoculate fresh Lund medium containing glucose. When the OD_{600} of the 100 ml culture reached 0.4-0.6, 0.2% *L*-(+)-arabinose was added to induce protein production. The cells were harvested 4h post-induction and resuspended in TES buffer (0.1M, pH8). Crude extracts were prepared using cell disruption and cell debris were removed by centrifugation. Crude extracts were used on the day and stored on ice during the duration of the activity assays. The assay was conducted using only NADH (0.1 mM) on sample ADH I (●) and on the control strain *E. coli* BW25113 containing an empty pBAD24 vector (■). A control experiment was carried out using only acetaldehyde (10mM) on the control strain *E. coli* BW25113 containing an empty pBAD24 vector with no addition of NADH (▲). Total protein concentration of the mixture was assayed using DC assay and estimated to 0.124mg of protein. Results represent the average of three repeated experiments. Standard deviations are shown on all curves, however some error bars are covered by the marker.

Further tests were performed by flushing nitrogen in order to remove any oxygen-triggered oxidation of NADH in the control crude extract. However, the same rate of NADH oxidation was observed as previously, suggesting that NADH oxidases are not responsible for the oxidation of NADH in these strains, and that an oxygen-independent enzyme might be responsible.

In *E. coli*, NADH dehydrogenases are central components of the respiratory chain for the transport of electrons [213], and are the main enzymes involved in the regeneration of NAD^+. NADH dehydrogenases are multisubunit complexes, which span the inner membrane with the NADH binding site facing the cytoplasm. However, activity of NADH dehydrogenases in crude extracts of *E. coli* produced using French press methods have been reported [214]. Therefore, observing consumption of NADH in crude extract of the control strain bearing an empty vector was coherent with what has been described in the literature. Further attempts were made to reduce the background effect such as increasing the centrifugation speed applied to remove the cell debris from the disrupted cells. NADH dehydrogenases aggregate as supercomplexes on the cytoplasmic membranes with therefore a significantly greater mass than the recombinant alcohol and acetaldehyde dehydrogenases investigated here. Unfortunately, the different increased speeds applied during the centrifugation steps did not make any difference on the consumption of NADH. Performing ultracentrifugation of the crude extract samples could have been a solution, assuming that the NADH dehydrogenase complexes would have remained intact after

the cell disruption treatment done; however, this latter point was unlikely. Furthermore, *E. coli* is a known facultative anaerobe, therefore other electron acceptors than oxygen were described in *E. coli*, such as fumarate *via* fumarate reductase, whose occurrence in crude extracts of *E. coli* would not be surprising [215], [216].

The recombinant ADH I enzyme was not His-tagged on the expression vectors, meaning quick, simple affinity-based purification could not be carried out. Due to time constraints, it was decided to carry on the project with the current construction, based on the more important, functional oxidation of ethanol route.

The same enzyme activity assay was performed on crude extracts from strains *E. coli* BW25113 pBAD24-*adhA-ALDH-cimA3.7* expressing the alcohol dehydrogenase from *C. glutamicum*, ADH A. ADH A was reported as a Zn-dependent enzyme in the literature [193]. Therefore, $ZnCl_2$ was added to the reaction mixture for the assay (Fig. 26). No activity was observed when compared to the control strain, regardless of the experimental condition investigated. However, an increase in absorbance was observed when $ZnCl_2$ was added to the assay. This was also observed when $ZnCl_2$ was added to the control strain assay, suggesting the reaction was due to $ZnCl_2$ (Fig. 26).

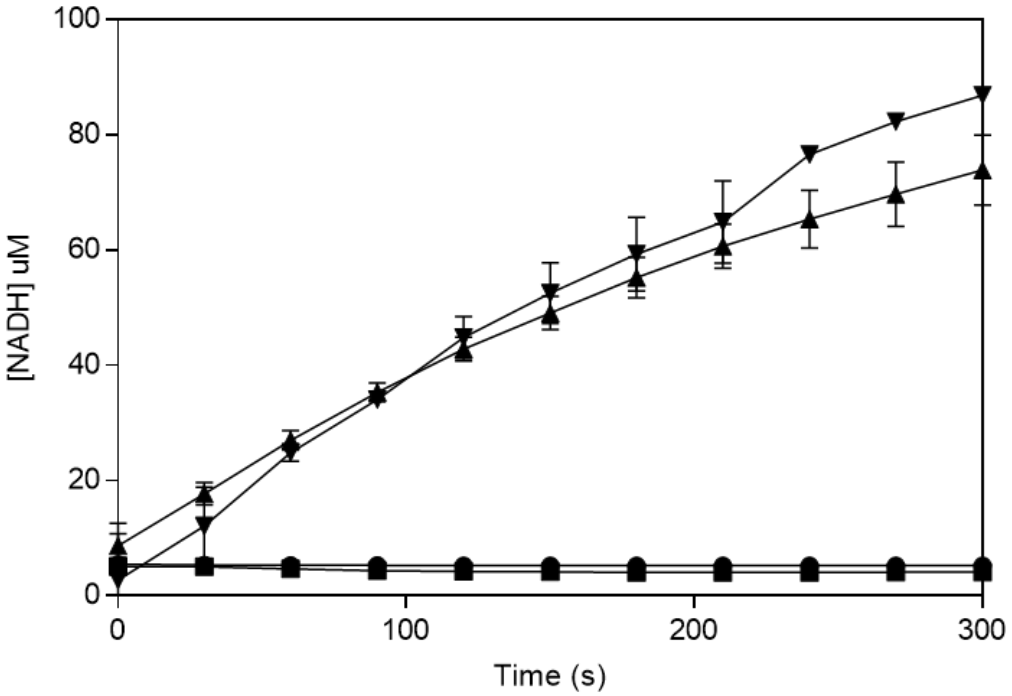


Figure 26: Oxidation assay on alcohol dehydrogenase ADH A

Overnight cultures of *E. coli* BW25113 Δ*ldhA* pBAD24-*adhA-ALDH-cimA3.7* and control strain of *E. coli* BW25113 Δ*ldhA* pBAD24 grown on Lund medium with glucose was used to inoculate fresh Lund medium containing glucose. When the OD_{600} of the 100 ml culture reached 0.4-0.6, 0.2% *L*-(+)-arabinose was added to induce protein production. The cells were harvested 4h post-induction and resuspended in TES buffer (0.1M, pH8). Crude extracts were prepared using cell disruption and cell debris were removed by centrifugation. Crude extracts were used on the day and stored on ice during the duration of the activity assays. The assay used to monitor the oxidation activity of ADH A is based upon the rate of increase in absorbance at 340 nm when cofactor NAD+ is reduced to NADH. The assay was conducted using ethanol (10 mM) and NAD^+ (1 mM) on sample of crude extract overexpressing ADH A (●). A control test using crude extract from *E. coli* BW25113 containing an empty pBAD24 vector, ethanol (10 mM) and NAD^+ (1 mM) was prepared (■). The same assay was conducted again using ethanol (10 mM), $ZnCl_2$ (10μM) and NAD^+ (1 mM) on sample of crude extract containing ADH A (▲), and on the control *E. coli* BW25113 containing an empty pBAD24 vector (▼). Total protein concentration of the mixture was assayed using DC assay and estimated to 0.124mg of protein. Results represent the average of three repeated experiments. Standard deviations are shown on all curves, however some error bars are covered by the marker.

In the absence of $ZnCl_2$ no change in absorbance was noticed between the control and *E. coli* BW25113 Δ*ldhA* pBAD24-*adhA-ALDH-cimA3.7* strains. Taken together, it was concluded that ADH A was inactive. The inactivity of the protein was assumed to be either due to the poor expression previously observed (Fig. 22) or misfolding or inactivity or all the above mentioned [217].

From the above results, only the alcohol dehydrogenase, ADH I, showed positive activity for the oxidation of ethanol, while the ADH A was completely inactive. Therefore, ADH I was used for the continuation of the project.

7.3.3.2 Acetaldehyde dehydrogenase enzyme assays

The activities of the two acetaldehyde dehydrogenases composing the second and central enzymatic step of the oxidation system were investigated. The irreversible conversion of acetaldehyde is central in completing the oxidation of ethanol as it provides the driving force in the reaction system.

The same enzyme activity test, as described previously, was conducted on both ALDH A and ALDH to examine their ability to oxidise acetaldehyde into acetate, while spectrophotometrically monitoring the increase in absorbance due to the formation of NADH.

An increase in absorbance was only observed in the reactions containing ALDH A, acetaldehyde and NAD^+. No catalytic activity was

detected in the control reactions that contained only crude extract from an empty pBAD24 vector strain (Fig. 27). This assay confirmed the catalytic activity of the overexpressed acetaldehyde dehydrogenase ALDH A in *E. coli*. The ALDH A enzyme showed an 8-fold higher activity compared to the ADH I and was estimated to be 180 µmol/min/mg, which is of the same order as the activity value (100U/mg) previously reported by Pateman and co-workers (1983). No activity of the ALDH A was detected when acetate and NADH were used in the reaction, which confirmed the irreversibility of the reaction.

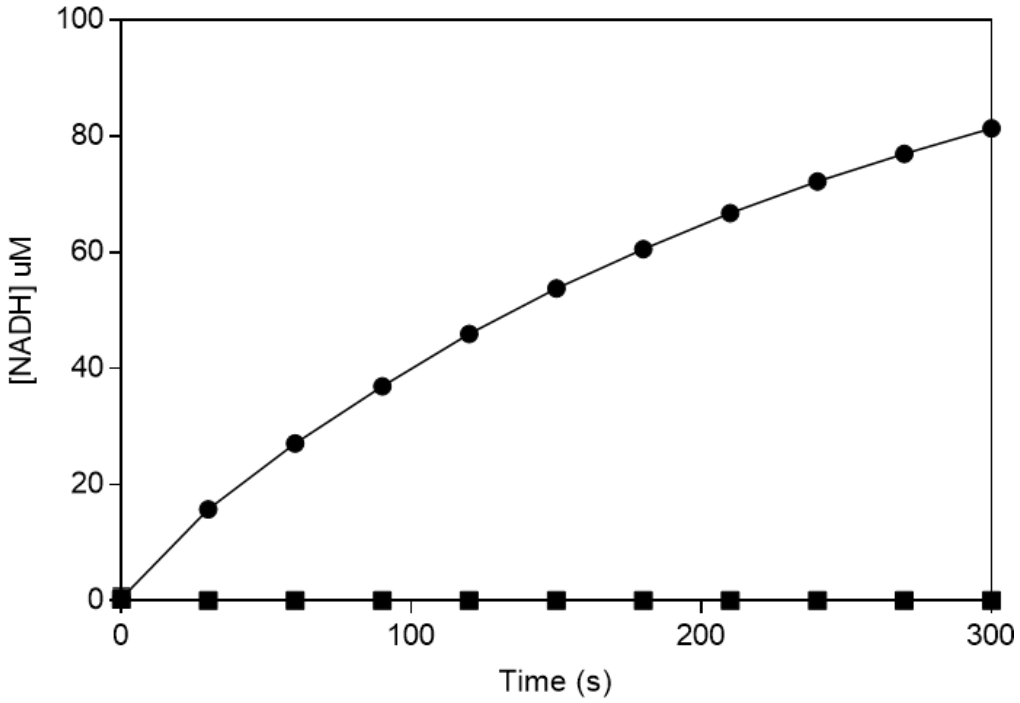


Figure 27: Acetaldehyde dehydrogenase, ALDH A, activity assay

Overnight cultures of *E. coli* BW25113 Δ*ldhA* pBAD24-*alcA*-*aldA*-*cimA3.7* and control strain of *E. coli* BW25113 Δ*ldhA* pBAD24 grown on Lund medium with glucose was used to inoculate fresh Lund medium containing glucose. When the OD_{600} of the 100 ml culture reached 0.4-0.6, 0.2% *L*-(+)-arabinose was added to induce protein production. The cells were harvested 4h post-induction and resuspended in TES buffer (0.1M, pH8). Crude extracts were prepared using cell disruption and cell debris were removed by centrifugation. Crude extracts were used on the day and stored on ice during the duration of the activity assays. The assay was conducted using acetaldehyde (10 mM) and NAD^+ (1 mM) on sample contraining crude extract from strain *E. coli* BW25113 Δ*ldhA* pBAD24-*alcA*-*aldA*-*cimA3.7* overexpressing ALDH A (●). A control reaction using crude extract from *E. coli* BW25113 containing an empty pBAD24 vector with acetaldehyde (10 mM) and NAD^+ (1 mM) was prepared (■). Total protein concentration was assayed using DC assay and estimated to 0.124mg/ml of protein. Results represent the average of three repeated experiments. Standard deviations are shown, however the error bars are covered by the marker.

Activity assay for the oxidation of acetaldehyde by the ALDH was also carried out. Unfortunately, no activity could be detected from the crude extract, under the same conditions, suggesting the enzyme was

inactive. As both enzymes from the same operon was inactive, it was concluded that the poor expression of these enzymes were the prime reason for undetectable activity.

From the results of the activity assays performed on all the recombinant alcohol and acetaldehyde dehydrogenases, it was concluded that the enzymes ADH I and ALDH A, both coming from *A. nidulans*, are the more suitable candidates to build an ethanol consuming pathway in *E. coli.* Despite some expression of ADH A and ALDH, no activity was detected *in vitro* and so work on these enzymes did not continue.

7.3.3.3 *In vitro* citramalate synthase assay

To confirm the feasibility of the biosynthetic route for ethanol co-utilisation for the bio-production of citramalate, the activity of the CimA3.7 needed to be confirmed. Therefore, activity assays of the citramalate synthase were performed on crude extracts from both strains *E. coli* BW25113 Δ*ldhA* pBAD24-*alcA*-*aldA*-*cimA3.7*, which overexpressed the citramalate synthase together with the ethanol-assimilation route.

To examine the activity of CimA3.7, a modified version of the assay described by Howell et *al*. (1999) was used [7]. The assay was based on Ellman's reagent using 5,5'-dithio-*bis*-(2-nitrobenzoic acid) (DTNB), which acted as a colorimetric indicator during the reaction. The catalytic activity of CimA3.7 in presence of pyruvate and acetyl-

CoA resulted in the generation of citramalate and the release of coenzyme A (CoA-SH). DTNB reacts with free thiol groups of CoA-SH to form 2-nitro-5-thiobenzoic acid, which absorbs at 412 nm, providing a colorimetric assay that could be monitored spectrophotometrically (Fig. 28).

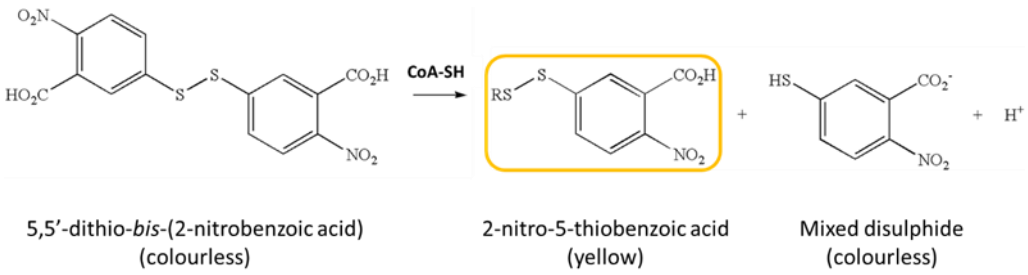


Figure 28: Reaction scheme for Ellman's reagent, DTNB, as colorimetric indicator for the formation of citramalic acid

Cell free extracts of strains *E. coli* BW25113 Δ*ldhA* pBAD24-*alcA-aldA-cimA3.7* and *E. coli* BW25113 Δ*ldhA* pBAD24 were prepared 5 h after induction with *L*-arabinose. CimA3.7 was partially purified from the cell crude extracts by performing a heat treatment step at 60°C for 10 minutes, based on reported methodology [7]. Heat treatment removed some of the native *E. coli* enzymes by precipitation of the denatured proteins. The assay was then carried out by incubating the partially purified CimA3.7 with pyruvate and acetyl-CoA. Samples of the incubated reaction mixtures were taken at regular intervals, and analysed for CoA-SH by mixing them with DTNB solution before measuring their absorbance at 412 nm (Fig. 29).

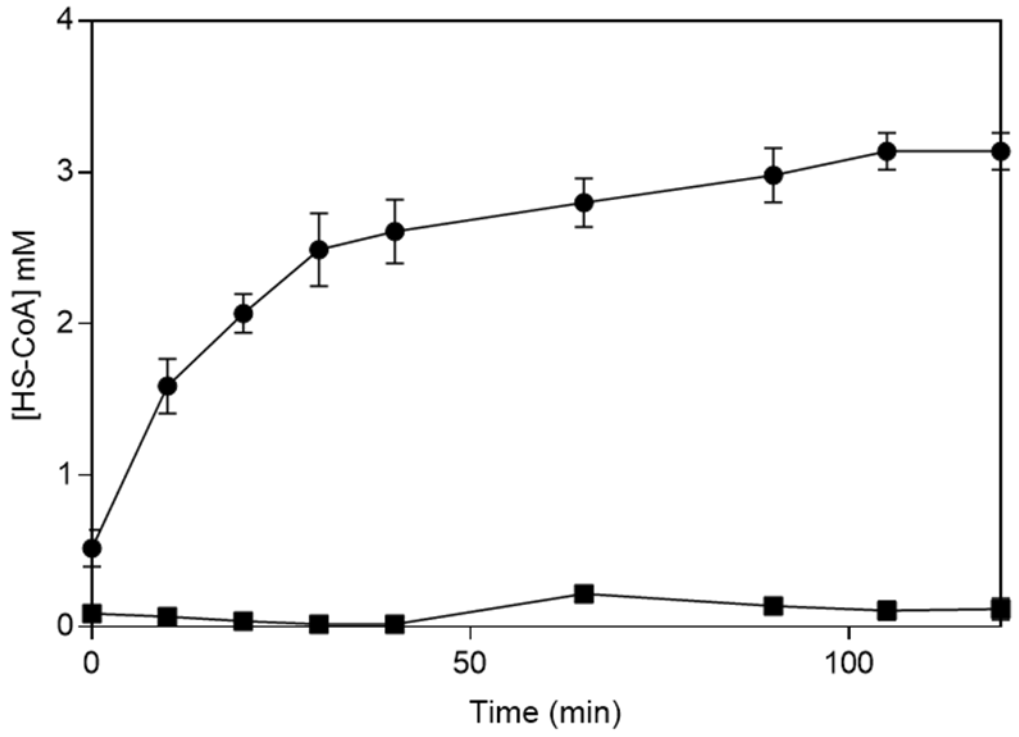


Figure 29: CimA3.7 activity assays

Overnight cultures of *E. coli* BW25113 Δ*ldhA* pBAD24-*alcA-aldA-cimA3.7* and control strain of *E. coli* BW25113 Δ*ldhA* pBAD24 grown on Lund medium with glucose was used to inoculate fresh Lund medium containing glucose. When the OD_{600} of the 100 ml culture reached 0.4-0.6, 0.2% *L*-(+)-arabinose was added to induce protein production. The cells were harvested 4h post-induction and resuspended in TES buffer (0.1M, pH8). Crude extracts were prepared using cell disruption and cell debris were removed by centrifugation. CimA3.7 is thermo-resistant, thus crude extracts were partially purified by performing a heat treated at 60°C for 10 min. The precipitated proteins were removed by centrifugation. The heat treated crude extract was used on the day and stored on ice during the duration of the activity assays. Samples of heat treated crude extracts from *E. coli* BW25113 Δ*ldhA* pBAD24-*alcA-aldA-cimA3.7* (●) were taken, and analysed for CoA-SH formation by the catalytic activity of CimA3.7 by measuring the absorbance of the reaction mixture at 412nm. A control reaction using heat treated crude extract from *E. coli* BW25113 Δ*ldhA* containing an empty pBAD24 vector with pyruvate, acetyl-CoA was prepared (■). Total protein concentration was assayed using DC assay and estimated to 62.5 µg/ml of protein and 74 µg/ml of protein in the heat treated crude extracts of *E. coli* BW25113 Δ*ldhA* pBAD24-*alcA-aldA-cimA3.7* and control strain of *E. coli* BW25113 Δ*ldhA* pBAD24, respectively. Results represent the average of three repeated experiments. Standard deviations are shown, however the error bars are covered by the marker.

Increases in absorbance were only observed in heat treated crude extracts from *E. coli* BW25113 Δ*ldhA* pBAD24-*alcA*-*aldA*-*cimA3.7* (Fig. 29). Activity was not detected in heat treated crude extract from the control strain containing an empty pBAD24 expression vector. Therefore, this assay confirmed that CimA3.7 was active in cell crude extracts of *E. coli* BW25113 Δ*ldhA* pBAD24-*alcA*-*aldA*-*cimA3.7*.

Furthermore, we also demonstrated that all the enzymes co-expressed in crude extracts of *E. coli* BW25113 Δ*ldhA* pBAD24-*alcA*-*aldA*-*cimA3.7* were active *in vitro*. Thus, the next step is to test their performances in whole-cell fermentations.

8. *In vivo* production of (*R*)-citramalate from two carbon sources

Two biosynthetic metabolic pathways were constructed for the production of citramalic acid from either glucose and ethanol or glucose and acetate. Enzymes assays confirmed that the expressed enzymes were active (see Section 7). This chapter will describe shake flask growth experiments demonstrating successful pathway construction and the design of fermentation processes to establish and optimise feeding regimes for each carbon source and to confirm citramalate production

8.1 Production of (*R*)-citramalate from the co-consumption of glucose and acetate in *E. coli* BW25113 Δ*ldhA*

8.1.1 Determination of optimal concentration of acetate for cell growth and (*R*)-citramalate conversion efficiency

In microbial fermentations, substrate toxicity and accumulation of toxic intermediate metabolites are known challenges that can impair the microbial biocatalyst by inhibiting cell growth or disrupting the biosynthetic metabolic processes [218]–[220]. Acetate is a known toxic compound to *E. coli* at concentrations of 5 g/L and above. Therefore, to further optimise the co-feeding strategy, the maximum concentration of acetate at which growth is not affected needed to be determined.

To identify optimal acetate concentrations, *E. coli* BW25113 Δ*ldhA* pBAD24-*ackA-pta-cimA3.7* was grown in Lund medium supplemented

with glucose (1%) and various concentrations of acetate (Appendix 11.15), and the co-expression of AckA-Pta and CimA3.7 was induced by adding *L*-arabinose (0.2%) to the medium. OD_{600nm} was monitored over 48h.

It was expected that adding acetate to the medium would decrease the growth rate, as it was observed from the previous experiment that glucose uptake was slowed down in presence of increased amounts of acetate (see Section 7.2.3). The decrease of the growth rate of *E. coli* BW25113 Δ*ldhA* pBAD24-*ackA-pta-cimA3.7* in response to the increase in acetate concentration (Table 14) confirmed our initial assumption.

Table 14: Growth rates of *E. coli* BW25113 Δ*ldhA* pBAD24 *ackA-pta-cimA3.7* challenged with increased acetate concentrations

Acetate concentrations	μ_{max}	Final DCW (g/L)
0 g/L	0.239 ±0.012	3.84 ±0.18
2.5 g/L	0.186 ±0.007	4.57 ±0.50
5 g/L	0.173 ±0.004	5.52 ±0.11
10 g/L	0.11 ±0.008	3.47 ±0.36

However, by adding acetate to the medium, it also increased the carbon source available for the strain. A strain engineered with the AckA-Pta pathway was expected to be able to show final greater biomass production. From a growth rate perspective, 2.5 g/L and 5 g/L of acetate gave the best growth results (Table 14). Indeed, when the strain was grown on glucose as sole carbon source, the dry cell weight (DCW) produced was lower. This observation was explained

by the availability of reduced amount of carbon source compared to experimentations where acetate was additionally supplemented to the medium. However, over 10 g/L of acetate supplementation, both growth rate and biomass production were impaired, suggesting a toxicity level not to be exceeded. Given the growth rate and the biomass production ability reported for each concentration of acetate tested, it was concluded that 5 g/L was the best compromise between μ_{max} and biomass production.

However, Tashiro and co-workers identified 10 g/L as the best acetate concentration in a co-feeding system with cells grown in M9 minimal medium supplemented with 50 g/L of glucose. M9 medium contained 5 g/L of yeast extract, which may explain the difference noticed in the optimum of acetate concentration that could be fed to the strain. It is then reasonable to conclude that the larger concentration of glucose and the presence of yeast extract in the culture medium used by Tashiro et *al*. (2015) provided a less stressful environment to *E. coli* even when challenged with greater acetate concentrations.

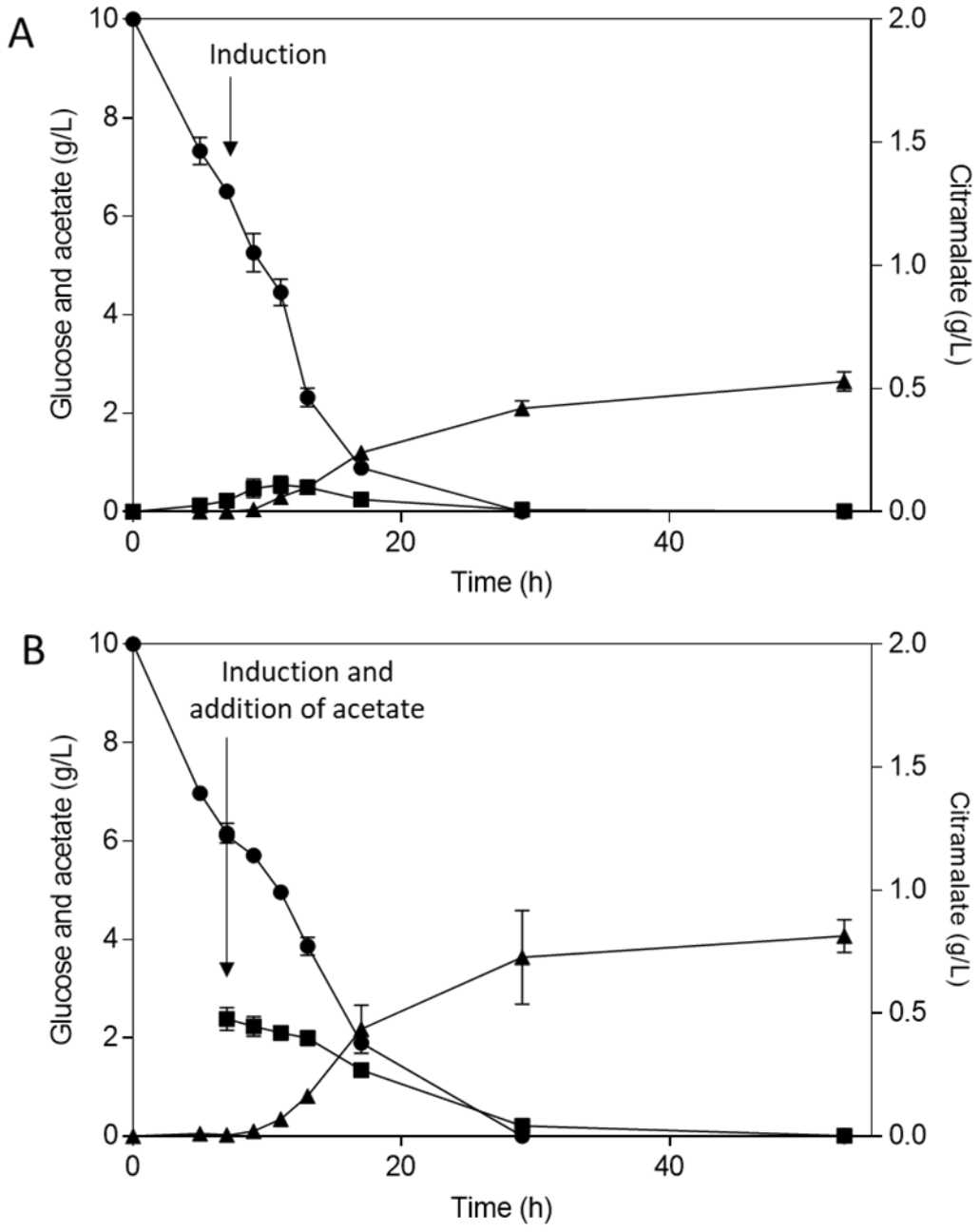
To confirm that supplementing 5 g/L of acetate was also the best choice regarding carbon conversion of both glucose and acetate into citramalate, we also studied the carbon yields of glucose and acetate consumption for citramalate production. Table 15 showed the carbon conversion ratio calculated from the glucose and acetate consumed and the citramalate formed. An example of calculation of the citramalate yield is given in Appendix 11.16.

Table 15: Citramalate titres (g/L) and carbon efficencies (g/g) under various concentrations of acetate supplemented to Lund medium

Concentration acetate supplemented	Citramalate titre (g/L)	$Y_{g\ citramalate/g\ glucose+acetate\ consumed}$
0 g/L	0.53 ±0.04	0.078 ±0.006
2.5 g/L	0.81 ±0.07	0.1 ±0.008
5 g/L	1.55 ± 0.03	0.151 ±0.008
10 g/L	1.09 ± 0.04	0.152 ±0.03

E. coli BW25113 Δ*ldhA* pBAD24-*ackA-pta-cimA3.7* was grown in Lund medium containing glucose (1%) at 30°C to an OD_{600nm} 0.6. AckA-Pta-CimA3.7 expression was induced by adding *L*-arabinose (0.2%) and various concentrations of acetate (0g/L, 2.5g/L, 5g/L and 10g/L) were supplemented to the growth medium, and further incubated at 30°C. Samples were taken regularly to be analysed for glucose and acetate consumption, as well as citramalate and organic acids contents by HPLC. Results and standard deviations are the average of triplicate experiments.

In all of the experiments (Fig. 30A-D), HPLC analysis showed that all the acetate added at induction and the glucose from the medium were completely and simultaneously consumed, except in the cultures supplemented with 10 g/L of acetate.


A
Induction
Glucose and acetate (g/L)
Citramalate (g/L)
Time (h)
B
Induction and
addition of acetate
Glucose and acetate (g/L)
Citramalate (g/L)
Time (h)

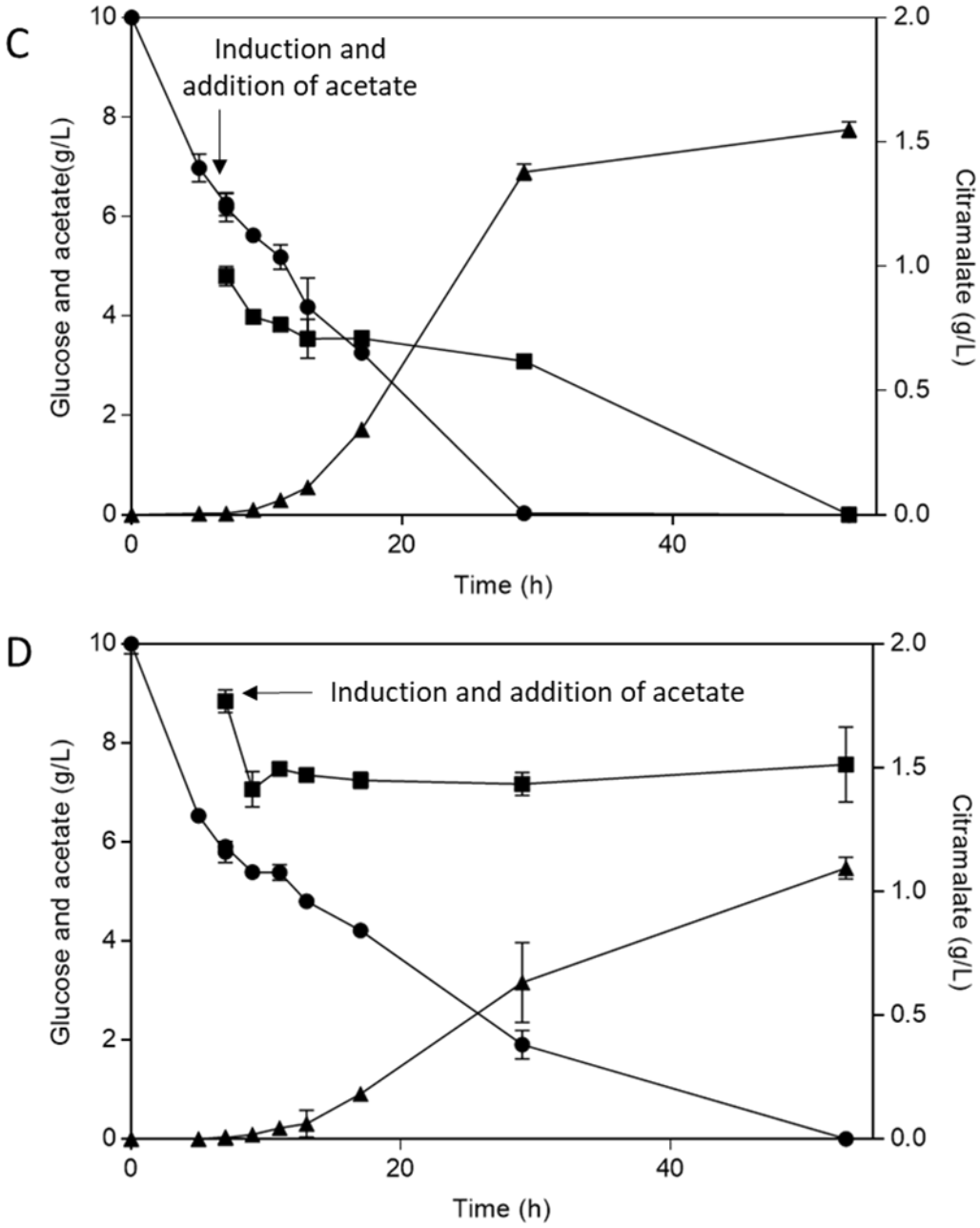


Figure 30: Glucose and acetate consumption and citramalate production in *E. coli* BW25113 Δ*ldhA* pBAD24-*ackA-pta-cimA3.7*

Cells of *E. coli* BW25113 Δ*ldhA* pBAD24-*ackA-pta-cimA3.7* were grown on glucose as sole carbon source in Lund medium. Protein expression was induced by adding *L*-(+)-arabinose (0.2%) at an OD_{600} of 0.6-0.8. Right after induction, various concentrations of acetate were supplemented to the culture medium. Samples were analysed for acetate consumption (■), glucose consumption (●), and citramalate production (▲) using HPLC. A: 0 g/L acetate; B: 2.5 g/L acetate; C: 5 g/L acetate and D: 10 g/L acetate.

Highest titre of citramalate was obtained when 5 g/L acetate was supplemented to the cultures medium (Table 15), and a yield of 0.151 g/ g $_{\text{glucose and acetate consumed}}$ ±0.008 was obtained. Although the carbon conversion ratio appeared to be similar with 10 g/L of acetate supplemented, *i. e.* 0.152 g/ g $_{\text{glucose and acetate consumed}}$ ±0.03, the limited amount of acetate consumed confirmed that 5 g/L of acetate supplementation was a better and more reliable compromise for growth, biomass formation, citramalate titres and carbon conversion yields. Moreover, the remaining high concentration of acetate in cultures, where 10 g/L of acetate was supplemented (Fig. 30D), suggested that citramalate was essentially produced from glucose under these circumstances. We also predicted that in presence of too high concentrations of acetate, a futile cycle of production-assimilation of acetate was triggered, making challenging to differentiate the proportion of the added acetate that was consumed, from the acetate generated by the cells themselves.

8.1.2 Conclusions from small-scale flask experiments

In this section, we demonstrated the co-consumption of glucose and acetate in *E. coli* engineered with the AckA-Pta acetate route. Additionally, the production of citramalate from the co-assimilation of carbon sources was also successfully confirmed. In the latter experiment, 5 g/L was identified as the optimum feeding regime, where all carbon sources could be completely consumed by the strain, and where the highest carbon conversion of glucose and acetate to

citramalate was obtained (Fig. 30A-D and Table 15). However, it was observed that growth in excess acetate generated a putative acetate futile cycle, whereby co-feeding acetate became counterproductive regarding carbon efficiency. Therefore, it was concluded that performing limited feeding of the carbon sources would enhance the carbon flux towards the bio-production of citramalate, as well as preventing any toxic effect caused by accumulation of acetate in the fermentation medium.

To our knowledge, this is the first demonstration of the bio-production of citramalate from the co-consumption of glucose and acetate. However, at this stage neither the citramalate titre, or its carbon efficiency was optimal yet. Thus, in order to assess whether or not acetate and glucose limited co-feeding could yield higher citramalate titres with improved carbon efficiency, the next step was to carry out fed-batch fermentations of *E. coli* BW25113 Δ*ldhA* pBAD24-*ackA*-*pta*-*cimA3.7* in 2L bioreactors.

8.1.3 Production of (*R*)-citramalate from glucose and acetate in fed-batch fermentation

8.1.3.1 Introduction

In small flask-scale (100 mL) using growing cells, the feasibility of producing (*R*)-citramalate from the co-consumption of glucose and acetate was demonstrated. To optimise further the carbon efficiency of the citramalate production route from carbon sources co-feeding

and demonstrate the industrial potentialities, scaled-up fermentations were performed.

There are three main types of fermentation process: batch, chemostat (or continuous) and fed-batch. In batch fermentations, all the nutrients are provided in the initial growth medium with no addition of removal of broth during the culture. In continuous fermentation, fresh medium is continually supplied to the culture, while the same volume of broth is being removed, ensuring the culture is run at its steady-state. Fed-batch fermentation fits itself in between as nutrients are first fed in the batch medium. Once they all have been consumed, a nutrient limited feed is applied to the culture until the maximum volume of the fermenter is reached, allowing the cell to further grow. Once the reactor is full, the fermentation is stopped. Of these three types, fed-batch fermentation is the most used process for biotechnological production, as it allows achieving high cell densities and therefore higher productivity per unit of volume, reducing the cost of capital investment. By contrast, continuous fermentation is the less applied technique, despite the idealistic aspect of a never-ending fermentation process. Fed-batch fermentation has indeed a number of advantages over continuous fermentation. First, fed-batch is a more robust process due to higher cell density reducing the risk of a contaminant taking over the culture, as well as reaching high volumetric productivity rendering the capital investment less costly. Then, the maintenance of the fed-batch culture is also easier and the mode of culture, as well as the feed can be modulated along the fermentation to optimise further the

productivity with no dramatic consequence such as wash-out effect, more common of continuous process. Thus, based on both capital and operating perspectives, fed-batch fermentations are more cost effective compared to continuous processes. Therefore, it was decided to use a fed-batch protocol for the bio-production of (*R*)-citramalic acid.

In a previous study [7], a multi-phase fed-batch fermentation protocol was successfully developed for the bio-production of (*R*)-citramalate from glucose using *E. coli* BW25113 Δ*pflB* Δ*ldhA* pBAD24 *cimA3.7* at high cell densities. Therefore, for the purpose of this project, the previously developed fermentation protocol was adjusted to a limited co-feeding system of glucose and acetate.

The fed-batch fermentation process was split into three distinct phases in order to allow the production of sufficient biomass for maximising both the co-consumption of carbon sources, and the citramalate production capacity of the strain in a carbon efficient manner. During the fermentation, samples were taken regularly to measure the OD_{600nm}, DCW, glucose, acetate and organic acids concentrations. The pH of the culture medium was constantly monitored and adjusted to 7 by either adding H_2SO_4 or $NH_4(OH)$ when required. The changes of fermenter volume caused by sampling and any feed, acid or base added to the fermenter were taken into account when calculating carbon efficiencies. Furthermore, in order to suit the

optimal expression conditions for the AckA-Pta route (see Section 7.1) all the fermentations were run at 30°C.

Phase 1, the batch phase of the fermentation, was started by inoculating *E. coli* BW25113 Δ*ldhA* pBAD24-*ackA-pta-cimA3.7* into the fermentation Lund medium, initially containing glucose (11.9 g/L) as sole carbon source (section 5.3.2). During the batch phase, the dissolved oxygen (DO) slowly decreased from 100% to 30% saturation, corresponding to the consumption of the glucose by the cells. Once the DO reached the value of 30% saturation, the stirred speed controller was triggered and adjusted the speed to maintain the DO at 30% saturation. The depletion of all the glucose from the batch medium was indicated by a sudden increase of the DO, indicating that cells entered the starving phase. The purpose of the batch phase was to enable the cell to grow at high cell density. The batch medium was supplemented with carbenicillin in order to ensure the growth at high cell concentration of the strain of interest. There was no further addition of antibiotic during the fermentation, as the high cell density itself allows preventing from contamination. The plasmid stability can appear as problematic as no continuous addition of antibiotic was performed during the fermentation. However, tests performed by successive flask cultures using selective and non-selective Lund medium showed a strong plasmid stability over generations.

The second phase was initiated by the start of a limited glucose feed, that was gradually increased until maximal growth rates were achieved [221]. The feed was made of a concentrated glucose

solution. The glucose feed also provided additional nutrients and salts, such as $MgSO_4$, trace elements and yeast extract. The rate of the glucose feed was set based on the existing protocol [7], and the complete uptake of the glucose was monitored *in situ* by using glucose monitoring sticks (section 5.3.2). In the initial fed-batch protocol developed in a previous study [7], the addition of yeast extract was added to reduce the putative formation of acetate, and also as a protective agent from the toxic effect of acetate accumulation. Furthermore, in the presence of complex carbon source, such as yeast extract, in the fermentation medium with limited glucose feeding, it was shown that the utilisation of acetate by *E. coli* was promoted [222] Given, that here, acetate was used as a substrate in a limited co-feeding, the yeast extract was then kept for the same reasons. Indeed, reducing the likelihood of acetate production while promoting its assimilation offered a preventive strategy against the potential occurrence of an acetate futile cycle.

Phase 3, the production phase, was started once the culture reached a high cell concentration of OD_{600nm} 40-45. The expression of the acetate assimilation route, AckA-Pta, and CimA3.7 was induced by adding *L*-arabinose (0.2%) to the fermenter. The glucose feed was maintained at limiting concentrations to ensure a high glycolytic flux. Glucose concentration was monitored throughout the run using dip-sticks (Millipore). Immediately post-induction, the acetate co-feed was started. The feed consisted of a separate concentrated solution of sodium acetate. The feeding rates were set and further optimised based on the acetate ang glucose uptake rates estimated from the

flask tests supplemented with 5 g/L acetate and 10g/L of glucose (Section 8.1.1., Fig. 30C), where optimal results for both carbon sources co-consumption and citramalate production were observed.

From a stoichiometric perspective, it was ideally considered that glucose and acetate or ethanol would respectively supply all the pyruvate and acetyl CoA needed for the production of citramalate. For each mole of glucose, an equivalent of 2 moles of either acetate or ethanol are necessary to obtain 2 moles of citramalate, based on the ideal assumption that acetyl-CoA would not be produced from the decarboxylation of pyruvate. Consequently, this system involved a requirement of a mass ratio of glucose:acetate and glucose:ethanol of 1.53 g/g and 1.96 g/g, respectively, which was used to set the co-feeding rates. Both glucose and acetate feeds were maintained throughout the fermentation. Fermentations were run until reaching the maximal working volume of the bioreactor. A picture describing the fermenter set up during the third phase was given in Appendix 11.17.

Exhaustively, the carbon balance in fermentations includes the proportion of carbon used in the production of biomass, the generation of CO_2, side products (organic acids), cell maintenance, energy and redox balance, as well as the target compound. In this body of work, the carbon balance was based on the knowledge of the glucose and acetate/ethanol consumed (assessed by the difference between what was supplied and what was remaining), the biomass, citramalate and organic acids produced during the fermentation. The carbon efficiencies in each fermentation situation was then

determined by comparing the amount of citramalate formed over the amount of carbon sources consumed and expressed as the carbon conversion yield. Additionally, theoretical maximum carbon yields (TMCY) were determined as the ratio of the quantity of citramalate measured over the theoretical maximum amount that would be obtained if all the carbon consumed had been used in the bio-route.

8.1.3.2 Benchmark fed-batch fermentation of *E. coli* BW25113 Δ*ldhA* for the production of (*R*)-citramalate from glucose only

In order to assess if the insertion of an acetate assimilation pathway improved the carbon flux from feedstocks to citramalate, it was needed to perform a benchmark fed-batch fermentation of *E. coli* BW25113 Δ*ldhA* pBAD24-*cimA3.7* fed with glucose only (Fig. 31). Furthermore, it was also needed to know what was the citramalate production capacity under our fermentation conditions, *i. e.* using 30°C as fermentation temperature. The same general fermentation protocol as described previously was used. The only change was that no acetate co-feeding was run.

At the end of the phases 1 and 2 of the fermentation (Fig. 31), 33.5 g of glucose was consumed and 13.75 g of biomass was produced, yielding a ratio of 0.41 $g/g_{glucose}$. This production ratio was similar to the biomass yield obtained in the previous study [7], showing that despite the change in temperature, the growth of the strain was not impaired. Once the OD_{600nm} reached 45, the expression of the CimA3.7 was induced by adding *L*-arabinose (0.2%) to the

fermentation medium and the phase 3 (production phase) was started and continued for another 24h. During this last phase, a further 133 g of glucose was consumed, and was converted into 44 g of biomass and 26.4 g of citramalate, yielding 0.33 $g/g_{glucose}$ and 0.20 $g/g_{glucose}$ respectively. A TMCY of 0.24 was obtained, describing a system where majority of the carbon was derived from the bio-route of interest. During the production phase, a (*R*)-citramalate production rate of 0.89 g/L/h and a specific production rate of 0.021 $g/L/g_{DCW}/h$ were obtained. The conversion ratio of glucose to biomass decreased by 20% between phase 1+2 and phase 3, confirming that the carbon atoms were derived from biomass production to citramalate biosynthesis.

After 40h of fermentation, some glucose started to accumulate (up to 0.17g/L at the end of the fermentation). As the fermentation was performed at 30°C, cells grew slower compared to 37°C. Thus, the reduced glucose uptake suggested that the cells were reaching the stationary phase. However, due to volume constraint of the vessel of the bioreactor, the fermentation could not be carried out any further.

Overall, from the total of 167 g of glucose fed during the fermentation, 26.4 g of citramalate and 58 g of biomass were produced, yielding a total conversion ratio of 0.16 $g/g_{glucose}$ and 0.35 $g/g_{glucose}$ respectively. When counting biomass and citramalate production, a conversion ratio of 0.51 $g/g_{glucose}$ was obtained. Despite the aeroby conditions of the fermentation, small amounts of organic acids (succinate and lactate) were noticed. It was concluded that the remaining carbon was lost *via* small side production of organic acid

and CO_2 emission from the formation of acetyl-CoA. Unfortunately, no off-gas analysis could have been performed, resulting in an overall limited assessment of the impact of CO_2 formation, only based on theoretical assumptions.

Therefore, to assess if the insertion of an alternative carbon source feed could improve the carbon proportion being converted into citramalate, another fed-batch fermentation using the exact same protocol was performed with *E. coli* BW25113 Δ*ldhA* pBAD24-*ackA-pta-cimA3.7*.

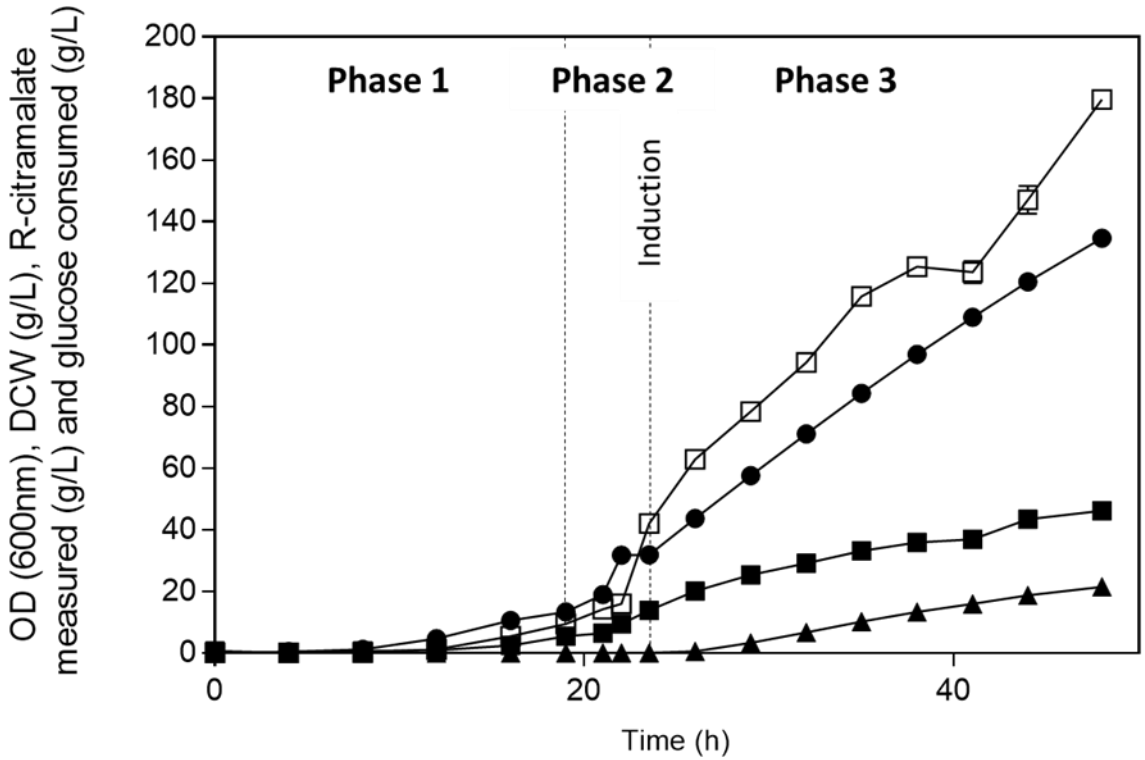


Figure 31: Benchmark aerobic fermentation of *E. coli* BW25113 Δ*ldhA* pBAD24-*cimA3.7* for the production of (*R*)-citramalate from glucose

E. coli BW25113 Δ*ldhA* pBAD24-*cimA3.7* was grown to starvation on glucose (11.9g/L) (Phase 1). A limited glucose feeding was used to grow the cells to an OD_{600nm} of 40-45 (Phase 2). Following this, the expression of CimA3.7 was induced by adding *L*-arabinose (0.2%) to the medium, which started the production phase (Phase 3). The glucose feed was maintained until the end of the fermentation. Samples were taken regularly to measure OD_{600nm} (□), concentration of dry cell weight (DCW; ■), glucose consumed (●) and citramalate produced (▲).

8.1.3.3 Fed-batch fermentation of *E. coli* BW25113 Δ*ldhA* for the production of (*R*)-citramalate from glucose and acetate

To examine if co-feeding acetate with glucose could be used for improving the carbon efficiency for the production of citramalate, the same three-phases fed-batch fermentation protocol was run. Citramalate titres, specific production and carbon yields were compared with the benchmark fermentation previously performed.

During phase 1 and 2 (Fig. 32), 35.6 g of glucose was consumed and converted to 14.8 g of biomass representing a conversion yield of 0.41 $g/g_{glucose}$. At the end of the phase 2, the co-expression of AckA-Pta and CimA3.7 was induced by adding *L*-arabinose (0.2%). The acetate co-feed was also immediately started after induction, while the glucose feed was maintained. Accumulation of glucose was carefully followed using monitoring glucose sticks and adjusted if needed. The feeding regimes were designed in a way that glucose and acetate were fed in stoichiometric proportion for the bio-production of citramalate. Therefore, starting the acetate feed involved reducing the glucose feed to reach a 2:1 molar ratio, respectively.

During phase 3 (Fig. 32), a further 36 g of glucose was co-consumed with 30.5 g of acetate, which corresponded to the stoichiometric uptake expected. Indeed, theoretically 36 g of glucose yields 0.4 mol of pyruvate, while 30.5 g of acetate provided 0.51 mol of acetyl-CoA, suggesting that a final 0.4 mol of citramalate (about 60 g) should be obtained with the conversion being slightly limited by the shortage of glucose. The use of acetate by the cells was confirmed as no acetate

accumulation was observed during the production phase. The co-consumption yielded a further 11 g of biomass and a smaller citramatate titre of 4.73 g/L (~5.25 g) compared to both expectations and the benchmark fermentation (Table 16). During the phase 3, a conversion yield of citramalate from both carbon source of 0.064g/$g_{glucose+acetate\ consumed}$, a TMCY of 0.07, and a production rate of 0.26g/L/h were obtained (Table 16). Overall, from the total of 77 g of glucose and 35 g of acetate fed during the whole fermentation, 5.25 g of citramalate were produced, yielding a total conversion ratio of 0.05 g/$g_{glucose\ +\ acetate\ consumed}$, 5 times lesser than the total conversion ratio obtained in the benchmark fermentation, confirming that more optimisation were necessary. Furthermore, from a carbon flow perspective, only a third of the carbon input could be recovered in the shape of biomass, citramalate and organic acids production, suggesting a predominant use (about 67%) of the carbon in cell maintenance, energy and redox balance and CO_2 formation instead of bioproduction.

Table 16: Efficiency parametres of the production phases (phase 3) in the benchmark *E. coli BW25113 ΔldhA* pBAD24-*ackA-pta-cimA3.7* fed-batch fermentations

Efficiency parameters during phase 3	Benchmark	Experiment 1
	BW25113 Δ*ldhA* pBAD24-*cimA3.7*	**BW25113 Δ*ldhA* pBAD24-*ackA-pta-cimA3.7***
Feeding regime	**Glucose**	**Glucose/Acetate**
R-citramalate concentration (g/L)	21.5	4.73
Glucose consumed (g) Acetate consumed (g) *Total (g)*	133 - *133*	36 30.5 *66.5*
$Y_{citramalate/total\ carbon\ source}$ (g/g – mol/mol)	0.20 g/g 0.24 mol/mol	0.06 g/g 0.04 mol/mol
R-citramalate production rate (g/L/h)	0.89	0.26
Biomass yield (g_{DCW}/g)	0.32	0.16
R-citramalate specific production rate (g/L/g_{DCW}/h)	0.021	0.019
TMCY ($g_{citramalate\ measured}/g_{citramalate\ theoretical}$)	0.24	0.07

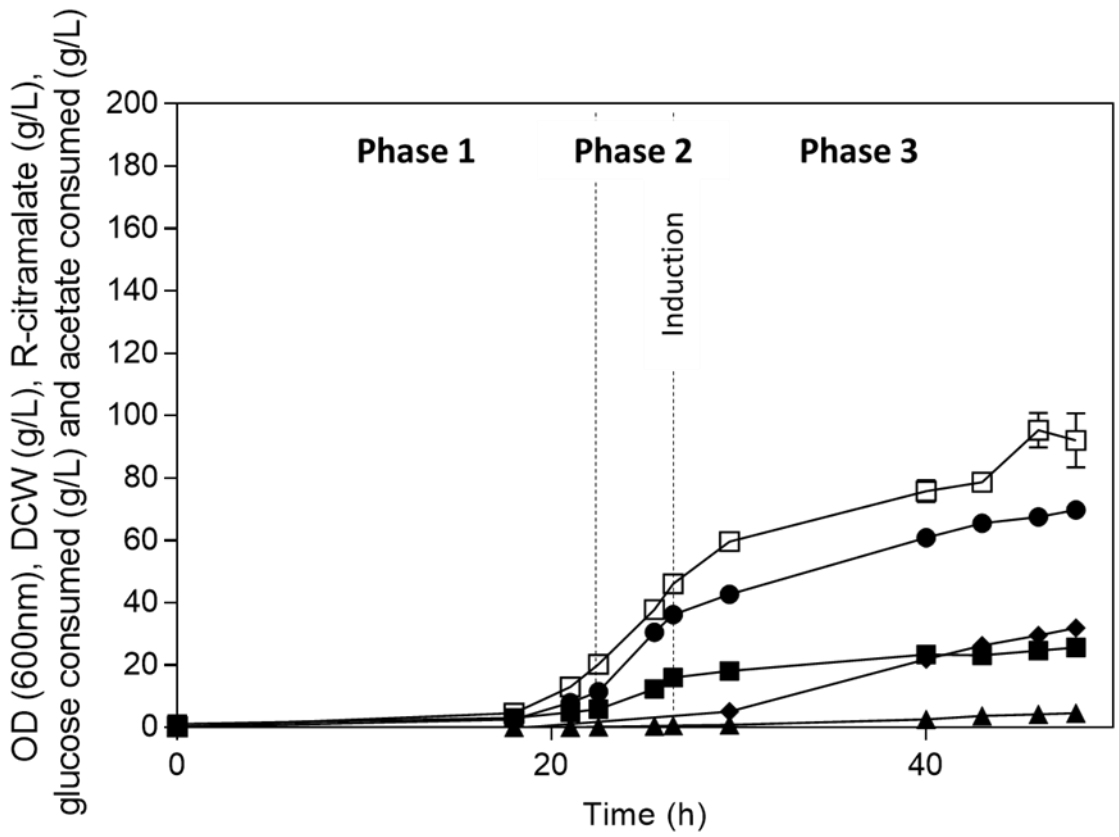


Figure 32: Aerobic fermentation of *E. coli* BW25113 Δ*ldhA* pBAD24-*ackA-pta-cimA3.7* for the production of (*R*)-citramalate from glucose and acetate

E. coli BW25113 Δ*ldhA* pBAD24-*ackA-pta-cimA3.7* was grown to starvation on glucose (11.9g/L) (Phase 1). A limited glucose feeding was used to grow the cells to an OD_{600nm} of 40-45 (Phase 2). Following this, the expressions of AckA-Pta and CimA3.7 were induced by adding *L*-arabinose (0.2%) to the medium, at which point the acetate feeding was also started (Phase 3). The glucose and acetate feeds were maintained until the end of the fermentation. Samples were taken regularly to measure OD_{600nm} (□), concentration of dry cell weight (DCW; ■), glucose consumed (●), acetate consumed (♦) and citramalate produced (▲).

Thus, the above results were rather disappointing. The discrepancy obtained between the stoichiometric expectations and the fermentation outcomes could be partly explained by the side production of organic acids such as lactate (despite the deletion of the *ldhA* as stated earlier in this work and also in the previous work of J. Webb [7]). Additionally, the fact that the strain was still growing represented also a significant carbon loss (Fig. 32). However, only about 11 g of biomass was formed during phase 3, which was not enough to explain such a little production of citramalate compared to the benchmark fermentation. It could also be argued that there was a possibility that the carbon feed was too restricted to satisfy the growing and citramalate production demands. Initially, it was decided to decrease the glucose feed in the fermentation process, based on observations previously made from flask experiments, where it was concluded that co-feeding acetate slowed down glucose uptake (see Section 7.2). If the lack of carbon atoms was actually occurring in the fermentation, this could explain the lower biomass and citramalate production. Moreover, the conflict for the carbon flux between biomass formation and citramalate production could have induced metabolic burdens impairing even more carbon efficiency of any direction. Therefore, another fermentation with an increased feed of acetate was performed (Appendix 11.18). The modulation of glucose and acetate feeds only succeeded in increasing the citramalate conversion yield during the production phase from 0.06g/$g_{glucose+acetate\ consumed}$ to 0.11 g/$g_{glucose+acetate\ consumed}$, which remained less than half of the yield obtained on the benchmark fermentation of *E. coli* BW25113

Δ*ldhA* pBAD24-*cimA3.7* (Appendix 11.18). Although, the increase of the acetate feeding enabled higher citramalate titres, as well as increase biomass production, this system remained inefficient as glucose and acetate had the tendency to accumulate during the production phase. Therefore, another strategy for improving the carbon efficiency of co-feeding process was needed.

8.1.3.4 Identification of a new strategy to improve carbon efficiency using a co-feed of glucose and acetate

In their study on glucose and acetate co-feeding using the overexpression of the AckA-Pta route, Tashiro and co-workers (2015) compared the impact of the deletion of the pyruvate dehydrogenase (PDHC) on the overall carbon efficiency. The PDHC is a central enzyme complex catalysing the conversion of pyruvate to acetyl-CoA aerobically *via* the release of CO_2 (Fig. 33). The PDHC is composed of three main subunits [223]. Pyruvate dehydrogenase (E_1 encoded by *aceE*) catalyses the decarboxylation of pyruvate and transfers the acyl chain to the second enzyme, dihydrolipoamide transacetylase (E_2 encoded by *aceF*) *via* the oxidised lipoyl-lysine arm linked to the E_2 subunit. E_2 generates acetyl-CoA, while the last subunit, dihydrolypoylamide dehydrogenase (E_3 encoded by *dhl*) acts as the final electron acceptor and regenerates the oxidised form of the lipoyllysine arm of the subunit E_2 for the chain reaction to continue. If one of the subunits is not functioning, the whole PDHC becomes inactive. Consequently, inactivating the PDHC enzyme renders an *E. coli* strain

auxotroph for a source of acetyl-CoA, therefore the cells have to obtain acetyl-CoA from an external source.

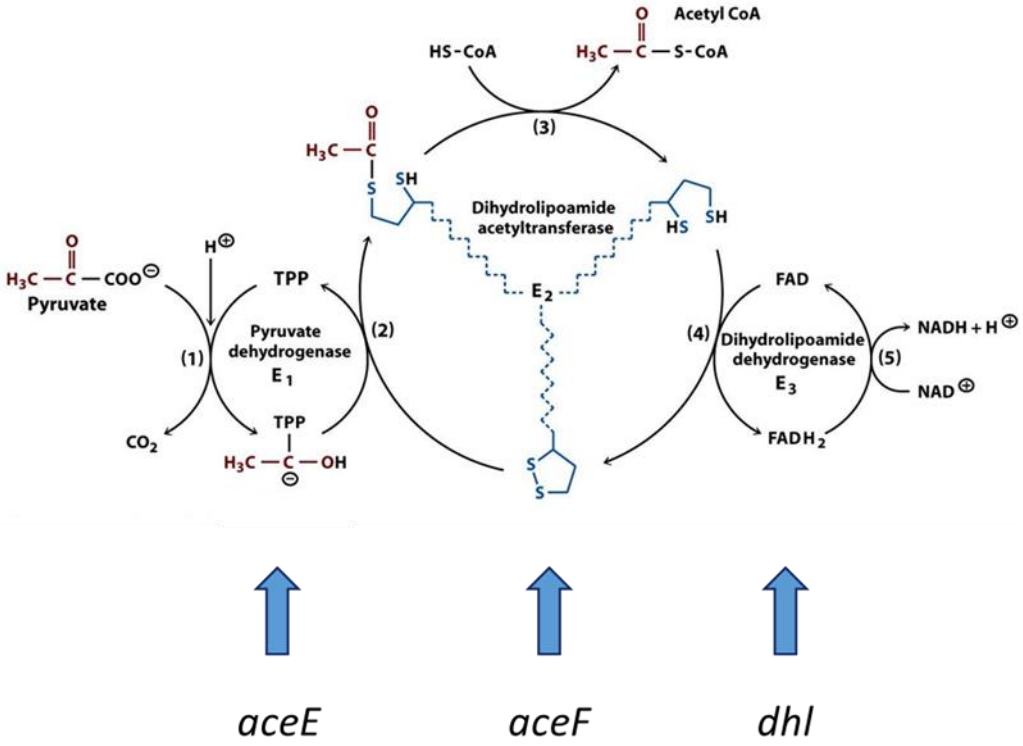


Figure 33: Structure of the pyruvate dehydrogenase complex

Interestingly, Tashiro and co-workers (2015) concluded that deleting PDHC did not improve further the carbon efficiency for their IBA production. They assumed that the counterproductive effect came from the slower carbon conversion. However, they performed all their fermentation assays and the corresponding carbon efficiency calculations in shake-flasks. Thus, glucose and acetate were provided in excess at the start of the experiments, which is likely to lead pyruvate accumulation and consequently repression of the TCA cycle.

By contrast, this study focused, here, on using limited carbon source feeds to maintain a high carbon flux in fed-batch fermentations, where culture conditions such as temperature, pH, and oxygenation were monitored and controlled more precisely. Given that, the AckA-Pta route alone did not provide improved carbon conversion compared to a citramalate-producing strain only fed on glucose, the deletion of the PDHC appeared as a promising strategy to investigate.

Therefore, an *E. coli* strain with the *aceF* gene (encoding the E_2 subunit, Fig. 33) deleted was used for the following fed-batch fermentations. New efficiency calculations were performed, and compared to the benchmark of *E. coli* BW25113 Δ*ldhA* pBAD24-*cimA3.7* and *E. coli* BW25113 Δ*ldhA* pBAD24-*ackA-pta-cimA3.7* fermentations. Deletion of the E_2 subunit was chosen arbitrarily, as the PDHC is inactivated by deleting any of its three genes. Nevertheless, the inability of growth of *E. coli* BW25113 Δ*aceF* when in presence of glucose as sole carbon was verified. Likewise, the restoration of growth by the supplementation of acetate to the glucose containing medium was also confirmed (Data not shown).

8.1.3.5 Fed-batch fermentation *E. coli* BW25113 Δ*aceF* for the production of (*R*)-citramalate from glucose and acetate

E. coli BW25113 Δ*aceF* was transformed with the expression vector pBAD24-*ackA-pta-cimA3.7.*

To assess if the deletion of the pyruvate dehydrogenase complex improved the carbon conversion efficiency, the same fed-batch fermentation protocol was applied to *E. coli* BW25113 Δ*aceF* pBAD24-*ackA-pta-cimA3.7* (Fig. 34). However, as the strain was an acetate auxotroph, 5 g/L of acetate was added to the batch medium in order to allow the strain to grow.

As mentioned by Tashiro et *al.* (2015), growth of *E. coli* BW25113 Δ*aceF* was slower even when the medium was supplemented with excess glucose and acetate. Therefore, the inoculum size was increased when starting the batch phase (OD_i=0.1; phase 1). The cells grew to an OD_{600nm} of 12 after 30h (Fig. 34, phase 1), and then reached starvation. No growth occurred in the period of starvation, suggesting all acetate and glucose had been used. Expression of AckA-Pta and CimA3.7 was induced by *L*-arabinose addition, and glucose and acetate feeding was initiated. The glucose and acetate feeds were adjusted proportionally and stoichiometrically to account for slower growth.

During the production phase, 50 g of glucose and 29 g of acetate were consumed, and converted into 23 g of biomass and 22.8 g of citramalate, which gave conversion ratios of 0.29 $g/g_{glucose+acetate\ consumed}$ and 0.29 $g/g_{glucose+acetate\ consumed}$ respectively (Table 17). At the

end of the production phase, we obtained a citramalate production rate of 0.74 g/L/h and a specific production rate of 0.032 g/L/g_{DCW}/h. Thus, despite a lower biomass production when using *E. coli* BW25113 Δ*aceF,* the production ability per unit of cells was increased by 50% compared to the benchmark strain. Moreover, the conversion yield of citramalate during the production phase as well as the TMCY were also improved by 50% compared to the *E. coli* BW25113 Δ*ldhA* strain (Table 17), confirming that the carbon flux was more directed towards the bio-production of citramalte.

Overall, from the total of 83 g of glucose and 46 g of acetate fed during the whole fermentation, 22.7 g of citramalate were produced, yielding a conversion ratio of 0.18 g/$g_{glucose\ +\ acetate\ consumed}$ of the complete process. Overall, a 12.5% increase in the carbon conversion to citramalate compared to the benchmark fermentation was obtained, while a lesser proportion of the carbon flow was recovered in the shape of biomass.

Table 17: Efficiency parameters of the production phases (phase 3) in the benchmark *E. coli* BW25113 Δ*ldhA* pBAD24-*cimA3.7* and *E. coli* BW25113 Δ*aceF* pBAD24-*ackA-pta-cimA3.7* fed-batch fermentations

Efficiency parameters during phase 3	Benchmark	Experiment 2
	BW25113 Δ*ldhA* pBAD24-*cimA3.7*	**BW25113 Δ*aceF* pBAD24-*ackA-pta-cimA3.7***
Feeding regime	**Glucose**	**Glucose/Acetate**
R-citramalate concentration (g/L)	21.5	19.36
Glucose consumed (g) Acetate consumed (g) *Total (g)*	133 - *133*	49.7 28.9 *78.7*
$Y_{citramalate/total\ carbon\ source}$ (g/g – mol/mol)	0.20 g/g 0.24 mol/mol	0.29 g/g 0.2 mol/mol
R-citramalate production rate (g/L/h)	0.89	0.74
Biomass yield (g_{DCW}/g)	0.32	0.29
R-citramalate specific production rate (g/L/g_{DCW}/h)	0.021	0.032
TMCY ($g_{citramalate\ measured}/g_{citramalate\ theoretical}$)	0.24	0.31

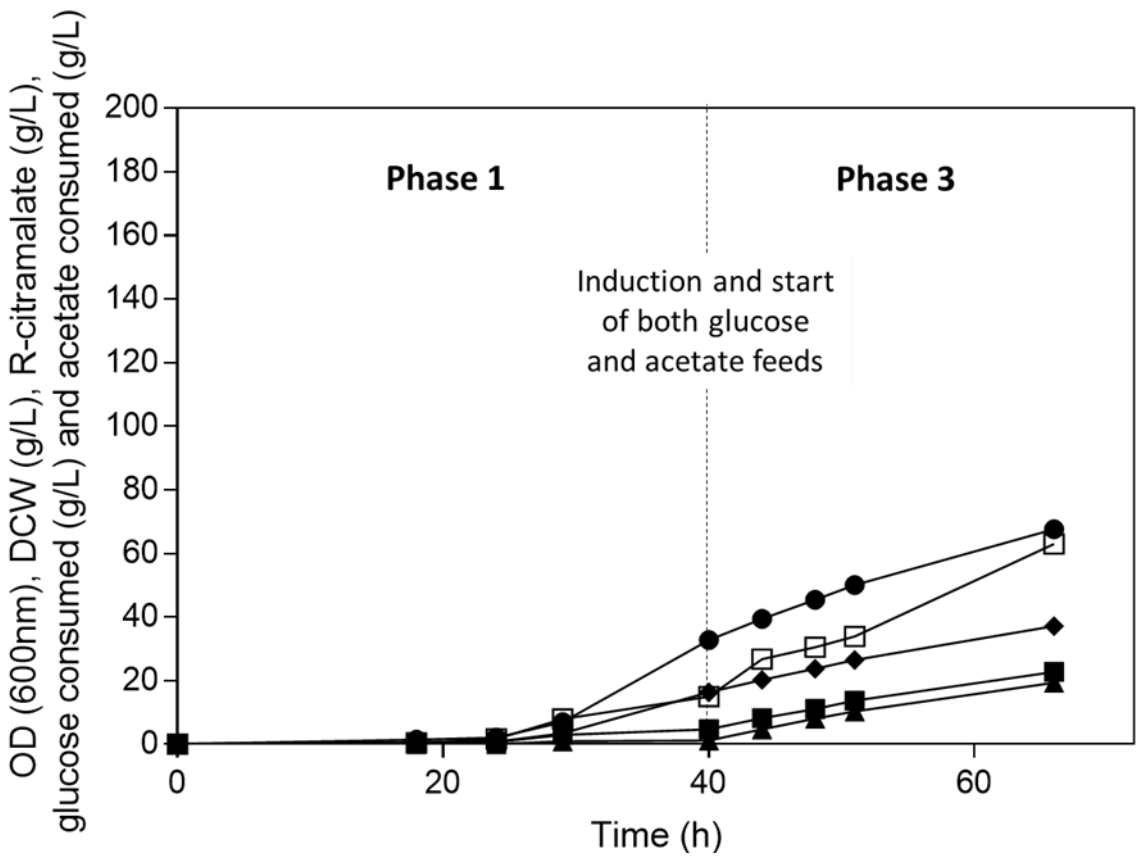


Figure 34: Aerobic fermentation of *E. coli* BW25113 Δ*aceF* pBAD24-*ackA-pta-cimA3.7* for the production of (*R*)-citramalate from glucose and acetate

E. coli BW25113 Δ*aceF* pBAD24-*ackA-pta-cimA3.7* was grown to starvation on glucose and acetate (11.9g/L and 5g/L, respectively) (Phase 1). Once glucoase and acetate from the batch phase were depleted (OD_{600nm} about 15), the expressions of AckA-Pta and CimA3.7 were induced by adding *L*-arabinose (0.2%) to the medium, at which point both the glucose and acetate feeds were started (Phase 3). The glucose and acetate feeds were maintained until the end of the fermentation. Samples were taken regularly to measure OD_{600nm} (□), concentration of dry cell weight (DCW; ■), glucose consumed (●), acetate consumed (♦) and citramalate produced (▲).

8.1.3.6 Conclusions

From the results obtained from the fed-batch fermentation of *E. coli* BW25113 Δ*aceF* overexpressing an acetate assimilation route, it was concluded that the deletion of the PDHC enhanced significantly the carbon flux towards the production of citramalate. Indeed, both a higher citramalate conversion yield and a TMCY were observed in *E. coli* BW25113 Δ*aceF* compared to the benchmark strain of *E. coli* BW25113 Δ*ldhA* (Table 16 and 17). More importantly, the absence of a functional PDHC prevented any decarboxylation of pyruvate to acetyl-CoA under aerobic conditions. Despite the constant requirement of acetate for growth, we succeeded in reaching similar citramalate titre as in the benchmark strain by using *E. coli* BW25113 Δ*aceF* pBAD24-*ackA-pta-cimA3.7* (19.36 g/L and 21.5 g/L, respectively; Table 17). Moreover, the production of citramalate by *E. coli* BW25113 Δ*aceF* pBAD24-*ackA-pta-cimA3.7* required, overall, almost half the amount of total carbon compared to *E. coli* BW25113 Δ*ldhA* pBAD24-*cimA3.7* (79 g instead of 133 g). Furthermore, the glucose required by *E. coli* BW25113 Δ*aceF* for citramalate production represented only 38% of the glucose needed by the benchmark strain for similar citramalate titres. This decrease in glucose consumption indicates: i) a significantly more carbon efficient process, and ii) improved overall process economics, since the requirement of additional acetate is offset by the low cost of this feedstock.

To further confirm that the deletion of the PDHC improved carbon efficiency in a co-feeding strategy, the use of another external acetate source was needed for comparison. Therefore, *E. coli* BW25113 Δ*aceF*

pBAD24-*alcA-aldA-cimA3.7* was generated, and the co-feed of glucose with ethanol was tested.

8.2 Production of (*R*)-citramalate from the co-consumption of glucose and ethanol in *E. coli* BW25113 Δ*aceF*

8.2.1 Demonstration of the co-consumption of glucose and ethanol and determination of the optimal concentration of ethanol for cell growth and *bio-production*

The ethanol assimilation pathway composed of ADH I and ALDH A, and associated with CimA3.7 were shown to be active *in vitro* (see Chapter 7), which suggested that the engineered strain of *E. coli* bearing pBAD24-*alcA-aldA-cimA3.7* should be able to produce (*R*)-citramalate from the co-utilisation of glucose and ethanol.

Previously, significantly improved carbon efficiency for the production of citramalate from glucose/acetate co-feeding was obtained by using *E. coli* BW25113 Δ*aceF*. Thus, the ethanol assimilation pathway was cloned into the Δ*aceF* strain, generating *E. coli* BW25113 Δ*aceF* pBAD24-*alcA-aldA-cimA3.7.* This strain was then characterised for its ability to co-consume ethanol and glucose and produce citramalate.

Firstly, confirmation that ethanol supplementation could be a suitable source of acetyl-CoA was required before any fermentation experiments were performed. Secondly, the ability to produce citramalate from glucose and ethanol needed to be verified too. And finally, the optimum concentration of ethanol to co-feed to ensure both proper growth and bio-product formation was also investigated.

Overnight cultures of *E. coli* BW25113 Δ*aceF* pBAD24-*alcA-aldA-cimA3.7* in Lund medium supplemented with glucose (1%) and acetate (2.5 g/L) was used to inoculate fresh Lund medium (100ml; $OD_{initial}$ =0.1) supplemented with glucose (1%) and various concentrations of ethanol as carbon sources at 30°C in 500 mL flasks (Appendix 11.19). Right after the inoculation, the co-expression of ADH I- ALDH A and CimA3.7 was induced by adding *L*-arabinose (0.2%) to the medium. OD_{600nm} was monitored over 48h.

Table 18: Growth rates, citramalate titres and yields of *E. coli* BW25113 Δ*aceF* pBAD24 *alcA-aldA-cimA3.7* challenged with increased ethanol concentrations

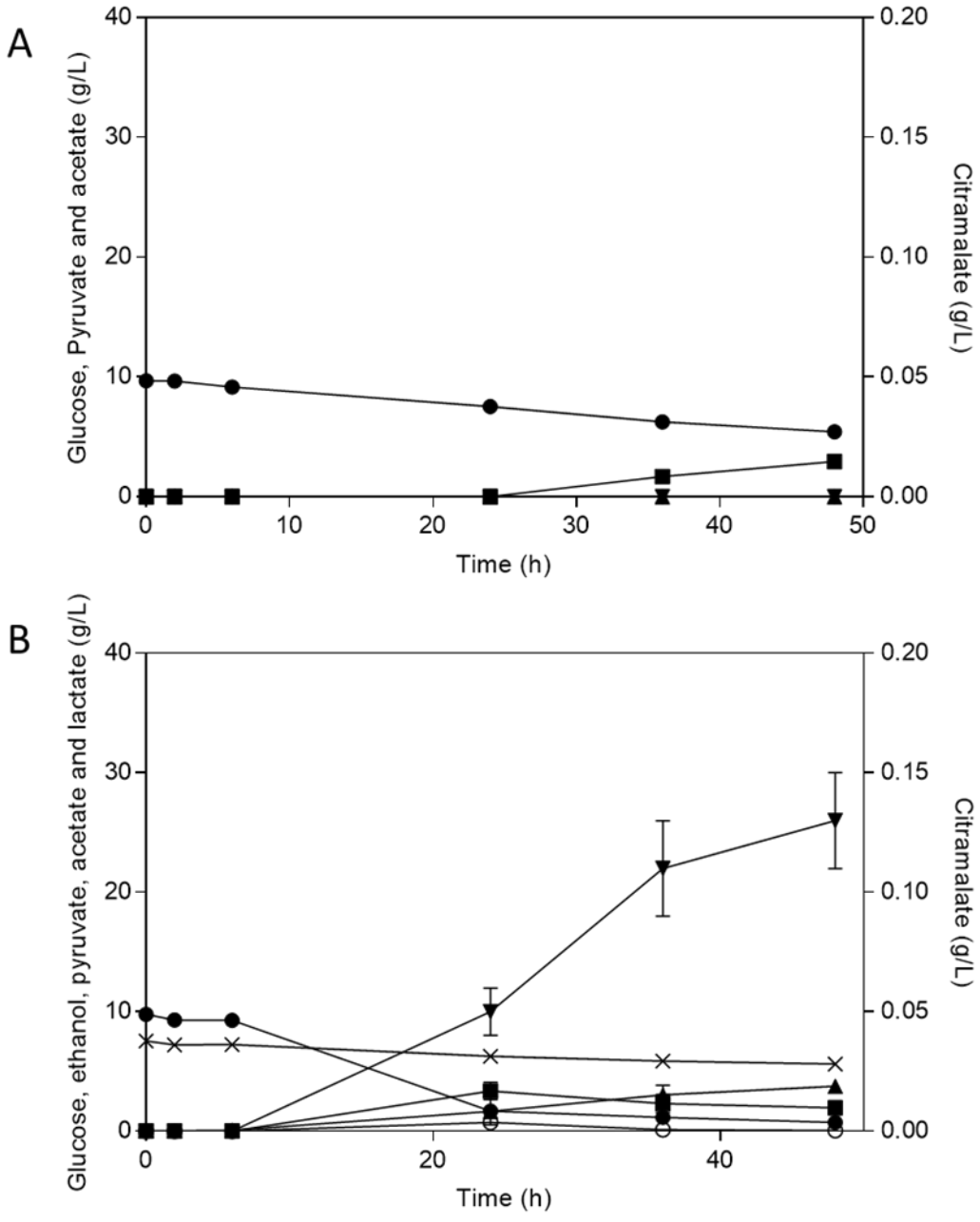
Ethanol concentrations	μ_{max}	Citramalate (g/L)	$Y_{citramalte}$ ($g/g_{glucose+ethanol}$)	Pyruvate accumulation
0%	0.107 ±0.005	0	0	++
1%	0.200 ±0.013	0.13± 0.02	0.011± 0.03	+
3%	0.120 ±0.007	0.12± 0.07	0.010± 0.07	++
5%	0.103 ±0.020	0.07± 0.02	0.006± 0.002	+++

As expected, in the absence of ethanol in the medium the strain was unable to grow (Table 18). The slight growth noticed was likely to be due to the small remaining of acetate from the seed culture. Adding concentrations of 1 or 3% of ethanol supported cell growth. However, ethanol at 3% already significantly impaired the growth compared to 1%, whilst 5% yielded non-growing cells. *E. coli* BW25113 Δ*aceF* was reported earlier [15] as growing slower than wild-type *E. coli* due to its slower glucose uptake. It was assumed that the likelihood of

pyruvate accumulation within the cell when grown on excess glucose repress glycolysis and therefore glucose uptake. Additionally, incrementing the concentration of ethanol available to the strain could lead to increased accumulation of NADH due to the oxidation of ethanol *via* ADH I-ALDH A, which may also impair cell growth. Indeed, the already slowed down metabolism rendered it even more challenging for the cell to balance the NADH/NAD ratio. Moreover, increased concentration of NADH could in turn repress the TCA cycle. Nevertheless, 1% of ethanol was enough to restore and support growth in a Δ*aceF* strain overexpressing an ethanol oxidising route (Appendix 11.19).

Citramalate was successfully produced from the co-utilisation of glucose and ethanol (Table 18 and Fig. 35A-D). No citramalate was produced in the absence of ethanol (Fig. 35A), and cells in presence of 5% ethanol showed poor final titres of citramalate (Fig. 35D). Although the citramalate titres and productivities were similar from the co-feeding of 1% and 3% of ethanol (Table 18), we noticed a higher accumulation of pyruvate within cells fed with 3% ethanol (Fig. 35B-C). The accumulation of pyruvate represented an unwanted feature for two main reasons. Firstly, increased amounts of pyruvate in the cell usually triggers the slowing down of the metabolism, and consequently might impair citramalate production. Second, cells generally limit pyruvate accumulation by converting it into lactate by the lactate dehydrogenase (LDH A), or by acetate formation through the Pyruvate oxidase (PoxB), yielding a net carbon loss regarding citramalate production. Given all these reasons, it was decided that

future ethanol feed would be performed based on a 1% supplementation.



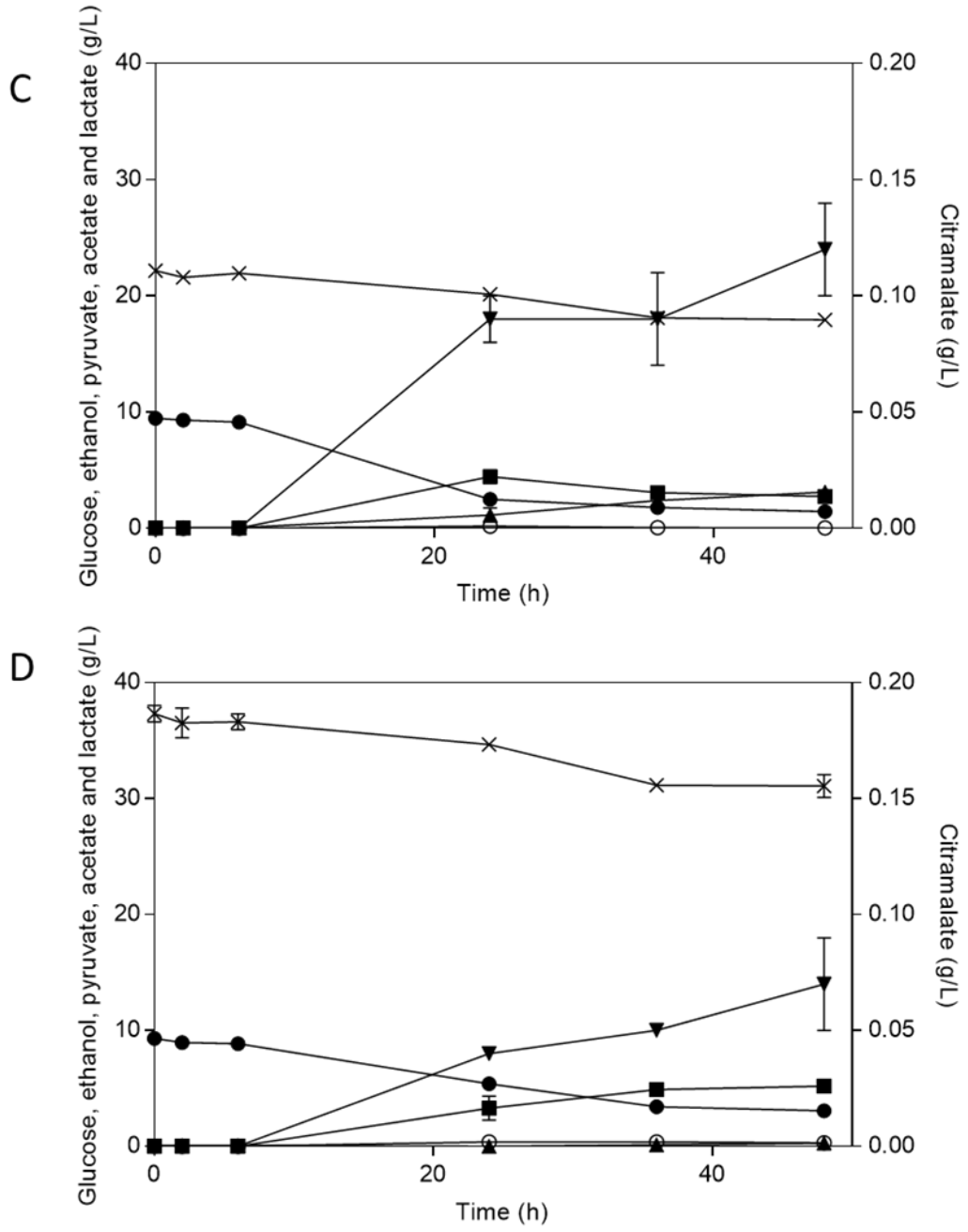


Figure 35: Glucose and ethanol consumption, citramalate and organic acids production in *E. coli* BW25113 Δ*aceF* pBAD24-*alcA-aldA-cimA3.7* when supplementing culture medium containing 1% glucose with 0% ethanol (A), 1% ethanol (B), 3% ethanol (C) and 5% ethanol (D).

Cells of *E. coli* BW25113 Δ*aceF* pBAD24-*alcA-aldA-cimA3.7* grown on glucose and acetate in Lund medium were used to inoculate fresh Lund medium containing glucose (1%) and various concentrations of ethanol. Proteins expression was induced by adding *L*-(+)-arabinose (0.2%) right after inoculation. Concentrations of ethanol were then supplemented to the culture medium. Samples were analysed for glucose (●), ethanol (**x**), pyruvate (■), citramalate (▼), acetate (▲) and lactate (○) concentrations (g/L). Standard deviations are shown, however the error bars are covered by the marker.

Nevertheless, we demonstrated three key points in this section:

- the feasibility of using ethanol as an acetyl-CoA source in a Δ*aceF* strain
- the production of citramalate from pyruvate and acetyl-CoA supplied by glucose and ethanol, respectively
- the optimum concentration of 1% ethanol to co-feed a Δ*aceF* strain with excess glucose showed the best growth rate, citramalate titre and carbon conversion.

To our knowledge, this was the first demonstration of the use of ethanol as a co-carbon source for the bio-production of citramalate and more widely of any bio-chemical. However, further improvements to carbon efficiency and product titre were required, and the strain was tested in fed-batch fermentations

8.2.2 Fed-batch fermentation of *E. coli* BW25113 Δ*aceF* for the production of (*R*)-citramalate from glucose and ethanol

As *E. coli* BW25113 Δ*aceF* pBAD24-*alcA-aldA-cimA3.7* required an external source of acetyl-CoA, the same strategy as previously described was used. (see Section 8.1.4.5). Once the cells consumed all the glucose and acetate from the batch medium, the co-expression of ADH I-ALDH A and CimA3.7 was induced by adding *L*-arabinose (0.2%) to the medium, and the co-feed of glucose and ethanol was started (Fig. 36).

Table 19: Efficiency parameters of the production phases (phase 3) in the benchmark *E. coli* BW25113 Δ*ldhA* pBAD24-*cimA3.7* and *E. coli* BW25113 Δ*aceF* pBAD24-*alcA-aldA-cimA3.7* fed-batch fermentations

Efficiency parameters during phase 3	Benchmark	Experiment 3
	BW25113 Δ*ldhA* pBAD24-*cimA3.7*	**BW25113 Δ*aceF* pBAD24-*alcA-aldA-cimA3.7***
Feeding regime	**Glucose**	**Glucose/Ethanol**
R-citramalate concentration (g/L)	21.5	27
Glucose consumed (g) Ethanol consumed (g) *Total (g)*	133 - *133*	99.7 55.9 *155.6*
$Y_{citramalate/total\ carbon\ source}$ (g/g – mol/mol)	0.20 g/g 0.24 mol/mol	0.23 g/g 0.15 mol/mol
R-citramalate production rate (g/L/h)	0.89	0.49
Biomass yield (g_{DCW}/g)	0.32	0.15
R-citramalate specific production rate ($g/L/g_{DCW}/h$)	0.021	0.031
TMCY ($g_{citramalate\ measured}/g_{citramalate\ theoretical}$)	0.24	0.22

During the production phase, 99.7 g of glucose and 55.9 g of ethanol were consumed, and converted into 23 g of biomass and 35.5 g of citramalate, which gave conversion ratios of 0.15 $g/g_{glucose+acetate\ consumed}$ and 0.23 $g/g_{glucose+acetate\ consumed}$ respectively (Table 19). At the end of the production phase, citramalate production rate was 0.49 g/L/h and a specific production rate of 0.031 $g/L/g_{DCW}/h$. Thus, despite a lower biomass production when using *E. coli* BW25113 Δ*aceF,* the production ability per unit of cells was increased by 50% compared to the benchmark strain. Moreover, a conversion yield of

citramalate similar to the *E. coli* BW25113 Δ*ldhA* strain was obtained, while using 25% less glucose (Table 19).

Overall, from the total of 110 g of glucose and 56 g of ethanol fed during the whole fermentation, 35.5 g of citramalate were produced, yielding a conversion ratio of 0.21 $g/g_{glucose + ethanol\ consumed}$ of the complete process. Overall, a 31% increase in the total carbon conversion to citramalate compared to the benchmark fermentation was obtained along with a reduced proportion of the carbon flow being used for biomass formation.

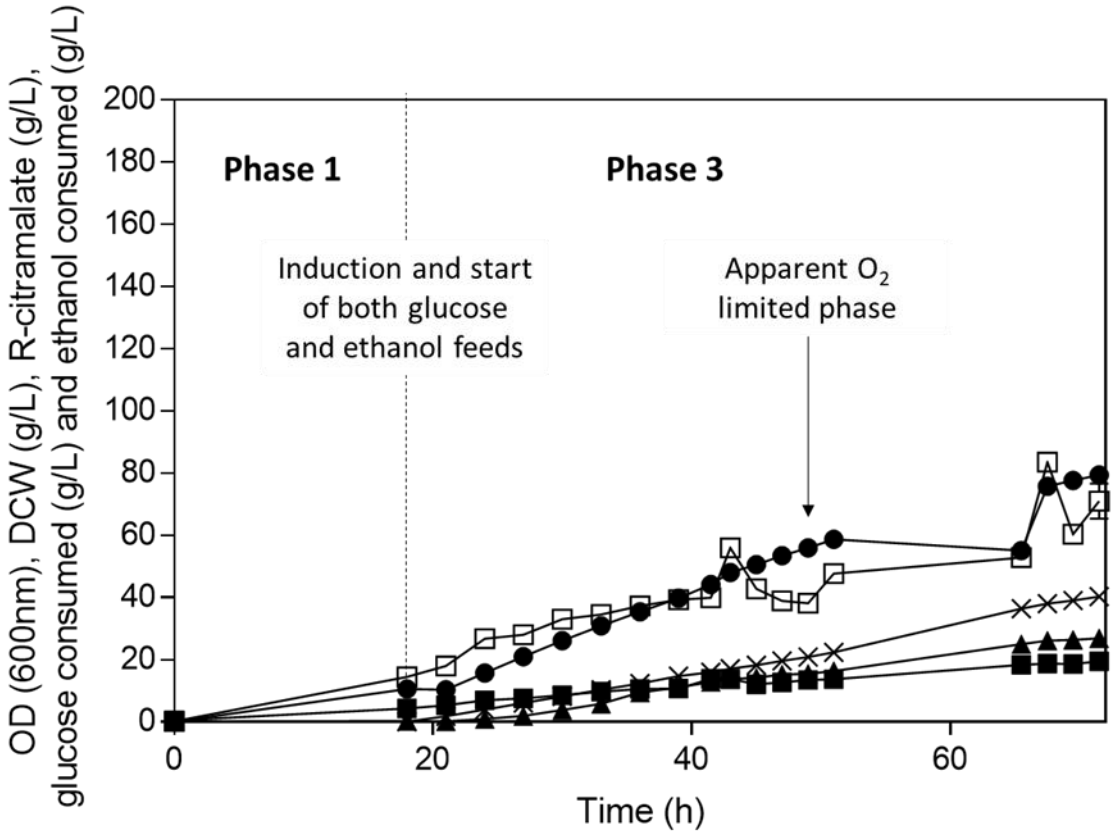


Figure 36: Aerobic fermentation of *E. coli* BW25113 Δ*aceF* pBAD24-*alcA-aldA-cimA3.7* for the production of (*R*)-citramalate from glucose and ethanol

E. coli BW25113 Δ*aceF* pBAD24-*alcA-aldA-cimA3.7* was grown to starvation on glucose and acetate (11.9g/L and 5g/L, respectively) (Phase 1). Once glucose and acetate from the batch phase were depleted (OD_{600nm} about 15), the expressions of ADH I-ALDH A and CimA3.7 were induced by adding *L*-arabinose (0.2%) to the medium, at which point both the glucose and ethanol feeds were started (Phase 3). The glucose and ethanol feeds were maintained until the end of the fermentation. Samples were taken regularly to measure OD_{600nm} (□), concentration of dry cell weight (DCW; ■), glucose consumed (●), ethanol consumed (**x**) and citramalate produced (▲).

During the batch phase (phase 1; Fig. 36-37), the cells accumulated some pyruvate, which was then consumed once the cells were induced. For the 30h post-induction, the cells grew and produced citramalate while consuming glucose and ethanol (Fig. 36). However, the pyruvate measured in the medium remained constant until 18h after induction, while all glucose was consumed and lactate started to accumulate (Fig. 37). This suggested that pyruvate was produced from glucose, and was consumed in one side with ethanol for citramalate, and on the other side was converted into lactate. Additionally, some acetate formation was observed (up to 0.3 g/L, Fig. 37), as well as ethanol accumulation, suggesting there were some bottlenecks. Two bottlenecks in the catalytic route for the conversion of ethanol to acetyl-CoA may have occurred. Firstly, the remaining ethanol concentration could be caused by the insufficient catalytic activity of the ADH I to completely oxidise ethanol. Secondly, the small acetate accumulation post-induction suggested there was limited conversion of the acetate generated *via* the ADH I-ALDH A route to acetyl-CoA. However, ethanol remained steadily consumed during the whole fermentation, and acetate did not accumulate but remained at low concentrations in the medium, which confirmed that it was converted into citramalate (Fig. 37).

Furthermore, worth was to mention that strains with Δ*aceF* could potentially obtain acetate from pyruvate *via* the catalytic activity of pyruvate oxidase (PoxB). PoxB can catalyse the decarboxylation of pyruvate directly to acetate, and its optimal activity has been reported to occur at early stationary phase. PoxB was also reported

to be induced by glucose depletion [91], [224]–[226]. Although this fed-batch was glucose limited, pyruvate and lactate slowly accumulated after 24h, while both glucose consumption and ethanol consumption remained constant (Fig. 37), which suggested that PoxB was unlikely to have had major impact on the production of acetate directly from pyruvate under these conditions.

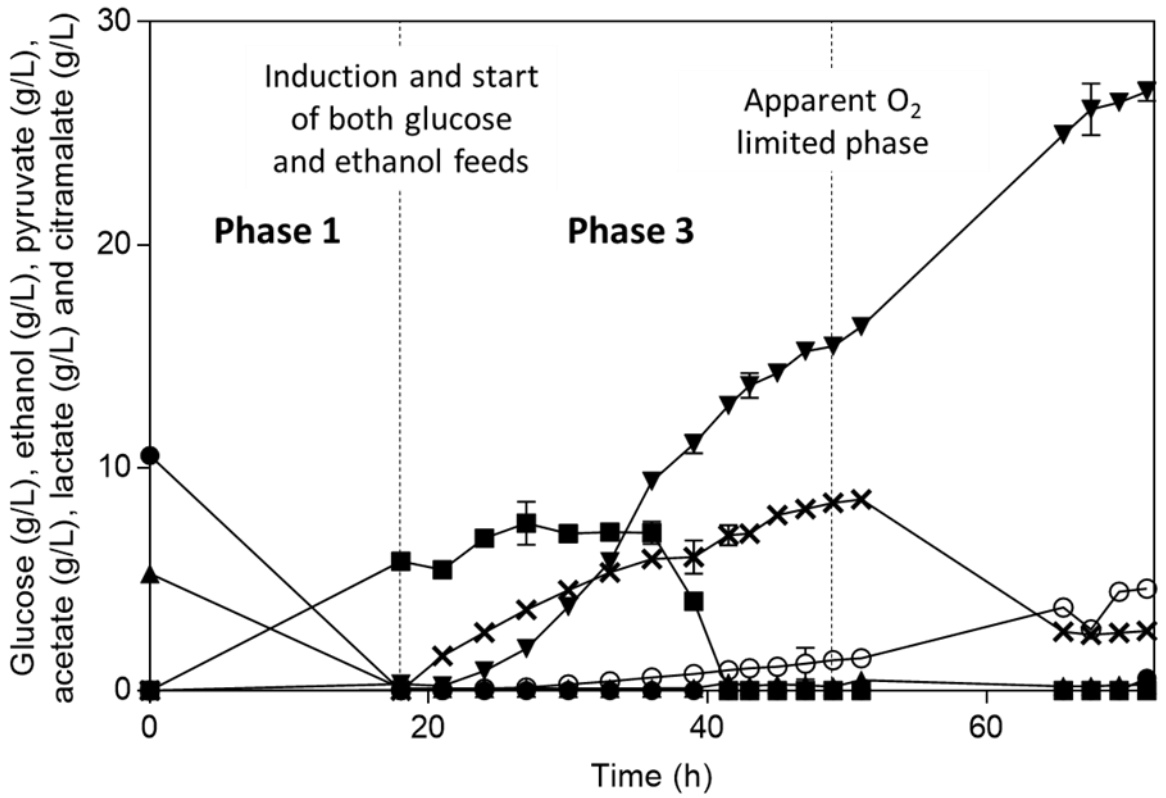


Figure 37: Citramalate and organic acids production (g/L) in fed-batch fermentation of *E. coli* BW25113 Δ*aceF* pBAD24-*alcA-aldA-cimA3.7*

E. coli BW25113 Δ*aceF* pBAD24-*alcA-aldA-cimA3.7* was grown to starvation on glucose and acetate (11.9g/L and 5g/L, respectively) (Phase 1). Once glucose and acetate from the batch phase were depleted (OD_{600nm} about 15), the expressions of ADH I-ALDH A and CimA3.7 were induced by adding *L*-arabinose (0.2%) to the medium, at which point both the glucose and ethanol feeds were started (Phase 3). The glucose and ethanol feeds were maintained until the end of the fermentation. Samples were taken regularly to measure glucose concentration (g/L; ●), ethanol concentration (g/L; **x**), citramalate produced (g/L; ▼), pyruvate concentration (g/L; ■), lactate concentration (g/L; ○) and acetate concentration (g/L; ▲).

Interestingly, after about 48 h, the fermentation appeared to enter a period of oxygen limitation (Fig. 37). During this period of 22 h, surprisingly an increase in ethanol consumption and production of lactate was observed (Fig. 36-37), while the production rate of citramalate decreased from 0.67 g/L/h (from 18 h to 49 h post induction) to 0.48 g/L/h (from 49 h post-induction until the end of the fermentation). Moreover, no more pyruvate accumulated in the medium, suggesting that all pyruvate formed from glucose was converted either into lactate or citramalate (Fig. 37). The apparent increase in ethanol consumption during this period did not result in acetate accumulation, meaning that catalytic activities for ethanol oxidation to acetate, followed by the generation of acetyl-CoA and finally the production of citramalate were matching each other activity levels. Interestingly, to our knowledge, no increase in activity level of the ADH I-ALDH A from *A. nidulans* under micro-oxygenation had been reported previously.

In order to confirm the effect of micro-oxygenation, we tried to reproduce it. Unfortunately, we were unable to repeat this period. Indeed, switching the oxygen off only resulted in asphyxiating the cells, becoming then unable to proceed to either ethanol oxidation or citramalate production (Data not shown). Then, due to time constraints, this putative micro-oxygenation period could not be further investigated.

8.2.3 Conclusions

Comparisons of the fed-batch fermentations of *E. coli* BW25113 Δ*aceF* overexpressing an ethanol assimilation route and *E. coli* BW25113 Δ*ldhA* confirmed the trends that the deletion of PDHC enhanced the carbon conversion from the feedstocks to citramalate (Table 20). From all the fermentations performed, the highest carbon conversion yields, theoretical maximum carbon yield (TMCY), and specific productivity of citramalate were obtained in *E. coli* BW25113 Δ*aceF* pBAD24-*ackA-pta-cimA3.7* with a limited co-feeding of glucose and acetate. Indeed, although, *E. coli* BW25113 Δ*aceF* pBAD24-*alcA-aldA-cimA3.7* showed the same specific productivity, yields of citramalate were lower. This was concluded to be due to a lower biomass production in *E. coli* BW25113 Δ*aceF* pBAD24-*alcA-aldA-cimA3.7*, consequently limiting the ability to convert carbon from the feedstocks into the product of interest. Moreover, despite the energetic advantage presented by the generation of NADH that can be further converted into ATP, accumulation of high concentrations of reduced co-factors in poorly growing cells may further impair growth.

In all fermentations, the cells were still growing, suggesting that the feedstocks were used to support both growth and citramalate synthesis. It was then shortly considered to grow cells until the stationary phase before inducing alternative carbon sources assimilation routes and CimA3.7. However, due to the growth temperature used in the present fed-batch protocol, it involved an extended batch phase, where glucose (and acetate if using Δ*aceF*)

would only be used for biomass production. Such a strategy is not cost-effective for an industrial process.

However, in this project only the impact of the removal of one pyruvate-consuming pathway at a time was investigated. Here, it was shown that carbon efficiency and production formation was improved overall in a *ΔaceF* strain expressing alternative carbon utilisation pathways. Future work will focus on the combination of this and other pyruvate consuming pathway deletion strains.

Table 20: Comparison of efficiencies parameters obtained for all fermentations during the production phase

Efficiency parameters during phase 3	Benchmark	Experiment 1	Experiment 2	Experiment 3
	BW25113 Δ*ldhA* pBAD24-*cimA3.7*	**BW25113 Δ*ldhA* pBAD24-*ackA-pta-cimA3.7***	**BW25113 Δ*aceF* pBAD24-*ackA-pta-cimA3.7***	**BW25113 Δ*aceF* pBAD24-*alcA-aldA-cimA3.7***
Feeding regime	**Glucose**	**Glucose/Acetate**	**Glucose/Acetate**	**Glucose/Ethanol**
R-citramalate concentration (g/L)	21.5	4.73	19.36	27
Glucose consumed (g) Acetate consumed (g) Ethanol consumed (g) *Total (g)*	133 - - *133*	36 30.5 - *66.5*	49.7 - 28.9 *78.7*	99.7 - 55.9 *155.6*
$Y_{\text{citramalate/total carbon source}}$ (g/g – mol/mol)	0.20 g/g 0.24 mol/mol	0.06 g/g 0.04 mol/mol	0.29 g/g 0.2 mol/mol	0.23 g/g 0.15 mol/mol
R-citramalate production rate (g/L/h)	0.89	0.26	0.74	0.49
Biomass yield (g_{DCW}/g)	0.32	0.16	0.29	0.15
R-citramalate specific production rate ($g/L/g_{DCW}/h$)	0.021	0.019	0.032	0.031
TMCY ($g_{\text{citramalate measured}}/g_{\text{citramalate theoretical}}$)	0.24	0.07	0.31	0.22

Table 21: Comparison of efficiencies parameters obtained for all fermentations during the total length of the fermentations

Efficiency parameters during total process	Benchmark	Experiment 1	Experiment 2	Experiment 3
	BW25113 Δ*ldhA* pBAD24-*cimA3.7*	**BW25113 Δ*ldhA* pBAD24-*ackA-pta-cimA3.7***	**BW25113 Δ*aceF* pBAD24-*ackA-pta-cimA3.7***	**BW25113 Δ*aceF* pBAD24-*alcA-aldA-cimA3.7***
Feeding regime	**Glucose**	**Glucose/Acetate**	**Glucose/Acetate**	**Glucose/Ethanol**
R-citramalate concentration (g/L)	21.5	4.73	19.36	27
Total Glucose cons (g) Total Acetate cons (g) Total Ethanol cons (g) *Total (g)*	167 - - *167*	77 35.5 - *112.5*	83.2 - 45.6 *128.8*	110.1 - 55.7 *165.8*
$Y_{\text{citramalate/total carbon source}}$ (g/g – mol/mol)	0.16 g/g 0.19 mol/mol	0.05 g/g 0.03 mol/mol	0.18 g/g 0.12 mol/mol	0.21 g/g 0.13 mol/mol

9. Conclusions, discussion and future direction

The work in this thesis aimed to improve the carbon efficiency of an existing process for the production of (*R*)-citramalate in *E. coli,* which was calculated at a $Y_{citramalate/glucose}$ of 0.20 g/g in the control strain *E. coli* BW25113 Δ*ldhA* pBAD24-*cimA3.7* grown on glucose as sole carbon source (Table 20). To improve this figure, two co-feeding strategies were designed and compared which used combinations of glucose/acetate or glucose/ethanol. *E. coli* production strains were constructed that were capable of co-consuming these different carbon sources and producing the target compound. Furthermore, the strains were constructed using simple and rational pathway design. To our knowledge this was the first time that production of (*R*)-citramalate from co-feeding of glucose and non-carbohydrates feedstocks had been reported. Additionally, it was also demonstrated that ethanol can be used as a suitable feedstock to support both growth and bio-production of target compounds in *E. coli*, which again, to our knowledge has not been previously reported.

Although the co-expression of CimA3.7 with either an acetate or ethanol assimilation route was enough to enable citramalate production from co-feeding, we demonstrated that the carbon efficiency, the TMCY during the production phase, as well as the overall carbon conversion ratio were further improved when *aceF*, a gene encoding the core subunit of the PDHC (E_2 enzyme) was deleted (Tables 20 & 21), removing the strain's ability to convert pyruvate to acetyl-CoA (Δ*aceF*). Carbon efficiencies of 0.29 $g/g_{glucose+acetate}$ and 0.23 $g/g_{glucose+ethanol}$ were obtained during the production phase by co-

feeding *E. coli* BW5113 Δ*aceF* with acetate and ethanol, respectively. In contrast, a carbon yield of only 0.06 g/g was observed in glucose/acetate co-feeding in the initial *E. coli* BW25113 Δ*ldhA*. Furthermore, removing the decarboxylation of pyruvate increased the citramalate production rate from 0.21 g/L/h in *E. coli* BW5113 Δ*ldhA* co-fed with glucose/acetate, to 0.74 g/L/h and 0.49 g/L/h in *E. coli* BW5113 Δ*aceF* co-fed with glucose/acetate and glucose/ethanol, respectively. Moreover, *E. coli* BW25113 Δ*aceF* showed a 50% increase in specific productivity compared to *E. coli* BW5113 Δ*ldhA* fed with glucose only or glucose/acetate. Considering the carbon conversion ratios of the complete fermentation processes (Table 21), a 12.5% and 31% increase were obtained in *E. coli* BW25113 Δ*aceF* co-fed with glucose/acetate and glucose/ethanol respectively, providing promising routes for future improvements. However, more in-depth carbon efficiencies calculations should be carried out, in order to assess the exact impact of CO_2 formation against the diversion of carbon towards cell maintenance, energy and redox balance, and carbon futile cycles *via* acetate node or the glyoxylate shunt.

Other studies investigated the carbon efficiency of the production of citramalate from glucose by inactivating or down-regulating the acetyl-CoA consuming routes [227], focusing on the citrate synthase (encoded by *gltA*), the acetate route (*ackA*) and the leucine pathway (*leuCD*). However, such metabolic engineering resulted in an *E. coli* strain auxotrophic for both glutamate and leucine, which are necessary to support both growth and the TCA cycle. Not only was

the supplementation of glutamate and leucine significantly costly from an industrial process perspective, but the strain grew poorly and displayed impaired production of citramalate. A final titre of 46.5 g/L citramalate was reached after 132h of fermentation, yielding a productivity of 0.35 g/L/h. Moreover, it was previously demonstrated that the degradation of citramalate into citraconate *via* the LeuCD enzymes (3-isopropylmalate dehydratase) belonging to the native leucine producing pathway in *E. coli* remained minor [228]. Considering both the metabolic burden and the additional cost generating by the deletion of *leuCD*, this knock-out did not appear as a suitable option here. Therefore, we focused on implementing simple metabolic engineering to allow the use of realistic and affordable feedstocks substrates for industrial applications.

The Δ*aceF* strains co-fed with either glucose/acetate or glucose/ethanol showed slightly lower carbon performances compared to production strains of other organic acids used as platform chemicals described in the literature, such as itaconic acid (0.54 $g/g_{glucose}$; 0.57 g/L/h; [229]) and fumaric acid (0.39 $g/g_{glucose}$; 0.45 g/L/h;[230]). However, we succeeded in developing more productive processes, yielding productivity values of 0.74g/L/h and 0.49 g/L/h in glucose/acetate and glucose/ethanol co-feeding, respectively.

Although, the current process is not yet optimised to become competitive based on industrial requirements [4], [5], [231]–[233], there is scope for further improvement. In the *E. coli* BW5113 Δ*aceF* fermentations presented here with either acetate or ethanol co-

feeding, the accumulation of pyruvate, lactate and acetate was observed, suggesting further metabolic engineering is required to optimise the process [234]. One strategy would be to delete all pyruvate consuming pathways catalysed by the lactate dehydrogenase (encoded by *ldhA*) and the pyruvate oxidase (encoded by *poxB*) (Fig. 38).

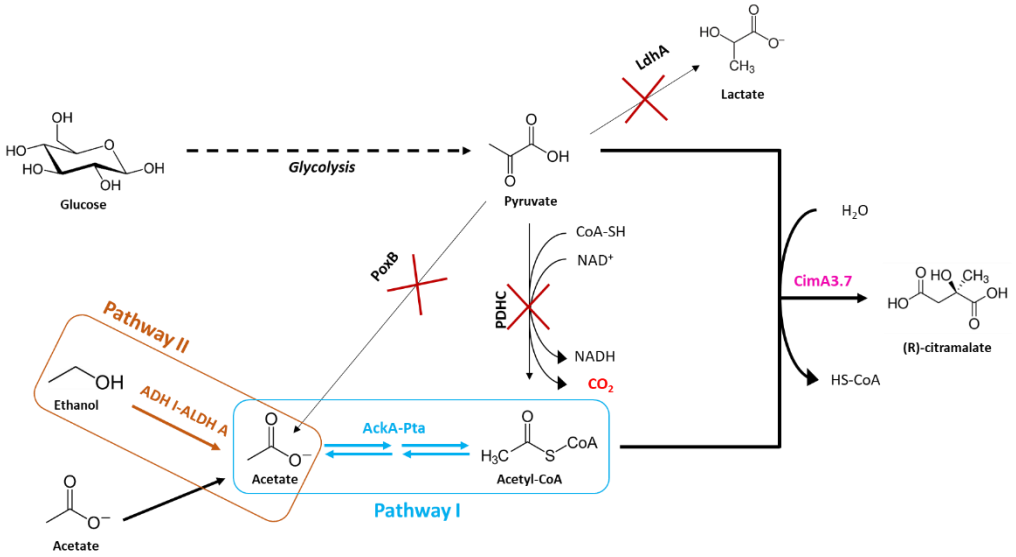


Figure 38: Schematic of future metabolic engineering to perform on *E. coli* BW25113 Δ*aceF*

PDHC: Pyruvate dehydrogenase complex; PoxB: Pyruvate oxidase; LdhA: lactate dehydrogenase; AckA-Pta: Acetate kinase-phosphoacetyltransferase node; ADH I-ALDH A: Alcohol dehydrogenase I –acetaldehyde dehydrogenase A; CimA3.7: Citramalate synthase.
Pathway I: Overexpression of the native acetate assimilation route from *E. coli*.
Pathway II: Insertion of exogenous ethanol assimilation route from *A. nidulans*.

Indeed, in either acetate or ethanol co-feeding systems, increased side productions of lactate in Δ*aceF* strains (up to 3.4 g/L) compared to Δ*ldhA* strains (about 0.5 g/L) were observed, suggesting that the deletion of the lactate dehydrogenase should be kept despite the fact that the fermentations are run under aerobic conditions.

The deletion of the phosphoenolpyruvate synthase (encoded by *pps*) can also be considered, to prevent any dissimilation of pyruvate *via* neoglucogenesis. Additionally, complimentary metabolic modelling [30], [61], [235]–[237] could be carried out to identify non-obvious pathways to delete; this strategy has already been used successfully to improve the tolerance of *S. cerevisiae* and *E. coli* to ethanol [42], [45], [46]. The challenge with such a strain is the high accumulation of pyruvate during the batch phase of the fermentation, which could generate metabolic burdens such as inhibiting glucose uptake and saturating the enzyme CimA3.7 (K_M=0.7mM for pyruvate). This could be addressed by performing a batch phase with acetate as the sole carbon source, in order to feed the TCA cycle and enable the strain to grow sufficiently. Once the cells reach a sufficient density, CimA3.7 and the alternative carbon source pathways would be induced, and the appropriate glucose and acetate-or ethanol feed could be started to provide the pyruvate needed for the production of citramalate. This would enable the formation of citramalate in a situation where less carbon would be used for biomass production. Interestingly, in a previous study [7], citramalate productivity decreased as the process time increased, therefore uncoupling growth and bio-production might not necessarily be the optimal strategy regarding carbon efficiency. Given this, it may be beneficial to try an alternative fermentation strategy, which would involve induction of the citramalate production route earlier during the batch phase. In parallel, another way to enhance the efflux of citramalate would be the *in situ* removal of citramalate from the fermentation broth, which

would result in pulling the biosynthetic pathway towards higher citramalate production, and increased uptake of carbon sources. However, the simultaneous extraction of citramalate remains challenging [238] and non-cost effective yet.

Another metabolic consideration worth further investigating is the possible up-regulation of the glyoxylate shunt. Under excess of glucose, the glyoxylate shunt is repressed, however key enzymes of the glyoxylate shunt become up-regulated under glucose-limiting condition and when acetate is the sole carbon source [239]. Therefore, there is a chance that this pathway was activated during the fermentation, resulting in decreasing the growth rate as well as diverted carbon atoms towards the production of biomass and metabolic intermediates [240] instead of the target compound. Only transcriptomic studies would be able to confirm or not this hypothesis. Nevertheless, the main key enzymes of the glyoxylate shunt are the isocitrate lyase (*aceA*) and the malate synthase (*aceB*), and their deletion would be an interesting strategy to explore to prevent the burden of carbon loss *via* the glyoxylate shunt, as well as the competition with the TCA cycle.

Even though the molecular cloning strategies used in these studies were both simple and rational, we did not further optimize at the transcriptional level for each gene. With this in mind, the modulation of the expression, solubility and activity of the catalytic enzymes is a route to explore. This is based on the assumption, that it is possible, that the level of activity of the citramalate, acetate and ethanol routes might not have been optimally matched to each other, thus

generating potential metabolic bottlenecks. It would be of interest to investigate the impact of either the strength of expression or copy number of each of the *cimA3.7*, *ackA-pta* (acetate node) and *alcA-aldA* (ethanol assimilation route) genes. Additionally, the impact of other ribosome binding sites on the expression levels of the different recombinant enzymes, as well as the tendency of forming inclusion bodies could be further experimented [209]. In parallel to this, inserting additional transport systems to enhance the uptake by the cells of the substrates (acetate or ethanol) is also a path worth exploring. In the case of ethanol, NADH-dependent-transporters could be an interesting option to sink the putative accumulation of NADH. Future work could also consider the chromosomal integration of the citramalate pathway along with either the acetate or ethanol route [241], [242]. In conjunction, it may be of benefit to make use of constitutive or non-chemically induced promoters, which would negate the need for chemical induction. This would remove the metabolic stresses caused by the necessity of using expression vectors, inducers and antibiotics, as well as the cost of both inducer and antibiotic.

Thus, more optimisation of the fermentation process is required to render *E. coli* based citramalate production from the co-feeding of glucose with acetate or ethanol cost-effective for the biological production of the commodity chemical MAA. Interestingly, citramalate also has the potential to be used as a key chiral intermediate for the production of drugs such as prostaglandins [243]–[245]. Therefore, if carbon efficiency and productivity could be further optimised, the

citramalate route would become attractive for further novel applications.

From a life cycle analysis (LCA) perspective, there are few key points to highlight. It becomes widely acknowledged that first generations of biofuels and biochemicals produced from purified glucose fermenting bacteria remain ineffective regarding life cycle analysis, and can show a relatively higher carbon footprint than as first imagined [246]. As example, LCA performed on first generation of bioethanol demonstrated very versatile results, depending of the origin of the sugar feedstock (maize, sugar cane, sugar beet or wheat) as well as the further use of the produced bioethanol as either a fuel or solvent [247]. More surprisingly, fossil-originated ethanol showed less impact on biodiversity and ecosystem, essentially due to the smallest proportion of land occupation involved in petrochemical processes compared to land use required for crop production. Ironically, one of the main challenge underlined by the overall poor LCA outcomes of bio-processes is the sustainability of the initial feedstock. Purified glucose was widely concluded as a poor long-term viable feedstock from both economic and environmental perspectives [247], [248]. Following its production, citramalate is then recovered from the culture broth by performing ion-exchange before being converted into MAA *via* the hot pressurised water process. If recovery of organic acids through ion-exchange chromatography is widely used in bio-processes and recognized as a low-energy demanding technique [238], the decarboxylation-dehydratation of citramalate to form MAA is expected to impact more on the overall carbon footprint

and LCA of the bio-process. However, the protocol for MAA generation from citramalate showed excellent yields and had already undergone a series of process optimization to reduce its energy and carbon impact. Therefore, more efforts should be yet focused on optimizing upstream steps in the bio-process. To this extend, the strategy described here provided two main points of progress regarding the overall improvement of sustainability in the bio-production of a commodity chemical as citramalate. First, the use of ethanol or acetate from gas-fermenting bacteria helped reducing the overall use of energy and GHG emissions compared to ethylene-based ethanol or acetate [249]. Second, despite the use of glucose as feedstock, performing co-feeding with either acetate or ethanol allowed a significant reduction of the proportion of purified sugar to be used in the whole bio-process (Section 8.2.3), directly improving the sustainability of such route. Then, more efforts should be undergone to further improve the LCA outcomes of the bio-production of citramalate, and implementing the use of more sustainable feedstock should be one of the first.

Nevertheless, the end goal of this project was to identify future directions of study, which would further aid the development of an industrial bio-process for carbon efficient production of citramalate. We demonstrated that co-consumption of glucose/acetate or glucose/ethanol is feasible, particularly in a pyruvate dehydrogenase inactivated strain (Δ*aceF*), and providing carbon-neutral acetate or ethanol. Amongst the two alternative carbon sources investigated, acetate was concluded as the more promising feedstock, despite the

energy cost incurred by the cell during its assimilation *via* the AckA-Pta node. Carbon-neutral fermentation of acetate is already established, ensuring availability and cost-effectivity of the substrate. Such a process would make the citramalate route more competitive compared to the current petroleum-based processes, and have the added benefit of providing a step forward in reducing carbon emission in bio-processes.

10. References:

[1] T. Witczak, J. Skrzypek, M. Grzesik, and M. Witczak, "Liquid-Phase Esterification of Methacrylic Acid with Methanol Catalyzed by Heteropolyacid," *Int. J. Chem. React. Eng.*, vol. 8, pp. 1–18, 2010.

[2] X. Chen, L. Zhou, K. Tian, A. Kumar, S. Singh, B. A. Prior, and Z. Wang, "Metabolic engineering of Escherichia coli: A sustainable industrial platform for bio-based chemical production," *Biotechnol. Adv.*, vol. 31, no. 8, pp. 1200–1223, 2013.

[3] B. J. Nikolau, M. A. D. N. Perera, L. Brachova, and B. Shanks, "Platform biochemicals for a biorenewable chemical industry," *Plant J.*, vol. 54, pp. 536–545, 2008.

[4] J. Nielsen, M. Fussenegger, J. Keasling, S. Y. Lee, J. C. Liao, K. Prather, and B. Palsson, "Engineering synergy in biotechnology.," *Nat. Chem. Biol.*, vol. 10, no. 5, pp. 319–22, 2014.

[5] S. Van Dien, "From the first drop to the first truckload: Commercialization of microbial processes for renewable chemicals," *Curr. Opin. Biotechnol.*, vol. 24, no. 6, pp. 1061–1068, 2013.

[6] J. D. Keasling, "Manufacturing molecules through metabolic engineering," *Science*, vol. 330, pp. 1355–1359, 2010.

[7] J. Webb, "Bio-production of C5 dicarboxylic acids for chemical

conversion to methyl methacrylate," *PhD diss. - Univ. Nottingham, UK*, 2015.

[8] M. Carlsson, C. Habenicht, L. C. Kam, M. J. Antal, N. Bian, R. J. Cunningham, and M. Jones, "Study of the Sequential Conversion of Citric to Itaconic to Methacrylic Acid in Near-Critical and Supercritical Water," *Ind. Eng. Chem. Res*, vol. 33, no. 8, pp. 1989–1996, 1994.

[9] I. W. Bogorad, T.-S. Lin, and J. C. Liao, "Synthetic non-oxidative glycolysis enables complete carbon conservation.," *Nature*, vol. 502, pp. 693–698, 2013.

[10] Y. Wu, X. Shen, Q. Yuan, and Y. Yan, "Metabolic Engineering Strategies for Co-Utilization of Carbon Sources in Microbes," *Bioengineering*, vol. 3, no. 10, pp. 1–10, 2016.

[11] J. Van Haveren, E. L. Scott, and J. Sanders, "Bulk chemicals from biomass," *Biofuels, Bioprod. Bioref*, vol. 2, pp. 41–57, 2008.

[12] P. Gawand, P. Hyland, A. Ekins, V. J. J. Martin, and R. Mahadevan, "Novel approach to engineer strains for simultaneous sugar utilization," *Metab. Eng.*, vol. 20, pp. 63–72, 2013.

[13] S. J. Moore, J. T. Macdonald, and P. S. Freemont, "Cell-free synthetic biology for in vitro prototype engineering," *Biochem. Soc. Trans.*, vol. 45, pp. 785–791, 2017.

[14] Y. Lu, "Cell-free synthetic biology: Engineering in an open

world," *Synth. Syst. Biotechnol.*, vol. 2, pp. 23–27, 2017.

[15] Y. Tashiro, S. H. Desai, and S. Atsumi, "Two-dimensional isobutyl acetate production pathways to improve carbon yield," *Nat. Commun.*, vol. 6, no. 7488, pp. 1–9, 2015.

[16] F. M. Liew, M. E. Martin, R. C. Tappel, B. D. Heijstra, C. Mihalcea, and M. Köpke, "Gas Fermentation-A flexible platform for commercial scale production of low-carbon-fuels and chemicals from waste and renewable feedstocks," *Front. Microbiol.*, vol. 7, no. 694, pp. 1–28, 2016.

[17] M. S. Chisholm, "Artificial Glass—The Versatility of Poly(methyl methacrylate) from Its Early Exploitation to the New Millennium," *J. Chem. Educ.*, vol. 77, no. 7, p. 841, 2000.

[18] K. Nagai and T. Ui, "Trends and future of monomer- MMA technologies," *R&D Report, Sumitomo Kagaru*, vol. 2, pp. 1–12, 2004.

[19] 2010 Chemical Weekly, "Methyl Methacrylate: A Techno-Commercial Profile. Part 1: Manufacturing Technology," *Chem. Wkly.*, vol. Special Re, p. 8, 2010.

[20] K. Nagai, "New developments in the productionof methyl methacrylate," *Appl. Catal. A Gen.*, vol. 221, pp. 367–377, 2001.

[21] J. Keijsper, P. Arnoldy, M. J. Doyle, and E. Drent, "'Green' MMA; an environmental benign and economically attractive process for the production of methyl methacrylate," *Reel. Trav. Chim.*,

vol. 115, p. 7, 1996.

[22] B. Harris, "Acrylics For The Future," *Ingenia*, vol. 45, pp. 18–22, 2010.

[23] J. Randolph and M. Masters, Gilbert, *Energy for sustainability: Technology, Planning, Policy*, Island Pre. 2008.

[24] T. Werpy and G. Petersen, "Top Value Added Chemicals from Biomass: Volume I — Results of Screening for Potential Candidates from Sugars and Synthesis Gas," *Pacific Northwest Natl. Lab.*, pp. 1–76, 2004.

[25] P. Anastas and N. Eghbali, "Green Chemistry: Principles and Practice," *Chem. Soc. Rev.*, vol. 39, pp. 301–312, 2009.

[26] D. Jullesson, F. David, B. Pfleger, and J. Nielsen, "Impact of synthetic biology and metabolic engineering on industrial production of fine chemicals," *Biotechnol. Adv.*, vol. 33, no. 7, pp. 1395–1402, 2015.

[27] Y. Luo, J.-K. Lee, and H. Zhao, "Challenges and opportunities in synthetic biology for chemical engineers," *Chem Eng Sci*, vol. 144, no. 5, pp. 724–732, 2015.

[28] V. G. Yadav, M. De Mey, C. Giaw Lim, P. Kumaran Ajikumar, and G. Stephanopoulos, "The future of metabolic engineering and synthetic biology: Towards a systematic practice," *Metab. Eng.*, vol. 14, no. 3, pp. 233–241, 2012.

[29] D. W. Johnson, G. R. Eastham, M. Poliakoff, and T. A. Huddle, "A process for the production of methacrylic acid and its

derivatives and polymers produced therefrom," WO 2012/069813, 2012.

[30] J. W. Lee, D. Na, J. M. Park, J. Lee, S. Choi, and S. Y. Lee, "Systems metabolic engineering of microorganisms for natural and non-natural chemicals," *Nat. Chem. Biol.*, vol. 8, no. 6, pp. 536–546, 2012.

[31] M. J. Burk, A. P. Burgard, R. E. Osterhout, and P. Pharkya, "Microorganisms for the production of methacrylic acid," WO 2009/135074, 2009.

[32] T. Rohwerder and R. H. Müller, "Biosynthesis of 2-hydroxyisobutyric acid (2-HIBA) from renewable carbon.," *Microb. Cell Fact.*, vol. 9, no. 13, pp. 1–10, Feb. 2010.

[33] M. J. Burk, A. P. Burgard, R. E. Osterhout, J. Sun, and P. Pharkya, "Microorganisms for producing methacrylic acid and methacrylate esters and methods related thereto," WO2012135789 A2, 2012.

[34] G. R. Eastham, G. Stephens, and A. Yiakoumetti, "Process for the biological production of methacrylic acid and derivatives thereof," WO2016185211 A1, 2016.

[35] H. Greim, J. Ahlers, R. Bias, B. Broecker, H. Hollander, H.-P. Gelbke, S. Jacobi, *et al.*, "Assessment of structurally related chemicals: Toxicity and ecotoxicity of acrylic acid and acrylic acid alkyl esters (acrylates), methacrylic acid and methacrylic acid alkyl esters (methacrylates)," *Chemosphere*, vol. 31, no.

2, pp. 2637–2659, 1995.

[36] V. Ansteinsson, H. B. Kopperud, E. Morisbak, and J. T. Samuelsen, "Cell toxicity of methacrylate monomers-The role of glutathione adduct formation," *J. Biomed. Mater. Res. Part A*, vol. 101, no. 12, pp. 3504–3510, 2013.

[37] E. Yoshii, "Cytotoxic effects of acrylates and methacrylates: Relationships of monomer structures and cytotoxicity," *J. Biomed. Mater. Res.*, vol. 37, no. 4, pp. 517–524, 1997.

[38] Z. Bereznowski, "In vivo assessment of methyl methacrylate metabolism and toxicity," *Int. J. Biochem. Cell Biol.*, vol. 27, no. 12, pp. 1311–1316, 1995.

[39] J. Trček, N. Pereira Mira, and L. R. Jarboe, "Adaptation and tolerance of bacteria against acetic acid," *Appl Microbiol Biotechnol*, vol. 99, pp. 6215–6229, 2015.

[40] M. J. Dunlop, "Engineering microbes for tolerance to next-generation biofuels," *Biotechnol Biofuels*, vol. 4, no. 32, pp. 1–9, 2011.

[41] K. M. Yang, J. M. Woo, S. M. Lee, and J. B. Park, "Improving ethanol tolerance of Saccharomyces cerevisiae by overexpressing an ATP-binding cassette efflux pump," *Chem. Eng. Sci.*, vol. 103, pp. 74–78, 2013.

[42] E. Ohta, Y. Nakayama, Y. Mukai, T. Bamba, and E. Fukusaki, "Metabolomic approach for improving ethanol stress tolerance in Saccharomyces cerevisiae," *J. Biosci. Bioeng.*, vol. 121, no.

4, pp. 399–405, 2016.

[43] C. Yamaoka, O. Kurita, and T. Kubo, "Improved ethanol tolerance of Saccharomyces cerevisiae in mixed cultures with Kluyveromyces lactis on high-sugar fermentation," *Microbiol. Res.*, vol. 169, no. 12, pp. 907–914, 2014.

[44] S. Hohmann, "Osmotic stress signaling and osmoadaptation in yeasts.," *Microbiol. Mol. Biol. Rev.*, vol. 66, no. 2, pp. 300–372, 2002.

[45] M. H. Rau, P. Calero, R. M. Lennen, K. S. Long, and A. T. Nielsen, "Genome-wide Escherichia coli stress response and improved tolerance towards industrially relevant chemicals," *Microb. Cell Fact.*, vol. 15, no. 176, pp. 1–18, 2016.

[46] M. C. Teixeira, L. R. Raposo, N. P. Mira, A. B. Lourenço, and I. Sá-Correia, "Genome-wide identification of Saccharomyces cerevisiae genes required for maximal tolerance to ethanol," *Appl. Environ. Microbiol.*, vol. 75, no. 18, pp. 5761–5772, 2009.

[47] M. Schwartz, *Smart Materials*. CRC Press, 2009.

[48] R. Bentley and C. Thiessen, "Biosynthesis of itaconic acid in Aspergillus terreus - I. Tracer studies with C14-labelled substrates," *J. Biol. Chem.*, vol. 226, pp. 673–687, 1957.

[49] R. Bentley and C. Thiessen, "Biosynthesis of itaconic acid in Aspergillus terreus - III. The properties and reaction mechanism of cis-aconitic acid and decarboxylase," *J. Biol. Chem.*, vol. 226, pp. 703–720, 1957.

[50] A. Hevekerl, A. Kuenz, and K.-D. Vorlop, "Influence of the pH on the itaconic acid production with Aspergillus terreus," *Appl Microbiol Biotechnol*, vol. 98, pp. 10005–10012, 2014.

[51] B. Max, J. M. Salgado, N. Rodríguez, S. Cortés, A. Converti, and J. M. Domínguez, "Biotechnological production of citric acid.," *Braz. J. Microbiol.*, vol. 41, pp. 862–875, 2010.

[52] M. G. Steiger, M. L. Blumhoff, D. Mattanovich, M. Sauer, N. P. Mira, and L. R. Jarboe, "Biochemistry of microbial itaconic acid production," *Front. Microbiol.*, vol. 4, no. 23, pp. 1–5, 2013.

[53] S. Kanamasa, L. Dwiarti, M. Okabe, and E. Y. Park, "Cloning and functional characterization of the cis-aconitic acid decarboxylase (CAD) gene from Aspergillus terreus," *Appl Microbiol Biotechnol*, vol. 80, pp. 223–229, 2008.

[54] M. Ueda, R. Sashida, H. Yamada, and Y. Asano, "Applied Microbiology Biotechnology Production of (S)-(+)-citramalic acid from itaconic acid by resting cells of Alcaligenes denitrificans strain MCI2775," *Appl Microbiol Biotechnol*, vol. 40, pp. 466–469, 1993.

[55] B.-F. He, T. Ozawa, T. Nakajima-Kambe, and T. Nakahara, "Efficient Conversion of Itaconic Acid to (s)-(+)-Citramalic Acid by Alcaligenes xylosoxydans IL 142," *J. Biosci. Bioeng.*, vol. 89, no. 4, pp. 388–391, 2000.

[56] H. A. Barker, "Citramalate Lyase of Clostridium tetanomorphum," *Arch. fiir Mikrobiol.*, vol. 59, pp. 4–12, 1967.

[57] S. Atsumi and J. C. Liao, "Directed evolution of Methanococcus jannaschii citramalate synthase for biosynthesis of 1-propanol and 1-butanol by Escherichia coli," *Appl. Environ. Microbiol.*, vol. 74, no. 24, pp. 7802–7808, 2008.

[58] Y. R. K. M. Sai, N. . Siva Kishore, A. . Dattatreya, S. Y. . Anand, and G. Sridhari, "A Review on Biotechnology and Its Commercial and Industrial Applications," *J. Biotechnol. Biomater.*, vol. 1, no. 121, pp. 1–5, 2011.

[59] B. Erickson, Nelson, and P. Winters, "Perspective on opportunities in industrial biotechnology in renewable chemicals," *Biotechnol. J.*, vol. 7, pp. 176–185, 2012.

[60] E. Shiue, I. M. Brockman, and K. L. J. Prather, "Improving product yields on D-glucose in Escherichi coli via knockout of pgi and zwf and feeding of supplemental carbon sources," *Biotechnol. Bioeng.*, vol. 112, no. 3, pp. 579–587, 2016.

[61] K. E. Tyo, K. Kocharin, and J. Nielsen, "Toward design-based engineering of industrial microbes," *Curr. Opin. Microbiol.*, vol. 13, pp. 255–262, 2010.

[62] M. J. Burk and S. Van Dien, "Biotechnology for Chemical Production: Challenges and Opportunities," *Trends Biotechnol.*, vol. 34, no. 3, pp. 187–190, 2016.

[63] N. Buschke, R. Schäfer, J. Becker, and C. Wittmann, "Metabolic engineering of industrial platform microorganisms for biorefinery applications - Optimization of substrate spectrum

and process robustness by rational and evolutive strategies," *Bioresour. Technol.*, vol. 135, pp. 544–554, 2013.

[64] V. Chubukov, A. Mukhopadhyay, C. Petzold, and J. Keasling, "Synthetic and systems biology for microbial production of commodity chemicals : from target selection to scale-up," *npj Syst. Biol. Appl.*, vol. 2, pp. 1–11, 2016.

[65] C. J. Chiang, H. M. Lee, H. J. Guo, Z. W. Wang, L. J. Lin, and Y. P. Chao, "Systematic approach to engineer Escherichia coli pathways for co-utilization of a glucose-xylose mixture," *J. Agric. Food Chem.*, vol. 61, pp. 7583–7590, 2013.

[66] K. Ohta, H. Hamasuna, J. Tsukamoto, M. Wakiyama, Y. Izumi, and K. Harada, "Disruption of ptsG gene and manXYZ operon of ethanol-producing Escherichia coli KO11: Effects on glucose and xylose utilization and ethanol production," *J. Biosci. Bioeng.*, vol. 113, no. 5, pp. 608–610, 2012.

[67] I. Y. Jung, J. W. Lee, W. K. Min, Y. C. Park, and J. H. Seo, "Simultaneous conversion of glucose and xylose to 3-hydroxypropionic acid in engineered Escherichia coli by modulation of sugar transport and glycerol synthesis," *Bioresour. Technol.*, vol. 198, pp. 709–716, 2015.

[68] R. Li, Q. Chen, P. G. Wang, and Q. Qi, "A novel-designed Escherichia coli for the production of various polyhydroxyalkanoates from inexpensive substrate mixture," *Appl. Microbiol. Biotechnol.*, vol. 75, no. 5, pp. 1103–1109, 2007.

[69] F.-F. Li, Y. Zhao, B.-Z. Li, J.-J. Qiao, and G.-R. Zhao, "Engineering Escherichia coli for production of 4-hydroxymandelic acid using glucose–xylose mixture," *Microb. Cell Fact.*, vol. 15, no. 90, pp. 1–11, 2016.

[70] S. M. Kim, B. Y. Choi, Y. S. Ryu, S. H. Jung, J. M. Park, G. H. Kim, and S. K. Lee, "Simultaneous utilization of glucose and xylose via novel mechanisms in engineered Escherichia coli," *Metab. Eng.*, vol. 30, pp. 141–148, 2015.

[71] K. Martínez, R. de Anda, G. Hernández, A. Escalante, G. Gosset, O. T. Ramírez, and F. G. Bolívar, "Coutilization of glucose and glycerol enhances the production of aromatic compounds in an Escherichia coli strain lacking the phosphoenolpyruvate: carbohydrate phosphotransferase system," *Microb. Cell Fact.*, vol. 7, no. 1, pp. 1–12, 2008.

[72] A. Sabido, J. C. Sigala, G. Hernández-Chávez, N. Flores, G. Gosset, and F. Bolívar, "Physiological and transcriptional characterization of Escherichia coli strains lacking interconversion of phosphoenolpyruvate and pyruvate when glucose and acetate are coutilized," *Biotechnol. Bioeng.*, vol. 111, no. 6, pp. 1150–1160, 2014.

[73] Organisation for Economic Co-operation and Development, "Industrial Biotechnology and Climate Change - Opportunities and challenges," 2011.

[74] C. Mihalcea, "Gas fermentation for fuel and chemical production at scale - LanzaTech Report," *LanzaTech*, 2014.

[75] C. Furdui and S. W. Ragsdale, "The role of pyruvate ferredoxin oxidoreductase in pyruvate synthesis during autotrophic growth by the Wood-Ljungdahl pathway," *J. Biol. Chem.*, vol. 275, no. 37, pp. 28494–28499, 2000.

[76] M. Devarapalli and H. K. Atiyeh, "A review of conversion processes for bioethanol production with a focus on syngas fermentation," *Biofuel Res. J.*, vol. 2, no. 3, pp. 268–280, 2015.

[77] J. Daniell, M. Koepke, and S. D. Simpson, "Commercial Biomass Syngas Fermentation," *Energies*, vol. 5, pp. 5372–5417, 2012.

[78] F. Gong, Z. Cai, and Y. Li, "Synthetic biology for CO 2 fixation," *Sci China Life Sci*, vol. 59, no. 11, pp. 1106–1114, 2016.

[79] X. Yang Qianqian Yuan Yangyang Zheng Hongwu Ma Tao Chen Xueming Zhao, "An engineered non-oxidative glycolysis pathway for acetone production in Escherichia coli," *Biotechnol. Lett.*, vol. 38, pp. 1359–1365, 2016.

[80] Y. Li, B. Huang, H. Wu, Z. Li, Q. Ye, and Y. H. P. Zhang, "Production of Succinate from Acetate by Metabolically Engineered Escherichia coli," *ACS Synth. Biol.*, vol. 5, no. 11, pp. 1299–1307, 2016.

[81] C. Ni, X. Wu, J. Dan, and D. Du, "Facile recovery of acetic acid from waste acids of electronic industry via a partial neutralization pretreatment (PNP) - Distillation strategy," *Sep. Purif. Technol.*, vol. 132, pp. 23–26, 2014.

[82] T. Yakushi and K. Matsushita, "Alcohol dehydrogenase of acetic

acid bacteria: structure, mode of action, and applications in biotechnology," *Appl Microbiol Biotechnol*, vol. 86, pp. 1257–1265, 2010.

[83] P. Raspor and D. Goranovič, "Biotechnological Applications of Acetic Acid Bacteria," *Crit. Rev. Biotechnol.*, vol. 28, no. 2, pp. 101–124, Jan. 2008.

[84] L. J. Jönsson and C. Martin, "Pretreatment of lignocellulose: Formation of inhibitory by-products and strategies for minimizing their effects," *Bioresour. Technol.*, vol. 199, pp. 103–112, 2016.

[85] Wolfe, "The Acetate Switch," *Microbiol. Mol. Biol. Rev*, vol. 69, no. 1, pp. 12–50, 2005.

[86] J. Shiloach and U. Rinas, "Glucose and acetate metabolism in Escherichia coli - System level analysis and biotechnological applications in protein production processes," in *System Biology and Biotechnology of Escherichia coli*, S. Y. Lee., S. Science, Ed. 2009, pp. 377–400.

[87] B. Enjalbert, F. Letisse, and J.-C. Portais, "Physiological and Molecular Timing of the Glucose to Acetate Transition in Escherichia coli.," *Metabolites*, vol. 3, no. 3, pp. 820–37, 2013.

[88] B. Enjalbert, M. Cocaign-Bousquet, J. C. Portais, and F. Letisse, "Acetate exposure determines the diauxic behavior of Escherichia coli during the glucose-acetate transition," *J. Bacteriol.*, vol. 197, no. 19, pp. 3173–3181, 2015.

[89] R. B. Gennis and L. P. Hager, "Pyruvate oxidase," in *The Enzymes and Biological Membranes*, vol. 2, A. Martonosi, Ed. New York, 1976, pp. 493–504.

[90] J. G. Koland, M. W. Mather, R. B. Gennis, J. S. White, and L. P. Hager, "Activation of Pyruvate Oxidase and Interaction with Membrane Components," in *Membranes and Transports*, A. N. Mart., P. Press, Ed. New York, 1982, pp. 83–92.

[91] A. M. Abdel-Hamid, M. M. Attwood, and J. R. Guest, "Pyruvate oxidase contributes to the aerobic growth efficiency of Escherichia coli," *Microbiology*, vol. 147, pp. 1483–1498, 2001.

[92] Y. Xiao, Z. Ruan, Z. Liu, S. G. Wu, A. M. Varman, Y. Liu, and Y. J. Tang, "Engineering Escherichia coli to convert acetic acid to free fatty acids," *Biochem. Eng. J.*, vol. 76, pp. 60–69, 2013.

[93] H. Wu, Z. M. Li, L. Zhou, and Q. Ye, "Improved succinic acid production in the anaerobic culture of an Escherichia coli pflB ldhA double mutant as a result of enhanced anaplerotic activities in the preceding aerobic culture," *Appl. Environ. Microbiol.*, vol. 73, no. 24, pp. 7837–7843, 2007.

[94] S. Leone, F. Sannino, M. L. Tutino, E. Parrilli, and D. Picone, "Acetate: friend or foe? Efficient production of a sweet protein in Escherichia coli BL21 using acetate as a carbon source.," *Microb Cell Fact*, vol. 14, pp. 1–10, 2015.

[95] H. Lin, N. M. Castro, and G. N. Bennett, "Acetyl-CoA synthase overexpression in Eschirichia coli demonstrates more efficient

acetate assimilation and lower acetate accumulation: a potential tool in metabolic engineering," *Appl Microbiol Biotechnol*, vol. 71, pp. 870–874, 2006.

[96] L. T. Cordova and H. S. Alper, "Central metabolic nodes for diverse biochemical production," *Curr. Opin. Chem. Biol.*, vol. 35, pp. 37–42, 2016.

[97] C. R. Shen, E. I. Lan, Y. Dekishima, A. Baez, K. M. Cho, and J. C. Liao, "Driving forces enable high-titer anaerobic 1-butanol synthesis in Escherichia coli," *Appl. Environ. Microbiol.*, vol. 77, no. 9, pp. 2905–2915, 2011.

[98] C. J. Paddon and J. D. Keasling, "Semi-synthetic artemisinin: a model for the use of synthetic biology in pharmaceutical development," *Nat. Rev. Microbiol.*, vol. 12, no. 5, pp. 355–367, 2014.

[99] R. V Vadali C E Horton F B Rudolph G N Bennett K-Y San, "Production of isoamyl acetate in ackA-pta and/or ldh mutants of Escherichia coli with overexpression of yeast ATF2," *Appl Microbiol Biotechnol*, vol. 63, pp. 698–704, 2004.

[100] R. V Vadali, G. N. Bennett, and K.-Y. San, "Applicability of CoA/acetyl-CoA manipulation system to enhance isoamyl acetate production in Escherichia coli," *Metab. Eng.*, vol. 6, pp. 294–299, 2004.

[101] T. Warnecke and R. T. Gill, "Organic acid toxicity, tolerance, and production in Escherichia coli biorefining applications.," *Microb.*

Cell Fact., vol. 4, pp. 25–32, 2005.

[102] Ingledew and Poole, "The Respiratory Chains of Escherichia coli," *Microbiol. Rev.*, vol. 48, no. 3, pp. 222–271, 1984.

[103] A. J. Roe, C. O'Byrne, D. McLaggan, and I. R. Booth, "Inhibition of Escherichia coli growth by acetic acid : A problem with methionine biosynthesis and homocysteine toxicity Inhibition of Escherichia coli growth by acetic acid : a problem with methionine biosynthesis and homocysteine toxicity," *Microbiology*, vol. 148, pp. 2215–2222, 2002.

[104] H. Wang, F. Wang, W. Wang, X. Yao, D. Wei, H. Cheng, Z. Deng, *et al.*, "Improving the Expression of Recombinant Proteins in Escherichia coli BL21 (DE3) under Acetate Stress: An Alkaline pH Shift Approach," *PLoS One*, vol. 9, no. 11, pp. 1–11, 2014.

[105] A. Saeki, K. Matsushita, S. Takeno, M. Tanigucm, H. Toyama, G. Theeragool, N. Lotong, *et al.*, "Enzymes responsible for acetate oxidation by acetic acid bacteria," *Biotechnol. Biochem*, vol. 63, no. 12, pp. 2102–2109, 1999.

[106] Y. Fujita, H. Matsuoka, and K. Hirooka, "Regulation of fatty acid metabolism in bacteria," *Mol. Microbiol.*, vol. 66, no. 4, pp. 829–839, 2007.

[107] D. P. Clark and J. E. Cronan, "Two-Carbon Compounds and Fatty Acids as Carbon Sources," *EcoSal Plus - Escherichia coli Salmonella Cell. Mol. Biol.*, vol. 1, no. 3, pp. 1–34, 2005.

[108] A. Krivoruchko, Y. Zhang, V. Siewers, Y. Chen, and J. Nielsen,

"Microbial acetyl-CoA metabolism and metabolic engineering," *Metab. Eng.*, vol. 28, pp. 28–42, 2015.

[109] D. P. Clark and J. E. Cronan, "Acetaldehyde coenzyme A dehydrogenase of Escherichia coli," *J Bacteriol.*, vol. 144, no. 1, pp. 179–184, 1980.

[110] M. R. Leonardo, Y. Dailly, D. P. Clark, M. R. Leonardo, Y. Dailly, and D. P. Clark, "Role of NAD in regulating the adhE gene of Escherichia coli," *J Bacteriol.*, vol. 178, no. 20, pp. 6013–6018, 1996.

[111] M. R. Leonardo, P. R. Cunningham, and D. P. Clark, "Anaerobic regulation of the adhE gene, encoding the fermentative alcohol dehydrogenase of Escherichia coli .," *J Bacteriol.*, vol. 175, no. 3, pp. 870–8, 1993.

[112] Y. M. Chen and E. C. C. Lin, "Regulation of the adhE gene, which encodes ethanol dehydrogenase in Escherichia coli," *J. Bacteriol.*, vol. 173, no. 24, pp. 8009–8013, 1991.

[113] D. Clark and E. J. Cronan, "Escherichia coli mutants with altered control of alcohol dehydrogenase and nitrate reductase," *J Bacteriol.*, vol. 141, no. 1, pp. 177–183, 1980.

[114] S. H. Mohd Azhar, R. Abdulla, S. A. Jambo, H. Marbawi, J. A. Gansau, A. A. Mohd Faik, and K. F. Rodrigues, "Yeasts in sustainable bioethanol production: A review," *Biochem. Biophys. Reports*, vol. 10, pp. 52–61, 2017.

[115] R. Muktham, S. K. Bhargava, S. Bankupalli, and A. S. Ball, "A

Review on first and second Generation Bioethanol Production-Recent Progress," *J. Sustain. Bioenergy Syst.*, vol. 6, pp. 72–92, 2016.

[116] H. B. Aditiya, T. M. I. Mahlia, W. T. Chong, H. Nur, and A. H. Sebayang, "Second generation bioethanol production: A critical review," *Renew. Sustain. Energy Rev.*, vol. 66, pp. 631–653, 2016.

[117] F. Alam, S. Mobin, and H. Chowdhury, "Third Generation Biofuel from Algae," *Procedia Eng.*, vol. 105, pp. 763–768, 2015.

[118] Y. S. Jang, J. M. Park, S. Choi, Y. J. Choi, D. Y. Seung, J. H. Cho, and S. Y. Lee, "Engineering of microorganisms for the production of biofuels and perspectives based on systems metabolic engineering approaches," *Biotechnol. Adv.*, vol. 30, no. 5, pp. 989–1000, 2012.

[119] K. Nakayama and H. Hagino, "Process for producing L-lysine," 3,595,751, 1971.

[120] T. Oki, Y. Sayama, Y. Nishimura, and A. Ozaki, "L-Glutamic Acid Formation by Microorganisms from Ethanol," *Agric. Biol. Chem.*, vol. 32, no. 1, pp. 119–120, 1968.

[121] S. J. Lee, E. K. Oh, Y. H. Oh, J. I. Won, S. O. Han, and J. W. Lee, "Increased ethanol resistance in Escherichia coli by insertion of heat-shock genes BEM1 and SOD2 from Saccharomyces cerevisiae," *Biotechnol. bioprocess Eng.*, vol. 15, pp. 770–776, 2010.

[122] S. Elleuche, K. Fodor, B. Klippel, A. Von Der Heyde, M. Wilmanns, and G. Antranikian, "Structural and biochemical characterisation of a NAD+-dependent alcohol dehydrogenase from Oenococcus oeni as a new model molecule for industrial biotechnology applications," *Appl. Microbiol. Biotechnol.*, vol. 97, no. 20, pp. 8963–8975, 2013.

[123] Elleuche and Antranikian, "Bacterial group III alcohol dehydrogenases-function, evolution and biotechnological applications," *Open Access Alcohol*, vol. 1, no. 3, pp. 1–6, 2013.

[124] M. F. Reid and C. A. Fewson, "Molecular Characterization of Microbial Alcohol Dehydrogenases," *Crit. Rev. Microbiol.*, vol. 20, no. 1, pp. 13–56, 1994.

[125] M. Flipphi, M. Mathieu, I. Cirpus, C. Panozzo, and B. Felenbok, "Regulation of the Aldehyde Dehydrogenase Gene (aldA) and its Role in the Control of the Coinducer Level Necessary for Induction of the Ethanol Utilization Pathway in Aspergillus nidulans," *J. Biol. Chem.*, vol. 276, no. 10, pp. 6950–6958, 2001.

[126] L. 0 Ingram and N. S. Vreeland, "Differential Effects of Ethanol and Hexanol on the Escherichia coli Cell Envelope," *J. Bacteriol.*, vol. 144, no. 2, pp. 481–488, 1980.

[127] T. Sawada, Y. Nakamura, and C. Media, "Growth Inhibitory and Lethal Effects of Ethanol on Escherichia coli," *Biotechnol. Bioeng.*, vol. 29, pp. 742–746, 1986.

[128] S. Huffer, M. E. Clark, J. C. Ning, H. W. Blanch, and D. S. Clark, "Role of alcohols in growth, lipid composition, and membrane fluidity of yeasts, bacteria, and archaea," *Appl. Environ. Microbiol.*, vol. 77, no. 18, pp. 6400–6408, 2011.

[129] H. Cao, D. Wei, Y. Yang, Y. Shang, G. Li, Y. Zhou, Q. Ma, *et al.*, "Systems-level understanding of ethanol-induced stresses and adaptation in Escherichia coli," *Nat. Sci. reports*, vol. 7, no. 44150, pp. 1–15, 2017.

[130] K. M. Dombek and L. 0 Ingram, "Effects of Ethanol on the Escherichia coli Plasma Membrane," *J. Bacteriol.*, vol. 157, no. 1, pp. 233–239, 1984.

[131] L. 0. Ingram, "Mechanism of Lysis of Escherichia coli by Ethanol and Other chaotropic agents," *J. Bacteriol.*, vol. 146, no. 1, pp. 331–336, 1981.

[132] J. Membrillo-Hernández, P. Echave, E. Cabiscol, J. Tamarit, J. Ros, and E. C. C. Lin, "Evolution of the adhE gene product of Escherichia coli from a functional reductase to a dehydrogenase: Genetic and biochemical studies of the mutant proteins," *J. Biol. Chem.*, vol. 275, no. 43, pp. 33869–33875, 2000.

[133] C. A. Holland-Staley, K. Lee, D. P. Clark, and P. R. Cunningham, "Aerobic activity of Escherichia coli alcohol dehydrogenase is determined by a single amino acid," *J. Bacteriol.*, vol. 182, no. 21, pp. 6049–6054, 2000.

[134] P. Ashtavinayak and E. Hill Annie, "Review : Gram Negative Bacteria in Brewing," *Adv. Microbiol.*, vol. 6, pp. 195–209, 2016.

[135] K. Kondo, T. Beppu, and S. Horinouchi, "Cloning, Sequencing, and Characterization of the Gene Encoding the Smallest Subunit of the three-Component Membrane-Bound Alcohol-Dehydrogenase From Acetobacter Pasteurianus," *J. Bacteriol.*, vol. 177, no. 17, pp. 5048–5055, 1995.

[136] S. Witthoff, A. Mühlroth, J. Marienhagen, and M. Bott, "C1 metabolism in Corynebacterium glutamicum: An endogenous pathway for oxidation of methanol to carbon dioxide," *Appl. Environ. Microbiol.*, vol. 79, no. 22, pp. 6974–6983, 2013.

[137] H. Yamada, K. C. Shin, N. Kato, S. Shimizu, and Y. Tani, "Purification and characterization of Alcohol Oxidase from Candida 25-A," *Agric. Biol. Chem.*, vol. 43, no. 4, pp. 877–878, 1979.

[138] F. O. Bryant, J. Wiegel, and L. G. Ljungdahl, "Purification and Properties of Primary and Secondary Alcohol Dehydrogenases from Thermoanaerobacter ethanolicus.," *Appl. Environ. Microbiol.*, vol. 54, no. 2, pp. 460–465, 1988.

[139] Y. Cao, L. Liao, X. W. Xu, A. Oren, C. Wang, X. F. Zhu, and M. Wu, "Characterization of alcohol dehydrogenase from the haloalkaliphilic archaeon Natronomonas pharaonis," *Extremophiles*, vol. 12, no. 3, pp. 471–476, 2008.

[140] Shim, Eun-Jung, S. Jeon, and K. Kong, "Overexpression,

Purification, and Biochemical Characterization of the Thermostable NAD-dependent Alcohol Dehydrogenase from Bacillus stearothermophilus," *J. Microbiol Biotechnol.*, vol. 13, no. 5, pp. 738–744, 2003.

[141] L. Feng, W. Wang, J. Cheng, Y. Ren, G. Zhao, C. Gao, Y. Tang, *et al.*, "Genome and proteome of long-chain alkane degrading Geobacillus thermodenitrificans NG80-2 isolated from a deep-subsurface oil reservoir.," *Proc. Natl. Acad. Sci. U. S. A.*, vol. 104, no. 13, pp. 5602–5607, 2007.

[142] Y. Ji, G. Mao, Y. Wang, and M. Bartlam, "Structural insights into diversity and n-alkane biodegradation mechanisms of alkane hydroxylases," *Front. Microbiol.*, vol. 4, no. 58, pp. 1–13, 2013.

[143] X. Liu, Y. Dong, J. Zhang, A. Zhang, L. Wang, and L. Feng, "Two novel metal-independent long-chain alkyl alcohol dehydrogenases from Geobacillus thermodenitrificans NG80-2," *Microbiology*, vol. 155, no. 6, pp. 2078–2085, 2009.

[144] A. Tani, Y. Sakai, T. Ishige, N. Kato, T. E. T. Al, and A. P. P. L. E. N. M. Icrobiol, "Thermostable NADP+ -Dependent Medium-Chain Alcohol Dehydrogenase from Acinetobacter sp . Strain M-1 : Purification and Characterization and Gene Expression in Escherichia coli," *Appl. Env. Microbiol.*, vol. 66, no. 12, pp. 5231–5235, 2000.

[145] J. Abbott, B., A. I. Laskin, and J. McCoy, "Growth of Acinetobacter calcoaceticus on ethanol," *Appl. Microbiol.*, vol. 25, no. 5, pp. 787–792, 1973.

[146] E. H. Creaser, R. L. Porter, K. A. Britt, J. A. Pateman, and C. H. Doy, "Purification and preliminary characterization of alcohol dehydrogenase from Aspergillus nidulans," *Biochem J*, vol. 225, no. 2, pp. 449–454, 1985.

[147] J. A. Pateman, C. H. Doy, E. Olsen, U. Norris, E. H. Creaser, and M. Hynes, "Regulation of alcohol dehydrogenase (ADH) and aldehyde dehydrogenase (AldDH) in Aspergillus nidulans," *Proc. R. Soc. London*, vol. 217, pp. 243–264, 1982.

[148] M. Auchter, A. Arndt, and B. J. Eikmanns, "Dual transcriptional control of the acetaldehyde dehydrogenase gene ald of Corynebacterium glutamicum by RamA and RamB," *J. Biotechnol.*, vol. 140, pp. 84–91, 2009.

[149] A. Arndt, M. Auchter, T. Ishige, V. F. Wendisch, and B. J. Eikmanns, "Ethanol catabolism in Corynebacterium," *J. Microbiol. Biotecnol.*, vol. 15, no. 4, pp. 222–233, 2008.

[150] A. Arndt and B. J. Eikmanns, "The Alcohol Dehydrogenase gene adhA in Corynebacterium glutamicum is subject to carbon catabolite repression," *J. Bacteriol.*, vol. 189, no. 20, pp. 7408–7416, 2007.

[151] G. Bokinsky, D. Groff, and J. Keasling, *Synthetic Biology of Microbial Biofuel Production: From Enzymes to Pathways to Organisms*, First Edit. Elsevier Inc., 2013.

[152] L. P. Wackett, "Novel biocatalysis by database mining," *Curr. Opin. Biotechnol.*, vol. 15, no. 4, pp. 280–284, 2004.

[153] L. S. Jing, F. F. M. Shah, M. S. Mohamad, N. L. Hamran, A. H. M. Salleh, S. Deris, and H. Alashwal, "Database and tools for metabolic network analysis," *Biotechnol. Bioprocess Eng.*, vol. 19, no. 4, pp. 568–585, 2014.

[154] K. Terpe, "Overview of bacterial expression systems for heterologous protein production: From molecular and biochemical fundamentals to commercial systems," *Appl. Microbiol. Biotechnol.*, vol. 72, no. 2, pp. 211–222, 2006.

[155] R. Machielsen, A. R. Uria, S. W. M. Kengen, and J. Van Der Oost, "Production and Characterization of a Thermostable Alcohol Dehydrogenase That Belongs to the Aldo-Keto Reductase Superfamily," *Appl. Environ. Microbiol.*, vol. 72, no. 1, pp. 233–238, 2006.

[156] M. M. Musa and R. S. Phillips, "Recent advances in alcohol dehydrogenase-catalyzed asymmetric production of hydrophobic alcohols," *Catal. Sci. Technol. Catal. Sci. Technol*, vol. 1, no. 1, pp. 1311–1323, 2011.

[157] R.-C. Zheng, Z. Ge, Z.-K. Qiu, Y.-S. Wang, and Y.-G. Zheng, "Asymmetric synthesis of (R)-1,3-butanediol from 4-hydroxy-2-butanone by a newly isolated strain Candida krusei ZJB-09162," *Appl Microbiol Biotechnol*, vol. 94, pp. 969–976, 2012.

[158] C. Saha, Badal and A. Cotta, Michael, "Ethanol production from lignocellulosic biomass by recombinant Escherichia coli strain FBR5," *Bioengineered*, vol. 3, no. 4, pp. 197–202, 2012.

[159] S. Suwannarangsee, S. Kim, O. C. Kim, D. B. Oh, J. W. Seo, C. H. Kim, S. K. Rhee, *et al.*, "Characterization of alcohol dehydrogenase 3 of the thermotolerant methylotrophic yeast Hansenula polymorpha," *Appl. Microbiol. Biotechnol.*, vol. 96, no. 3, pp. 697–709, 2012.

[160] P. Pharkya, E. V. Nikolaev, and C. D. Maranas, "Review of the BRENDA Database," *Metab. Eng.*, vol. 5, no. 2, pp. 71–73, 2003.

[161] R. Apweiler, A. Bairoch, C. H. Wu, W. C. Barker, B. Boeckmann, S. Ferro, E. Gasteiger, *et al.*, "UniProt: the Universal Protein knowledgebase," *Nucleic Acids Res.*, vol. 32, no. Database issue, pp. 115–119, 2004.

[162] M. Kanehisa and S. Goto, "Kyoto Encyclopedia of Genes and Genomes," *Nucleic Acids Res.*, vol. 28, no. 1, pp. 27–30, 2000.

[163] V. Egelhofer, I. Schomburg, and D. Schomburg, "Automatic Assignment of EC Numbers," *PLoS Comput Biol*, vol. 6, no. 1, pp. 1–7, 2010.

[164] D. Kessler, I. Leibrecht, and J. Knappe, "Pyruvate-formate-lyase-deactivase and acetyl-CoA reductase activities of Escherichia coli reside on a polymeric protein particle encoded by adhE," *FEBS Lett.*, vol. 281, no. 1–2, pp. 59–63, 1991.

[165] T. Nosova, H. Jousimies-Somer, P. Kaihovaara, K. Jokelainen, R. Heine, and M. Salaspuro, "Characteristics of alcohol dehydrogenases of certain aerobic bacteria representing human

colonic flora.," *Alcohol. Clin. Exp. Res.*, vol. 21, no. 3, pp. 489–494, 1997.

[166] C. Thurner, C. Vela, L. Thony-Meyer, L. Meile, and M. Teuber, "Biochemical and genetic characterization of the acetaldehyde dehydrogenase complex from Acetobacter europaeus," *Arch. Microbiol*, vol. 168, pp. 81–91, 1997.

[167] P. Chinnawirotpisan, G. Theeragool, S. Limtong, H. Toyama, O. O. Adachi, and K. Matsushita, "Quinoprotein alcohol dehydrogenase is involved in catabolic acetate production, while NAD-dependent alcohol dehydrogenase in ethanol assimilation in Acetobacter pasteurianus SKU1108.," *J. Biosci. Bioeng.*, vol. 96, no. 6, pp. 564–571, 2003.

[168] U. Masud, K. Matsushita, and G. Theeragool, "Molecular cloning and characterization of two inducible NAD+-adh genes encoding NAD+-dependent alcohol dehydrogenases from Acetobacter pasteurianus SKU1108," *J. Biosci. Bioeng.*, vol. 112, no. 5, pp. 422–431, 2011.

[169] S. Reiser and C. Sommerville, "Isolation of mutants of acinetobacter calcoaceticus dificient in wax ester synthesis and complementation of one mutation with a gene encoding a fatty acyl coenzyme A reductase," *J. Bacteriol.*, vol. 179, no. 9, pp. 2969–2975, 1997.

[170] M. G. Smith, T. A. Gianoulis, S. Pukatzki, J. J. Mekalanos, L. N. Ornston, M. Gerstein, and M. Snyder, "New insights into Acinetobacter baumannii pathogenesis revealed by high-density

pyrosequencing and transposon mutagenesis," *Genes Dev.*, vol. 21, no. 5, pp. 601–614, 2007.

[171] A. Kotrbova-Kozak, P. Kotrba, M. Inui, J. Sajdok, and H. Yukawa, "Transcriptionally regulated adhA gene encodes alcohol dehydrogenase required for ethanol and n-propanol utilization in Corynebacterium glutamicum R," *Appl. Microbiol. Biotechnol.*, vol. 76, no. 6, pp. 1347–1356, 2007.

[172] J. Kalinowski, B. Bathe, D. Bartels, N. Bischoff, M. Bott, A. Burkovski, N. Dusch, *et al.*, "The complete Corynebacterium glutamicum ATCC 13032 genome sequence and its impact on the production of L-aspartate-derived amino acids and vitamins," *J. Biotechnol.*, vol. 104, pp. 5–25, 2003.

[173] J. Pelechova, F. Smekal, V. Koura, J. Plachy, and V. Krumphanzl, "Biosynthesis of L-Lysine in Corynebacterium glutamicum on Sucrose, Ethanol and Acetic Acid," *Folia Microbiol.*, vol. 25, no. 4, pp. 341–346, 1980.

[174] X. Li, Y. Li, D. Wei, P. Li, L. Wang, and L. Feng, "Characterization of a broad-range aldehyde dehydrogenase involved in alkane degradation in Geobacillus thermodenitrificans NG80-2," *Microb. Res.*, vol. 165, pp. 706–712, 2010.

[175] D. R. Zeigler, "The Geobacillus paradox: why is a thermophilic bacterial genus so prevalent on a mesophilic planet?," *Microbiology*, vol. 160, pp. 1–11, 2014.

[176] D. Jendrossek, A. Steinbüchel, and H. G. Schlegel, "Alcohol

dehydrogenase gene from Alcaligenes eutrophus: subcloning, heterologous expression in Escherichia coli, sequencing, and location of Tn5 insertions.," *J. Bacteriol.*, vol. 170, no. 11, pp. 5248–5256, 1988.

[177] H. Sakoda and T. Imanaka, "Cloning and sequencing of the Gene Coding for Alcohol Dehydrogenase of Bacillus stearothermophilus and rational shift of the optimum pH," *J. Bacteriol.*, vol. 174, no. 4, pp. 1397–1402, 1992.

[178] B. Felenbok and J. M. Kelly, "Regulation of carbon metabolism in mycelial fungi," in *The Mycota, Vol. 3 -Biochemistry and Molecular Biology*, 1996, pp. 369–380.

[179] H. M. Sealy-Lewis and R. A. Lockington, "Regulation of two alcohol dehydrogenases in Aspergillus nidulans," *Curr. Genet.*, vol. 8, pp. 253–259, 1984.

[180] I. Nikolaev, M. Mathieu, P. J. I. Van De Vondervoort, J. Visser, and B. Felenbok, "Heterologous expression of the Aspergillus nidulans alcR-alcA system in Aspergillus niger," *Fungal Genet. Biol.*, vol. 37, no. 1, pp. 89–97, 2002.

[181] H. M. Sealy-Lewis and V. Fairhurst, "Substrate specificity of nine NAD+-dependent alcohol dehydrogenases in Aspergillus nidulans," *Microbiology*, vol. 141, pp. 2295–2300, 1995.

[182] T. Ito, S. Fujimura, M. Uchino, N. Tanaka, Y. Matsufuji, T. Miyaji, K. Takano, *et al.*, "Distribution, diversity and regulation of alcohol oxidase isozymes, and phylogenetic relationships of

methylotrophic yeasts," *Yeast*, vol. 24, no. 6, pp. 523–532, Jun. 2007.

[183] G. Daniel, J. Volc, L. Filonova, O. Plíhal, E. Kubátová, and P. Halada, "Characteristics of Gloeophyllum trabeum Alcohol Oxidase, an Extracellular Source of H2O2 in Brown Rot Decay of Wood," *Appl. Environ. Microbiol.*, vol. 73, no. 19, pp. 6241–6253, 2007.

[184] P. Goswami, S. S. R. Chinnadayyala, M. Chakraborty, A. K. Kumar, and A. Kakoti, "An overview on alcohol oxidases and their potential applications," *Appl. Microbiol. Biotechnol.*, vol. 97, pp. 4259–4275, 2013.

[185] N. R. Asad, L. M. B. O. Asad, A. B. Silva, and I. Felzenszwalb, "Hydrogen peroxide effects in Escherichia coli cells," *Acta Biochem. Pol.*, vol. 45, no. 3, pp. 677–690, 1998.

[186] R. Kumar, S. and J. A. Imlay, "How Escherichia coli Tolerates Profuse Hydrogen Peroxide Formation by a Catabolic Pathway," *J. Bacteriol.*, vol. 195, no. 20, pp. 4569–4579, 2013.

[187] V. Vasiliou, A. Pappa, and D. R. Petersen, "Role of aldehyde dehydrogenases in endogenous and xenobiotic metabolism," *Chem. Biol. Interact.*, vol. 129, pp. 1–19, 2000.

[188] S. Singh, C. Brocker, V. Koppaka, C. Ying, B. Jackson, A. Matsumoto, D. C. Thompson, *et al.*, "Aldehyde Dehydrogenases in Cellular Responses to Oxidative/ electrophilic Stress," *Free Radic Biol Med*, vol. 56, pp. 89–101, 2013.

[189] N. A. Sophos and V. Vasiliou, "Aldehyde dehydrogenase gene superfamily: The 2002 update," *Chem. Biol. Interact.*, vol. 143–144, pp. 5–22, 2003.

[190] Murooka; Yoshikastu and T. Imanaka, *Recombinant Microbes for Industrial and Agricultural Applications*. New York City, 1994.

[191] S. H. Hong, H. P. T. Ngo, H. K. Nam, K. R. Kim, L. W. Kang, and D. K. Oh, "Alternative biotransformation of retinal to retinoic acid or retinol by an aldehyde dehydrogenase from Bacillus cereus," *Appl. Environ. Microbiol.*, vol. 82, no. 13, pp. 3940–3946, 2016.

[192] N. Kamimura, T. Goto, K. Takahashi, D. Kasai, Y. Otsuka, M. Nakamura, Y. Katayama, *et al.*, "A bacterial aromatic aldehyde dehydrogenase critical for the efficient catabolism of syringaldehyde," *Nat. Publ. Gr.*, 2017.

[193] Zhao, Lei, Wu, Wang, Zhang, Deng, and Wang, "Molecular cloning and expression of the complete DNA sequence encoding NAD+-dependent acetaldehyde dehydrogenase from Acinetobacter sp strain HBS-2," *Ann. Microbiol.*, vol. 59, no. 1, pp. 97–104, 2009.

[194] B. Omokoko, U. K. Jäntges, M. Zimmermann, M. Reiss, and W. Hartmeier, "Isolation of the phe-operon from G. stearothermophilus comprising the phenol degradative meta-pathway genes and a novel transcriptional regulator.," *BMC Microbiol.*, vol. 8, pp. 197–206, 2008.

[195] J. Zhu, A. Sanchez, G. N. Bennett, and K.-Y. San, "Manipulating Respiratory Levels in Escherichia coli for Aerobic Formation of Reduced Chemical Products," *Metab Eng*, vol. 13, no. 6, pp. 704–712, 2011.

[196] R. Caspi, R. Billington, L. Ferrer, H. Foerster, C. A. Fulcher, I. M. Keseler, A. Kothari, *et al.*, "The MetaCyc database of metabolic pathways and enzymes and the BioCyc collection of pathway/genome databases," *Nucleic Acids Res.*, vol. 42, pp. 459–471, 2014.

[197] "Coli Genetic Stock Center, Yale University." [Online]. Available: https://cgsc2.biology.yale.edu/StrainQueryForm.php.

[198] J. R. L. Walker, "Spectrophotometric determination of enzyme activity: Alcohol Dehydrogenase (ADH)," *Biochem. Educ.*, vol. 20, no. 1, p. 42-, 1992.

[199] D. M. Howell, H. Xu, and R. H. White, "(R)-Citramalate Synthase in Methanogenic Archaea," *J. Bacteriol.*, vol. 181, no. 1, pp. 331–333, 1999.

[200] M. R. Antoniewicz, "Methods and advances in metabolic flux analysis: a mini-review," *J Ind Microbiol Biotechnol*, vol. 42, pp. 317–325, 2015.

[201] J. D. Orth, I. Thiele, and B. Ø. Palsson, "What is flux balance analysis?," *Nat Biotechnol.*, vol. 28, no. 3, pp. 245–248, 2010.

[202] K. J. Kauffman, P. Prakash, and J. S. Edwards, "Advances in flux balance analysis," *Curr. Opin. Biotechnol.*, vol. 14, no. 5, pp.

491–496, 2003.

[203] P. D. N. Pissarra and J. Nielsen, "Thermodynamics of Metabolic Pathways for Penicillin Production: Analysis of Thermodynamic Feasibility and Free Energy Changes During Fed-Batch Cultivation," *Biotechnol. Prog.*, vol. 13, no. 2, pp. 156–165, Apr. 1997.

[204] M. L. Mavrovouniotis, "Estimation of standard Gibbs energy changes of biotransformations," *J. Biol. Chem.*, vol. 266, no. 22, pp. 14440–14445, 1991.

[205] Thauer, Jungermann, and Decker, "Energy Conservation in Chemotrophic Anaerobic Bacteria," *Bacteriol. Rev.*, vol. 41, no. 1, pp. 100–180, 1977.

[206] M. Ataman and V. Hatzimanikatis, "Heading in the right direction: thermodynamics-based network analysis and pathway engineering," *Curr. Opin. Biotechnol.*, vol. 36, pp. 176–182, 2015.

[207] S. D. Finley, L. J. Broadbelt, V. Hatzimanikatis, and V. H. Ch, "Thermodynamic Analysis of Biodegradation Pathways," *Biotechnol Bioeng*, vol. 103, no. 3, pp. 532–541, 2009.

[208] G. R. Eastham, D. W. Johnson, I. Archer, R. Carr, J. Webb, and G. Stephens, "A process for production of methacrylic acid and derivatives thereof," WO2015022496-A2, 2015.

[209] M. Kozak, "Comparison of initiation of protein synthesis in procaryotes, eucaryotes, and organelles," *Microbiol. Rev.*, vol.

47, no. 1, pp. 1–45, 1983.

[210] M. Kozak, "Regulation of translation via mRNA structure in prokaryotes and eukaryotes," *Gene*, vol. 361, pp. 13–37, 2005.

[211] J. E. Bailey, "Toward a science of metabolic engineering," *Science (80-.).*, vol. 252, no. 5013, pp. 1668–1675, 1991.

[212] C. G. Miyada, L. Stoltzfus, and G. Wilcox, "Regulation of the araC gene of Escherichia coli: Catabolite repression, autoregulation, and effect on araBAD expression (cAMP receptor protein/in vitro transcription/DNase I protection/oligonucleotide-directed mutagenesis)," *Proc. Natl. Acad. Sci.*, vol. 81, pp. 4120–4124, 1984.

[213] Unden and Bongaerts, "Alternative respiratory pathways of Escherichia coli: energetics and transcriptional regulation in response to electron acceptors," *Biocheimica Biophys. Acta*, vol. 1320, pp. 217–234, 1997.

[214] J. H. Chung, P. Karageorgiou, P. Yang, N. Yang, and F. Levitt, "The Enzyme Kinetics of NADH Dehydrogenase After the Addition of the Inhibitory Molecules, EDTA and Mg," *J. Exp. Microbiol. Immunol.*, vol. 7, pp. 7–13, 2005.

[215] D. G. Nicholls and S. J. Ferguson, *Bioenergetics 2*, Second edi. Academic Press, 1992.

[216] J. R. Guest, "Anaerobic Growth of Escherichia coli K12 with Fumarate as Terminal Electron Acceptor. Genetic Studies with Menaquinone and Fluoroacetate-resistant Mutants," *J. Gen.*

Microbiol., vol. 115, pp. 259–271, 1979.

[217] G. L. Rosano and E. A. Ceccarelli, "Recombinant protein expression in Escherichia coli: Advances and challenges," *Front. Microbiol.*, vol. 5, no. 172, pp. 1–17, 2014.

[218] S. A. Nicolaou, S. M. Gaida, and E. T. Papoutsakis, "A comparative view of metabolite and substrate stress and tolerance in microbial bioprocessing: From biofuels and chemicals, to biocatalysis and bioremediation," *Metab. Eng.*, vol. 12, pp. 307–331, 2010.

[219] N. Wei, J. Quarterman, S. R. Kim, J. H. D. Cate, and Y.-S. Jin, "Enhanced biofuel production through coupled acetic acid and xylose consumption by engineered yeast.," *Nat. Commun.*, vol. 4, no. 2580, pp. 1–8, 2013.

[220] L. R. Jarboe, P. Lu, and L. Royce, "Engineering inhibitor tolerance for the production of biorenewable fuels and chemicals," *Curr. Opin. Chem. Eng.*, vol. 1, no. 1, pp. 1–24, 2011.

[221] H. Lin, G. N. Bennett, and K. Y. San, "Fed-batch culture of a metabolically engineered Escherichia coli strain designed for high-level succinate production and yield under aerobic conditions," *Biotechnol. Bioeng.*, vol. 90, no. 6, pp. 775–779, 2005.

[222] A. K. Panda, R. H. Khan, S. Mishra, K. B. C. A. Rao, and S. M. Totey, "Influences of yeast extract on specific cellular yield of

Ovine growth hormone during fed-batch fermentation of Escherichia coli," *Bioprocess Eng.*, vol. 22, pp. 379–383, 2000.

[223] H. R. Horton, *Principles of biochemistry*. Pearson Education International, 2006.

[224] A. Tomar, M. A. Eiteman, and E. Altman, "The effect of acetate pathway mutations on the production of pyruvate in Escherichia coli," *Appl. Microbiol. Biotechnol.*, vol. 62, no. 1, pp. 76–82, 2003.

[225] S. Castaño-Cerezo, J. M. Pastor, S. Renilla, V. Bernal, J. L. Iborra, and M. Cánovas, "An insight into the role of phosphotransacetylase (pta) and the acetate/acetyl-CoA node in Escherichia coli," *Microb Cell Fact*, vol. 8, pp. 54–72, 2009.

[226] K. Martínez-Gómez, N. Flores, H. M. Castañeda, G. Martínez-Batallar, G. Hernández-Chávez, O. T. Ramírez, G. Gosset, *et al.*, "New insights into Escherichia coli metabolism: carbon scavenging, acetate metabolism and carbon recycling responses during growth on glycerol.," *Microb. Cell Fact.*, vol. 11, pp. 46–66, 2012.

[227] X. Wu and M. A. Eiteman, "Production of citramalate by metabolically engineered Escherichia coli," *Biotechnol. Bioeng.*, vol. 113, no. 12, pp. 2670–2675, 2016.

[228] J. P. Webb, S. A. Arnold, S. Baxter, S. J. Hall, G. Eastham, and G. Stephens, "Efficient bio-production of citramalate using an engineered Escherichia coli strain."

[229] M. Okabe, D. Lies, S. Kanamasa, and E. Y. Park, "Biotechnological production of itaconic acid and its biosynthesis in Aspergillus terreus," *Appl Microbiol Biotechnol*, vol. 84, no. 4, pp. 597–606, 2009.

[230] C. Cho, S. Y. Choi, Z. W. Luo, and S. Y. Lee, "Recent advances in microbial production of fuels and chemicals using tools and strategies of systems metabolic engineering," *Biotechnol. Adv.*, vol. 33, no. 7, pp. 1455–1466, 2015.

[231] A. Burgard, M. J. Burk, R. Osterhout, S. Van Dien, and H. Yim, "Development of a commercial scale process for production of 1,4-butanediol from sugar," *Curr. Opin. Biotechnol.*, vol. 42, pp. 118–125, 2016.

[232] S. Y. Lee and H. U. Kim, "Systems strategies for developing industrial microbial strains," *Nat. Biotechnol.*, vol. 33, no. 10, pp. 1061–1072, 2015.

[233] G. Stephanopoulos, "Challenges in engineering microbes for biofuels production.," *Science*, vol. 315, no. 5813, pp. 801–804, 2007.

[234] G. Stephanopoulos, H. Alper, and J. Moxley, "Exploiting biological complexity for strain improvement through systems biology," *Nat. Biotechnol.*, vol. 22, no. 10, pp. 1261–1267, 2004.

[235] J. H. Park, S. Y. Lee, T. Y. Kim, and H. U. Kim, "Application of systems biology for bioprocess development," *Trends*

Biotechnol., vol. 26, no. 8, pp. 404–412, 2008.

[236] C. Bro and J. Nielsen, "Impact of 'ome' analyses on inverse metabolic engineering," *Metab. Eng.*, vol. 6, no. 3, pp. 204–211, 2004.

[237] K. Shimizu, "Toward systematic metabolic engineering based on the analysis of metabolic regulation by the integration of different levels of information," *Biochem. Eng. J.*, vol. 46, no. 3, pp. 235–251, 2009.

[238] Q.-Z. Li, X.-L. Jiang, X.-J. Feng, J.-M. Wang, C. Sun, H.-B. Zhang, M. Xian, *et al.*, "Recovery Processes of Organic Acids from Fermentation Broths in the Biomass-Based Industry," *J. Microbiol. Biotechnol*, vol. 26, no. 261, pp. 1–8, 2016.

[239] R. P. Maharjan, P. L. Yu, S. Seeto, and T. Ferenci, "The role of isocitrate lyase and the glyoxylate cycle in Escherichia coli growing under glucose limitation," *Res. Microbiol.*, vol. 156, no. 2, pp. 178–183, 2005.

[240] K. Walsh and D. E. J. Koshland, "The Determination of Flux through the Branch Point of Two Metabolic Cycles," *J. Biol. Chem.*, vol. 259, no. 15, pp. 9646–9655, 1984.

[241] P. Gu, F. Yang, T. Su, Q. Wang, Q. Liang, and Q. Qi, "A rapid and reliable strategy for chromosomal integration of gene(s) with multiple copies," *Sci. Rep.*, vol. 5, no. 9684, pp. 1–9, 2015.

[242] M. E. Chung, I. H. Yeh, L. Y. Sung, M. Y. Wu, Y. P. Chao, I. S. Ng, and Y. C. Hu, "Enhanced integration of large DNA into

Escherichia coli chromosome by CRISPR/Cas9," *Biotechnol. Bioeng.*, vol. 114, no. 1, pp. 172–183, 2017.

[243] A. Kutner, M. Chodyñski, and S. J. Halkes, "Citramalic Acid As Chiral Synthon. Synthesis of Chiral Aliphatic Sulfones," *Synth. Commun.*, vol. 26, no. 6, pp. 1175–1182, 1996.

[244] Y. Fujimoto, J. S. Yadav, and C. J. Sih, "(S)-citramalic acid, a useful chiral synthon for the synthesis of 15-deoxy-16(S)-hydroxy-16-methylprostaglandins," *Tetrahedron Lett.*, vol. 21, no. 26, pp. 2481–2482, 1980.

[245] S. V. Frye and E. L. Eliel, "Asymmetric chemical synthesis of (R)- and (S)-citramalate in high enantiomeric purity," *Croat. Chem. Acta*, vol. 58, no. 4, pp. 647–652, 1985.

[246] S. M. Clay and S. S. Fong, *Developing biofuel bioprocesses using systems and synthetic biology*. Springer, 2013.

[247] I. Muñoz, K. Flury, N. Jungbluth, G. Rigarlsford, L. Milà Canals, and H. King, "Life cycle assessment of bio-based ethanol produced from different agricultural feedstocks," *Int J Life Cycle*, 2013.

[248] S. C. Davis, K. J. Anderson-Teixeira, and E. H. Delucia, "Life-cycle analysis and the ecology of biofuels."

[249] X. Ou, X. Zhang, Q. Zhang, and X. Zhang, "Life-cycle analysis of energy use and greenhouse gas emissions of gas-to-liquid fuel pathway from steel mill off-gas in China by the LanzaTech process."

11. Appendices

11.1 Wood-Ljungdahl pathway:

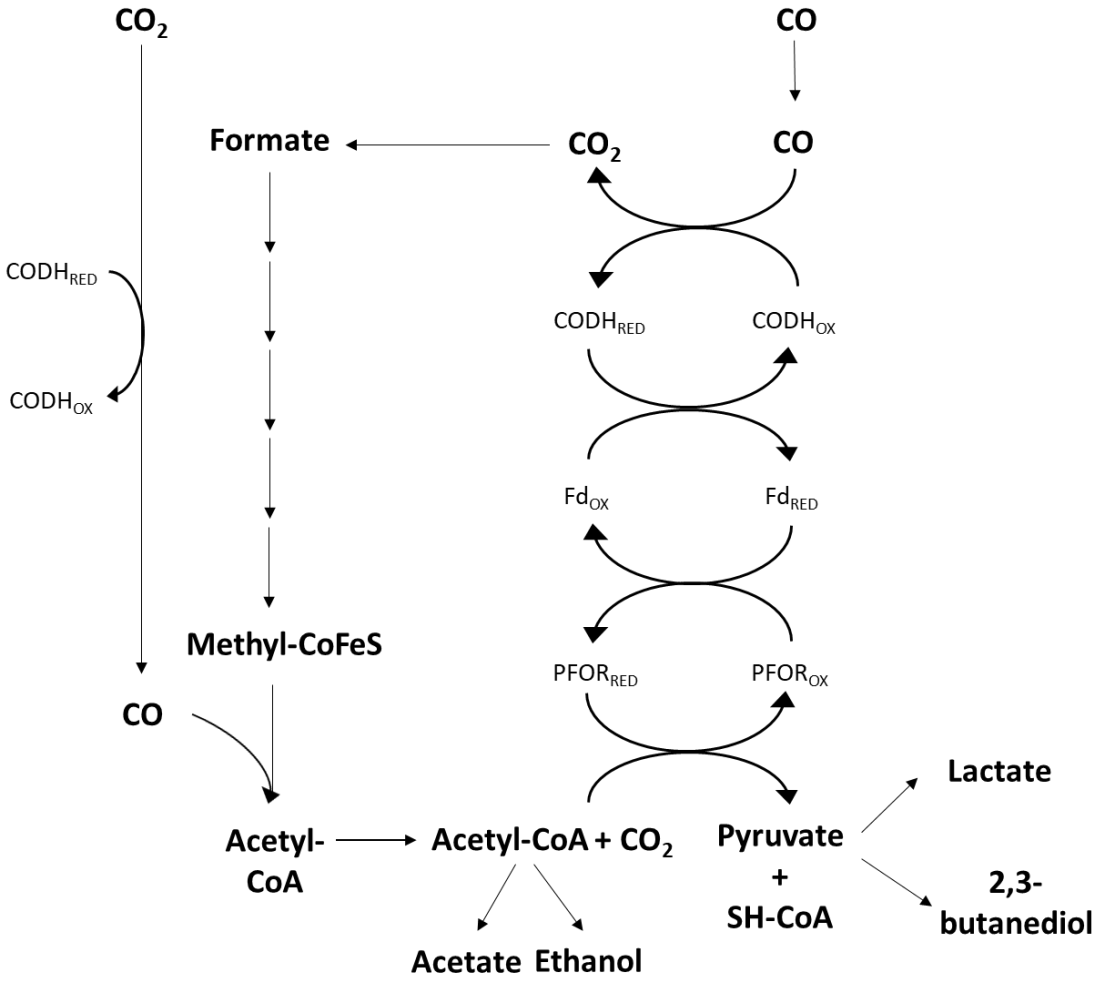


Figure 39: Overview of the Wood-Ljungdahl pathway for the production of acetyl CoA and pyruvate from the fixation of CO and CO_2

CO: Carbon monoxide; CO_2: Carbon dioxide; COASH: Coenzyme A; $CODH_{OX/RED}$: Carbon monoxide dehydrogenase oxidised form/reduced form; $Fd_{OX/RED}$: Ferredoxin oxidised form/reduced form; $PFOR_{OX/RED}$: Pyruvate: ferredoxin oxidaoreductase oxidised form/reduced form.

Adapted from Liew et *al.* 2016.

11.2 Nucleotide sequence of the *E. coli* native *ackA:*

Escherichia coli str. K-12 substre MG1655, complete genome

NCBI Reference Sequence: NC_000913.3

>NC_000913.3:2413470-2414672 *Escherichia coli* str. K-12 substr. MG1655, complete genome

ATGTCGAGTAAGTTAGTACTGGTTCTGAACTGCGGTAGTTCTTCACTGAAATTTGCC
ATCATCGATGCAGTAAATGGTGAAGAGTACCTTTCTGGTTTAGCCGAATGTTTCCAC
CTGCCCGAAGCACGTATCAAATGGAAAATGGACGGCAATAAACAGGAAGCGGCTTTA
GGTGCAGGCGCCGCTCACAGCGAAGCGCTCAACTTTATCGTTAATACTATTCTGGCA
CAAAAACCAGAACTGTCTGCGCAGCTGACTGCTATCGGTCACCGTATCGTACACGGC
GGCGAAAAGTATACCAGCTCCGTAGTGATCGATGAGTCTGTTATTCAGGGTATCAAA
GATGCAGCTTCTTTTGCACCGCTGCACAACCCGGCTCACCTGATCGGTATCGAAGAA
GCTCTGAAATCTTTCCCACAGCTGAAAGACAAAAACGTTGCTGTATTTGACACCGCG
TTCCACCAGACTATGCCGGAAGAGTCTTACCTCTACGCCCTGCCTTACAACCTGTAC
AAAGAGCACGGCATCCGTCGTTACGGCGCGCACGGCACCAGCCACTTCTATGTAACC
CAGGAAGCGGCAAAAATGCTGAACAAACCGGTAGAAGAACTGAACATCATCACCTGC
CACCTGGGCAACGGTGGTTCCGTTTCTGCTATCCGCAACGGTAAATGCGTTGACACC
TCTATGGGCCTGACCCCGCTGGAAGGTCTGGTCATGGGTACCCGTTCTGGTGATATC
GATCCGGCGATCATCTTCCACCTGCACGACACCCTGGGCATGAGCGTTGACGCAATC
AACAAACTGCTGACCAAAGAGTCTGGCCTGCTGGGTCTGACCGAAGTGACCAGCGAC
TGCCGCTATGTTGAAGACAACTACGCGACGAAAGAAGACGCGAAGCGCGCAATGGAC
GTTTACTGCCACCGCCTGGCGAAATACATCGGTGCCTACACTGCGCTGATGGATGGT
CGTCTGGACGCTGTTGTATTCACTGGTGGTATCGGTGAAAATGCCGCAATGGTTCGT
GAACTGTCTCTGGGCAAACTGGGCGTGCTGGGCTTTGAAGTTGATCATGAACGCAAC
CTGGCTGCACGTTTCGGCAAATCTGGTTTCATCAACAAAGAAGGTACCCGTCCTGCG
GTGGTTATCCCAACCAACGAAGAACTGGTTATCGCGCAAGACGCGAGCCGCCTGACT
GCCTGA

11.3 Nucleotide sequence of the *E. coli* native *pta*

Escherichia coli str. K-12 substre MG1655, complete genome

NCBI Reference Sequence: NC_000913.3

>NC_000913.3:2414747-2416891 *Escherichia coli* str. K-12 substr. MG1655, complete genome

GTGTCCCGTATTATTATGCTGATCCCTACCGGAACCAGCGTCGGTCTGACCAGCGTC
AGCCTTGGCGTGATCCGTGCAATGGAACGCAAAGGCGTTCGTCTGAGCGTTTTCAAA
CCTATCGCTCAGCCGCGTACCGGTGGCGATGCGCCCGATCAGACTACGACTATCGTG
CGTGCGAACTCTTCCACCACGACGGCCGCTGAACCGCTGAAAATGAGCTACGTTGAA
GGTCTGCTTTCCAGCAATCAGAAAGATGTGCTGATGGAAGAGATCGTCGCAAACTAC
CACGCTAACACCAAAGACGCTGAAGTCGTTCTGGTTGAAGGTCTGGTCCCGACACGT
AAGCACCAGTTTGCCCAGTCTCTGAACTACGAAATCGCTAAAACGCTGAATGCGGAA
ATCGTCTTCGTTATGTCTCAGGGCACTGACACCCCGGAACAGCTGAAAGAGCGTATC
GAACTGACCCGCAACAGCTTCGGCGGTGCCAAAAACACCAACATCACCGGCGTTATC
GTTAACAAACTGAACGCACCGGTTGATGAACAGGGTCGTACTCGCCCGGATCTGTCC
GAGATTTTCGACGACTCTTCCAAAGCTAAAGTAAACAATGTTGATCCGGCGAAGCTG
CAAGAATCCAGCCCGCTGCCGGTTCTCGGCGCTGTGCCGTGGAGCTTTGACCTGATC
GCGACTCGTGCGATCGATATGGCTCGCCACCTGAATGCGACCATCATCAACGAAGGC
GACATCAATACTCGCCGCGTTAAATCCGTCACTTTCTGCGCACGCAGCATTCCGCAC
ATGCTGGAGCACTTCCGTGCCGGTTCTCTGCTGGTGACTTCCGCAGACCGTCCTGAC
GTGCTGGTGGCCGCTTGCCTGGCAGCCATGAACGGCGTAGAAATCGGTGCCCTGCTG
CTGACTGGCGGTTACGAAATGGACGCGCGCATTTCTAAACTGTGCGAACGTGCTTTC
GCTACCGGCCTGCCGGTATTTATGGTGAACACCAACACCTGGCAGACCTCTCTGAGC
CTGCAGAGCTTCAACCTGGAAGTTCCGGTTGACGATCACGAACGTATCGAGAAAGTT
CAGGAATACGTTGCTAACTACATCAACGCTGACTGGATCGAATCTCTGACTGCCACT
TCTGAGCGCAGCCGTCGTCTGTCTCCGCCTGCGTTCCGTTATCAGCTGACTGAACTT
GCGCGCAAAGCGGGCAAACGTATCGTACTGCCGGAAGGTGACGAACCGCGTACCGTT
AAAGCAGCCGCTATCTGTGCTGAACGTGGTATCGCAACTTGCGTACTGCTGGGTAAT
CCGGCAGAGATCAACCGTGTTGCAGCGTCTCAGGGTGTAGAACTGGGTGCAGGGATT
GAAATCGTTGATCCAGAAGTGGTTCGCGAAAGCTATGTTGGTCGTCTGGTCGAACTG
CGTAAGAACAAAGGCATGACCGAAACCGTTGCCCGCGAACAGCTGGAAGACAACGTG
GTGCTCGGTACGCTGATGCTGGAACAGGATGAAGTTGATGGTCTGGTTTCCGGTGCT
GTTCACACTACCGCAAACACCATCCGTCCGCCGCTGCAGCTGATCAAAACTGCACCG
GGCAGCTCCCTGGTATCTTCCGTGTTCTTCATGCTGCTGCCGGAACAGGTTTACGTT
TACGGTGACTGTGCGATCAACCCGGATCCGACCGCTGAACAGCTGGCAGAAATCGCG
ATTCAGTCCGCTGATTCCGCTGCGGCCTTCGGTATCGAACCGCGCGTTGCTATGCTC
TCCTACTCCACCGGTACTTCTGGTGCAGGTAGCGACGTAGAAAAAGTTCGCGAAGCA
ACTCGTCTGGCGCAGGAAAAACGTCCTGACCTGATGATCGACGGTCCGCTGCAGTAC
GACGCTGCGGTAATGGCTGACGTTGCGAAATCCAAAGCGCCGAACTCTCCGGTTGCA
GGTCGCGCTACCGTGTTCATCTTCCCGGATCTGAACACCGGTAACACCACCTACAAA
GCGGTACAGCGTTCTGCCGACCTGATCTCCATCGGGCCGATGCTGCAGGGTATGCGC
AAGCCGGTTAACGACCTGTCCCGTGGCGCACTGGTTGACGATATCGTCTACACCATC
GCGCTGACTGCGATTCAGTCTGCACAGCAGCAGTAA

11.4 Matrix analysis for ADHs selection –Satisfactory percentage table

Factors		**K_M (EtOH)**	**K_M (Actd)**	**K_{cat} (EtOH)**	**Mesophilic activity**	**DNA seq. available**	**Heterolog. Expr.**	**Total**	**Score**
Proteins	Relative Weights	10%	7%	21%	24%	35%	3%	5	100%
ADH C	*E.coli*	1	0	2	5	4	5	3.27	65%
ADH I	*A.nidulans*	4	2	4	5	5	3	4.42	88%
ADH II	*Acetobacter*	3	4	0	4	1	2	1.95	39%
ADH A	*C.glutamicum*	1	2	3	5	5	5	3.97	79%
ADH A	*Acinetobacter sp. HSB-2*	0	0	0	4	0	2	1.02	20%
ADH2	*G. thermodenitrificans*	2	2	5	0	5	2	3.2	64%
ADH	*G. stearothermophilic*	3	3	3	0	1	2	1.55	31%

11.5 Nucleotide sequence of the *alcA* gene encoding alcohol dehydrogenase from *A. nidulans:*

ATGTCCATCCCCACTATGCAATGGGCCCAGGTCGCCGAGAAGGTCGGCGGCCCGCTC
GTCTACAAGCAGATCCCCGTCCCTAAGCCCGGTCCCGACCAGATCCTTGTGAAGATC
CGCTACTCTGGGGTTTGCCACACCGACCTACACGCTATGATGGGTCACTGGCCAATC
CCCGTCAAAATGCCGCTCGTCGGTGGGCACGAAGGAGCAGGAATCGTCGTGGCAAAG
GGCGAACTGGTCCACGAATTCGAGATCGGCGACCAAGCTGGCATCAAATGGCTCAAT
GGTTCCTGCGGAGAGTGCGAGTTCTGCCGCCAATCGGACGACCCCCTCTGTGCACGC
GCCCAGCTCTCTGGGTATACTGTTGACGGCACGTTCCAGCAGTATGCGCTCGGAAAG
GCGAGTCATGCGTCGAAGATCCCTGCGGGCGTCCCGCTGGATGCCGCGGCCCCAGTA
CTCTGTGCCGGTATTACAGTGTACAAGGGATTGAAAGAGGCCGGGGTCCGGCCGGGC
CAGACCGTGGCGATCGTGGGTGCCGGTGGCGGCCTGGGATCCCTTGCACAGCAGTAT
GCGAAGGCGATGGGGATCAGGGTTGTCGCGGTCGATGGGGGAGATGAGAAGCGGGCC
ATGTGTGAGTCGCTTGGAACAGAGACATATGTCGACTTCACCAAATCTAAAGACCTG
GTGGCCGACGTCAAGGCAGCGACGCCGGATGGTCTCGGTGCGCACGCGGTGATCCTG
CTTGCCGTGTCAGAGAAGCCCTTCCAGCAAGCCACTGAATATGTGCGCTCTCGCGGG
ACAATTGTTGCTATTGGCTTGCCGCCAGATGCGTACCTCAAGGCCCCTGTGATCAAC
ACAGTTGTTCGCATGATCACTATCAAGGGCAGCTACGTTGGAAACCGACAGGACGGT
GTCGAGGCTCTGGACTTCTTCGCTCGCGGCCTGATCAAGGCTCCGTTCAAGACGGCT
CCTCTGAAGGATCTGCCGAAGATTTACGAGCTTATGGAACAAGGCAGAATCGCCGGT
CGTTATGTGCTAGAGATGCCAGAATAA

11.6 Nucleotide sequence of the *adhA* gene encoding alcohol dehydrogenase from *C. glutamicum:*

ATGACCACTGCTGCACCCCAAGAATTTACTGCTGCTGTTGTTGAAAAATTCGGTCAT
GAGGTGACCGTGAAGGATATTGACCTTCCAAAGCCAGGACCAAACCAGGCATTGGTG
AAGGTACTCACCTCCGGCATCTGCCACACCGACCTCCACGCCTTGGAGGGCGATTGG
CCAGTAAAGCCGGAACCACCATTCGTACCAGGACACGAAGGTGTAGGTGAAGTTGTT
GAGCTCGGACCAGGTGAACACGATGTGAAGGTCGGCGATATTGTCGGCAATGCATGG
CTCTGGTCAGCGTGTGGCACCTGCGAATACTGCATCACCGGCAGGGAAACTCAGTGC
AACGAAGCTGAGTATGGTGGCTACACCCAAAATGGATCCTTCGGCCAGTACATGCTG
GTGGATACCCGTTACGCCGCTCGCATCCCAGACGGCGTGGACTACCTCGAAGCAGCA
CCAATTCTGTGTGCAGGCGTGACTGTCTACAAGGCACTCAAAGTCTCTGAAACCCGC
CCGGGCCAATTCATGGTGATCTCCGGTGTCGGCGGACTTGGCCACATCGCAGTCCAA
TACGCAGCGGCGATGGGCATGCGTGTCATTGCGGTAGATATTGCCGATGACAAGCTG
GAACTTGCCCGTAAGCACGGTGCGGAATTTACCGTGAATGCTCGCAATGAAGATCCA
GGCGAAGCTGTACAGAAGTACACCAACGGTGGCGCACACGGCGTGCTTGTGACTGCA
GTTCACGAGGCAGCATTCGGCCAGGCGCTGGATATGGCTCGACGTGCAGGAACGATT
GTGTTCAACGGCCTGCCACCGGGAGAGTTCCCAGCATCCGTGTTCAACATCGTATTC
AAGGGCCTGACCATCCGTGGATCCCTCGTGGGAACCCGCCAAGACTTGGCCGAAGCG
CTCGATTTCTTTGCACGCGGACTAATCAAGCCAACCGTGAGTGAGTGTTCCCTCGAT
GAGGTCAATGATGTTCTTGACCGCATGCGAAACGGCAAGATTGATGGTCGTGTGGCA
ATTCGCTACTAA

11.7 Paired comparison table for weighing each factor considered in the selection process against each others

Factors		A	B	C	D	E	F
		K_M(Adl)	K_M (Acetate)	K_{cat} (Ald ox)	Mesophilic activity	DNA seq. available	Heterol Expr. *E. coli*
A	K_M(Adl)		A, 1	C, 3	D, 2	E, 3	A, 2
B	K_M (Acetate)			B, 2	B, 0	E, 3	B, 2
C	K_{cat} (Ald ox)				C, 1	E, 1	C, 1
D	Mesophilic activity					E, 2	F, 1
E	DNA sequence available						E, 1
F	Heterologous expression in *E. coli*						

11.8 Relative importance of the factors used for the selection of ALDHs

	Factor	Score	Relative weight	Rank
A	K_M(Adl)	3	12%	4
B	K_M (Acetate)	4	16%	3
C	K_{cat} (Ald ox)	5	20%	2
D	Mesophilic activity	2	8%	5
E	DNA sequence available	10	40%	1
F	Heterolog. Expr. in *E. coli*	1	4%	6
	Total	25	100%	-

11.9 Matrix analysis for ALDHs selection - Satisfactory percentage table

Factors		K_M (Ald)	K_M (Acetate) ~irreversibility	K_{cat} (Ald)	Mesophil. activity	DNA seq. available	Heterolog. expr	Total	Score
Proteins	**Relative Weights**	12%	16%	20%	8%	40%	4%	5	100%
ADH C	*E.coli*	1	0	3	5	4	5	2.92	58%
ALDH A	*A.nidulans*	5	5	4	5	5	4	4.76	95%
ALDH II	*Acetobacter*	2	2	3	3	0	0	1.4	28%
ALDH A	*C.glutamicum*	0	5	0	5	5	2	3.28	66%
ALDH	*Acinetobacter sp. HSB-2*	5	5	3	5	5	2	4.48	90%
ALDH	*G. thermodenitrificans*	5	5	3	0	5	2	4.08	82%
ALDH	*G. stearothermophilic*	2	5	5	0	0	2	2.24	45%

11.10 Growth profiles of *E. coli* BW25113 Δ*ldhA* pBAD24-*ackA-pta-cimA3.7* and *E. coli* BW25113 Δ*ldhA* pBAD24 in flask experiment

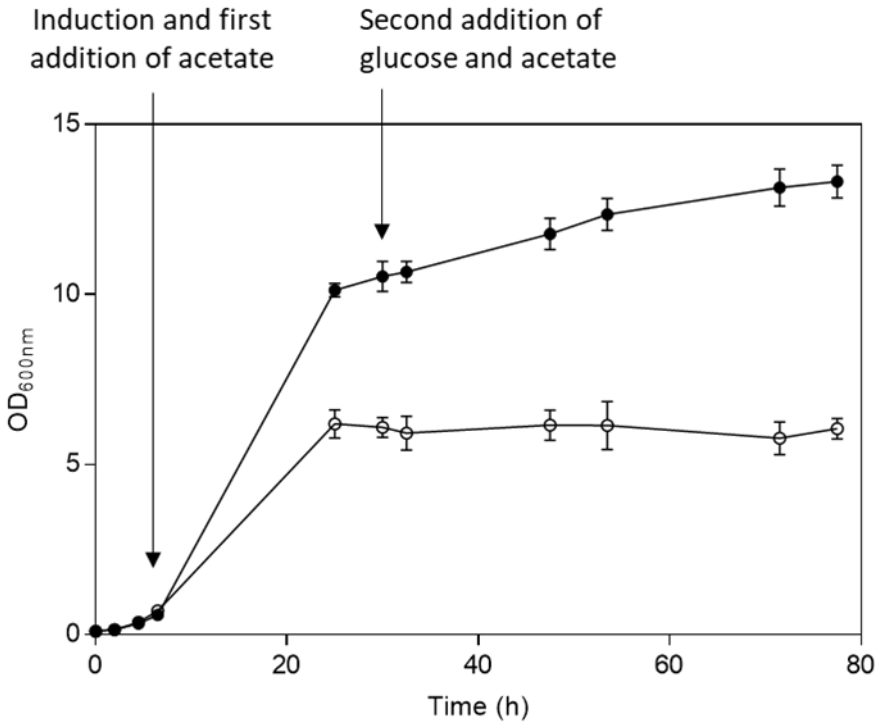


Figure 40: Growth profiles of *E. coli* BW25113 Δ*ldhA* pBAD24 and *E. coli* BW25113 Δ*ldhA* pBAD24-*ackA-pta-cimA3.7* in glucose and acetate co-feed in flask experiment

Growth profiles of control strain of *E. coli* BW25113 Δ*ldhA* pBAD24 (○) and *E. coli* BW25113 Δ*ldhA* pBAD24-*ackA-pta-cimA3.7* (●) grown on Lund minimal medium supplemented with glucose (1%). Acetate was added right after the induction (50mM) and a second time with fresh glucose after 25h.

11.11 Example of SDS-PAGE of insoluble ADH I-ALDH A-CimA3.7

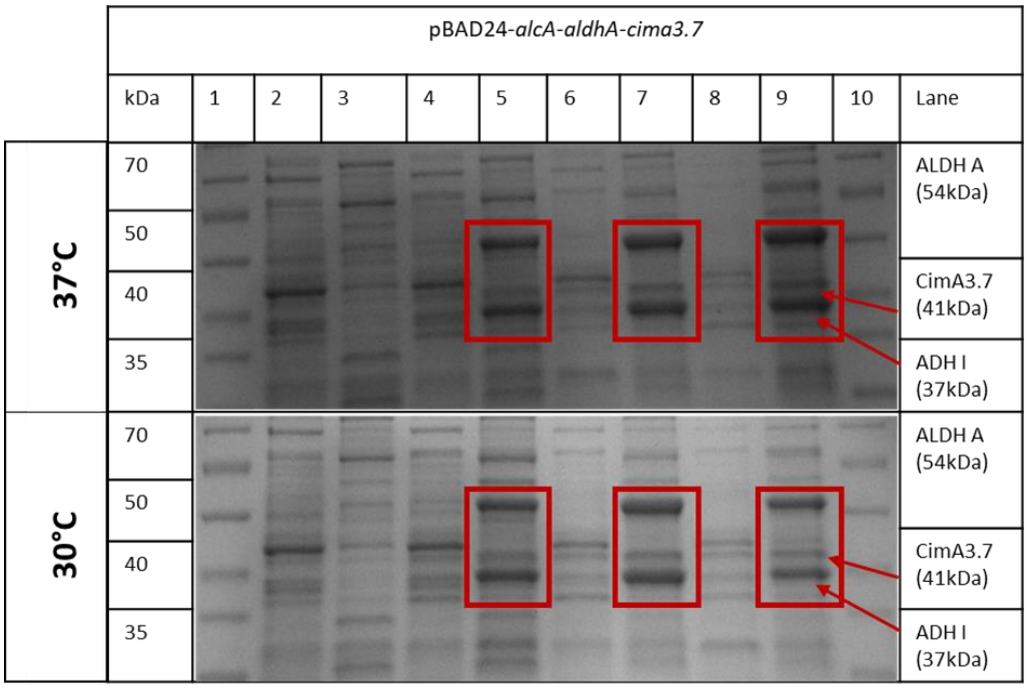


Figure 41: Example of SDS-PAGE showing insoluble ADH I –ALDH A – CimA3.7 when expressed on Lund medium supplemented with glycerol as sole carbon source at 37°C and 30°C.

Overnight seed cultures of *E. coli* BW25113 Δ*ldhA* pBAD24-*alcA-aldA-cimA3.7* grown on Lund medium with glycerol as sole carbon source were used to inoculate fresh Lund medium containing glycerol and incubated at 30°C or 37°C. When the OD_{600} of the 50 ml culture reached 0.4-0.6, 0.2% *L*-(+)-arabinose was added to induce protein production. Samples were taken at regular intervals to measure the OD_{600}. Cells were lysed using BugBuster protein extraction reagent and run on an SDS-PAGE. **Lane 1 and 10**: ladder. **Lane 2-3**: soluble and insoluble fractions of sample at 0h, before induction. **Lane 4-5**: soluble and insoluble fraction of sample 4h after induction. **Lane 6-7**: soluble and insoluble fraction of sample 8h after induction. **Lane 8-9**: soluble and insoluble fraction of sample 24h after induction. Red squares highlight the production of insoluble proteins.

11.12DC assay calibration curve

DC Protein assay was used to determine total protein concentrations in enzyme activity assays. Bovine Serum Albumin (BSA) was used as the protein standard. BSA (2 mg) was dissolved in the same buffer as the reactions for enzyme activity were to be perfomed, and a serie of dilutions prepared (0.2 to 2 mg/L). Each sample (100 µL) was transferred to a new tube and mixed with reagent A' (500 µL) and reagent B (4 mL). The mix was incubated at room temperature for 15 minutes and the absorbance at 750 nm measured. The calibration curve was then produced by plotting the absorbance against the concentration of BSA. The same experiment was performed with a series of dilution of the unquantified protein samples. The calibration curve was then used to estimate the total protein content of samples. A calibration curve was freshly prepared for each experiment. An example of BSA calibration curve is shown in Fig. 40.

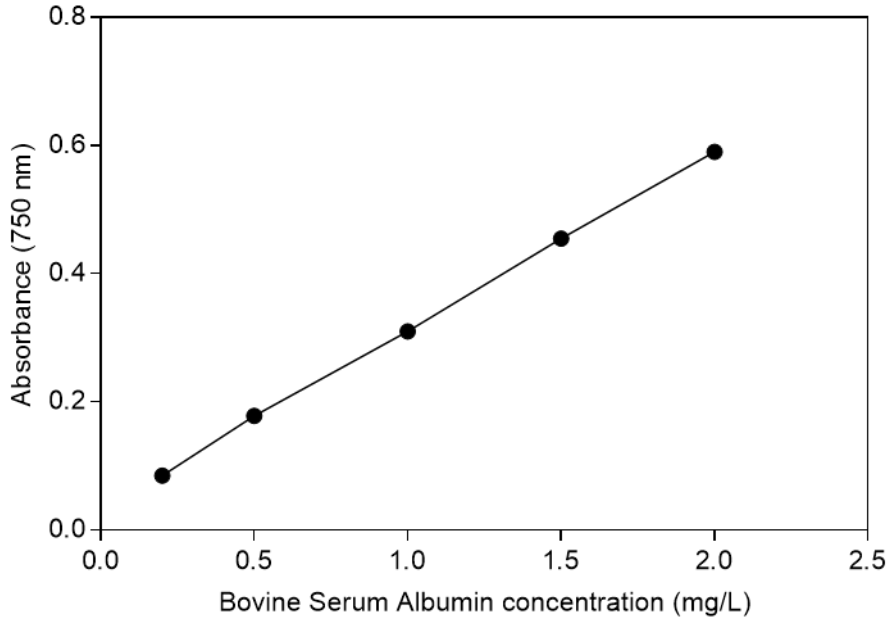


Figure 42: Bovine Serum Albumin concentration calibration curve

11.13 2-Mercaptoethanol calibration curve

2-Mercaptoethanol (2-ME) was used as a standard for citramalate synthase assays. It contains a free thiol group, which reacts with DTNB and produce the yellow chromophore of 2-nitro-5-thiobenzoic acid, which absorbs strongly at 412 nm. The change in absorbance at various concentrations of 2-ME was used to produce a standard curve to calculate the concentration of SH-CoA liberated by the catalytic reaction of CimA3.7 on pyruvate and acetyl-CoA. This provided a convienient and quick way to measure CimA3.7 activity. An example of a calibration curve is given in Fig. 41.

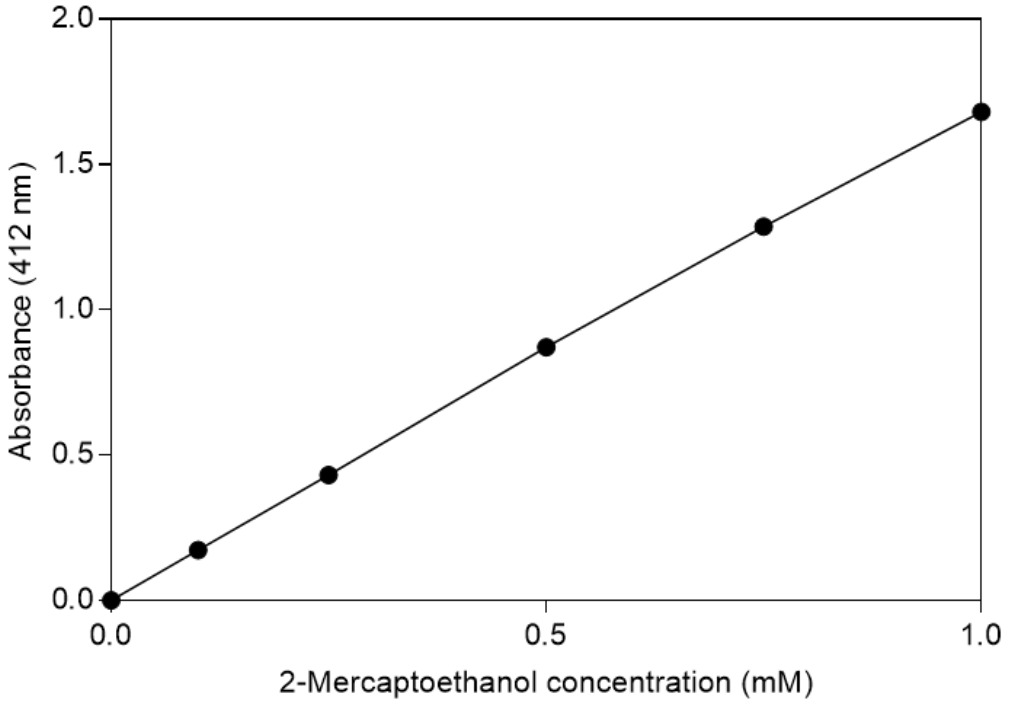


Figure 43: 2-Mercaptaethanol concentration calibration curve

11.14 HPLC calibration curves

HPLC standard curves were produced to calculate the concentrations of compounds consumed and produced during flasks assays and fed-batch fermentations. Pure compounds purchased from Sigma-Aldrich were used to generate the standard curves. Various solutions of known concentrations were produced for each compounds. Serial dilutions were done and injected onto the HPLC column. The peak area for each injection volume was measured. The standard curves were done by plotting peak area against compound concentration. The amount of compound used to generate the standard curve was varied depending on the expected titre of the compounds, so that the amount produced would fall within the range of the calibration curve. An example of a calibration curve used for flask assay and fed-batch fermentations is given in Fig. 42.

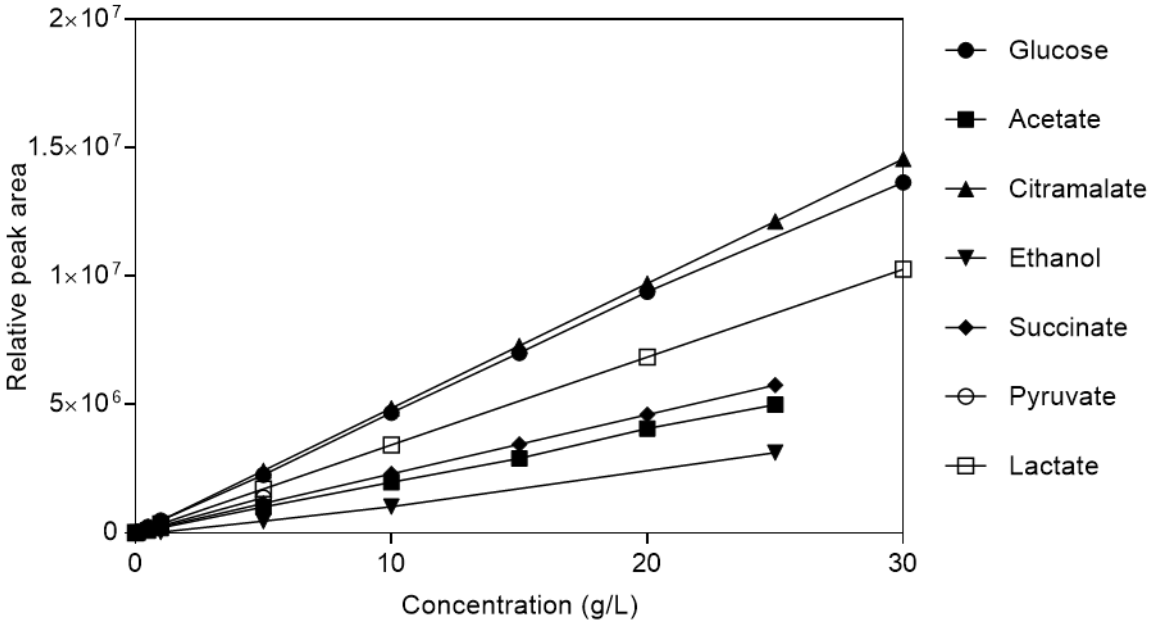


Figure 44: HPLC calibration curves

11.15 Growth profiles of *E. coli* BW25113 Δ*ldhA* pBAD24-*ackA-pta-cimA3.7*

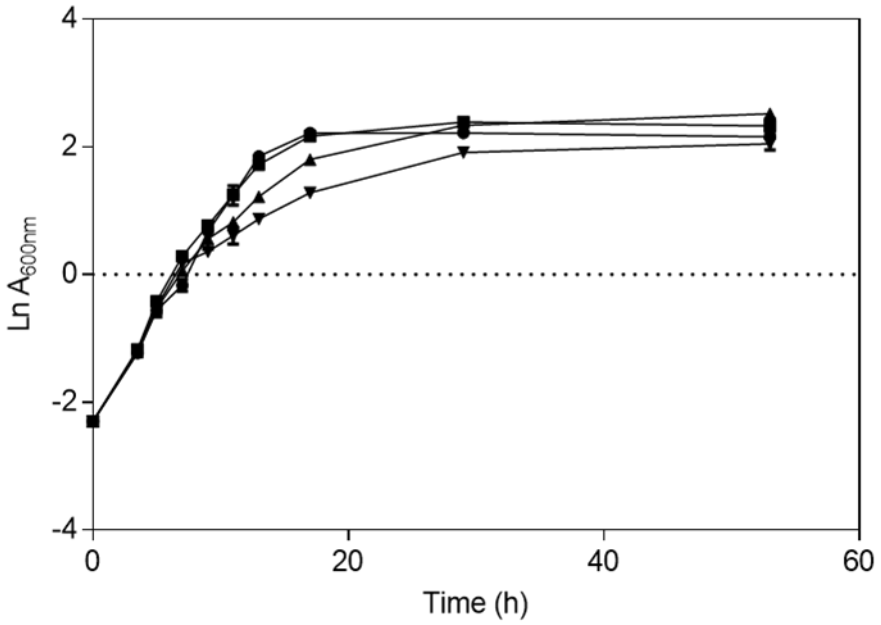


Figure 45: Growth profile of *E. coli* BW25113 Δ*ldhA* pBAD24-*ackA-pta-cimA3.7* in presence of various concentrations of acetate

Cells of *E. coli* BW25113 Δ*ldhA* pBAD24-*ackA-pta-cimA3.7* were grown on glucose as sole carbon source. Proteins expression was induced by adding L-(+)-arabinose (0.2%) at an OD_{600} of 0.6-0.8. Right after induction, 0 g/L (●), 2.5 g/L (■), 5 gL/ (▲) and 10 g/L (▼) of acetate was supplemented to the culture medium. Growth was monitored by measuring the OD_{600nm}. Growth rates, μ_{max}, were calculated as described in section 5.2.

11.16 Sample calculation of yield of carbon source conversion to citramalate

Table 22: Glucose and acetate consumed for the production of citramalate, and yields of carbon source conversion to citramalate when 0% and 2.5% of acetate was supplemented to the medium

0% acetate	Flask 1	Flask 2	Flask 3
Glucose consumed (g/L)	7.42	7	7.55
Citramalate produced (g/L)	0.53	0.57	0.62
$Y_{citramalate/carbon\ source}$ (g/g)	0.071	0.081	0.082
Average	**$Y_{citramalate/glucose}$ = 0.078 ± 0.006**		

E. coli BW25113 Δ*ldhA* pBAD24-*ackA-pta-cimA3.7* was grown in Lund medium containing glucose (1%) as sole carbon source at 30°C to an OD_{600nm} 0.6. AckA-Pta-CimA3.7 expression was induced by adding *L*-arabinose (0.2%), and further incubated at 30°C. Samples were taken regularly to be analysed by HPLC and were used to calculate the glucose consumed and the correspondant citramalate produced. Results of the three experiments conducted are shown and were used to calculate average and standard deviations.

The $Y_{citramalate/\ carbon\ source}$ was calculated for each flask as followed:

$Y_{citramalate/\ carbon\ source}$ = citramalate produced / carbon source consumed

Flask 1 : **$Y_{citramalate/\ carbon\ source}$ = 0.53 / 7.42 = 0.071 g/g.**

Flask 2 : **$Y_{citramalate/\ carbon\ source}$ = 0.57 / 7 = 0.081 g/g.**

Flask 3 : **$Y_{citramalate/\ carbon\ source}$ = 0.62 / 7.55 = 0.082 g/g**

Therefore, an average for $Y_{citramalate/\ carbon\ source}$ of **0.078 ± 0.006 g/g** was obtained.

Similar calculations were performed on each of the other acetate concentrations tests. In the experiments, where 2.5, 5 and 10 g/L of acetate were added to the medium, the amounts of acetate consumed for citramalate production were added to the amount of glucose consumed to calculate the $Y_{citramalate/\ carbon\ source}$.

11.17 Fed-batch fermentation set-up

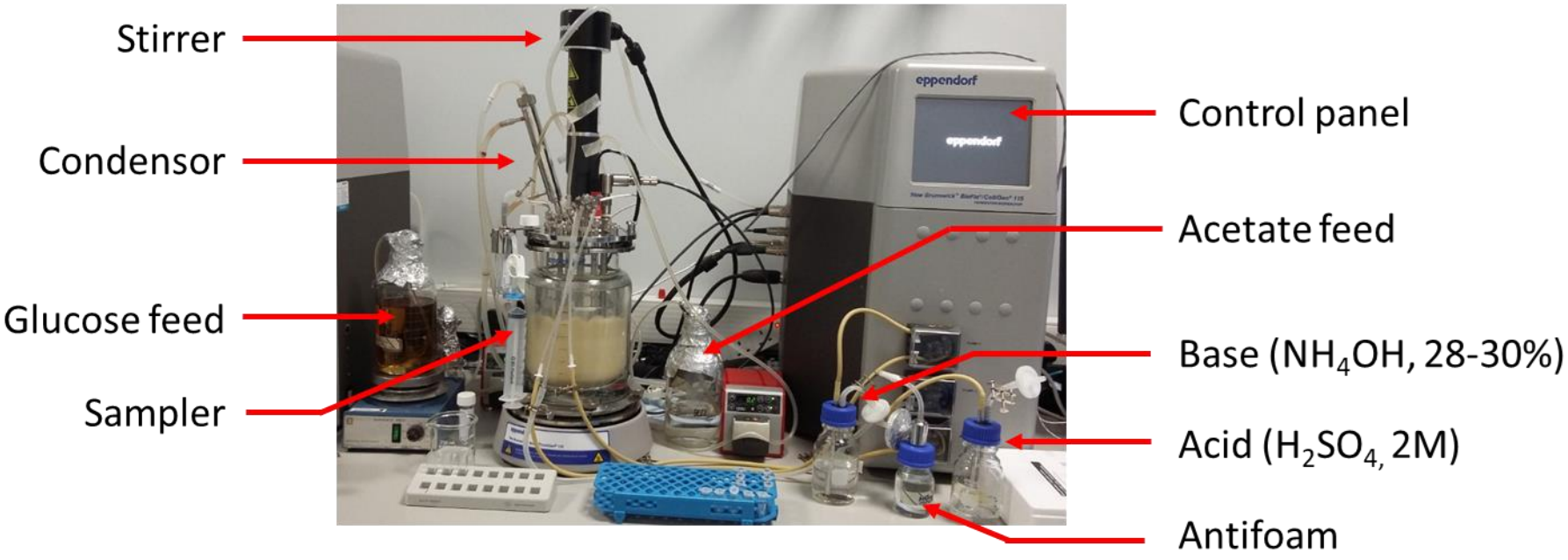


Figure 46: Description of the fed-batch fermentation devices and set-up

11.18 Comparison of efficiency parameters in fed-batch fermentation with different glucose and acetate co-feeds

Table 23: Comparison of efficiency parameters obtained in the benchmark fed-batch fermentation and in various glucose/acetate co-feeding regimes

STRAINS	BW25113 Δ*ldhA* pBAD24-*cimA3.7* 30°C Glucose only	BW25113 Δ*ldhA* pBAD24-*ackA-pta-cimA3.7* 30°C Glucose+acetate 1	BW25113 Δ*ldhA* pBAD24-*ackA-pta-cimA3.7* 30°C Glucose+acetate 2
Phase 1+2 (pre-induction)			
$Y_{BM/glucose}$	0,45 g/g	0,41 g/g	0.45 g/g
Phase 3 (production phase)			
$Y_{BM/glucose}$	0.32 g/g	-	-
$Y_{BM/glucose+acetate}$	-	0.16 g/g	0.26 g/g
Citramalate titre (g/L)	21.5	4.73	9.64
$Y_{citramalate/glucose}$	0.20 g/g	-	-
$Y_{citramalate/glucose+acetate}$	-	0.06 g/g	0.11 g/g
Citramalate production rate (g/L/h)	0.89	0.26	0.64
Citramalate specific production ($g/L/g_{DCW}/h$)	0.021	0.019	0.028

11.19 Growth profiles of *E. coli* BW25113 Δ*aceF* pBAD24-*alcA-aldA-cimA3.7*

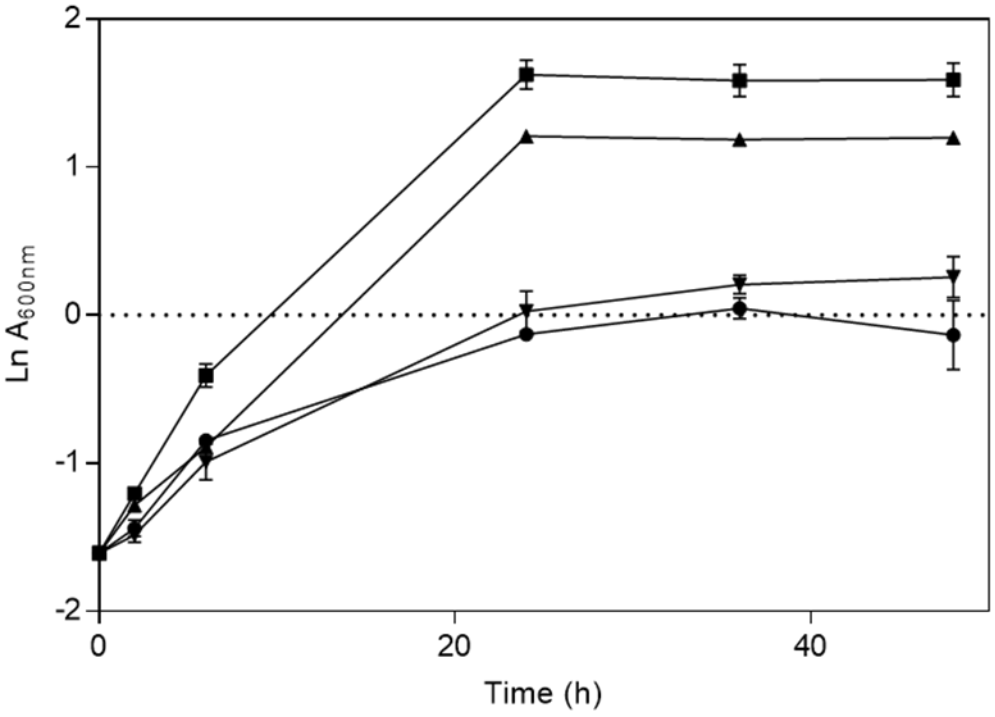


Figure 47: Growth profile of *E. coli* BW25113 Δ*aceF* pBAD24-*alcA-aldA-cimA3.7* in presence of various concentrations of ethanol

Cells of *E. coli* BW25113 Δ*aceF* pBAD24-*alcA-aldA-cimA3.7* grown on glucose and acetate were used to inoculate fresh Lund medium containing glucose (1%) and various concentrations of ethanol as carbon sources. Proteins expression was induced by adding L-(+)-arabinose (0.2%) right after inoculation. Concentrations of ethanol were then added, 0% (●), 1% (■), 3% (▲) and 5% (▼) of acetate was supplemented to the culture medium. Growth was monitored by measuring the OD_{600nm}. Growth rates, μ_{max}, were calculated as described in section 5.2.

12. Addendum: DTP- PIP placement

Professional Internships for PhD Students

Reflection Form

Name of Organization

University of Reunion Island, IUT de Saint-Pierre Laboratory LCSNSA (EA 2212)

Details of Placement

Please describe your main activities during the placement (150-200 words)

Teaching mission: - The student will be responsible for temporary teaching with first and second year students doing a Technology university degree (DUT) in Biological Engineering at the University of Saint Pierre (Reunion Island, France); preparation and conduction of the practical lab classes over the first semester 2015-2016; supervision and marking of the students reports. - The student will be under the status of temporary teaching (CEV). Research mission: - The student will have to get involved into the innovative Research projects of the LCSNSA laboratory (E2 2212) at the University of Reunion Island and lead research actions targeted on the development of innovative extraction technics for microbial pigments (as part of the main theme of the laboratory on New Molecules with biological activity); - The student will have to do a technological survey and a literature review on the above mentioned theme "eco-extraction of microbial pigments", and write down a review article;

- The student will participate to the academically valorisation of the work achieved during the placement (participation in writing scientific articles);
- The student will participate to the seminars and internal meetings of the Council of the laboratory.

Placement Achievements

Please detail all outcomes from the placement, including any publications, presentations given and reports written etc. (150-200 words)

An oral presentation supported by a powerpoint presentation was done at the University of Reunion Island at the end of the placement. It was followed by a discussion with all the scientists involved in the project, and new axes to investigate were drawned.

For the teaching hours that I have done, I prepared slides for the students as a teaching support during the lecture. I was also in charge of preparing demonstration and group exercices to do in class. To complete the teaching hours on industrial fermentation, I also prepared an examination and made the correction and markings, which were used for the students' final grades. During the research project, I was involved in writing a book chapter, which was published earlier in 2016. I am part of the cited authors. I also was asked to produced 2 posters (I signed as primary author on them), that were used for a conference talk in July 2016.
As a follow up after the PIP placement, I wrote a scientific paper with the lab group from Reunion Island. The paper was published earlier this year in Journal of Fungi, and I am the first author as well.

Book chapter:

Caro, Y.; Venkatachalam, M.; Lebeau, J.; Fouillaud, M.; Dufossé, L. Pigments and Colorants from Filamentous Fungi. In Fungal Metabolites, 1st ed.; Mérillon, J.-M., Ramawat, K.G., Eds.; Springer International Publishing: Berlin, Germany, 2015; pp. 499–568.

Posters made for the conference Pigments in Food, July 2016.

Poster 1:

Lebeau, J. ; Venkatachalam, M.; Fouillaud, M.; Dufossé, L. ; Caro, Y. Extraction of fungal polyketides using ionic liquids. 2016.

Poster 2:

Lebeau, J. ; Venkatachalam, M.; Fouillaud, M.; Dufossé, L. ; Caro, Y. Emerging greener extraction systems for fungal pigments isolation. 2016.

Scientific article:

Lebeau, J. ; Venkatachalam, M.; Fouillaud, M.; Petit, T. ; Vinale, F. ; Dufossé, L. ; Caro, Y. Production and New Extraction Method of Polyketide Red Pigments Produced by Ascomycetous Fungi from Terrestrial and Marine Habitats. *Journal of Fungi*, 3(34), 2017.

Skill development

Has this Placement helped you developed any new skills or enhanced your previous skill set? (100-150 words)

This placement has enhanced my communication skills as I had to teach teenagers (16-17 years old) about industrial fermentation, as well as leading a demonstration class with them. It was an excellent way to learn how to be clearer in explaining complex systems, but also teaching to others teaches you to be patient and constantly questioning yourself on how to improve your explanations.
The research part of the placement was very valuable too as it led to take part in the writing of a book chapter for a comprehensive review on pigments produced by fungal strains and their biotechnological interests. Therefore, dealing with a different field of research during my PhD, was also a good training for improving my capacities of adaptation.

Future Work

Has this Placement influenced your future career aspirations? If so, in what way? (150-200 words)

The three angles offered by this placement gave me a great experience and the opportunity to touch to multiple things! I really enjoyed teaching to undergrads, preparing the lecture, the demonstration class as well as preparing the exam and marking it. I really enjoyed being involved in a research project with a team, where everyone is working on a part of the same project. It confirmed that I need and want to be involved in a team project rather than focusing on my own independent project. However, this is the human management side that I did like the most (managing people susceptibilities is a real challenge, and always full of surprises!). Thus, it makes me consider careers paths where more social interactions are involved, but obviously still in the science field!